Université de Toulouse

THÈSE

En vue de l'obtention du

DOCTORAT DE L'UNIVERSITÉ DE TOULOUSE

Délivré par :

Université Toulouse 3 Paul Sabatier (UT3 Paul Sabatier)

Présentée et soutenue par :
Abbas FAYAD

Le mardi 18 avril 2017

Titre :

EVALUATION DE LA RESSOURCE EN EAU ASSOCIÉE AU MANTEAU NEIGEUX SUR LE MONT LIBAN À PARTIR D'OBSERVATIONS ET DE LA MODÉLISATION

ED SDU2E : Hydrologie, Hydrochimie, Sol, Environnement

Unité de recherche :

CESBIO (IRD, CNES, CNRS, UPS) - Centre d'Etudes Spatiales de la BIOsphère, (UMR 5126)

Directeur(s) de Thèse :

Richard ESCADAFAL (CESBIO, Toulouse), Simon GASCOIN (CESBIO, Toulouse), Ghaleb FAOUR (CNRS, Liban)

Rapporteurs :

Thomas CONDOM (IGE, Grenoble),
Denis RUELLAND (HydroSciences, Montpellier)

Autre(s) membre(s) du jury :

Laurent POLIDORI (CESBIO, Toulouse), Janine SOMMA (USJ, Liban), Fadi COMAIR (Ministère de l'Énergie et de l'Eau, Liban), Mouin HAMZE (CNRS, Liban)

EVALUATION OF THE SNOW WATER RESOURCES IN MOUNT LEBANON USING OBSERVATIONS AND MODELLING

by:
Abbas FAYAD

University of Toulouse 3 Paul Sabatier (UT3 Paul Sabatier)

CESBIO - Centre d'Etudes Spatiales de la BIOsphère (UMR 5126)
(IRD, CNES, CNRS, UPS)

Advisors:
Richard ESCADAFAL (CESBIO, Toulouse), Simon GASCOIN (CESBIO, Toulouse), Ghaleb FAOUR (CNRS, Liban)

Reviewers:
Thomas CONDOM (IGE, Grenoble),
Denis RUELLAND (HydroSciences, Montpellier)

Committee Members:
Laurent POLIDORI (CESBIO, Toulouse), Janine SOMMA (USJ, Liban), Fadi COMAIR (Ministry of Energy and Water, Lebanon), Mouin HAMZE (CNRS, Lebanon)

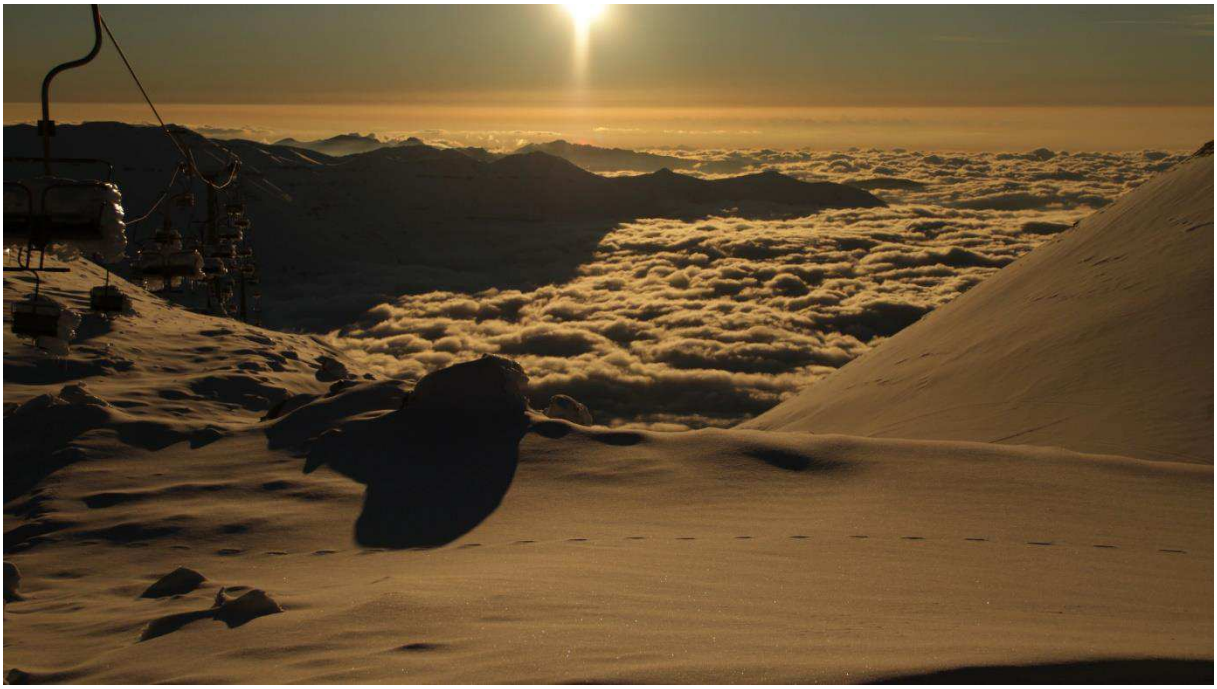

Sunset at Cedars (2790 m), Mount Lebanon, 12 Jan 2016.
Photograph by A. Fayad

ACKNOWLEDGEMENTS

Funding for this PhD work was possible thanks to a Scholarship from the Institut de Recherche pour le Developpement (IRD). Fieldwork in the Mount Lebanon was supported by a grant from The National Council for Scientific Research (CNRS).

First and foremost, I wish to thank Dr. Simon Gascoin for his guidance, support, and for giving me the freedom to conduct independent research in the interesting and physically challenging mountain regions. I am very indebted for his patience and willingness to help me with virtually every aspect of my PhD. The countless hours spent together modeling and analyzing the snow data made this PhD possible. Second, thanks to Dr. Ghaleb Faour, for this helpful feedback, and for providing the opportunity and funding to spend two years in the Mount Lebanon wandering and exploring. Thanks to Dr. Richard Escadafal for accepting to direct this PhD work, his comments and administrative support during the last-minute race against time were appreciated.

I am very grateful to Laurent Drapeau friendship, support, and his shared passion of hiking to remote places. I am also thankful to Pascal Fanise for the perspective he has given me on meteorological and snow censors, and for his keen good humor. Additionally, they both have provided devotion and tremendous effort on keeping the snow stations running over the past six years.

Thanks to Dr. Thomas Condom and Dr. Denis Ruelland for reviewing this manuscript. Their insightful comments and helpful feedback have improved the quality of this dissertation.

I am furthermore grateful to Dr. Fadi Comair for his tremendous support, encouragement, and endorsement during the past five years. Dr. Mouin Hamze continued interest and support for my work was a tremendous boost. I would also like to thank Dr. Janine Soma and Dr. Laurent Polidori for accepting to serve on my committee, your time and discussions were appreciated.

I would like to thank colleagues from the National Council for Scientific Research (CNRS), the Institut de Recherche pour le Developpement (IRD), and the University of Saint Joseph (USJ), for their noteworthy support in the field and managing to find time for fun in the process. My experiences with coworkers at CNRS and CESBIO, in the field and in the office, will be always remembered.

It would be difficult to forget the hospitality of Père Samir and Père Pierre at the Monastery of the Nativity. Their support and endless conversations will be fondly remembered.

Finally, I am so fortunate to have an amazing family, whom I owe everything.

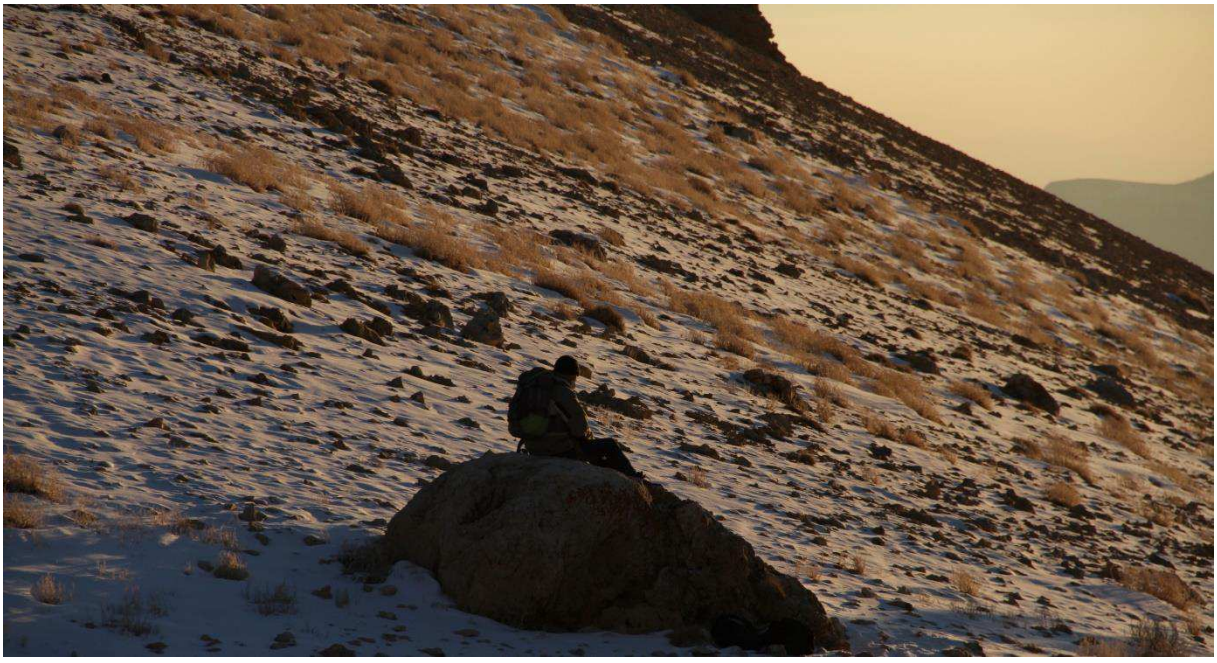

Early snow: Hiking the Cedars slopes (1800-2850 m) with L. Drapeau., 26 Dec 2016. Photograph by A. Fayad

ABSTRACT

Lebanon's water resources are under increasing pressure due to economic development, demographic growth, unsustainable water resource management, and climate change. The Mount- and Anti-Lebanon Mountains are natural water towers for Lebanon as they play an important role in enhancing orographic precipitation. Due to the influence of the Mediterranean climate, most precipitation above 1200 m a.s.l. falls as snow during winter season. As a result, snowmelt is an important contributor to the national water balance. In particular, snowmelt from Mount-Lebanon feeds the karst groundwater systems, which provide key water resources to the coastal region. Despite the importance of the snow cover in the Lebanese mountains, the actual snowpack spatial and temporal variability and its contribution to the spring and river discharges in Lebanon remains poorly constrained. The objective of this work is to reduce this lack of knowledge using a combination of in situ measurements, remote sensing observations and modelling of the snowpack in Mount-Lebanon.

1. We first present an extensive review of the literature about the snow hydrological processes in Mediterranean-like mountain regions. Many studies - mainly from Western USA and Southern Europe mountains - emphasize the strong impact of the interannual Mediterranean climate variability on the snowpack dynamics. The high incoming solar radiation is an important driver of the snowpack energy balance, but the contribution of heat fluxes is stronger at the end of the snow season. Snow sublimation and rapid densification are important processes to consider. Hybrid approaches combining weather station data with optical remote sensing of the snow extent through modelling are recommended to tackle the lack of spatially-distributed observations of the meteorological forcing.

2. Then, we introduce an original dataset on the snow cover in Mount-Lebanon for the period 2013-2016. We collected field observations of the snow height (HS), snow water equivalent (SWE), and snow density between 1300 and 2900 m a.s.l. in the western slope of Mount-Lebanon. In addition, continuous meteorological data were acquired by three automatic weather stations located in the snow dominated region of Mount-Lebanon. The MODIS snow product was used to compute the daily snow cover area in three snow dominated basins. We find that HS and SWE have large variances and that snow density is high. The strong correlation between HS and SWE may be useful to reduce the amount of field work for future operational monitoring.

3. Using these data we set up a distributed snowpack energy balance in the Mount-Lebanon at 100 m resolution. The model is validated at different scales using the observed SWE, snow density, HS and SCA. A simulation with very limited adjustments to the default parameterization is found to correctly capture most of the observations. This simulation allows the estimation of the SWE evolution and snow melt in the three study basins between 2013 and 2016.

This research highlighted the importance of conducting simultaneous field surveys and meteorological observations to gain insights into the physical processes driving snowpack evolution in Mount-Lebanon. Finally, the influence of snow erosion by wind and the influence of dust deposits on snowmelt, remains less known, and are warrant for future research.

Keywords: Snow monitoring, Remote sensing of snow, Snow water equivalent, Snow hydrology, Mediterranean climate, Climate change, Water resources, Lebanon

Snow, a major source for the karst groundwater in Lebanon. Balaa (1485 m), 20 Feb 2016. Photograph by A. Fayad

RÉSUMÉ

Les ressources en eau du Liban sont soumises à une pression croissante due au développement économique, à la croissance démographique, à la gestion non-durable des ressources en eau et au changement climatique. Les montagnes du Mont et Anti-Liban sont des châteaux d'eau naturels pour le Liban car elles augmentent les précipitations par le soulèvement orographique des masses d'air. En raison de l'influence du climat méditerranéen, la plupart des précipitations au-dessus de 1200 m a.s.l. tombe sous la forme de neige en hiver. Par conséquent, la fonte des neiges contribue de façon importante au bilan hydrique national. En particulier, la fonte des neiges du Mont-Liban alimente les réseaux d'eau souterraine karstiques, qui fournissent des ressources en eau essentielle pour la région côtière. Malgré l'importance du manteau neigeux au Liban, sa variabilité spatiale et temporelle est insuffisament observée si bien que sa contribution au débit des fleuve et des sources reste méconnue. L'objectif de ce travail est de réduire ce manque de connaissance en utilisant des mesures in situ, des observations satellite et de la modélisation du manteau neigeux.

1. Nous présentons d'abord une revue de la littérature sur les processus nivo-hydrologiques dans les régions montagneuses méditerranéennes. De nombreuses études - principalement aux Etats-Unis de l'Ouest et dans les montagnes au sud de l'Europe - soulignent l'impact fort de la variabilité interannuelle du climat méditerranéen sur la dynamique du manteau neigeux. Le rayonnement solaire élevé est un facteur important du bilan énergétique du manteau neigeux, mais la contribution des flux de chaleur est plus forte à la fin de la saison nivale. La sublimation de la neige et la densification rapide sont des processus importants dans ce contexte. Les approches hybrides combinant des données de stations météorologiques et la télédétection optique de la surface enneigée à travers la modélisation sont recommandées pour compenser l'absence d'observations spatialisées du forçage météorologique.

2. Ensuite, nous présentons un ensemble original de données sur le manteau neigeux au Mont-Liban pour la période 2013-2016. Nous avons recueilli des observations sur le terrain de la hauteur de neige (HS), de l'équivalent en eau de neige (SWE) et de la densité de neige entre 1300 et 2900 m d'altitude sur le flanc occidental du Mont-Liban. De plus, des données météorologiques continues ont été acquises par trois stations météorologiques automatiques situées dans la partie enneigée du Mont-Liban. Le produit MODIS a été utilisé pour calculer la superficie couverte par la neige dans trois bassins hydrographiques couverts par les observations in situ. Nous remarquons la grande variabilité de HS et SWE et une densité élevée du manteau neigeux. Nous trouvons une corrélation significative entre HS et SWE qui peut être utile pour réduire la quantité de travail de terrain en vue d'un suivi opérationnel futur.

3. Grâce à ces données, nous avons mis en place un modèle distribué du manteau neigeux sur le Mont-Liban à une résolution de 100 m. Le modèle est validé à différentes échelles en utilisant les observations de SWE, densité, HS et SCA. Une simulation avec des modifications très limitées du paramétrage par défaut permet de capturer correctement la plupart des observations. Cette simulation permet donc d'estimer l'évolution du SWE et la fonte dans les trois bassins étudiés entre 2013 et 2016.

Cette recherche a mis en évidence l'importance de réaliser simultanément des mesures sur le terrain et des observations météorologiques continues pour mieux appréhender les processus physiques qui contrôlent l'évolution du manteau neigeux sur le Mont-Liban. Enfin, l'influence du transport de la neige par le vent et des dépôts de poussière sur la fonte des neiges reste à évaluer en perspective de ce travail.

Measuring snow height (HS) and snow density. Cedars (2870 m), 6 Mar 2016.
Photograph by C. Abou Chakra

In Loving Memory of the Late Samih Fayad (1946-2012)

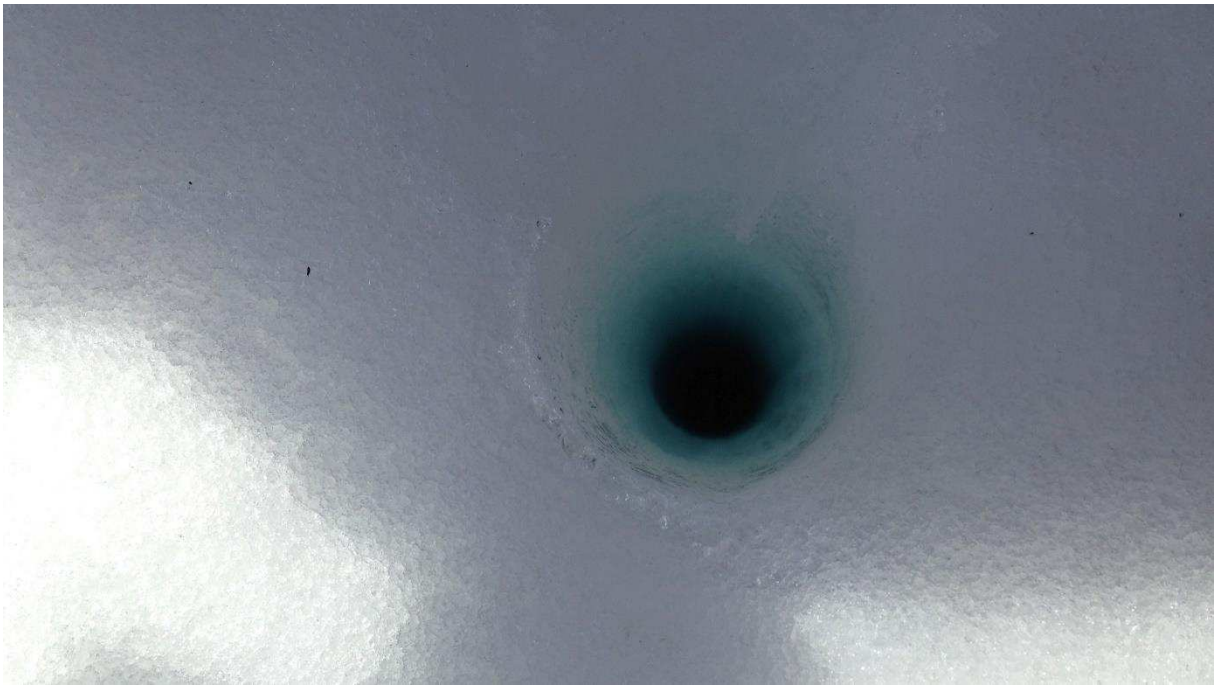

Snow course revisited: trace of the federal snow sampler in Mzar (2300 m), 10 Mar 2015. Photograph by A. Fayad

Déyé món, gen món

Beyond mountains there are mountains

Derriere les montages se cachent d’autres montagnes

خلف الجبل جبال

Moutain ponds are a major source of water for agriculture. Laqlouq (1800 m), 20 Mar 2016. Photograph by A. Fayad

TABLE OF CONTENTS

LIST OF FIGURES

LIST OF TABLES

Snowmelt starting in late March at the high elevation plateau. Cedars (2830 m), 23 Mar 2016. Photograph by A. Fayad

1 INTRODUCTION

1.1 Water scarcity in Lebanon

Mediterranean like mountain regions (e.g., López-Moreno et al., 2011) are among the most vulnerable to global warming (e.g., Nogués-Bravo et al., 2007; Giorgi and Lionello, 2008; Harpold and Molotch, 2015; Grouillet et al., 2016). In addition, temperature is expected to increase with elevation (Kotlarski et al., 2015; Pepin et al., 2015). As a result, the mid-elevation mountain regions, in many Mediterranean like climate, are expected to shift from snow dominated to rain dominated hydrologic regimes (e.g., Maurer et al., 2007; Berghuijs et al., 2014; Goulden and Bales, 2014). Furthermore, Mediterranean mountain regions are characterized with high seasonal snow depth variance and snow densification rates when compared to other mountain regions such as Prairies or Tundra's (e.g., Sturm et al., 2010). Understanding, different climate drivers and topographic influence on the snow variability is needed and provides the basis for investigating the link between snowmelt and hydrologic processes (e.g., Bales et al., 2006). Solving the snow mass balance is important to anticipate the effects of climate change (Molotch and Meromy, 2014; Lopez-Moreno et al., 2015).

The Mount- and Anti-Lebanon are major water tower in the Levant region. With average elevations above 2200 m a.s.l., these mountain ranges play an important role in enhancing orographic precipitation. Snowfall is more common at elevations above 1200 m a.s.l. and snow season usually extends over 6 months in the high elevation regions (above 2200 m a.s.l.). The hydrologic regime in these mountain catchments is snow dominated and influenced by (1) the Mediterranean climate which influences both the seasonal snowpack accumulation and melt processes and (2) the karst system characterized by a fast response between snowmelt and spring discharge (Margane et al. 2013; Königer et al. 2016). The meltwater released from the snowpack between March and May is a major source of fresh water for lowland coastal regions and inland plains, where most of the population and the economic activities are concentrated (mostly are irrigated agriculture). More specifically, the snowmelt from the Mount- and Anti-Lebanon plays a major role in the sustainability of spring water supply during the dry season (May-August) because it contributes to the replenishment of groundwater resources (e.g., Königer and Margane, 2014; UNDP, 2014; Königer et al. 2016). This groundwater resource is essential to the water supply of the major urban agglomerations in coastal Lebanon. For instance Beirut receive 75% of its potable water supply from the Jeita karstic spring (Margane et al.,

2013). In addition, snowmelt contributes to the storage of surface water (e.g. mountainous hill lakes, reservoirs, and dams), and the sustainability of agricultural and ecological systems.

Despite the amount of the water captured by the Lebanese mountains, there is growing concerns in Lebanon regarding its sustainability. The current situation is characterized by the overexploitation of surface water resources and the increased over-abstraction from groundwater resources (MOEW, 2010; UNDP, 2014). The problem has been attributed to the lack in the quantification of surface and groundwater resources, the unsustainable water resource management, access to improved drinking water sources, increased water demand by all sectors, and the increased water pollution and seawater intrusion (MOEW, 2010; UNDP, 2014).

The focus of this research is to quantify the snowmelt contribution in the major snow-dominate basins located in the windward side (west slope) of Mount-Lebanon. Due to the lack of an established snow monitoring program in Lebanon we started by an extensive review of the key concepts and methods to quantify snowmelt in Mediterranean mountain regions. Then, we present the new snow observations that were collected in the frame of this thesis and the snow observatory that was established in Lebanon to address this issue. Finally, we apply a distributed snowpack model to compute the spatio-temporal distribution of SWE and snowmelt during three snow seasons in three basins of Mount-Lebanon (Fig 1.1.)

Next section (Section 1.2) describes the study area. Section 1.3) focuses on the existing knowledge regarding the snow hydrology in Lebanon. Section 1.4) presents the rationale of the thesis and the main objectives. Section 1.5) outlines the organization of the dissertation.

1.2 Study area

The study region is part of the Mount- and Anti Lebanon mountain regions. We focus on three snow dominated basins located on the windward side on Mount-Lebanon (Fig. 1.1). The climate is Mediterranean, i.e. most precipitation falls mainly between December and March, over a period of 90 days (MOEW, 2010). The Mount- and Anti-Lebanon play a critical role in enhancing orographic precipitation. The average annual precipitation volume is estimated at 830 mm (equivalent to 8.6 billion cubic meters (MOEW, 2010). Due to the influence of the Mediterranean climate, the precipitation varies between years. For example, the total precipitation ranged between 577 and 899 mm for the water years between 2008 and 2012 (UNDP, 2014). Mean annual observed precipitation at the Beirut international airport is 744.5 mm (1932-2010) and the normal over the time period between 1981 and 2010 is equal to

711.9 mm (Fig 1.2). It is estimated that between 30 to 40% of the annual precipitation over Lebanon falls as snow (Shaban et al., 2004; UNDP, 2014). On an average water year (September - August), the mountain regions receive between 50 to 67% of the total annual precipitation as snow (UNDP, 2014).

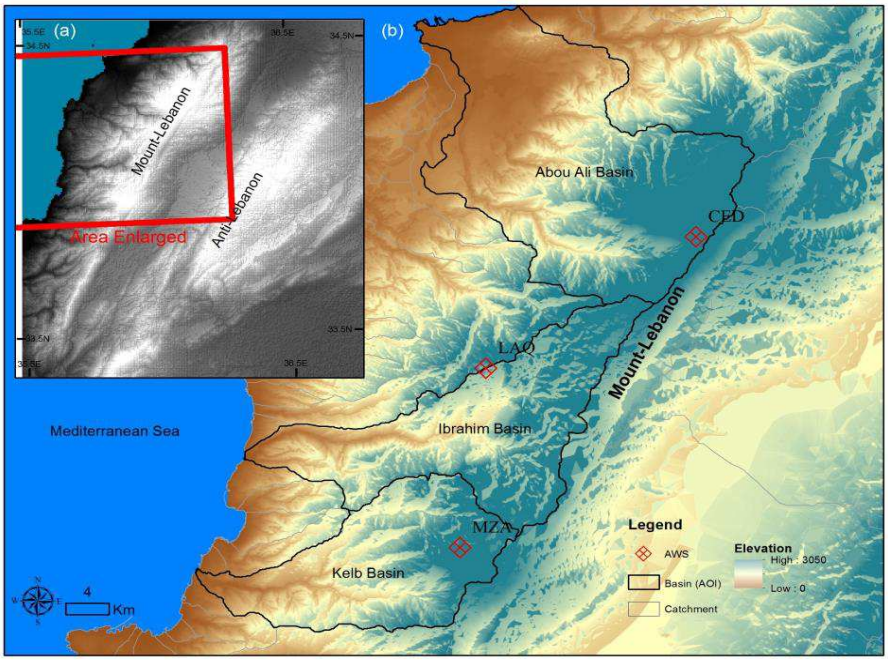

Fig. 1.1. Study Area showing (a) the Mount- and Anti-Mount Lebanon and (b) the location of the three major snow dominated basins of Abou ALi, Ibrahim and Kelb.

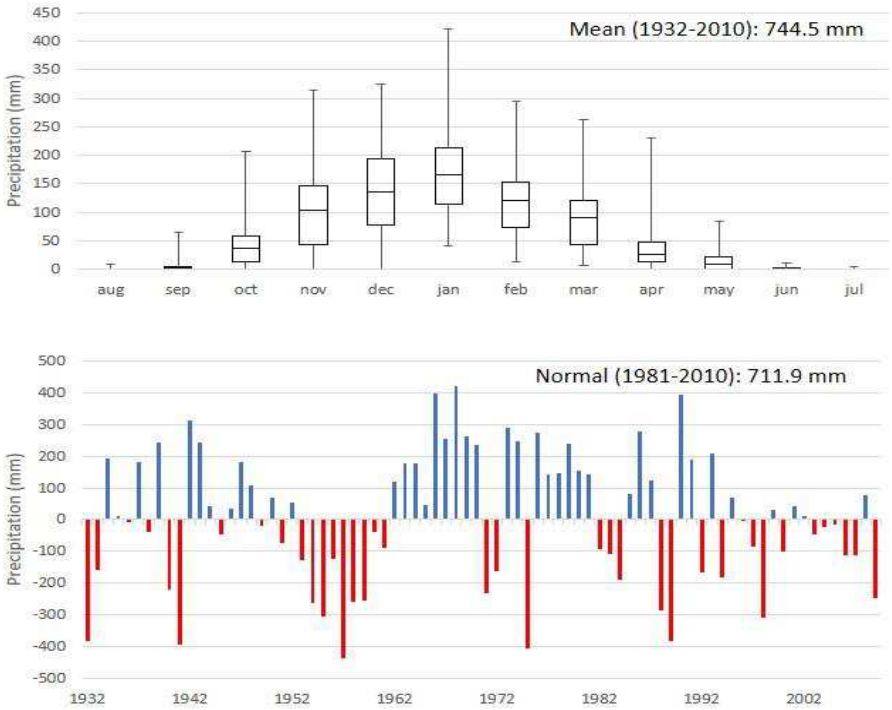

Fig. 1.2. (a) Mean monthly precipitation at the Beirut international Airport (1932-2010) and (b) annual precipitation over the same time period.

Renewable water resources for the entire Lebanon are estimated at 2.7 billion cubic meters (258 mm) for the average water year (i.e., 2.2 billion cubic meters as surface water and 0.5 billion cubic meter for groundwater storage) (MOEW, 2010). The SWE contributes to 26% of the national hydrologic budget (Mhawej et al., 2014). In Mount-Lebanon, the SWE contributes to 31% of the rivers and springs discharges (Telesca et al., 2014). Basin scale studies (e.g., Margane et al., 2013), on the other hand, estimates that snowmelt contribution to 75% of the groundwater recharge in the El Kelb Basin.

Surface water is available via more than 2000 major springs (with discharge above 30 l/s) originating mostly from the karst mountainous regions. Most of the fresh-water in the coastal basins is used to meet urban demands. The flows of these springs is usually characterized by a high seasonal variability (i.e., during a single water year (September-August) and inter-annual variability (i.e., between dry and wet years). The total surface yield from springs is estimated to 1.2 billion cubic meters on an average year, with around 0.2 billion cubic meter being available during the dry summer period. Surface water yield from springs decreases to 0.85 billion cubic meter in dry years. These springs, however, are currently intensively exploited (MOEW, 2010).

Surface water resources use in Lebanon was estimated to 0.63 billion cubic meter in 2010 – preliminarily supplied from springs. Withdrawal from groundwater was estimated to 0.71 billion cubic meter exceeding the natural recharge rate of 0.50 billion cubic meter per average year. The current available annual water per capita is estimated to 830 m^3 which is less that than the water stress threshold (i.e. 1000 m^3 cap^{-1} yr^{-1}) (MOEW, 2010). In contrast, the country current water deficit is estimated at 0.28 billion cubic meter per average water year (MOEW, 2010).

Lebanon, as part of the Mediterranean basin is particularly exposed to climate change (Nohara et al., 2006; Giorgi and Lionello, 2008; Morán-Tejeda et al., 2014). More particularly, the Levant region has witnessed consecutive dry periods over the past two decades (1998-2012) (Cook et al., 2016) characterized by above-normal temperature and below-normal winter (November - April) precipitation (1931-2008) (Kelley et al., 2015).

Future climate projections indicate that many Mediterranean mountain catchments would shift from the snow dominated to the rain dominated hydrologic regime (e.g., Maurer et al., 2007; Goulden and Bales, 2014). Furthermore, mid-altitude regions (elevation ~2000 m a.s.l.) are most sensitive to global warming (Pepin et al., 2015). These expected climatic changes will have a direct impact on the different hydrological processes of snowmelt, runoff,

and evapotranspiration (e.g., Knowles and Cayan, 2004; Lundquist and Loheide, 2011; Milano et al., 2013; Godsey et al., 2014). The Lebanese mountains are among this category of mountain vulnerable to global warming. As a result, there are reasonable grounds for strong concern as to the sustainability of the water resources from Mount-Lebanon and Anti-Lebanon under projected warming scenarios. Under a 2 °C warming by 2040, snow depth is projected to reduce by 50% at 2000 m a.s.l. resulting in the retreat of winter snowline from 1500 to 1700 m a.s.l. (MOEW, 2010). Under the same scenario the snow season is projected to be 2 to 6 weeks shorter and the annual SWE volume would decrease by 40% (MOEW, 2010).

1.3 The delineation of the Mont- and Anti-Lebanon mountainous regions

A better representation of the mountain regions is needed for the separation between lowland and mountain areas. We used a modified Viviroli et al. (2007) scheme in order to better identify the mid-elevation climate-vulnerable zones in the Mount- and Anti-Lebanon mountains. The Viviroli et al. (2007) scheme is based on Meybeck et al., (2001) land form classes with a modified mountain clustering. The Meybeck et al., (2001) scheme clusters mountains into four different classes (low, middle, high and very high altitude mountains) based on a set of 15 different land form classes (see Fig. 1.3). The landform classes are derived from digital elevation model using a combination of relief roughness (RR in ‰) and mean elevation range (in meters) (Meybeck et al., 2001). The modified Viviroli et al. (2007) scheme, on the other hand, recommends to add the landform classes of hills, mid-altitude plains above 1000 m a.s.l. and plateaus of medium, high and very high altitude to the four mountain classes defined by Meybeck et al., (2001). In this study, we further expanded the Viviroli et al. (2007) scheme by including regions with snow cover (Table 1.1). We found that when using the Meybeck (2001) scheme only 25.8% of Lebanon's area was classified as mountain regions. This classification, in fact, excluded most of the high plateaus, especially those above 2200 m a.s.l. where most snow falls. This classification also excluded mid-altitude areas with relatively high roughness (e.g. the steep coastal rugged terrains at the base of Mount-Lebanon) (Fig. 1.3). The estimated mountain region under the Viviroli (2007) scheme increased to 59.9% of Lebanon's area. The areal difference between the two schemes is due to the previously excluded (1) mid-altitude areas, which are considered as potential sources of runoff production and groundwater recharge, and (2) mid- and high altitude and high plateaus, which are the major regions for snow accumulation and groundwater recharge (Fig. 1.3). We also found that 14.9% of Lebanon's area

is classified as mid-altitude plateaus between 1000 and 2000 m a.s.l. and 6.6% as high altitude plateaus with elevations above 2000 m a.s.l. (Table 1.1 and Fig. 1.3).

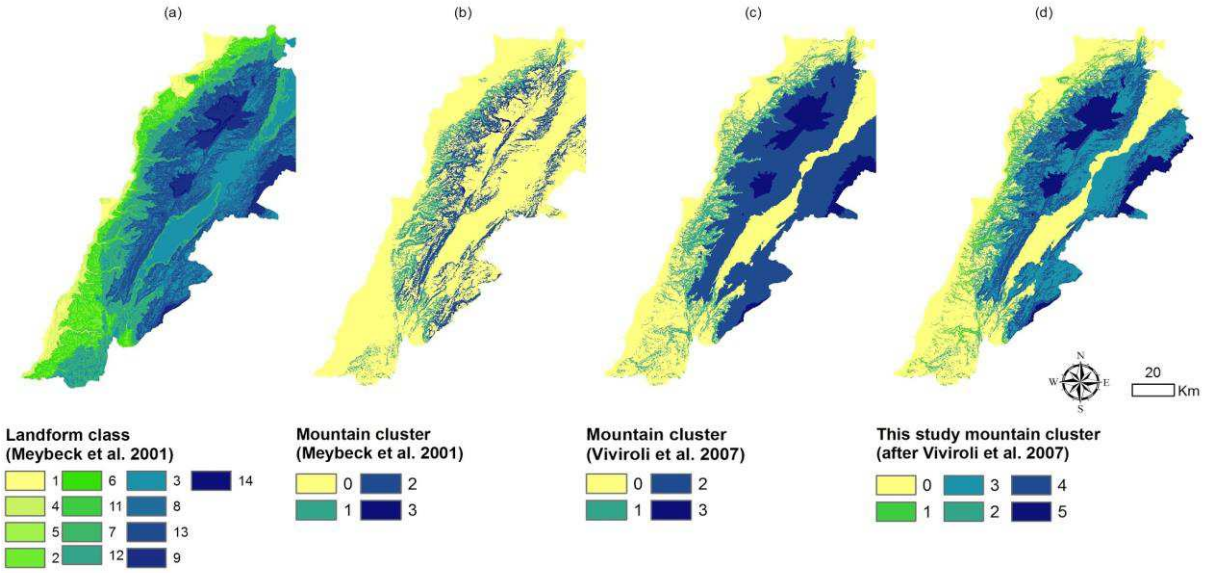

Fig. 1.3. (a) Landforms for Lebanon after Meybeck et al. (2001) where: (1) plains, (2) mid-altitude plains, (3) high-altitude plains, (4) lowlands, (5) rugged lowlands, (6) platforms, (7) low plateaus, (8) mid-altitude plateaus, (9) high plateaus, (10) very high plateaus, (11) hills, (12) low mountains, (13) mid-altitude mountains, (14) high mountains, (15) very high mountain; (b) and (c) are mountain clustering according to Meybeck et al. (2001) and Viviroli et al. (2007) respectively where: (0) lowland, (1) low mountains, (2) mid-altitude mountains, and (3) high mountains; and (d) current study mountain clustering where: (0) lowland, (1) low areas with no snow contribution, (2) low with coarse to no snow contribution, (3) mid-altitude areas with coarse snow contribution, (4) mid-altitude with partial snow contribution, and (5) high mountains with snow contribution (see Table 1.1).

The snow cover of the different topographies in the study area are presented in Fig. 1.4. All photos were taken, in the three major basins of Mount-Lebanon, during field work conducted during winter seasons 2015 and 2016 (courtesy of the author). The snow dominated region, in general presents little to no vegetated surfaces. Sparse scrublands are located below the treeline (~1550 m a.s.l.) (Fig. 1.4a). Home settlements are below 1800 m and gricultural crops are found in terraces and in the low elevation plateau regions (elevation below 1800 m) (e.g., Fig. 1.4b). The low elevation plateau region between Laqlouq and Aaqoura is rich in mountain pounds (elevation range 1600 and 1900 m) (e.g., Fig. 1.4b). The mid-elevation mountain regions at elevations between 1800 and 2300 m are characterized with rugged topography (e.g. Fig 1.4c). Mid-elevation region between 2100 and 2400 m a.s.l in Mzar and Ouyoun Al Siman are rich in Dolines and sinkholes (e.g. Fig 1.4d). The mid-elevation plateau is located at the elevation between 2300 m and 2500 m between Ouyoun Al Siman and Mount Sannine (Fig. 1.4e). The mountainous regions in the three basins is characterized with steep slopes and valleys and the winter snowline is usually above 1500 m (Fig. 1.4f). Medium and high elevation mountain regions are in the Cedars region (elevation range 1860 and 2750 m)

(Fig. 1.4g). The high-elevation plateau has an elevation range between 2750 and 3000 m (Fig. 1.4h).

Table 1.1. Classification of the Lebanese mountains and lowland areas.

Mountain Class: Meybeck et al. (2001) and Viviroli et al. (2007)	Mountain Class: This Study	Area in % (by Landform class)		
		Meybeck et al. (2001)	Viviroli et al. (2007)	This Study
Lowland	Lowland	74.2 (1-11)	40.1 (1-2; 3*-7)	40.1 (1-2; 3*-7)
Low mountains	Low areas with no snow contribution	8.5 (12)	12.5 (11, 12)	4 (11, 12†)
	Low areas with coarse snow contribution			8.5 (12†)
Mid-altitude mountains	Mid-altitude areas with temporal snow cover	16.4 (13)	39.9 (3*, 8, 13)	23.5 (3*, 8‡, 13‡)
	Mid-altitude with persistent snow cover			16.4 (8‡, 13‡)
High mountains	High mountains with persistent snow cover	0.9 (14)	7.5 (9, 14)	7.5 (9,14)
	Total lowland (%)	74.2	40.1	40.1
	Total mountains (%)	**25.8**	**59.9**	**59.9**

* high-altitude plains range in elevation between 500 and 2000 m a.s.l. in the modified Vivorili et al. (2007) cluster suggested the need to include all regions above 1000 m a.s.l. as part of the mid altitude mountains.
† Snowfall in not uncommon in the elevation regions between 800 and 1000 m a.s.l., but usually remains for around a week following major storm events.
‡ Snow persist above 1400 m a.s.l. (personal note)

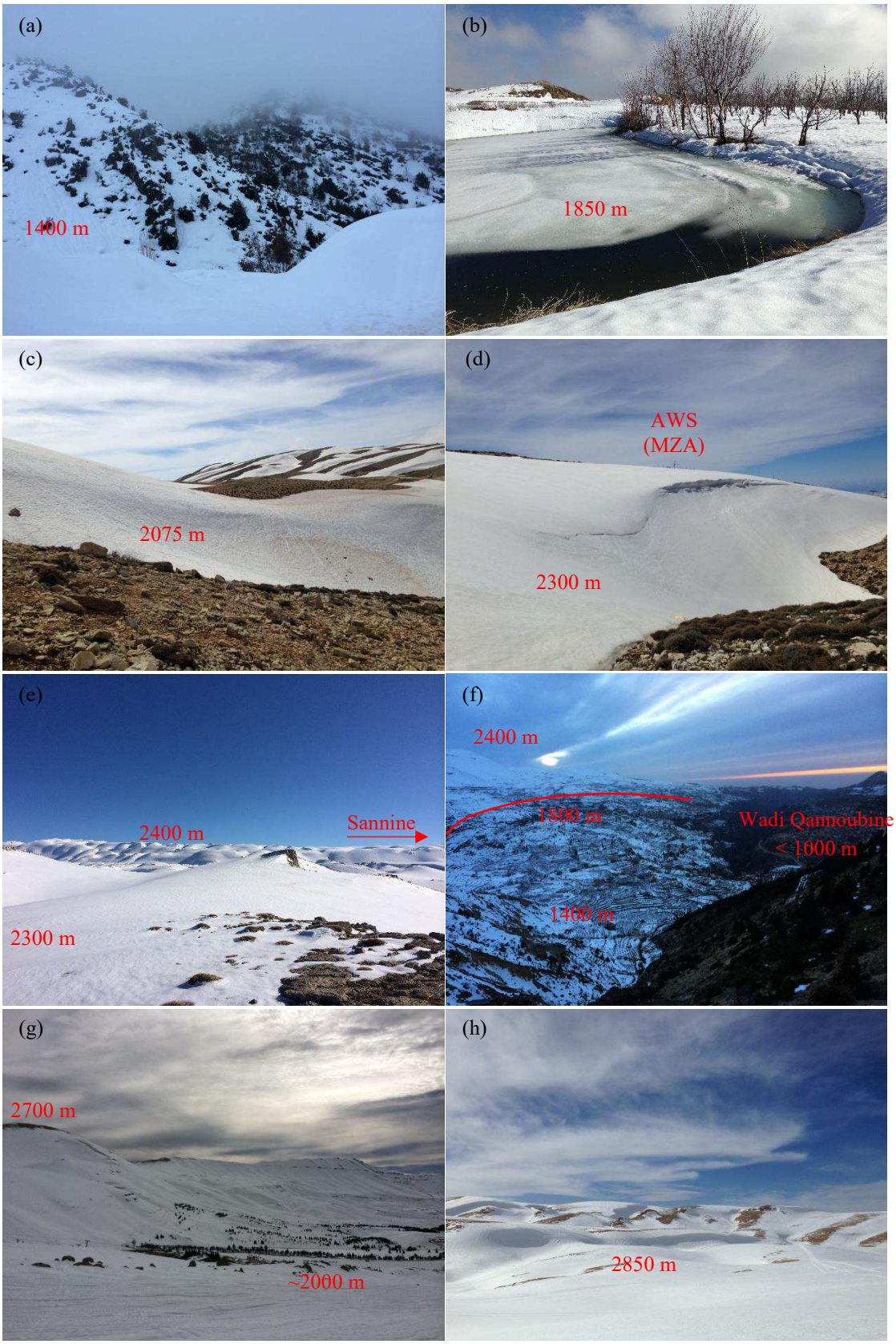

Fig. 1.4. Example of the different snow cover in Mount-Lebanon: (a) sparse scrublands in Ehmej (16 Feb, 2015); (b) mountain ponds and tree crops in Laqlouq (20 Feb, 2016); (c) rugged topography in Mzaar (1800- 2300 m a.s.l.) (2 Apr, 2015); (d) Dolines at 2300 m a.s.l (2 Apr, 2015); (e) mid-elevation plateau (shown here for elevations 2200–2400 m) (5Mar, 2015); (f) low-land and mountainous region between Wadi Qannoubine and Bcharre (27 Jan, 2015); (g) high elevation mountain regions at Cedars (27 Jan, 2015); (h) high elevation plateau at Cedars, shown here for the elevations between 2820–2900 m (23 Mar, 2016). All images are courtesy of the author.

1.4 Existing snow hydrological studies

Despite the importance of snow in Lebanon, the knowledge on the seasonal snowmelt contribution to the hydrologic budget, especially during dry season, remains limited. This can be attributed to: (1) the limited number of meteorological and snow observations in the high-elevation regions; (2) the fact that most existing knowledge is usually limited either to national scales studies with monthly or yearly means or to point scale studies with observations over short time periods; and (3) the fact that groundwater is dominated by a wide karstic system (around 65 % of the country's total area), which hinders the evaluation of snowmelt contribution to surface runoff, spring discharge, and groundwater recharge.

1.4.1 Point scale snow observations

Observation networks in mountainous regions and complex terrain are usually sparse (e.g., Raleigh et al., 2016). In Lebanon, the meteorological network operated by the Lebanese meteorological department (Part of the directorate general of civil aviation), is below the snowline (highest operational weather station is located at 1220 m a.s.l). Snow and meteorological observations in snow dominated regions are usually carried via (1) cooperation projects (e.g., Margane et al., 2013) or through research programs with observations of 1 to 3 years on average (e.g., Shaban et al., 2004; Aouad-Rizk et al., 2005; Hreiche et al., 2007). The newly established network for snow observations (NSO) is the first attempt to measure snowfall, snow depth, and SWE, and standard meteorological variables on a regular basis in the windward snow dominated regions of Mount-Lebanon (elevation range between 1830 and 2830 m a.s.l.). The NSO is a joint collaboration between the 'Institut de Recherche pour le Développement' IRD (France), the 'Centre d'Etudes Spatiales de la Biosphere' CESBIO (France), the National Council for Scientific Research – Remote Sensing Center (CNRS\NCRS) (Lebanon), and the University of Saint Joseph USJ (Lebanon). The network includes three automatic weather stations (AWS) and became fully operational in 2014 via the installation of the third AWS at Laqlouq (Fig. 1.1).

1.4.2 Monitoring snow cover extent using satellite imagery

At present, the technique for mapping the Snow Cover Area (SCA) using satellite remote sensing is well established; such technique relies on the high reflectance of snow surface in the visible wavelengths and low reflectance in the near-infrared (e.g., Dozier et al., 1989;

Seidel and Martinec, 2004; Tedesco (ed.), 2015). Various studies assessed the accuracy of snow maps derived from optical sensors (e.g., Painter et al., 2003; Frei et al., 2012). The MODIS data have been used to generate a global, daily, snow cover extent product at 500 m resolution (Hall and Riggs, 2007; Painter et al., 2009). Despite their advantage to detect snow, optical satellite images are subject to cloud obstruction (Parajka and Blöschl, 2008). In this context, different methodologies were used to interpolate the missing data (e.g., Andreadis, 2006; Boudhar, et al., 2009; Gascoin et al., 2015). Another limitation of remote sensing is that space-borne sensors do not allow an accurate estimation of the SWE in mountain regions due to the facts that: (1) in case of orbiting spaceborne Radar measurements, the complex topography causes multiple reflections of the emitted microwave signal, which limits the interpretation of the data, and (2) in case of passive microwave, the ground spatial resolution of current spaceborne radiometer is too coarse to be useful over mountainous regions.

Deriving the snow cover extent is useful to the quantification of the spatial and temporal distribution of the snowpack properties and melt through the implementation of snow hydrologic model (De Jong et al., 2005). In fact, while the snow coverage is best observed using remote sensing, the assessment of hydrologic processes requires field observations which are most of the time difficult to obtain in mountainous environments. The proper understanding of the spatio-temporal dynamics of a snowpack is fundamental for the hydrologic modeling of mountain basins (e.g., Liston, 1995; De Jong, et al., 2005). Therefore, many studies pointed out that, in order to extend the usefulness of remote sensing data for mountain hydrology, there is a need to combine remote sensing observations (i.e., SCA) with a snow model that takes into consideration the surface meteorological variables (e.g., precipitation, air temperature, humidity, wind, etc) and radiative variables (e.g., longwave and shortwave radiation) (Sun et al., 2004; De Jong, et al., 2005; Clark et al., 2006; Andreadis, 2006; Tedesco (ed.) 2015; Dozier et al., 2016).

In Lebanon, the MODIS snow product (MOD10) was used to compute the SCA evolution with time and map the snow cover duration (SCD). These data served to estimate the SWE using index based approaches (Mhawej et al. 2014; Telesca et al. 2014). It is worth noting, that Mhawej et al. (2014) data set did not account for cloud gap filling which may be one of the gaps that still requires attention. Telesca et al. (2014), on the other hand, used a gap-filling algorithm that is described by Gascoin et al. (2015) in the case of the Pyrenees to interpolate the missing data due to clouds. The gap-filling step is necessary to draw meaningful climatological variables from the MODIS products.

1.4.3 Snow water equivalent (SWE)

The proper quantification of the SWE is crucial for basin scale hydrology (DeWalle and Rango, 2008). SWE which is the depth of water that is contained in the snowpack and is expressed as the product of the snowpack height (HS) and the bulk snowpack density. In Lebanon, the average annual SWE is estimated to range between 1.82 and 2.57 billion cubic meter (174-246 mm equivalent) for the water years between 2008 and 2012 (UNDP, 2014). The average annual SWE is estimated at 2.42 billion cubic meter for Mount-Lebanon and Anti-Lebanon combined (2002-2011) (Mhawej et al., 2014) (Appendix A1). The average annual SWE for Mount-Lebanon is estimated to range between 0.77 billion cubic meter (average over the time priod 2000-2012) (Telesca et al., 2014) and 1.1 billion cubic meter (2001-2002) (Shaban et al., 2004). Such differences in the estimation of SWE can be attributed to (1) the different methods used for the estimation, and (2) the limited number of ground observations used to validate model estimates. Hence, the proper quantification of SWE remains incomplete.

1.4.4 Snowpack dynamics

Snowmelt dynamics are thermodynamic in nature and thus are best evaluated in function of an energy balance model (Corripio, et al., 2005). Different methods have been proposed and used for the estimation of SWE in mountain regions (Dozier et al., 2016). These methods rely on the use of ground observations (e.g. meteorological stations) and in situ measurements (e.g., snow depth snow density measurements). However, in many cases, methods based on snow observations usually lack the spatial coverage of snow cover (Takala et al., 2011). Spatial interpolation (e.g., Girotto et al., 2014) and the integrated approach between remote sensing derived SCA and ground measurements are among the most used to derive spatial SWE (Molotch et al., 2005; Jonas et al., 2009; Brown et al., 2010; Skaugen et al., 2011).

Solving for the snow energy balance requires good knowledge of meteorological variables (e.g. precipitation, temperature, wind speed, and solar radiation) and snow data (e.g., snow depth, SWE) for model forcing and model validation (e.g., Liston et al., 1999). To simplify, two main approaches are used for the evaluation of snowmelt from snowpack: (1) the Degree-Day or Temperature Index Method (DDM) (e.g., Hock, 2003) and (2) Snowpack Energy Balance (SEB) (e.g., Liston et al., 1999; Corripio, et al., 2005). The application of DDM is practical, due to its simplicity and minimal data requirement (i.e., can be derived based on temperature data only), but it requires snowmelt observations to calibrate the degree-day factor. The SEB, on the other hand, enables the computation of the snowmelt based on physically-based equations provided that meteorological forcing of precipitation, wind speed, air humidity,

air temperature, and of the incoming radiation (i.e., longwave and shortwave radiation) are available (e.g., Liston and Elder, 2006).

Modeling attempts in Mount-Lebanon are so far limited to the experimental watershed scale using point scale models. For example, Aouad-Rizk et al., (2005) investigated snowmelt in the El Kelb River Basin using both an energy balance and a degree day method. This study highlights the importance to account for the snow density and the SWE variation with altitude when assessing snowmelt contribution. Hreiche et al., (2007), on the other hand, used a coupled rainfall–runoff with a DDM module to investigate changes in runoff under projected climate change scenarios in the Ibrahim river basin. A 2 ℃ increase in temperature would result in 2 months shift towards earlier peak flow in the snow-dominated catchment of the Ibrahim Basin (Hreiche et al., 2007). These research efforts give a global picture on the temporal variability of snow in Lebanon and its melting behavior. However, the spatial-temporal distribution of SWE and the link between snowmelt and surface runoff and groundwater recharge remains largely unidentified.

1.4.5 Snow hydrology and the Importance of Karst system

In Lebanon, most snow falls over the cretaceous plateau (the "roof" of the karstic rock formation, ~ 40% of the country) (Fig 1.5). The karst system constitutes between 62 to 79% of the three basins areas (Table 1.2).Snow melt (between November and May) recharges the groundwater karst system (e.g., Margane et al., 2013). Example from the El Kelb Basin (e.g., Margane et al., 2013) revealed that the high mountain regions, with elevation between 1000 and 2600 m a.s.l., contributes to around 75% of the karst groundwater recharge (e.g., Margane et al., 2013). The snowmelt was estimated to contribute to 56% of the spring discharge located in the lowland area of Mount-Lebanon at the Jeita spring (outlet at 60 m a.s.l.) (Margane et al., 2013). The spring discharge response to precipitation in the El Kelb Basin is fast (can be seen within 24-48h after precipitation events) and usually depends on the distribution and type of precipitation (rainfall or snowfall) (Margane et al., 2013; Koeniger and Margane, 2014). The spring response to snow is common to most coastal basins, for instance we show below the map of the snow detection probability from the daily "binary" (snow/no snow) MODIS snow product (MOD10A1) (Hall et al., 2006) in Mount-Lebanon and Anti-Lebanon mountain ranges over the period 2000-2011 after the application of the gap-filling method of Gascoin et al. (2015) (Fig. 1.6a). The mean monthly snow cover area evolution from the same product is compared to the spring discharge at Afaq, a major spring and the source of the Ibrahim river,

for the time period between 2000 and 2011 (Fig. 1.6b). Fig. 1.7 illustrates the correlation between the observed spring discharge at the Afqa Spring and the SCA in the Afqa spring topographic catchment over 2000-2011, a period which includes dry, average and wet years. Here, as a first introductory example, we used the SCA as a proxy of the SWE. We found 86% correlation with a 2-month time lag between SCA and the Afqa Spring (1113 m a.s.l.) discharge. Such correlation highlights the importance of snowmelt in the hydrologic responses of the karst system in Mount-Lebanon. These findings go along with Margane et al. (2013) investigations on the fast response of the karst system in the El Kelb River Basin.

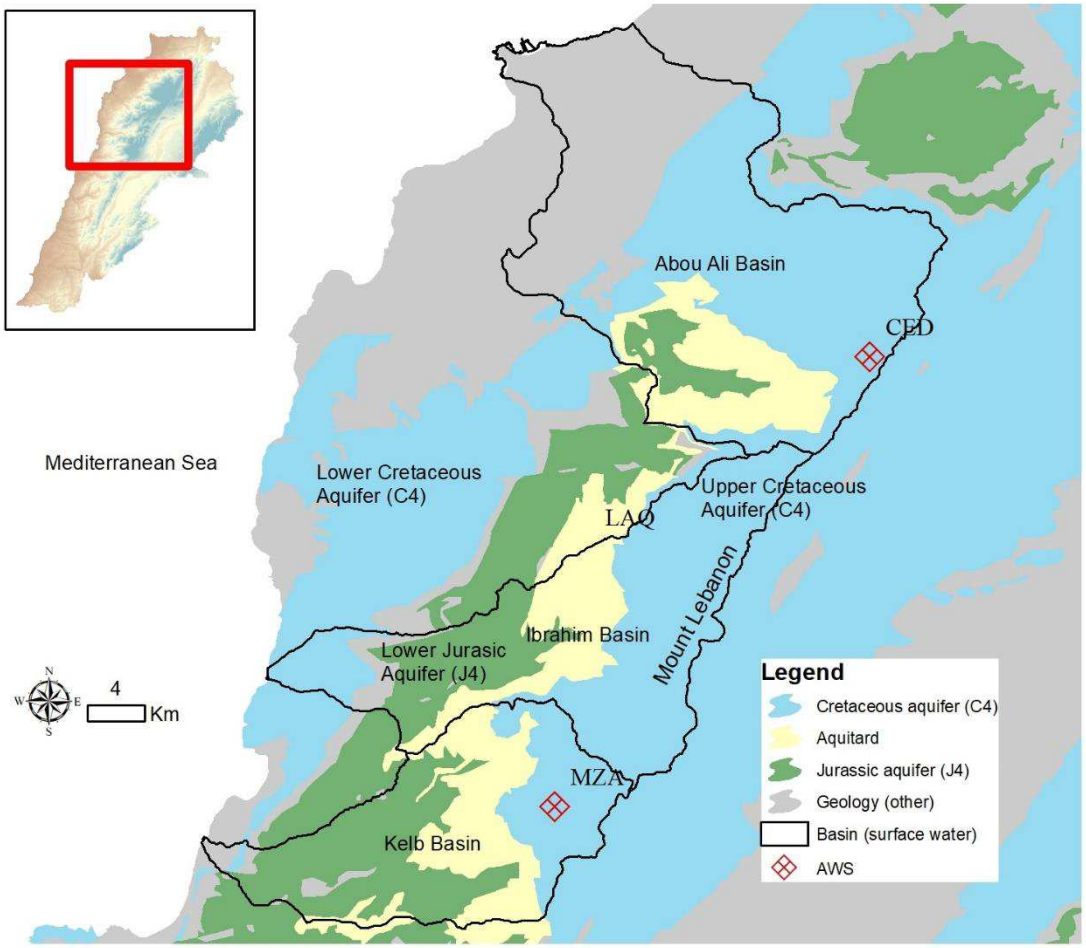

Fig. 1.5. Major groundwater system showing the major upper Cretaceous aquifer (C4) where most the snow falls in the Mount Lebanon. Both the Cretaceous (C4) and Jurasic (J4) aquifer systems are chareteized by their high Karstification.

Table 1.2. Major geologic formations in the three snow dominated basins.

Basin[a]	Area (km^2)	Elevation range (average)[b], m a.s.l.	Karst exposure (% total area)	Cretaceous aquifer (C4) (% total area)	Jurassic aquifer (J4) (% total area)	Aquitard[c] (% total area)
1	513	0–3088 (1202)	62%	49%	5%	14%
2	323	0–2681 (1547)	79%	60%	19%	17%
3	256	0–2619 (1381)	65%	26%	39%	31%

[a]Basins are Abou Ali (1), Ibrahim (2), and El Kelb (3) (Fig. 3.1). [b]Values are derived for the national 10 meter DEM (NCRS). [c] Namely the lower Creataceous and upper Jurasic (C3-J5).

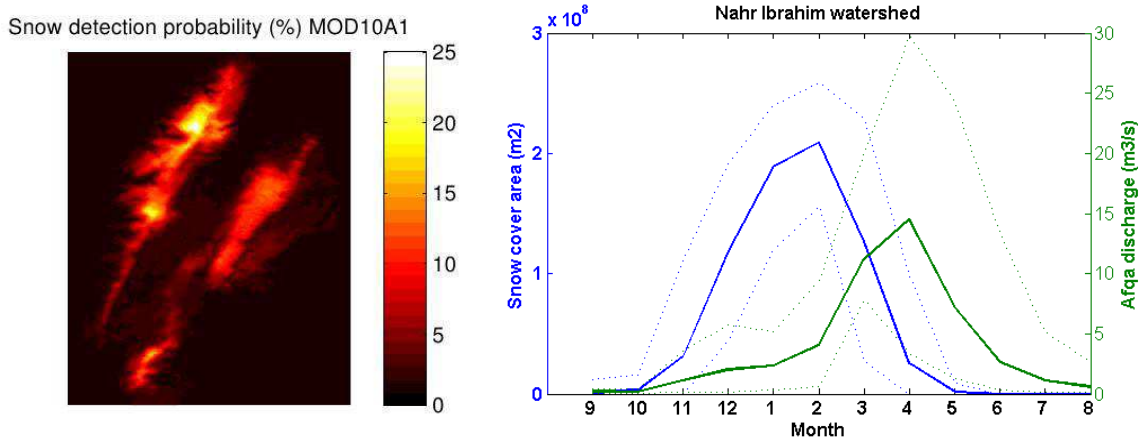

Fig. 1.6. (a) Snow detection probability (% of 1 year) computed from MOD10A1 product over Mount Lebanon and Anti Lebanon mountain ranges, and (b) Mean monthly discharges of Afqa spring and snow cover area derived from the same MOD product (2000-2011). The dotted lines indicate the minimum and maximum observed over the period between 2000 and 2011.

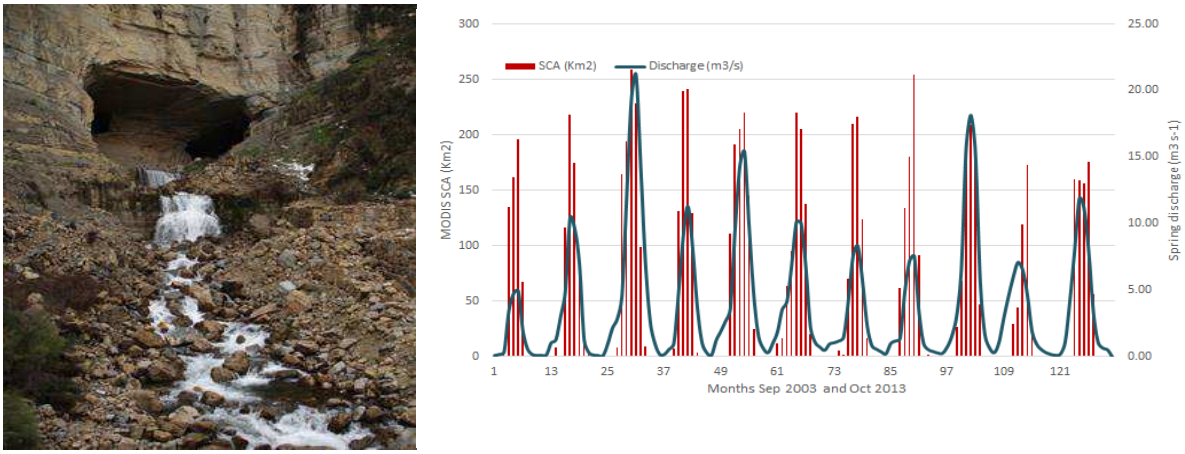

Fig. 1.7. (a) The Afqa spring (1113 m a.s.l) in the Ibrahim River Basin captured in the mid-snow season where flow is still minimal. The image was taken on February 24th, 2015 (courtesy of the author); and (b) the correlation between MODIS SCA and Afqa spring discharge for the water years (September-October) between 2003 and 2013.

Hence, snowmelt, which usually occurs during spring, at the time where there is little contribution from rainfall, has great influence on the observed discharges of most springs and rivers. Fig. 1.8 illustrates the different discharges of the at the Afqa spring (Ibrahim River Basin in Mount Lebanon), a typical snow fed spring, over the last decade (2000-2011). Discharge remains minimal during winter season (December to March) and peaks between end of March and May depending on the snow amount and the onset of snowmelt.

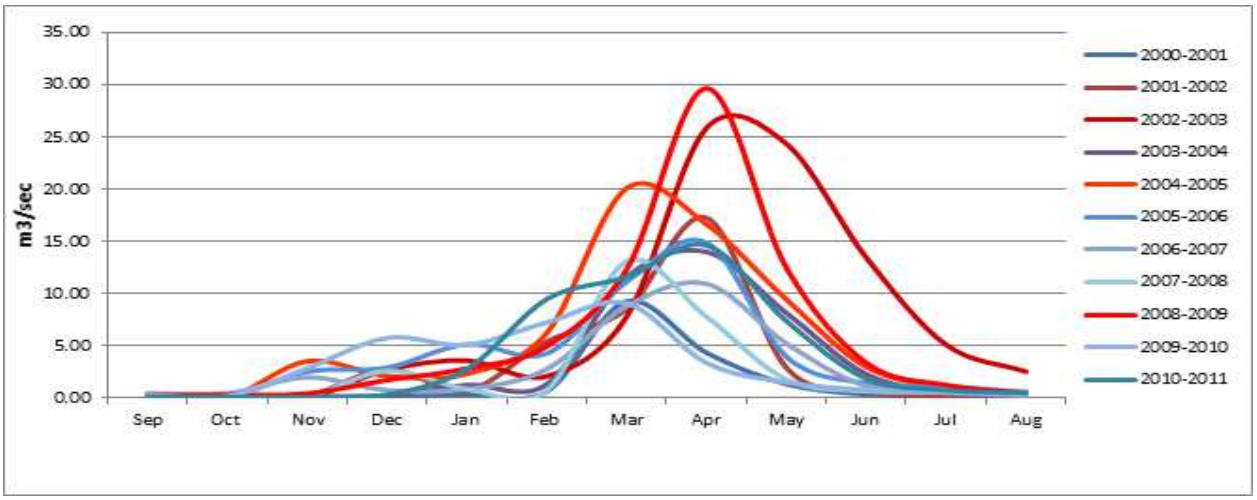

Fig. 1.8. Mean monthly spring discharge at the Afqa spring (1113 m a.s.l.), Ibhrahim Basin, between 2000 and 2011.

1.5 Rationale

The rationale behind this study is that groundwater recharge and spring discharge from the karst system are strongly linked to snowmelt in Mount and Anti-Lebanon (Koeniger and Margane, 2014; Doummar et al., 2014; UNDP, 2014). The proper understanding of these processes is only achievable with the proper quantification of SWE and snowmelt. So far, this problem had been approached using (1) point scale DDM or EB models to estimate SWE at the point or small pilot catchment scales (e.g., Aouad-Rizk et al., 2005; Hreiche et al., 2007) or (2) using a combined spatially distributed MODIS SCA data with average snow density (Telesca et al., 2014) or bulk AMSR-E SWE averages (Mhawej et al. 2014) to estimate average annual SWE at a relatively medium spatial resolution (i.e. 500 m). However, there remain large uncertainties in the quantification of the snowmelt due to a lack of continuous meteorological data in the Mount- and Anti-Lebanon Mountain Chains.

One of the most persistent questions in Lebanon are (1) how much water is stored as snow, in the Mount- and Anti-Lebanon during the winter season? and (2) what is the contribution of snowmelt to springs and groundwater resources?

To answer these two questions, we conducted field measurements over two snow seasons 2014-2016, and used new automatic weather station observations and remote sensing snow cover data, to set up and evaluate a spatially- distributed snowpack model for the first time in the snow dominated regions of Mount-Lebanon between (elevation range between 1300 and 2900 m a.s.l.). The specific objectives of this thesis are to answer the following questions:

1- What are the major meteorological and physiographic factors controlling the snow processes in Mediterranean like regions and what is the fate of snowmelt in the hydrologic system of these regions?

2- What is the spatio-temporal variability of the SWE at different elevation range (1300-2900 m a.s.l.), in the snow dominated regions of Mount-Lebanon?

3- To which extent can we accurately estimate the spatial distribution of daily SWE at a fine spatial scale (100 grid)?

4- Given the difficulty and relatively high cost needed for conducting intensive field measurements and maintaining meteorological stations in mountainous areas, which temporal scale is most suitable for conducting field measurements? And which meteorological forcing are considered a priority for running energy balance snow models?

1.6 Content of the report

In addition to this introductory chapter this dissertation contains four chapters. In Chapter 2 we try to answer question 1 by presenting a synthesis of the snow studies in Mediterranean like mountain regions. This work is based on a review of more than 650 papers published in peer review journals.

Chapter 3 addresses question 2 and introduces the snow observatory in Lebanon which cover the upper area of three snow dominated basins located in the windward side of Mount-Lebanon. This chapter presents the three AWS collecting continuous meteorological and snow observations in the snow dominated regions of Mount-Lebanon. In addition, this chapter shows the results of field surveys of snow depth, SWE, and snow density that were conducted by the author of this dissertation across different elevation regions (1300-2900 m a.s.l.). Eventually, SCA data from MODIS are presented to define the snow cover area and snow cover duration in these basins.

Chapter 4 tackles question 3 using a distributed energy balance model (Liston et al. 1999; 2006). The model is ran at a 100 m resolution grid across the Mount- and Anti-Lebanon but we focused on the three study basins introduced in Chapter 3. The model is forced and validated using the novel dataset presented in Chapter 3.

Chapter 5 addresses question 4, presents the main conclusions of this research work, highlights the major limitations and proposes potential ideas for future research.

1.7 References

Andreadis, K. M. and Lettenmaier, D. P., 2006. Assimilating remotely sensed snow observations into a macroscale hydrology model. Adv. Water Resour. 29: 872–886.

Aouad–Rizk, A., Job, J.–O., Khalil, S., Touma, T., Bitar, C., Boqcuillon, C. and Najem, W., 2005. Snow in Lebanon: a preliminary study of snow cover over Mount Lebanon and a simple snowmelt model / Etude préliminaire du couvert neigeux et modèle de fonte des neige pour le Mont Liban. Hydrological Sciences Journal, 50(3), doi:10.1623/hysj.50.3.555.65023.

Bales, R., Molotch, N., Painter, T., Dettinger, M., Rice, R., Dozier, J., 2006. Mountain hydrology of the western United States. Water Resources Research 42.

Berghuijs, Woods, Hrachowitz, 2014. A precipitation shift from snow towards rain leads to a decrease in streamflow. Nature Climate Change 4, 583–586.

Boudhar, A., et al., 2009. Long-term analysis of snow-covered area in the Moroccan High-Atlas through remote sensing. Int. J. Appl. Earth Observ. Geoinform.

Brown, R., C. Derksen, and L. Wang., L. 2010. A multi-dataset analysis of variability and change in Arctic spring snow cover extent 1967–2008. Journal of Geophysical Research.

Clark, M., Hendrikx, J., Slater, A., Kavetski, D., Anderson, B., Cullen, N., Kerr, T., Hreinsson, E., Woods, R., 2011. Representing spatial variability of snow water equivalent in hydrologic and land-surface models: A review. Water Resources Research 47.

Cook, B.I., Anchukaitis, K.J., Touchan, R., Meko, D.M., Cook, E.R., 2016. Spatiotemporal drought variability in the Mediterranean over the last 900 years. J. Geophys. Res. Revised.

Corripio, J.G., and Pruves., R.S., 2005. Surface Energy Balance of High Altitude Glaciers in the Central Andes: the Effects of Snow Penitents. In Climate and Hydrology in Mountain Areas, by C De Jong, D. Collins and R. Ranzi. WILEY, 2005.

DeWalle, D R, Rango, A. 2008. Principles of Snow Hydrology. Cambridge Univ. Press. (ISBN-10: 0511535678) 410 pp.

Doummar, J., Geyer, T., Baierl, M., Nödler, K., Licha, T., Sauter, M., 2014. Carbamazepine breakthrough as indicator for specific vulnerability of karst springs: Application on the Jeita spring, Lebanon. Applied Geochemistry 47, 150–156.

Dozier, J., 1989. Spectral signature of alpine snow cover from the Landsat Thematic Mapper. Remote sensing of Environment, 29: 9–22.

Dozier, J., Bair, E., Davis, R., 2016. Estimating the spatial distribution of snow water equivalent in the world's mountains. Wiley Interdisciplinary Reviews: Water 3, 461–474.

Frei, A., Tedesco, M., Lee, S., Foster, J., Hall, D., Kelly, R., Robinson, D., 2012. A review of global satellite-derived snow products. Advances in Space Research 50, 1007–1029.

Gascoin, S., Hagolle, O., Huc, M., Jarlan, L., Dejoux, J.-F., Szczypta, C., Marti, R., and Sánchez, R., 2015. A snow cover climatology for the Pyrenees from MODIS snow products, Hydrol. Earth Syst. Sci., 19, 2337–2351, doi:10.5194/hess-19-2337- 2015.

Giorgi, F., Lionello, P., 2008. Climate change projections for the Mediterranean region. Global and Planetary Change 63, 90–104.

Girotto, M., Margulis, S., Durand, M., 2014. Probabilistic SWE reanalysis as a generalization of deterministic SWE reconstruction techniques. Hydrological Processes 28, 3875–3895.

Godsey, Kirchner, Tague, 2014. Effects of changes in winter snowpacks on summer low flows: case studies in the Sierra Nevada, California, USA. Hydrological Processes 28, 5048–5064.

Goulden, M., Bales, R., 2014. Mountain runoff vulnerability to increased evapotranspiration with vegetation expansion. Proceedings of the National Academy of Sciences 111, 14071–14075.

Grouillet, B., Ruelland, D., Vaittinada Ayar, P., and Vrac, M., 2016. Sensitivity analysis of runoff modeling to statistical downscaling models in the western Mediterranean. Hydrol. Earth Syst. Sci., 20, 1031-1047, doi:10.5194/hess-20-1031-2016.

Hall DK, Riggs GA, Salomonson VV., 2006. MODIS snow and sea ice products. In Earth Science Satellite Remote Sensing–Volume I: Science and Instruments, Qu J (ed.). Springer-Verlag Press: Berlin, Heidelburg.

Harpold, A., Molotch, N., 2015. Sensitivity of soil water availability to changing snowmelt timing in the western U.S. Geophysical Research Letters 42, 8011–8020.

Hock, R. 2003. Temperature index melt modelling in mountain areas. J. Hydrol., 282(1–4), 104–115.

Hreiche, A., Najem, W. and Bocquillon, C., 2007. Hydrological impact simulations of climate change on Lebanese coastal rivers /Simulations des impacts hydrologiques du changement climatique sur les fleuves côtiers Libanais. Hydrological Sciences Journal, 52(6), 11191133, doi:10.1623/hysj.52.6.1119.

Jonas, T., Marty, C., and Magnusson, J., 2009. Estimating the snow water equivalent from snow depth measurements in the Swiss Alps, Journal of Hydrology, 378(1–2), 161167, doi:10.1016/j.jhydrol.2009.09.021.

Jong, C. de (ed.), David N. Collins D.N., Ranzi, R. (eds.) 2005. Climate and Hydrology of Mountain Areas. Wiley. (ISBN: 978-0-470-85814-1) 338 pp.

Kelley, C.P., Mohtadi, S., Cane, M.A., Seager, R., & Kushnir, Y., 2015. Climate change in 300 the Fertile Crescent and implications of the recent Syrian drought. Proc. Natl. Acad. 301 Sci., 112 (11), 3241-3246.

Knowles, N, Cayan, DR, 2004. Elevational dependence of projected hydrologic changes in the San Francisco estuary and watershed. Climatic Change. 62:319–336.

Köeniger, P., Margane, A., 2014. Stable Isotope Investigations in the Jeita Spring catchment, Technical Cooperation Project Protection of Jeita Spring, BGR Technical Report No. 12. 56 pp. Hannover, Germany.

Koeniger, P., Toll, M., Himmelsbach, T., 2016. Stable isotopes of precipitation and spring waters reveal an altitude effect in the Anti- Lebanon Mountains, Syria. Hydrol Process 30, 2851–2860.

Kotlarski, S., Lüthi, D., Schär, C., 2015. The elevation dependency of 21st century European climate change: an RCM ensemble perspective. International Journal of Climatology 35, 3902–3920.

Liston, G. E., 1995: Local advection of momentum, heat, and moisture during the melt of patchy snow covers. J. Appl. Meteor. 34, 1705–1715.

Liston GE, Winther J-G, Bruland O, Elvehøy H, Sand K. 1999. Below surface ice melt on the coastal Antarctic ice sheet. J. Glaciol. 45: 273–285, doi: 10.3189/002214399793377130.

Liston, G.E., Elder, K., 2006. A meteorological distribution system for high-resolution terrestrial modeling (MicroMet). J. Hydrometeorol. 7, 217–234.

López-Moreno, J., Revuelto, J., Fassnacht, S., Azorín-Molina, C., Vicente-Serrano, S., Morán-Tejeda, E., Sexstone, G., 2015. Snowpack variability across various spatio-temporal resolutions. Hydrological Processes 29, 1213–1224.

López-Moreno, J.L., Vicente-Serrano, S.M., Morán-Tejeda, E., Lorenzo-Lacruz, J., Kenawy, A., Beniston, M., 2011. Effects of the North Atlantic Oscillation (NAO) on combined temperature and precipitation winter modes in the Mediterranean mountains: observed relationships and projections for the 21st century. Global and Planetary Change 77 (1-2), 62–76.

Lundquist, J., Loheide, S., 2011. How evaporative water losses vary between wet and dry water years as a function of elevation in the Sierra Nevada, California, and critical factors for modeling. Water Resources Research 47. doi:10.1029/2010WR010050.

Margane, A., Schuler, P., Königer, P., Abi Rizk, J., Stoeckl, L., and Raad, R., 2013. Hydrogeology of the Groundwater Contribution Zone of Jeita Spring. Technical Cooperation Project Protection of Jeita Spring, BGR Technical Report No. 5, 317pp. Raifoun, Lebanon.

Maurer, Stewart, Bonfils, Duffy, Cayan, 2007. Detection, attribution, and sensitivity of trends toward earlier streamflow in the Sierra Nevada. Journal of Geophysical Research: Atmospheres (1984–2012) 112.

Meybeck, M., Green, P., and Vörösmarty, C., 2001. A New Typology for Mountains and Other Relief Classes: An Application to Global Continental Water Resources and Population Distribution. Mountain Research and Development, 21, 34-45.

Mhawej, M., Faour, G., Fayad, A., Shaban, A., 2014. Towards an enhanced method to map snow cover areas and derive snow-water equivalent in Lebanon. Journal of Hydrology 513, 274–282.

Milano, M., Ruelland, D., Fernandez, S., Dezetter, A., Fabre, J., Servat, E., Fritsch, J.-M., Ardoin-Bardin, S., and Thivet, G., 2013. Current state of Mediterranean water resources and future trends under climatic and anthropogenic changes, Hydrolog. Sci. J., 58, 498–518.

Ministry of Energy and Water (MOEW), 2010. National Water Sector Strategy (NWSS) Report, Beirut, Lebanon.
Molotch, N. P., and Meromy, L., 2014. Physiographic and climatic controls on snow cover persistence in the Sierra 20 Nevada Mountains. Hydrological Processes. 28, 4573-4586, 2014.
Molotch, N., Colee, M., Bales, R., Dozier, J., 2005. Estimating the spatial distribution of snow water equivalent in an alpine basin using binary regression tree models: the impact of digital elevation data and independent variable selection. Hydrol Process 19, 1459–1479.
Morán-Tejeda, E., Lorenzo-Lacruz, J., López-Moreno, J., Rahman, K., Beniston, M., 2014. Streamflow timing of mountain rivers in Spain: Recent changes and future projections. Journal of Hydrology 517, 1114–1127.
Nogués-Bravo, Araújo, Errea, Martínez-Rica, 2007. Exposure of global mountain systems to climate warming during the 21st Century. Global Environmental Change 17, 420–428.
Nohara, D., Kitoh, A., Hosaka, M., Oki, T., 2006. Impact of Climate Change on River Discharge Projected by Multimodel Ensemble. Journal of Hydrometeorology 7, 1076–1089.
Painter, T., Dozier, J., Roberts, D., Davis, R., Green, R., 2003. Retrieval of subpixel snow-covered area and grain size from imaging spectrometer data. Remote Sensing of Environment 85, 64–77.
Painter, T., Rittger, K., McKenzie, C., Slaughter, P., Davis, R., Dozier, J., 2009. Retrieval of subpixel snow covered area, grain size, and albedo from MODIS. Remote Sensing of Environment 113, 868–879.
Parajka, J., and Blöschl., G, 2008. Spatio-temporal combination of MODIS images: potential for snow cover mapping. Water Resour. Res., 44.
Pepin, Bradley, Diaz, Baraer, Caceres, Forsythe, Fowler, Greenwood, Hashmi, Liu, Miller, Ning, Ohmura, Palazzi, Rangwala, Schöner, Severskiy, Shahgedanova, Wang, Williamson, Yang, 2015. Elevation-dependent warming in mountain regions of the world. Nature Climate Change 5, 424–430.
Raleigh, M., Livneh, B., Lapo, K., Lundquist, J., 2016. How Does Availability of Meteorological Forcing Data Impact Physically Based Snowpack Simulations?. Journal of Hydrometeorology 17, 99–120.
Seidel, K. and Martinec, J., 2004. Remote Sensing in Snow Hydrology. Runoff Modelling, Effect of Climate Change. (ISBN: 978-3-540-40880-2) 150 pp.
Shaban, A., Faour, G., Khawlie, M. and Abdallah, C., 2004. Remote sensing application to estimate the volume of water in the form of snow on Mount Lebanon / Application de la télédétection à l'estimation du volume d'eau sous forme de neige sur le Mont Liban. Hydrological Sciences Journal, 49(4), doi:10.1623/hysj.49.4.643.54432.
Skaugen, T., and F. Randen., F. 2011. Modelling the spatial distribution of snow water equivalent at the catchment scale taking into account changes in snow covered area. Hydrol. Earth Syst. Sci. Discuss 8.
Sturm, M., Taras, B., Liston, G., Derksen, C., Jonas, T., Lea, J., 2010. Estimating Snow Water Equivalent Using Snow Depth Data and Climate Classes. Journal of Hydrometeorology 11, 1380–1394.
Sun, C., J. P. Walker, and Houser, P.R., 2004. A methodology for snow data assimilation in a land surface model. J. Geophys. Res. 109.
Takala, M., et al., 2011. Estimating northern hemisphere snow water equivalent for climate research through assimilation of space-borne radiometer data and ground-based measurements, Remote Sensing of Environment, doi:10.1016/j.rse.2011.08.014
Tedesco M (ed.) 2015. Remote Sensing of the Cryosphere. Wiley. (ISBN: 978-1-118-36885-5) 432 pp.
Telesca, L., Shaban, A., Gascoin, S., Darwich, T., Drapeau, L., Hage, M., Faour, G., 2014. Characterization of the time dynamics of monthly satellite snow cover data on Mountain Chains in Lebanon. Journal of Hydrology 519, 3214–3222.
UN Development Programme (UNDP), 2014. Assessment of Groundwater Resources of Lebanon. Beirut. www.lb.undp.org/ content/lebanon.
Viviroli, D., Dürr, H., Messerli, B., Meybeck, M., Weingartner, R., 2007. Mountains of the world, water towers for humanity: Typology, mapping, and global significance. Water Resources Research 43.

1.8 INTRODUCTION (VERSION FRANÇAISE)

I. 1. Pénurie d'eau au Liban

Les régions méditerranéennes de montagne sont parmi les plus vulnérables au réchauffement climatique (Nogués-Bravo et al., 2007; Giorgi et Lionello, 2008; Harpold et Molotch, 2015). En outre, la hausse de température causée par le changement climatique a tendance à augmenter avec l'altitude (Kotlarski et al., 2015; Pepin et al., 2015). On s'attend donc à ce que de nombreuses régions de montagne passent d'un régime hydrologique dominé par la neige à un régime hydrologique dominé par la pluie (Maurer et al., 2007, Goulden et Bales, 2014). De plus, les régions méditerranéennes sont naturellement caractérisées par une forte variabilité de la hauteur de neige par rapport à d'autres régions de montagne comme les prairies ou la toundra (Sturm et al., 2010). La compréhension des différents facteurs climatiques et topographiques qui contrôlent l'évolution du manteau neigeux est nécessaire pour établir le lien entre la neige et les ressources en eau associées (Bales et al., 2006) et pour anticiper les effets du changement climatique (Molotch et Meromy, 2014 , Lopez-Moreno et al., 2015).

Le Mont-Liban et l'Anti-Liban sont deux châteaux d'eau naturels au Proche-Orient. Avec des altitudes moyennes supérieures à 2200 m.s.l., ces chaînes de montagnes reçoivent d'importantes précipitations déclenchées par le soulèvement orographique des masses d'air chaudes et humides en provenance de la mer Méditerranée. Ainsi, on estime que le Liban reçoit en moyenne 830 mm de précipitations par année hydrologique (septembre-août). A cause de l'altitude, le Mont et l'Anti-Liban, reçoivent entre 50 et 67% des précipitations annuelles totales sous forme de neige (MOEW, 2010; PNUD, 2014). Les chutes de neige sont plus fréquentes aux altitudes supérieures à 1200 m. La saison nivale s'étend généralement sur six mois dans la partie haute (au-dessus de 2200 m). Le régime hydrologique de ces bassins montagneux est dominé par (1) la fonte des neige sous l'influence du climat méditerranéen et (2) le système karstique caractérisé par une réponse rapide entre la fonte et le débit de printemps (Königer et al., 2016). L'eau de fonte entre le mois de mars et le mois de mai est une source d'approvisionnement essentiel en eau douce pour la région de plaine côtière et la plaine intérieure où se concentrent la majorité de la population et les activités économiques, y compris l'agriculture irriguée. Plus spécifiquement, la fonte des neiges sur le Mont-Liban qui recharge les aquifères karstiques, joue un rôle majeur dans la durabilité de l'écoulement des sources qui alimentent les zones urbaines du littoral libanais pendant la saison sèche (mai-août) (e.g. Königer et Margane, 2014 ; PNUD, 2014, Königer et al., 2016). Par exemple, Beyrouth reçoit 75% de son approvisionnement en eau potable à partir de la source karstique de Jeita (Margane

et al., 2013). Enfin, il ne faut pas négliger le fait que la fonte des neiges contribue au remplissage des réservoirs de surface artificiels ou naturels utiles pour l'agriculture notamment, et au fonctionnement des écosystèmes.

Malgré la quantité d'eau captée par ses montagnes, le Liban est de plus en plus préoccupé par la durabilité de la ressource en eau. La situation actuelle se caractérise par la surexploitation des eaux de surface et par des prélèvements excessifs des eaux souterraines (MOEW, 2010; PNUD, 2014). Cette situation s'explique par un manque de connaissance concernant les quantités d'eau disponibles, par une gestion non raisonnée, une demande accrue d'eau par tous les secteurs. On constate une augmentation de la pollution de l'eau de surface et l'intrusion d'eau salée dans la nappe souterraine en bord de mer (Fayad et al., 2013, PNUD, 2014).

Le but de cette recherche est de quantifier la contribution de la fonte des neiges en provenance du Mont-Liban. Nous nous sommes concentrés sur les bassins versant situés sur le flanc ouest du Mont-Liban car ils approvisionnent la région côtière qui est aussi la plus peuplée. Comme il n'existe aucun programme opérationnel de suivi du manteau neigeux au Liban, nous avons commencé par un examen approfondi des concepts et des méthodes clés pour quantifier la fonte des neiges dans les régions de montagne méditerranéennes. Ensuite, nous présentons les nouvelles observations qui ont été recueillies dans le cadre de cette thèse et dans le cadre de l'observatoire de la neige qui a été établi au Liban pour remédier à ce manque. Enfin, nous appliquons un modèle de neige distribué pour calculer la fonte pendant trois saisons pour trois bassins hydrographiques majeurs.

La section suivante (section 1.2) décrit la zone d'étude. Section 1.3) se concentre sur les connaissances actuelles concernant l'hydrologie des neiges au Liban. Section 1.4) présente la logique de la thèse et les principaux objectifs. Section 1.5) décrit l'organisation de la dissertation.

I. 2. Zone d'étude

Le climat du Liban est méditerranéen, donc les précipitations sont abondantes entre décembre et mars (MEE, 2010). Le volume moyen annuel des précipitations est estimé à 8,6 milliards de mètres cubes (MEE, 2010). En raison de l'influence du climat méditerranéen, les précipitations sont assez variables d'une année à l'autre. Par exemple, le total des précipitations varie entre 577 et 899 mm pour les années hydrologiques 2008 et 2012 (PNUD, 2014). On estime qu'entre 30 à 40% des précipitations annuelles au Liban tombent sous forme neige

(Shabanet al, 2004; PNUD, 2014). Les régions de montagne du Liban reçoivent quant à elles entre 50 à 67% des précipitations annuelles sous forme neige (UNDP, 2014).

Les ressources en eau renouvelables annuelles sont estimées à 2,7 milliards de mètres cubes (258 mm) (2,2 milliards de mètres cubes d'eau de surface et 0,5 milliard de mètres cubes d'eaux souterraines) (MEE, 2010). La fonte de la neige contribuerait à 26% du bilan hydrologique national (Mhawej et al., 2014). Dans la région du Mont-Liban, la neige apportait 31% du débit rivières et des sources (Telesca et al., 2014). Margane et al. (2013) ont estimé que la neige contribue à hauteur de 75% de la recharge des eaux souterraines dans le bassin versant El Kelb.

Les eaux de surface sont issues de plus de 2000 sources (dont le débit est supérieur à 30 l/s) principalement dans la région montagneuse karstique. Les débits de ces sources sont généralement caractérisés par une forte variabilité saisonnière et inter-annuelles. La production totale des sources est estimée à 1,2 milliards de mètres cubes par an, dont environ 0,2 sont disponibles durant la période estivale sèche. La production annuelle diminue à 0,85 milliards de mètres cubes lors des années sèches. Ces sources sont exploitées de façon intensive (MEE, 2010).

L'utilisation de l'eau de surface en 2010 a été estimé à 0,63 milliards de mètres cubes - principalement depuis les sources karstiques. Les pompages d'eau souterraine sont estimés à 0,71 milliards de mètres cubes, ce qui est supérieur à la recharge naturelle estimée à 0,50 milliards mètres cubes par an. L'eau disponible est estimée à 830 m^3 par habitant et par an, ce qui est inférieur au seuil de stress hydrique qui est fixé à 1000 m^3 cap^{-1} $an^{-1)}$ (MEE, 2010). Le déficit actuel en eau du pays est estimé à 0,275 milliards mètres cubes par an (MEE, 2010).

Le Liban, faisant partie du bassin Méditerranéen est particulièrement exposé au changement climatique (Nohara et al, 2006; Giorgi et Lionello, 2008; Milano et al., 2013; Morán-Tejeda et al, 2014.). Plus particulièrement, le Proche-Orient a connu une période de sécheresse (1998-2012) (Cook et al., 2016) caractérisée par une température supérieure à la normale et des précipitations inférieures à la normale en hiver (Novembre - Avril) telle que définie sur la période 1931-2008 (Kelleyet al., 2015). Les tendances et projections climatiques suggèrent que les montagnes libanaises sont fortement vulnérables au réchauffement climatique. La hauteur de neige pourrait réduire de 50% à 2000 m sous 2 degrés de réchauffement en 2040, conduisant à un retrait de la ligne d'altitude de la neige de 1500 à 1700 m d'altitude (MEE, 2010). Dans le même scénario la saison de neige devrait être 2 à 6 semaines plus courte et le volume annuel de SWE diminuerait de 40% (MEE, 2010). Par conséquent, il

y a des motifs de vive préoccupation quant à la durabilité des ressources en eau en provenance du Mont-Liban et de l'Anti-Liban.

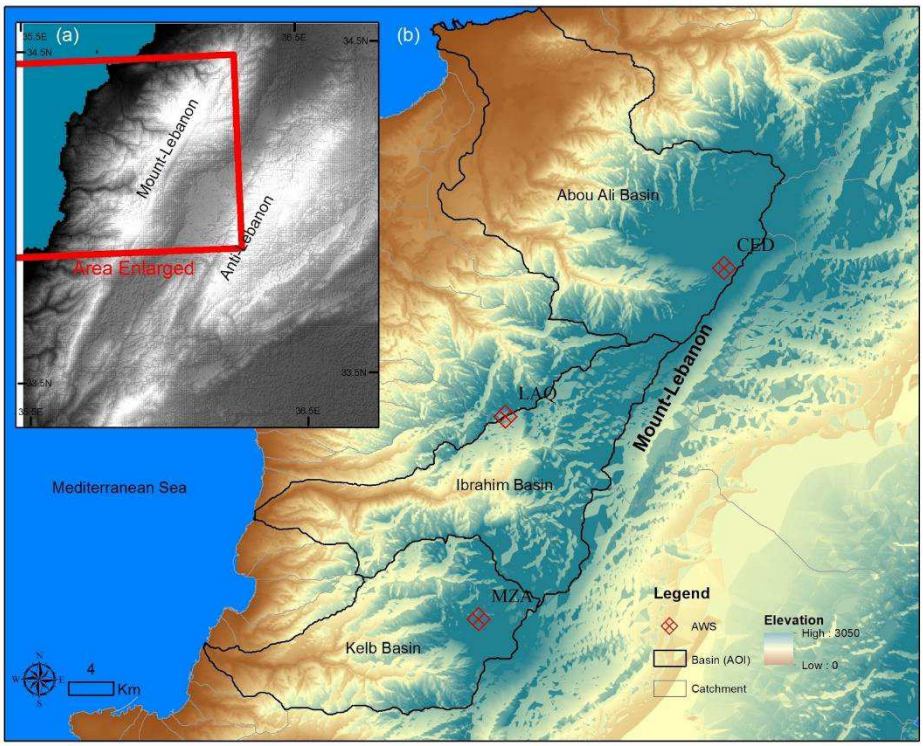

Figue. 1.1 Zone d'étude montrant (a) le Mont-Liban et l'Anti-Liban (b) l'emplacement des trois grands bassins étudiés dans cette thèse: Abou ALi, Ibrahim et Kelb.

I. 3. Etudes précédentes en hydrologie nivale au Liban

Malgré l'importance de la neige au Liban, les connaissances sur la contribution de la fonte des neiges au bilan hydrologique, en particulier pendant la saison sèche, restent limitées. Ceci peut être attribué à: 1) le peu d'observations météorologiques dans les régions de montagne 2) le fait que la plupart des connaissances existantes sont limitées soit à des études à l'échelle nationale avec des moyennes mensuelles ou annuelles, soit à des études à l'échelle ponctuelle avec des observations sur de courtes périodes; 3) le fait que l'eau souterraine est dominée par un système karstique qui couvre environ 65% de la superficie totale du pays, ce qui complique l'évaluation de la contribution de la fonte des neiges au ruissellement.

I. 3.1. Échelle ponctuelle

Les réseaux d'observation dans les régions montagneuses sont généralement insuffisants (Raliegh et al., 2015). Au Liban, tout le réseau météorologique opéré par l'agence météorologique (faisant partie de la direction générale de l'aviation civile) se trouve en-dessous de la limite d'enneigement hivernale (la plus haute station météorologique opérationnelle est

située à 1220 m.a.s.l). Les observations nivales et météorologiques dans les régions d'altitude sont habituellement réalisées via (1) des projets de coopération (par exemple, Margane et al., 2013) ou par des programmes de recherche avec des observations de 1 à 3 ans en moyenne (Shaban et al. Aou-Rizk et al., 2005, Hreiche et al., 2007). Le réseau nouvellement créé dans le cadre de l'observatoire de la neige est la première tentative de mise en place d'un réseau stable de mesure de la hauteur de neige ainsi que des variables météorologiques standards sur le Mont-Liban (altitude entre 1830 et 2830 m.a.s.l.). Cet observatoire est une collaboration entre l'Institut de Recherche pour le Développement (IRD), le Centre d'Etudes Spatiales de la Biosphère CESBIO (France), le Conseil National de la Recherche Scientifique - Centre de télédétection (CNRS \ NCRS, Liban), et l'Université de Saint Joseph (USJ, Liban). Le réseau comprend trois stations météorologiques automatiques (AWS) et est devenu entièrement opérationnel en 2014 avec l'installation de la troisième AWS à Laqlouq (Fig. 1.1).

I. 3.2. Suivi de la surface enneigée par satellite

À l'heure actuelle, la technique de cartographie de la surface enneigée (snow cover area, SCA) par télédétection satellite est bien établie. Elle repose sur la réflectance élevée de la surface enneigée dans les longueurs d'onde visibles et une faible réflectance dans le proche infrarouge (Dozier et al., 1989, Seidel et Martinec 2004, Salomonson et Appel, 2004, Tedesco (éd.) 2015) . Diverses études ont évalué favorablement des cartes de neige dérivées de capteurs optiques (Simic et al., 2004). En particulier les données MODIS ont été utilisées pour générer un produit global, quotidien, de SCA à une résolution de 500 m (Hall et Riggs, 2007). Mais les images satellites optiques sont sujettes à l'obstruction par les nuages (Parajka et Blöschl, 2008). Dans ce contexte, différentes méthodes ont été proposées pour interpoler les données manquantes (par exemple, Andreadis, 2006, Boudhar et al., 2009; Gascoin et al., 2015). Une autre limitation de la télédétection est que les capteurs spatiaux ne permettent pas une estimation fiable du SWE dans les régions montagneuses en raison des faits suivants: (1) en cas de mesures radar, la topographie complexe provoque des réflexions multiples du micro-onde émis, et l'absorption par l'eau liquide du signal limite l'interprétation des données (2) en cas de micro-ondes passives, la résolution spatiale atteinte par les radiomètres est trop grossière (~25 km) pour être utile sur les régions montagneuses.

La compréhension correcte de la dynamique spatio-temporelle d'un manteau neigeux est fondamentale pour la modélisation hydrologique des bassins de montagne (Liston, 1999, De Jong et al., 2005). Le calcul de l'étendue du manteau neigeux aide à la quantification de la répartition spatiale et temporelle des propriétés physiques du manteau neigeux lorsque les

observations sur le terrain sont insuffisantes. Par conséquent, de nombreuses études ont souligné que, pour étendre l'utilité des données de télédétection pour l'hydrologie de montagne, il est nécessaire de combiner les observations de télédétection avec un modèle de neige qui tient compte des variables météorologiques de surface : les précipitations, la température de l'air, l'humidité, le vent et le rayonnement de courte et de grande longueur d'ondes (Sun, et al., 2004; 2006, Tedesco (éd.) 2015, Dozier et al., 2016).

Au Liban, le produit de neige MODIS (MOD10) a été utilisé pour calculer l'évolution de SCA dans le temps et cartographier la durée d'enneigement (snow cover duration SCD). Ces données ont servi à estimer le SWE en utilisant des approches empiriques (Mhawej et al., 2014, Telesca et al., 2014). Il convient de noter que Mhawej et al. (2014) ne tiennent pas compte du remplissage des lacunes causés par les nuages. Telesca et al. (2014), d'autre part, ont utilisé un algorithme d'interpolation qui est décrit par Gascoin et al. (2015) dans le cas des Pyrénées. Cette étape est nécessaire pour tirer des variables climatologiques utiles des produits MODIS.

I. 3.3. Équivalent en eau de neige (SWE)

La quantification correcte du SWE est cruciale pour l'hydrologie à l'échelle du bassin (DeWalle et Rango, 2008). Le SWE est la lame d'eau équivalent qui est contenue dans le manteau neigeux. Il peut être exprimé comme le produit de la hauteur du manteau neigeux (HS) et de la densité du manteau neigeux. Au Liban, on estime que le SWE annuel moyen se situerait entre 1,82 et 2,57 milliards de mètres cubes (équivalent de 174-246 mm) pour les années entre 2008 et 2012 (PNUD, 2014). Une autre étude suggère que la moyenne annuelle SWE est de 1,1 milliard de mètres cubes (2001-2002) (Shaban et al., 2004). Plus récemment, le SWE annuel moyen a été estimé à 2,42 milliards de mètres cubes pour le Mont-Liban et l'Anti-Liban combinés (Mhawej et al., 2014) et 0,77 milliard de mètres cubes pour le Mont-Liban (Telesca et al. 2014). Ces différences dans l'estimation de SWE peuvent être attribuées à (1) les différentes méthodes utilisées pour l'estimation, et (2) au nombre limité d'observations au sol utilisées pour valider les estimations du modèle.

I. 3.4. Dynamique du manteau neigeux

La dynamique de la fonte des neiges est un phénomène thermodynamique qui est donc modélisable par un bilan énergétique (Corripio, et al., 2005). Différentes méthodes ont été proposées et utilisées pour l'estimation du SWE dans les régions de montagne (Dozier et al., 2016). Ces méthodes reposent sur l'utilisation d'observations au sol (par exemple, des stations météorologiques) et sur des mesures in situ (par exemple, des mesures de la densité de neige de

profondeur de neige). Cependant, dans de nombreux cas, les méthodes basées sur les observations de neige manquent généralement de couverture spatiale (Takala et al., 2011). L'interpolation spatiale (par exemple, Girotto et al., 2014) et les approches qui combinent le SCA dérivé de la télédétection et les mesures au sol sont parmi les plus utilisées pour calculer le SWE spatialisé (Molotch et al., 2005; Al., 2010; Skaugen et al., 2011).

Une autre approche consiste à utiliser un modèle de manteau neigeux forcé par les données météorologiques. Pour simplifier, deux approches principales sont utilisées pour l'évaluation de la fonte du manteau neigeux: (1) la méthode degrés-jours (degree day model DDM) ou d'indice de température (Hock, 2003) et (2) la méthode du bilan d'énergie (surface energy balance SEB, Liston et al., 1999, Corripio, et al., 2005). L'approche DDM est pratique, en raison de sa simplicité et de son exigence minimale de données (uniquement des données de température), mais elle nécessite des observations de fonte pour évaluer le facteur degré-jour. D'autre part, le SEB permet de calculer la fonte des neiges à partir d'équations physiques, à condition que le forçage météorologique de la précipitation, de la vitesse du vent, de l'humidité de l'air, de la température de l'air et du rayonnement entrant (radios à ondes longues et ondes courtes) soit disponible (Liston et Elder, 2006).

Les tentatives de modélisation sur le Mont-Liban avaient jusqu'ici été limitées à l'échelle du bassin expérimental à l'aide de modèles à l'échelle ponctuelle. Aouad-Rizk et al., (2005) ont étudié la fonte des neiges dans le bassin de la rivière El Kelb à l'aide d'un bilan énergétique et d'une méthode de degré jour. Cette étude met en évidence l'importance de la densité de neige et la variation SWE avec l'altitude lors de la prise en compte de la contribution de la fonte des neiges. D'autre part, Hreiche et al. (2007) ont utilisé un couplage d'un modèle pluie-débit avec un module DDM pour étudier les effets des scénarios de changement climatique dans le bassin Ibrahim. Une augmentation de 2 ° C de la température se traduirait par une avance de 2 mois de l'écoulement de pointe dans le bassin versant dominé par la neige de Nahr Ibrahim (Hreiche et al., 2007). Ces travaux de recherche donnent une image globale de la variabilité temporelle de la neige au Liban et de son comportement de fonte. Cependant, la répartition spatio-temporelle du SWE et la relation entre la fonte des neiges et le ruissellement superficiel et la recharge des eaux souterraines reste largement méconnue.

I. 3.5. Hydrologie nivale et importance du karst

Au Liban, la plupart des chutes de neige tombe sur le plateau crétacé (le «toit» de la formation karstique, soit environ 40% du pays). La fonte des neiges (entre novembre et mai) recharge le système karstique (par exemple, Margane et al., 2013). Un exemple du bassin d'El

Kelb (Margane et al., 2013) a révélé que les régions de haute montagne, entre 1000 et 2600 m d'altitude, contribuent à environ 75% de la recharge des eaux souterraines karstiques (Margane et al. 2013). On a estimé que la fonte des neiges contribuait à 56% du débit de la source dans la zone de plaine du Mont-Liban au printemps à Jeita (à 60 m a.s.l.) (Margane et al., 2013). La réponse du débit de la souce aux précipitations dans le bassin El Kelb est rapide (peut être observée dans les 24-48h après les précipitations) et dépend généralement de la distribution et du type de précipitation (pluie ou chute de neige) (Margane, 2014). La réponse des sources à la neige est commune à la plupart des bassins côtiers, par exemple nous montrons ci-dessous la carte de la probabilité de détection de neige du produit de neige MODIS (MOD10A1) (Hall et al., 2006) Dans les chaînes de montagnes du Mont-Liban et de l'Anti-Liban sur la période 2000-2011 après l'application de la méthode de gap-filling de Gascoin et al. (2015) (Fig. 1.2a). L'évolution mensuelle moyenne de la surface de couverture neigeuse du même produit est comparée à la moyenne mensuelle dérivée du SCA et du débit pour la période entre 2000 et 2011 de la source d'Afqa, source importante qui aliment la rivière Ibrahim (Fig. 1.2b). Fig 1.3 illustre la corrélation entre le débit observé à Afqa et la SCA dans le bassin topographique d'Afqa sur la période 2003-2013, période qui comprend des années sèches, moyennes et humides. Ici, comme c'est un exemple préliminaire, nous avons utilisé le SCA comme indicateur du SWE. Nous avons trouvé une corrélation de 86% avec un décalage de 2 mois entre la SCA et la sortie du printemps Afqa (1113 m a.s.l.). Une telle corrélation souligne l'importance de la fonte des neiges dans les réponses hydrologiques du système karstique au Mont-Liban. Ces résultats vont de pair avec Margane et al. (2013) sur la réponse rapide du système karst dans le bassin de la rivière El Kelb.

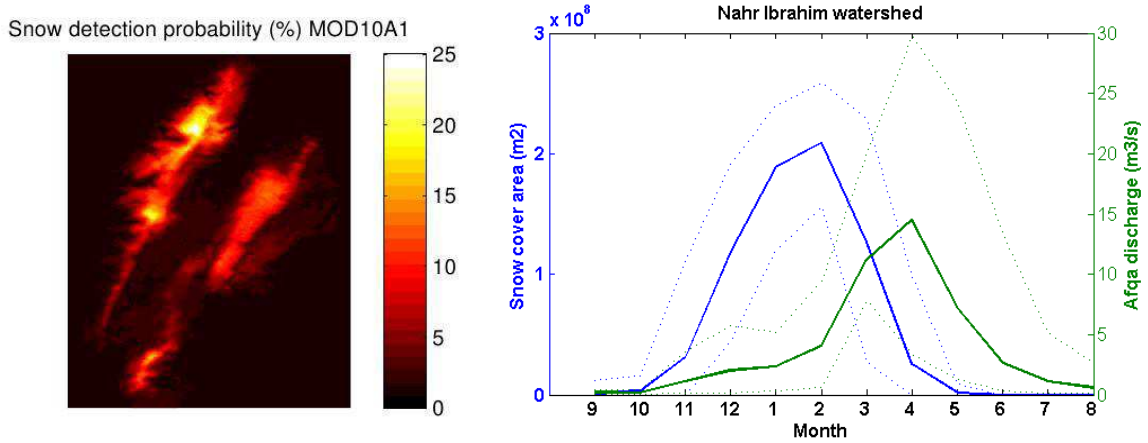

Figue. 1.2. (a) probabilité de détection de neige (% de 1 an) calculée à partir du produit MOD10A1 sur le Mont Liban et Anti Liban, et (b) débits moyens mensuels et surface enneigée du bassin de la source Afqa dérivé du même produit (2000-2011) . Les lignes pointillées indiquent le minimum et maximum observés.

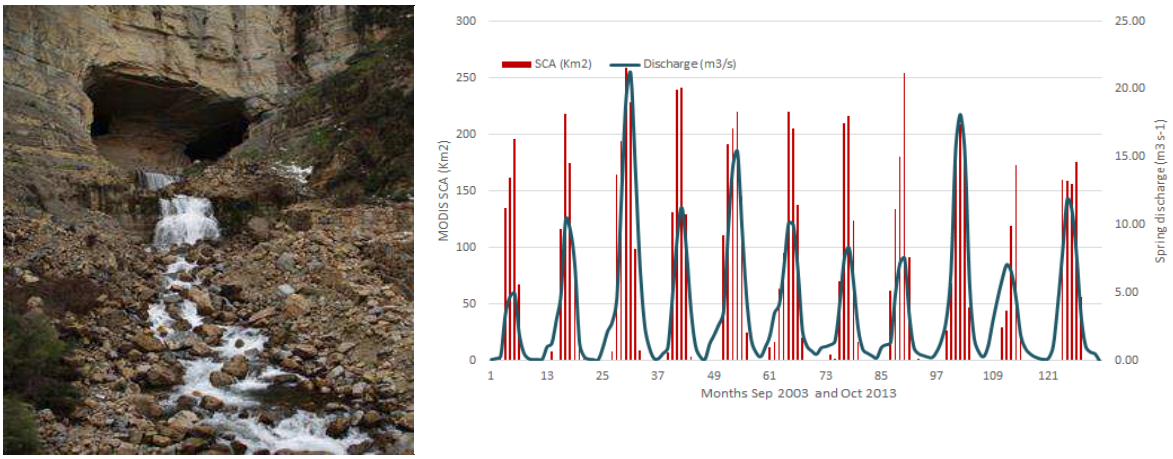

Figue. 1.3 (a) La source Afqa (altitude 1113 m) dans le bassin de la rivière Ibrahim en hiver quand le débit est encore minime. L'image a été prise le 24 Février 2015 (avec l'aimable autorisation de l'auteur); et (b) la corrélation entre MODIS SCA et le débit d'Afqa pour les années 2003 à 2013.

Par conséquent, la fonte des neiges, qui se produit habituellement au printemps, au moment où il ya peu de contribution des précipitations, a une grande influence sur les débits de la plupart des sources et des rivières du Liban. Fig. 1.4 illustre les débits d'Afqa au cours de la dernière décennie. Les débits sont faibles pendant la saison hivernale (de décembre à mars) et atteignent leur maximum entre fin mars et mai en fonction de la quantité de neige.

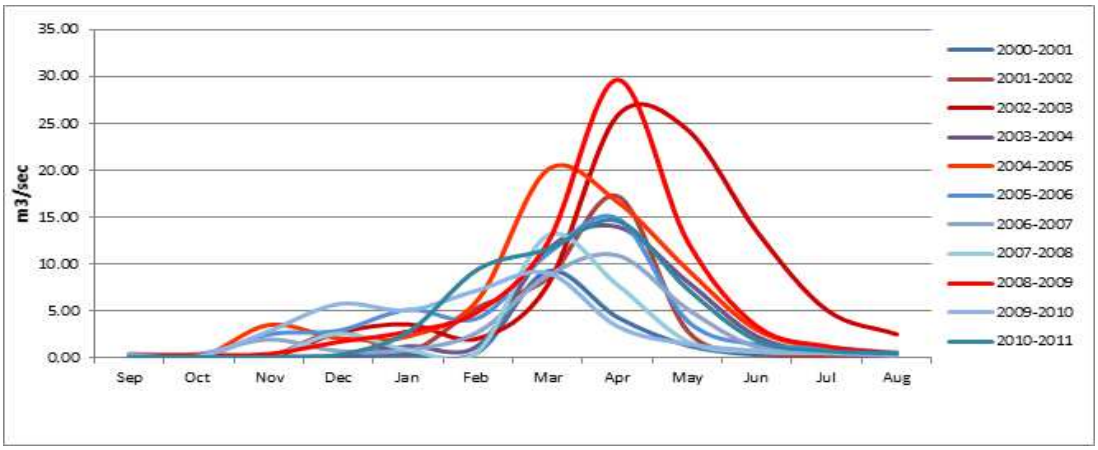

Figue. 1.4 Débit de la source d'Afqa, bassin du Nahr Ibhrahim, moyenne mensuelle entre 2000 et 2011

I. 4. Problématique

Cette thèse est motivée par le fait que la recharge des eaux souterraines et les débits du système karstique sont fortement liés à la fonte de la neige sur le Mont-Liban (Koeniger et Margane, 2014, Doummar et al., 2014 et PNUD, 2014). Jusqu'à présent, ce problème a été abordé à l'aide de deux types d'approches (1) à l'aide de modèles DDM ou SEB à l'échelle

ponctuelle ou de petits bassin pilotes (Aouad-Rizk et al., 2005, Hreiche et al. , 2007) ou (2) en combinant des données de MODIS SCA avec des mesures manuelles du SWE (Telesca et al., 2014), ou par micro-ondes passives à faible résolution (Mhawej et al., 2014) . Cependant, il subsiste de grandes incertitudes quant à la quantification de la fonte des neiges à l'échelle régionale, principalement en raison du manque de données météorologiques continues dans les zones d'altitudes au Liban.

Parmis les questions les plus pressantes au Liban sont (1) quelle est la quantité d'eau stockée sous forme de neige en hiver? (2) quelle est la contribution de la fonte des neiges aux à la recharge des eaux souterraines?

Pour répondre à ces deux questions, nous avons effectué des mesures sur deux saisons de 2014 à 2016, nous avons utilisé les nouvelles observations de stations météorologiques, et de télédétection pour mettre en place et évaluer un modèle du couvert neigeux distribué spatialement pour la première fois sur le Mont-Liban entre de 1300 et 2900 m. Les objectifs spécifiques de cette thèse sont:

1- Quels sont les principaux facteurs météorologiques et physiographiques qui contrôlent les processus nivaux dans les régions méditerranéennes et quel est le rôle de la fonte des neiges dans l'hydrologie de ces régions?

2- Quelle est la variabilité spatio-temporelle du SWE à différentes altitude (1300-2900 m a.s.l.) sur le versant ouest du Mont-Liban?

3- Dans quelle mesure pouvons-nous estimer avec précision la répartition spatiale du SWE au pas de temps journalier à une résolution spatiale fine (100 m)?

4- Compte tenu de la difficulté et des coûts relativement élevés pour effectuer des mesures sur le terrain et maintenir les stations météorologiques dans les zones montagneuses, quelle périodicité convient le mieux pour effectuer des mesures sur le terrain? Et quels forçages météorologiques sont considérés comme prioritaires pour le bon fonctionnement d'un modèle du manteau neigeux?

I. 5. Contenu du rapport

En plus de ce chapitre introductif cette thèse comporte quatre chapitres. Dans le chapitre 2 nous essayons de répondre à la question 1 en présentant une synthèse des études nivologiques

dans les régions Méditerranéennes. Ce travail est basé sur un l'examen de plus de 650 articles publiés dans des revues scientifiques.

Le Chapitre 3 aborde la question 2 et introduit l'observatoire de la neige au Liban sur le Mont-Liban. Ce chapitre présente les trois AWS et montre les résultats des mesures de terrain de hauteur, SWE, et densité de la neige qui ont été menées par l'auteur de cette thèse entre 1300 et 2900 m d'altitude. Finalement, les données de surface enneigées MODIS sont présentées.

Le chapitre 4 aborde la question 3 en utilisant un modèle de bilan d'énergie (Liston et al., 1999;2006). Le modèle a été appliqué sur une grille de résolution 100 m et nous nous sommes concentrés sur son évaluation dans les trois bassins d'étude présentés au chapitre 3. Le modèle est forcé et validé en utilisant le l'ensemble des données présentées au chapitre 3.

Le chapitre 5 aborde la question 4, et présente les principales conclusions de ces travaux de recherche, met en évidence les principales limites et propose des pistes de recherches futures.

Summary of chapter: "Snow hydrology in mediterranean mountain regions: a review"

This chapter in its current form is published in the Journal of Hydrology: Fayad, A., Gascoin, S., Faour, G., López-Moreno J. I., Drapeau L., Le Page M., Escadafal, R.: Snow hydrology in Mediterranean mountain regions: a review, J. Hydrol. doi:10.1016/j.jhydrol.2017.05.063

The objective of this paper is to provide a review on the snow hydrological processes in Mediterranean like mountain regions. In order to investigate this issue, we collected 620 peer-reviewed papers published between 1913 and 2016, and dealing with Mediterranean-like mountainous regions namely those located in the western USA, the Central Andes in South America, and the Mediterranean basin (South Europe, North Africa and Western Asia).

This chapter contributed to highlighting the major meteorological and physiographic factors controlling the snow processes in Mediterranean like regions and what is the fate of snowmelt in the hydrologic system of these regions. We found that (1) the persistence of snow cover is highly variable in space and time but mainly controlled by elevation and precipitation; (2) the snowmelt is driven by radiative fluxes, but the contribution of heat fluxes is stronger at the end of the snow season and during heat waves and rain-on-snow events; (3) the snow densification rates are higher in these regions than other climate regions; and (4) the snow sublimation is an important component of snow ablation, especially in high-elevation regions.

Despite snow importance in Mediterranean like mountainous regions the proper investigation of snow dynamics and SWE is still hindered by the lack of consistent ground observation especially in high-elevation regions. The spatial representation of SCA and SCD can be well achieved using remotely sensed snow data. A better spatial characterization of snow cover, however, can be achieved by combining ground observations with remotely sensed snow data. SWE reconstruction using satellite snow cover area and a melt model provides reasonable information that is suitable for hydrological applications.

Among the pressing issues is the lack of stable ground observation in high-elevation regions. However, a few years of snow depth (HS) and snow water equivalent (SWE) data can provide realistic information on snowpack variability. Further advances in our understanding of the snow processes in Mediterranean snow-dominated basins will be achieved using finer and more accurate climate forcing. Finally, while the theory on the snowpack energy and mass balance is now well established the connections between the snowpack and the water pathways in the critical zone (soil, groundwater) require further investigation.

2 SNOW HYDROLOGY IN MEDITERRANEAN MOUNTAIN REGIONS: A REVIEW

Abstract

Water resources in Mediterranean regions are under increasing pressure due to climate change, economic development, and population growth. Many Mediterranean rivers have their headwaters in mountainous regions where hydrological processes are driven by snowpack dynamics and the specific variability of the Mediterranean climate. A good knowledge of the snow processes in the Mediterranean mountains is therefore a key element of water management strategies in such regions. The objective of this paper is to review the literature on snow hydrology in Mediterranean mountains to identify the existing knowledge, key research questions, and promising technologies. We collected 620 peer-reviewed papers, published between 1913 and 2016, that deal with the Mediterranean-like mountain regions in the western United StatesA, the central Chilean Andesthe Central Andes in South America, and the Mediterranean basin (south Europe, North Africa and western Asia). We find a large amount of studies in the western US that form a strong scientific basis for other Mediterranean mountain regions. This review led to the followings highlights: (1) the persistence of snow cover is highly variable in space and time but mainly controlled by elevation and precipitation; (2) the snowmelt is driven by radiative fluxes, but the contribution of heat fluxes is stronger at the end of the snow season and during heat waves and rain-on-snow events; (3) the snow densification rates are higher in these regions than other climate regions; and (4) the snow sublimation is an important component of snow ablation, especially in high-elevation regions. Among the pressing issues is the lack of stable ground observation in high-elevation regions. However, a few years of snow depth (HS) and snow water equivalent (SWE) data can provide realistic information on snowpack variability. A better spatial characterization of snow cover can be achieved by combining ground observations with remotely sensed snow data. SWE reconstruction using satellite snow cover area and a melt model provides reasonable information that is suitable for hydrological applications. Further advances in our understanding of the snow processes in Mediterranean snow-dominated basins will be achieved by finer and more accurate climate forcing. While the theory on the snowpack energy and mass balance is now well established, the connections between the snow cover and the water resources involve complex interactions with the sub-surface processes, which demand future investigation.

Keywords: Snowpack; Snow hydrology; Mountain hydrology; Mediterranean regions

2.1 Introduction

Mountains regions are a major source of surface water and groundwater recharge in the world (Viviroli et al., 2007; Dettinger, 2014). The water balance in mountainous regions is defined by the interactions between the climate, cryospheric, and hydrological systems (de Jong et al. eds. 2005; DeWalle and Rango, 2008). In mountainous regions that are under the influence of the Mediterranean climate (Bolle 2003; Lionello et al. 2006), the wet-winters and hot and dry-summers climate, orographic enhanced precipitation, variability of temperature and the

partitioning of rain and snow with elevation, and the high seasonal variability of the snow cover make the hydrologic processes in these mountainous regions significantly different from those found in other cryospheric regions and or dry or wet climates. Under the influence of the Mediterranean climate, an important fraction of the precipitation occurs during winter months (e.g., Demaria et al., 2013a; López-Moreno et al., 2013a; Valdés-Pineda et al., 2014), with the highest elevation areas receiving most of this winter precipitation as snow while the mid-elevation areas have a mixed precipitation regime (McCabe et al., 2007; Surfleet and Tullos, 2013; Guan et al., 2016). Winter precipitation is orographically enhanced along with elevation (Dettinger et al., 2004; Behrangi et al., 2016; Derin et al., 2016). The snowmelt from the Mediterranean mountain occurs in the spring and summer when precipitation is otherwise scarce, and thus, this snowmelt is an essential water resource for many communities living in the surrounding low land regions (Morán-Tejeda et al., 2010; López-Moreno et al., 2008a, 2014).

The Mediterranean mountain regions include thecountries around the Mediterranean Sea (e.g., Morocco, Spain, France, Italy, Bulgaria, Croatia, Greece, Turkey, and Lebanon.), the western USA (California) and the mid-latitude area of Chile and Argentina. In almost all these regions, agriculture is an important source of income and employment and snowmelt provides runoff during the crop growing season, when irrigation is the most needed. However, the sustainability of the water resources is threatened by the pressure of a growing population, increasing irrigation, and climate change (e.g., Barnett et al., 2008). While Mediterranean region have been considered as climate change "hot spots" since the first IPCC reports (Milly et al., 2005; Giorgi, 2006; Nohara et al., 2006; Nogués-Bravo et al., 2007; Giorgi and Lionello, 2008; Loarie et al., 2009; Kyselý et al., 2012; Kapnick and Delworth, 2013; Morán-Tejeda et al., 2014; Prudhomme et al., 2014; Harpold and Molotch, 2015; Vano et al., 2015; Kumar et al., 2016), there is also new evidence that the rate of atmospheric warming increases with elevation (Kotlarski et al., 2015; Pepin et al., 2015), which strengthens the concern about the climate change in Mediterranean mountain regions. The impact of atmospheric warming is expected to be strong in snow-dominated watersheds since snow accumulation and ablation are highly sensitive to air temperature (Beniston, 2003; Barnett et al., 2005; Howat and Tulaczyk, 2005; Brown and Mote, 2009; Cooper et al., 2016). The main consequence to warming is a shift in the hydrological regimes from a snow-dominated regime towards a rain-dominated regime (Berghuijs et al., 2014; Goulden and Bales, 2014). For example, in the western USA, areas with elevations between 2000 to 2800 m are the most sensitive to global warming (Maurer et al., 2007). Regions in the western US where the average winter-wet-day minimum temperature

increased by +3 °C are witnessing a reduction in the winter-total snowfall to precipitation ratio (Knowles et al., 2006). Most Northern-Hemisphere's snow-dependent regions are likely to experience increasing stress from low snow years within the next three decades (Diffenbaugh et al., 2012). Areas with an average winter temperature between -4 and -2 °C are expected to witness shifts towards earlier streamflow peaks (changes that exceed 45 days relative to those from 1961–1990) (Maurer et al., 2007). Similar results were reported in the Southern Alpine river basins (Zampieri et al., 2015). The Mediterranean climate is also characterized by a high inter-annual variability, although the underlying mechanisms depend upon the specific region. North and South American Mediterranean regions are under the influence of the climatic variability of the Pacific Ocean, while the Mediterranean climate in Europe and North Africa is relatively connected to the North-Atlantic climatic variability (López-Moreno et al., 2013a).

Research on the seasonal snow and snow hydrology in mountains is well established and several authors have already produced review articles or chapters on the following: (1) the physical properties of the snowpack (e.g., Armstrong and Burn (eds) 2008; Kinar and Pomeroy, 2015; Sturm, 2015); (2) remote sensing of snow (Dozier and Painter, 2004; Seidel and Martinec 2004; Dozier et al., 2009; Dietz et al., 2012; Frei et al., 2012; Deems et al., 2013; Lettenmaier et al., 2015; Sturm, 2015; Tedesco (ed.) 2015); (3) spatial distribution of the snow water equivalent, SWE (Dozier et al., 2016); (4) snow and mountain hydrology (e.g., Seidel and Martinec 2004; de Jong et al. (eds.) 2005; Bales et al., 2006; Armstrong and Burn (eds) 2008; DeWalle and Rango 2008; Varhola et al., 2010; Hrachowitz et al., 2013; Bierkens, 2015; Sturm, 2015); (5) snow spatial representation in hydrologic and land-surface models (e.g., Clark et al., 2011); and the (6) projected climate impact on the cryospheric and hydrological systems in mountains (e.g., Beniston, 2003; de Jong et al. (eds.) 2005; Huber et al. (eds.) 2005; Vicuña and Dracup, 2007; Viviroli et al., 2007; Brown and Mote, 2009; Stewart, 2009; García-Ruiz et al., 2011; Diffenbaugh et al., 2012; Kapnick and Delworth, 2013; Beniston and Stoffel, 2014; Pepin et al., 2015; Sturm 2015; Wu et al., 2015; Meixner et al., 2016).

Snow processes are driven by meteorological forcing (energy and mass fluxes), and land surface physiography (topography and vegetation). Therefore, the snowpack present different characteristics depending on the region. The standard snow classification that was introduced by Sturm et al. (1995) defines seven classes of seasonal snow according to their physical properties: Tundra, Taiga, Alpine, Maritime, Ephemeral, Prairie, or Mountain. The "Mediterranean snow" can be observed as a subset of the Maritime class and it is characterized by a warmer snowpack, a shorter snow season, and a higher variance in both the intra-annual snow depth and mean monthly snow density compared to the Tundra, Taiga, and Prairie snow

regions (Brown and Mote, 2009; Sturm et al., 2010; Bormann et al., 2013) (Fig. 2.1). In comparison with the Tundra and Taiga regions, the snowpack in Mediterranean mountains is characterized by higher mean annual snow densities and annual densification rates (Bormann et al., 2013; Trujillo and Molotch, 2014) (Fig. 2.1).

To our knowledge, no review to date has explicitly addressed the characterization of snow hydrologic processes related to snow in one of the major snow regions. Given the significance of the snowmelt as a water resource in Mediterranean regions, we considered that a review of the previous snow studies undertaken in Mediterranean mountain regions is needed. This review may be helpful, for example, in defining a new research program in this climate region, which is highly sensitive to global warming and where snowmelt is an important contributor to the hydrologic cycle (Grouillet et al., 2016).

More specifically this review seeks to answer the following questions: (1) what are the major forcing variables and controls that drive the snow dynamics in Mediterranean mountain regions? (2) To what extent are we able to estimate the spatiotemporal properties of snowpack (i.e., SCA, HS, and SWE)? (3) What are the current limitations and opportunities associated with available observational networks and methods used to assess the snowpack dynamics and hydrologic responses in these mountain regions?

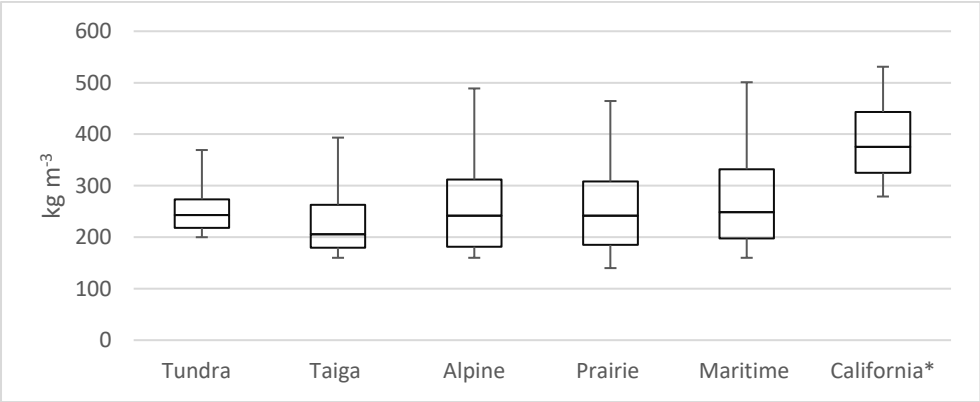

Fig. 2.1. Variation in the mean monthly snow density (Oct-June) (kg m-3) adopted from Brown and Mote (2009) for the major climate regions. *California monthly snow density means (Jan-June) are based on long-term monthly data records (more than 20 years) retrieved from 46 snow courses and 26 SNOTEL stations (data are available online at wcc.nrcs.usda.gov/snow/). The average snow depth and standard deviation, not shown, were as follows: Tundra (43.8 cm, 24.7 std dev), Taiga (59.6, 22.7), Alpine (130, 82.5), Prairie (88.5, 72.8), and Maritime (176.6, 149.9) (Sturm et al., 2010), and the average for California calculated from long term monthly snow courses and SNOTEL data was 146.1 cm (std dev = 97.5).

We collected 620 peer-reviewed articles published between 1913 and 2016, which dealing with the snowpack and snow hydrology in Mediterranean regions. From this large number of papers, we adopted a hybrid quantitative (metadata analysis from the papers) and qualitative approach (literature review) to gain insight into the major issues, trends, and

advances in this already large and growing research field. We present the geographic extent of the papers and the methodology to analyze them in section (2). The key indicators obtained from the papers dataset are presented in section (3). The second part of the paper is devoted to the review of the three key issues that emerge from this article database: Section (4) addresses the characterization of the climatic forcing in snow-dominated Mediterranean regions; Section (5) describes the main features of the snowpack obtained from ground measurements and remote sensing techniques; Section (6) focuses on the studies dedicated to the snowmelt modeling; and Section (7) draws conclusions and opportunities for future work.

We focused on papers that address snowfall, snowpack and snow hydrology processes in Mediterranean mountains. We did not focus on the climate change impact studies, which already represent an important body of the literature *per se*. Interested readers can refer to Beniston (2003), Beniston and Stoffel, (2014), de Jong et al., (eds) (2005), and de Jong et al., 2012) for additional information regarding the potential impact of climate changes on mountain hydrology and water resources in Mediterranean regions.

2.2 Method

2.2.1 Geographic extent of the review

The Mediterranean climate is found on the western part of the continents between latitudes 30° and 45° (Bolle (ed.), 2003). The land regions around the Mediterranean Sea (southern Europe, Northern Africa and the Levantine region) form the largest area of this type of climate. The Mediterranean climate is also found in the western Coastal USA (California, and western Oregon), and the Central Andes of Chile and Argentina (Fig. 2.2). Limited regions in Southern Australia and southern Africa are also classified as Mediterranean (not shown). A combined Koppen (Kottek et al., 2006) and mountain classification scheme (Viviroli et al., 2007) was used to better distinguish the mountain regions associated with the Mediterranean climate (Fig. 2.2). The Koppen climate scheme defines five main groups and multi subtypes according to the long-time annual and monthly temperature means and precipitation totals. Of particular interest to this study are the Mediterranean (Csa, Csb) regions and the regions influenced by Mediterranean climate, such as the adjacent maritime zones (Cfb, Cfc) and the semi-arid regions (BSh, BSk). The Viviroli et al., (2007) scheme distinguishes a total of 15 relief patterns by combining elevation and a relief roughness indicator, and it was used to distinguish between mountainous and lowland areas.

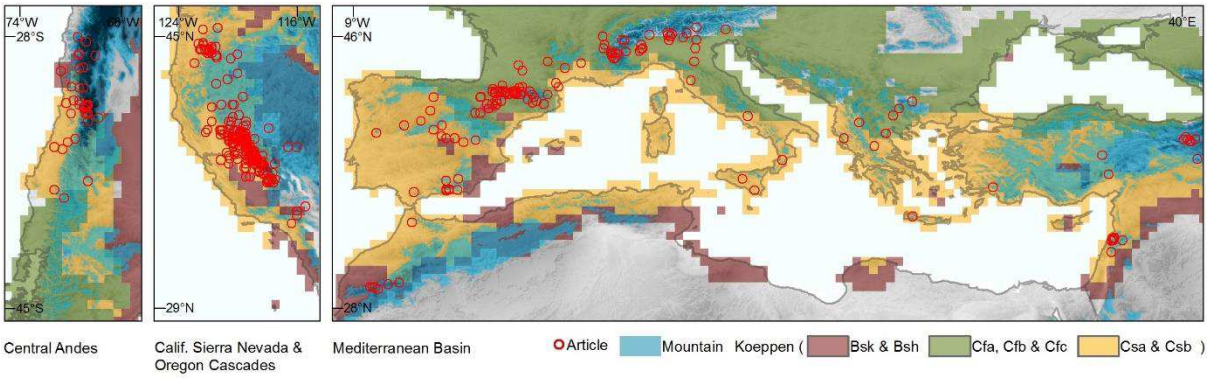

Fig. 2.2. Mediterranean mountain regions (a) Central Chile (b) western USA and (c) Mediterranean Basin. Mountain regions were derived using the Viviroli et al., (2007) scheme based on the global multi-resolution terrain elevation data (GMTED2010) at 15-arc second resolution (Danielson et al., 2011), and they are shown in light blue; the three main distinct climates portray the Mediterranean (Csa, Csb) shown in light orange, oceanic and maritime climates (Cfb, Cfc) in dark olive, and the semi-arid regions (BSh, BSk) in plum (Kottek et al., 2006). The red dot indicates the coordinates associated with each paper in the database.

2.2.2 Bibliographic sources

We used the website of the three major scientific publishers (Elsevier, Wiley, and Springer), Google Scholar, ReadCube, and open access journals websites to find articles from the early 1900's to the present, in which snow, hydrology, and mountain hydrology and climatology appeared in the title or abstract, or as a keyword. Only articles published in peer-reviewed journal with an impact factor greater than one and articles related to the Mediterranean regions presented above were considered. A second round of screening focused on reading the abstract and identifying articles where snow properties, snow hydrology and mountain hydroclimatology are considered as part of the article's main objectives. As much as possible, we avoided papers where snow was addressed in a marginal context. Hundreds of articles were identified during the initial screening. A total of 620 articles, (published in 82 different journals) (Fig. 2.3a.), were retained after the second screening. A table with the metadata for the articles is provided in Appendix (A2).

We identified a list of 35 different indicators that correspond to key research areas (Appendix A3). These were classified under three major groups (science, methods, and data) and subdivided into different categories. The first group focuses on science and it includes three categories: (1) meteorology and climatology in mountains (e.g., mountain climate, climate change and variability, climatology and meteorology, and hydrometeorology (inc. hydroclimatology), (2) snow (e.g., snow hydrometeorology (inc. climatology), snow properties,

and snow hydrology) and (3) hydrology (e.g., mountain hydrology, hydrology in snow-dominated basins, and hydrogeology in mountains). The second group focuses on the following methods: (4) methods used to quantify the snow cover extent (e.g., remote sensing of snow); methods used to describe the spatial distribution of snowpack indicators (e.g., spatial statistics and trends in climate, snowpack, and hydrology); and methods used to simulate the main characteristics of snow accumulation, snow duration, and snowmelt processes (e.g., snow energy and mass balance simulation, hydrological modeling). The third group emphasizes the following: (5) data (i.e., length of data used, source and type of data (i.e., ground observations, projections, and reanalysis), and spatial scales (extent of the study area and elevation range). Each article was associated with a pair of longitude and latitude coordinates, which represent the approximate centroid of the study area highlighted in the paper, and each article was reported on a map that shows both the Koppen climate classes and the mountain regions, as defined by Viviroli et al., (2007) (Fig. 2.2).

Using our personal criteria, each article was classified under one or two major science topics (see categories 1-3 above) and a methodological approach (see category 4 above). We then combined both in a single label. For instance, Maurer et al. (2007) addressed streamflow trends in snow dominated regions where climate change, hydrology, snow and streamflow timing were all considered. Hence, since the article emphasizes on the use of a hydrologic model for streamflow in mountain regions the paper was categorized under the "trends in snowpack and hydrology, using distributed hydrological model".

2.3 Description of the articles database

2.3.1 Mountain ranges

Mountain regions covered in this review include the following (Fig. 2.3b): (1) the coastal regions of western United States (Bales et al., 2006) including the Oregon Cascade (Sproles et al., 2013) and California Sierra Nevada Mountains (Guan et al., 2013a; Molotch and Meromy, 2014); (2) the central Andes that cover two of Chile's major natural regions – Chile's central and southern zones (Favier et al., 2009; Cortés et al., 2011; Valdés-Pineda et al., 2014); the major mountain chains around the Mediterranean Sea (López-Moreno et al., 2011a) namely; (3) Spanish (López-Moreno et al., 2014) and French (Gascoin et al., 2015) Pyrenees; (4) Spanish Sierra Nevada Mountains (Pimentel et al. 2015); (5) French and Italian Maritime Alps (Dedieu et al., 2014) – which are under the influence of the Mediterranean climate (Durand et

al. 2009); (6) Turkey and the Armenian Plateau (Tekeli, 2008); (7) Mount Lebanon and Anti Lebanon Ranges (Mhawej et al., 2014); and (8) Moroccan Atlas (Marchane et al., 2015). Little information was found on other Mediterranean Sea Mountains (López-Moreno et al., 2011a) such as the Iberian Peninsula Mountains (Morán-Tejeda et al., 2014), Italian Apennines (Martelloni et al., 2013), Southern Calabrian mountains in Italy (Senatore et al., 2011), Julian Alps (Italy and Slovenia), Dinaric Alps (mostly over Croatia and Bosnia and Herzegovina), Bulgarian mountains (Brown and Petkova, 2007), Pindos (Greece), Rhodope (Greece), and Taurus (Turkey).

2.3.2 Bibliometric analysis

Papers that covered local and regional scale studies accounted for ~90% (of all 620 papers), the remaining (~10%) were global studies and review papers. The majority of all articles (90.5%) were published between 2000 and 2016 inclusive, and half of all articles (53.4%) were published over the past five years (2011-2016) (Fig. 2.3a). The remaining (<10%, not shown) were published between 1913 and 1999, of which ~85% were published between 1990 and 1999. Approximately 66.5% of all articles were published in 10 journals (Fig. 2.3a). Over the past 16 years (2000-2016), papers covering the California, Sierra Nevada Mountains amounted to 30% of the local and regional scale studies (41% when the regional scale studies over the western United States are included). Spanish Pyrenees (10%) and the Chilean central Andes (6%) were among the most studied mountain regions (Fig. 2.3b). Fig. 2.3c highlights the yearly number of published papers in the first three major Mediterranean regions (2000-2016).

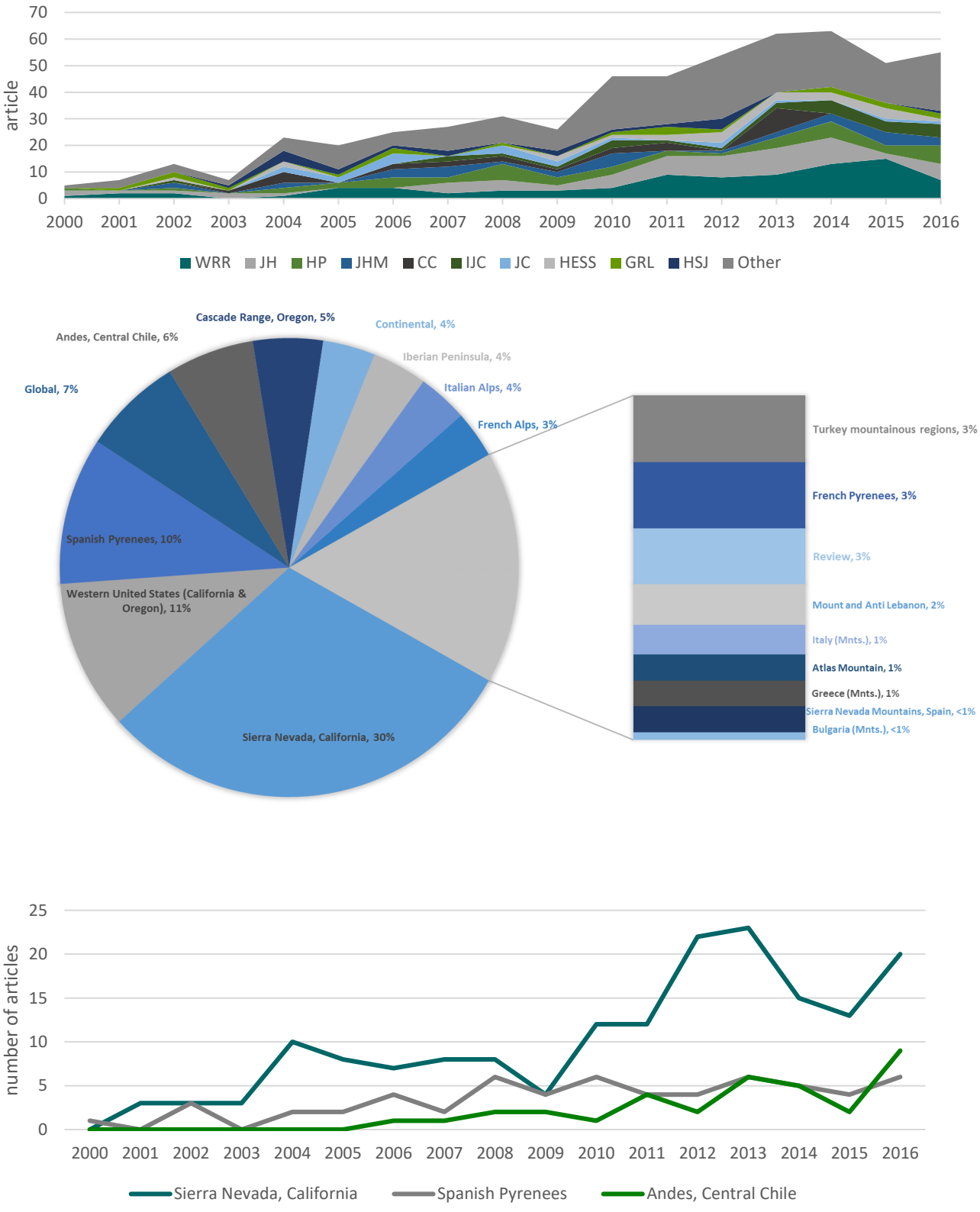

Fig. 2.3. Key bibliometric indicators were the following (from top to bottom): (a) cumulative yearly number of publications per journal (based on 561 articles published between 2000 and 2016); (b) Distribution of studies by major mountain regions shown; and (c) number of yearly published papers in California (excluding western US regional studies) (30%), Spanish Pyrenees (10%), and Chilean Central Andes (6%).

2.3.3 Thematic analysis

The papers cover multiple scales: (1) experimental sites and small catchments (Storck et al., 2002; Franz et al., 2010; López-Moreno et al., 2010, 2013b; Bales et al., 2011; Liu et al., 2013; Raleigh et al., 2013; Harpold et al., 2014; Girotto et al., 2014; Revuelto et al., 2016a; Marti et al., 2016); (2) snow-dominated basins (Lundquist et al., 2010; Powell et al., 2011; Rousselot et al., 2012; Smith et al., 2013; Welch et al., 2013; Cortés et al., 2014; Franz et al., 2014; Telesca et al., 2014; Marchane et al., 2015); (3) multiple basins, mountain ranges, and regional scales (Painter et al., 2009; López-Moreno et al., 2011a; Pavelsky et al., 2011; Guan et al., 2013b; Núñez et al., 2013; Slater et al., 2013; Stewart, 2013; Avanzi et al., 2014; Hüsler et al., 2014; Cornwell et al., 2016); and (4) continental scales and the global scale (e.g., Nohara et al., 2006; Pepin et al., 2015). The studies provide information on (1) mountain climatology and meteorology (Bonfils et al., 2008; Herrero and Polo, 2012; Pavelsky et al., 2012; Lute and Abatzoglou, 2014; Lundquist et al., 2015a; Guan et al., 2016); (2) long-term hydroclimatology and snowpack trends in mountains (López-Moreno and García-Ruiz, 2004; Hamlet et al., 2005; Mote et al., 2005; Stewart et al., 2005; Masiokas et al., 2006; McCabe et al., 2007; Pierce et al., 2008; Das et al., 2009); (3) meteorological forcing and topographic controls on snowfall and snowpack in mountains (Anderton et al., 2004; Guan et al., 2010; Rice et al., 2011; Musselman et al., 2012; Trujillo et al., 2012; Wayand et al., 2013; Ayala et al., 2014; Molotch and Meromy, 2014; Hinkelman et al., 2015; Lapo et al., 2015; López-Moreno et al., 2015; Harpold, 2016); (4) snowpack properties (Mizukami and Perica, 2008; Perrot et al., 2014; Trujillo and Molotch, 2014); (5) snow accumulation and ablation (Harpold et al., 2012; Meromy et al., 2013; Guan et al., 2013a; Avanzi et al., 2014; Sade et al., 2014); (6) snowmelt runoff (Tekeli et al., 2005a; Herrero et al., 2009; Şorman et al., 2009; Franz and Karsten, 2013; Liu et al., 2013; Jepsen et al., 2016a); and (7) different hydrological (Aguilar et al., 2010; Kourgialas et al., 2010; Lundquist and Loheide, 2011; Goulden et al., 2012; Schlaepfer et al., 2012; Harpold et al., 2015; Penna et al., 2015; Harpold, 2016); and (8) hydrogeological processes (Tague and Grant, 2009; Lowry et al., 2010) in snow-dominated mountain regions.

Given the variety of the topics covered in the literature, we found that the most relevant approach for synthesizing them is to treat the three main vertical levels of the hydrosystem from the atmosphere to the bedrock separately: (1) climate forcing to the snowpack, (2) snowpack spatio-temporal variability, and (3) snowmelt hydrology and hydrogeology. A synthesis on climate forcing, snowpack dynamics, and hydrological processes is presented in Table 2.1 and

further discussed in detail under sections 4-6, respectively. Fig. 2.4 summarizes the key elements of the energy fluxes and mass balance in a typical Mediterranean mountain context.

Early studies published prior to the '90s emphasized on mountain meteorology, ground observations of the snowpack, and the theoretical aspects of snow energy balance and snowmelt-runoff models. The time period between 1990 and 1999 witnessed a diversification in the topics with a focus on the quantification of the snow water equivalent, snow interception in forests, hydrology and hydrogeology in snow-dominated basins– including hydrochemical analysis of snowmelt runoff. In this period, the first studies on the changes in snowpack and streamflow under global warming were published. Few studies were based on remote sensing (5%).

After 2000, the number of scientific publications increased exponentially each five years. Such a growth rate is higher than the doubling time for natural sciences, which is estimated at 8.7 years (Bornmann and Mutz, 2015). Fig. 2.5 summarizes the number of published papers (2000-2016) based on their key category. The main scientific area was the effect of meteorological and climatological variables on the snow hydrology that accounted for 29% of the studies (Fig. 2.5), of which about a half were dedicated to assessing climate change impacts on the hydrology and the snowpack. 25% and 7% of the studies were dedicated to hydrology and hydrogeology, respectively. The snowpack modeling accounted for 13% of the studies, and the snow remote sensing for 8% (Fig. 2.5).

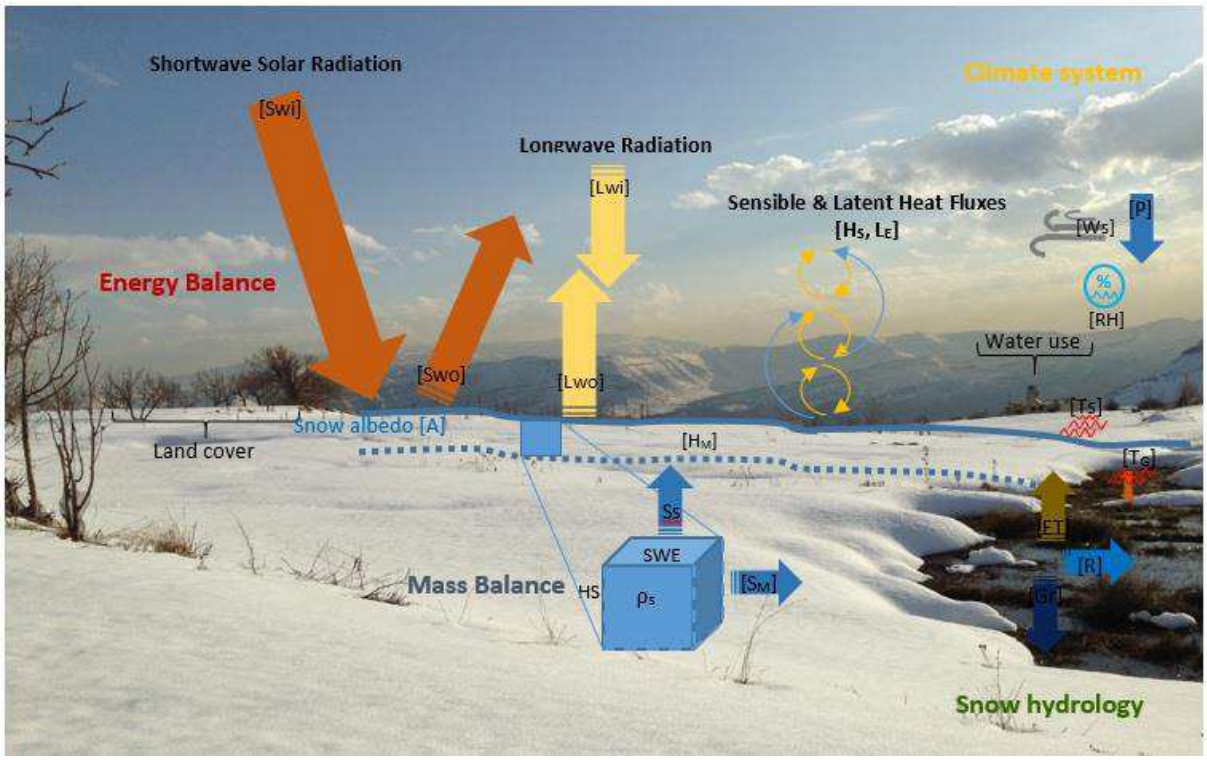

Fig. 2.4. Major climate forcing and snow processes in Mediterranean-like mountainous regions with emphasis on the specific objectives shown here for mountain hydrology and snowpack dynamics. Where SWi and SWo are incoming and outgoing shortwave radiation, respectively; Lwo and Lwi are the emitted and incoming longwave radiation, respectively; P is precipitation, Ws is wind speed, and RH is relative humidity; HM is sensible heat fluxe; Ts is surface temperature and Tg is ground temperature; HS is snow depth, ds is snow density, and SWE is snow water equivalent; Ss is snow sublimation and Sm is snow melt; ET is evapotranspiration, R is surface runoff, G is subsurface and groundwater flow. The background image was taken in Laqlouq at 1850 m a.s.l. (Mount-Lebanon) on February 20th, 2016 (courtesy of the author).

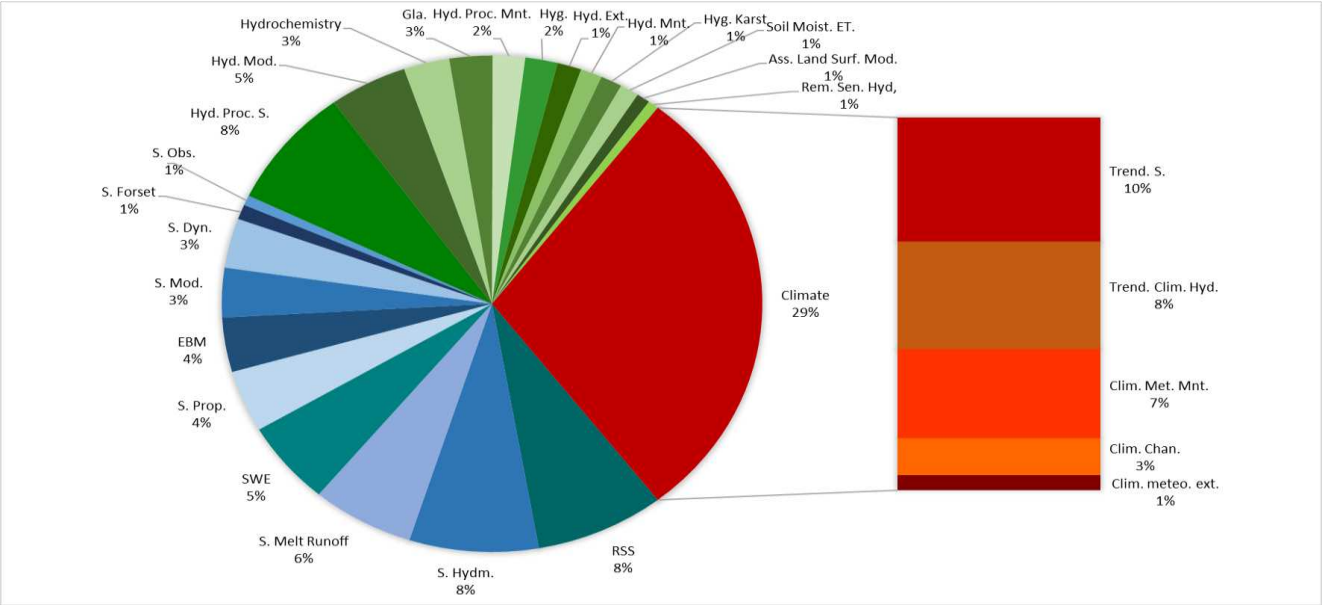

Fig. 2.5. Distribution of papers by science groups and key sub-categories with emphasis on climate forcing to the snowpack (29% of all studies, shown in red), snow studies (39%, blue), and snowmelt hydrology and hydrogeology (32%, green). S. is snow; Trend S. indicates a study that emphasis addressing climate change impacts on snow. RSS indicates a paper that focuses on remote sensing of snow. EBM indicates a study that describes and testes an energy balance model (see appendix A3 for a detailed list of indicators).

Table 2.1. Summary of key science topics identified in the literature; in addition, the table lists major variables, scales and sources of uncertainty.

Topic	Main variables of interest	Main source of data	Main methods	Major sources of uncertainty
Climate forcing to the snowpack	Near-surface meteorological variables (air temperature, air humidity, precipitation, longwave and shortwave radiation); latent and sensible heat.	Ground observations (automatic weather stations); reanalysis data.	Mesoscale atmospheric model (e.g., WRF); assimilation techniques; downscaling; spatial interpolation.	Lack of weather stations at high-elevation; high spatial variability of the climate in mountains; lack of long time series; snowfall undercatch by precipitation gauges; few radiation and flux measurements
Snowpack spatio-temporal variability	Snow cover area, snow depth, snow density, snow water equivalent, snow albedo.	Field measurements; Automatic weather stations, space borne remote sensing products; terrestrial remote sensing (Lidar, camera).	Temperature index model; regression analysis; modeling of snowpack mass and energy balance.	Spatial variability of snow depth; inter-annual variability of SWE; difficulty to sample large areas in the field; cloud and canopy obstruction in optical remote sensing; large errors of SWE retrievals in complex topography by microwave remote sensing.
Meltwater hydrology	Surface runoff, soil moisture, evapotranspiration, groundwater flow and recharge.	Gauging stations; remote sensing; hydro-chemical testing for streamflow and groundwater recharge.	Water balance, hydrological and hydrogeological modeling.	Medium to high difficulty in conducting measurements; heterogeneity of mountain topography and land cover; mixed rain/snow regimes; lack of sub-surface measurements.

2.4 Climate forcing to the snowpack

The two processes that control snowpack dynamics in mountains are snow accumulation and ablation. The accumulation is mainly forced by snowfall and this mainly depends on precipitation and temperature (López-Moreno, 2005), while the ablation is driven by radiation and heat fluxes between the atmosphere, the snowpack and the underlying soil (Herrero et al., 2009). The near-surface wind also influences both accumulation and ablation (e.g., Gascoin et al., 2013) (see Sect. 5).

2.4.1 Near-surface meteorological observations

The minimum meteorological data to run a temperature index snowmelt model are the precipitation and the air temperature (DeWalle and Rango, 2008). A typical 1D (vertical) snowpack energy balance model requires additional data of air relative humidity, incoming shortwave and longwave radiation and wind speed. The wind direction is only useful to simulate wind drift and lateral heat advection (e.g., Burns et al., 2014), in case of a patchy snow cover (e.g., Liston, 1995). However, information on the spatial distribution of the main meteorological variables remains incomplete in Mediterranean mountains, such as in most of the world's mountains (e.g., Bales et al., 2006). This has been attributed to the following:

(1) The sparseness of the automatic weather stations (AWS) networks (Horel and Dong, 2010; Gottardi et al., 2012; Valdés-Pineda et al., 2014; Henn et al., 2015). Even in well-monitored regions most of the AWS are usually below 3000 m a.s.l, although meltwater production generally increases with elevation (Favier et al., 2009).

(2) The number of variables being measured at the AWS (Raleigh et al., 2016). A survey based on 1318 AWS across the western US, where meteorological data and either SWE or snow depth are measured, indicated that near-surface forcing variables of air temperature and precipitation are among the most sampled (99-83%) whereas wind speed, humidity (often as relative humidity RH), and incoming shortwave radiation are measured 24-36% of the time. Incoming longwave radiation is the least measured (1.4%). Nearly 99% of all AWSs do not measure all six forcing variables (Raleigh et al., 2016).

(3) Biases and uncertainties that arise from observational data. AWS are prone to data logging failure; some sensors require periodic calibration and the data must undergo specific quality control given the harsh climatic conditions encountered in high-elevation areas (Estévez et al., 2011; Filippa et al., 2014; Lundquist et al., 2015a).

Radiative and turbulent fluxes in Mediterranean mountain regions can be calculated from meteorological and incident solar radiation and thermal radiation observations (e.g., using pyranometer and pyrgeometer) at experimental sites (e.g., Marks et al., 1992). There are few flux tower locations (e.g., Goulden et al., 2012; Burns et al, 2014) and specific research sites, such as the CUES in California, which feature a full range of censors for measuring the snow energy balance (Bair et al., 2015). Flux towers equipped with eddy covariance system and specific stations equipped with pyranometers and pyrgeometers remain the two options for measuring the sensible heat, latent heat, and radiative fluxes. However, most of the available flux towers are generally located at flatter lowland areas and provide little information needed

to evaluate fluxes in snow ablation in complex mountain regions (Bales et al., 2006; Raleigh et al., 2016). Studies that address snow energy balance in snow-dominated regions (e.g., Sproles et al., 2013; Mernild et al., 2016a) rely on solving the energy balance solely from meteorological observations (e.g., Liston et al., 1999; Herrero et al., 2009). This led has resulted in the current availability of limited information for validating the contribution of radiative and turbulent fluxes (Lapo et al., 2015; Raleigh et al., 2016).

2.4.1.1 Precipitation

In Mediterranean mountain regions, more than 80% of the annual precipitation falls during winter (November to March for the Northern Hemisphere and May to September in the Southern Hemisphere) (Mazurkiewicz et al., 2008; Demaria et al. 2013a; López-Moreno et al. 2013a). Mountain regions such as the Sierra Nevada, California receive 75-90% of winter precipitation in the form of snow (Jepsen et al., 2012). Mountain regions tend to receive more precipitation than surrounding lowland areas due to the orographic enhancement (Favier et al., 2009; Neiman et al., 2014; Lundquist et al., 2015a; Derin et al., 2016).

The assessment of the distribution of precipitation amounts in mountain regions and an accurate identification of the precipitation type (snow or rain) emerge as the most uncertain factors in the literature (Gottardi et al., 2012; Neiman et al., 2014; Dettinger, 2014; Buisan et al., 2014; Derin et al., 2016). Uncertainties in the precipitation distribution over mountain regions are associated with (1) snow gauge undercatch (Sevruk et al, 1991; Rasmussen et al., 2012), (2) precipitation phase determination (e.g., Harpold et al., 2017), (3) methods for estimating spatial precipitation distribution, including the precipitation lapse rates (Lundquist et al., 2015a; Henn et al., 2017), and (4) the heterogeneity of the precipitation network (Favier et al., 2009; Rice and Bales, 2010; and Gottardi et al., 2012).

Wind-induced precipitation undercatch affects the accuracy of precipitation data and is more pronounced for solid precipitation than for liquid precipitation (Rasmussen et al., 2012; Buisan et al., 2016; Smith et al., 2016; Pan et al., 2016). Measurement errors due to gauge undercatch frequently range between 20% and 50% (Rasmussen et al., 2012). The factors that govern snow undercatch are related to the gauge setting (i.e. shielded and unshielded) (Colli et al., 2015), snowflake characteristics (Theriault et al., 2012), and wind speed (Rasmussen et al., 2012). Despite its importance little information was found in the literature on snow undercatch in Mediterranean regions.

Precipitation phase determination is often done as post-processing given that most gauges do not detect the phase. The phase is required to determine the water equivalent during

the accumulation season, but also to properly correct precipitation undercatch, and for investigating rain-on-snow events which contribute to the snowpack ablation. Determining precipitation phase from ground observation can be achieved using (1) thresholds for temperature (e.g., air, dewpoint, and wet bulb) (see Marks et al., 2013), (2) linear transition, range, and sigmoidal curve methods based on near-surface air temperature (e.g., Harpold et al., 2017), and (3) psychrometric energy balance method (Harder and Pomeroy, 2013). Despite the availability of these methods, one of the major limitation for the proper determination of precipitation phase from ground data is attributed to the lack of meteorological observations for stations in near locations to the precipitation gauges (Harpold et al., 2017).

Rain-on-snow events are not uncommon in Mediterranean mountains (Guan et al., 2016). These events help in warming the snowpack and add very high sensible heat to the snowpack through condensation, which accelerates melting and sometimes triggers catastrophic floods (McCabe et al., 2007; Surfleet and Tullos, 2013). In the western United States, rain-on-snow-events appear to be partly driven by the El Niño–Southern Oscillation (ENSO), the Pacific Decadal Oscillation (PDO) (McCabe et al., 2007; Lute and Abatzoglou, 2014) and atmospheric rivers (Trujillo and Molotch, 2014; Guan et al., 2016). To our knowledge, the impacts of rain-on-snow events were not specifically addressed in regions other than the western USA. The analysis of rain-on-snow events remain challenging and warrant future investigation (Wayand et al., 2015).

Uncertainties associated with the spatial distribution of precipitation increases with elevation, where differences between datasets ranged between 5 to 60%, exceeding 200 mm yr-1 on average, were reported across the Western United States (Henn et al., 2017). Different methodologies were developed to compute the integrated precipitation in high-elevation watersheds (Valery et al., 2010) and to generate gridded precipitation maps from daily ground observation (see Demaria et al., (2013b) and Lundquist et al., (2015a) for a list of gridded precipitation products). The emergence of gridded precipitation products over the 2000s has boosted the research in snow hydrology and facilitated the upscaling of point-scale studies. Precipitation grids are invaluable data for distributed hydrological modeling in both the operational and research context, e.g., to perform climate change impact studies at the scale of river basins (Mernild et al., 2016b). While the overall accuracy of gridded precipitation products has been deemed satisfactory, the biases increase with elevation (Mizukami et al., 2011; Lundquist et al., 2015a). Precipitation-gauge undercatch, a poor knowledge of wind patterns to correct the undercatch, and the lack of in situ input data are sources of errors in the gridded precipitation products (Dettinger, 2014; Lundquist et al., 2015b; Mizukami and Smith, 2012).

In addition, temporal inconsistencies in multi-year gridded precipitation biases tend to increase the uncertainty in simulating hydrological responses in snow-dominated basins (Mizukami and Smith, 2012).

Acquiring precipitation and snowfall from high-resolution satellite-based rainfall (SBR) products (e.g., TRMM and GPM) in mountain regions (Derin et al., 2016), such as the western US (Behrangi et al., 2016), and northeastern Spain (Kenawy et al., 2015), is still hindered by the facts that (1) capturing solid precipitation is practically challenging for TRMM and results are highly biased over snow surfaces, (2) precipitation satellites tend to underestimate the wet season and overestimate dry season precipitation rates over land and should be corrected using in situ measurements; and (3) the performance of gauge correction to SRB is less effective in mountain regions and depends on the representativeness of the observation networks.

Over the past decade there had been an increase in the use of assimilation techniques and the downscaling of atmospheric model (e.g., Vionnet et al., 2016, Mernild et al., 2016a). These different techniques to estimate precipitation using a combination of ground observations, numerical weather prediction, and remote sensing observations are still not complete and the generated gridded data is at coarser and medium resolution at best (e.g., Quéno et al., 2016). There is more work needed to understand how atmospheric circulation (Jin et al., 2006; Lundquist et al., 2010) and the complex topography at the finer scales (López-Moreno et al., 2015) affects precipitation and snowfall and both topics are interesting field of research. An intercomparison between different gridded precipitation datasets (e.g., Lundquist et al., 2015a; Henn et al., 2017) across different mountain regions is needed. Reducing the bias in precipitation estimates along altitude and enhancing the spatial resolution of gridded precipitation could be the next breakthrough in mountain hydrology.

2.4.1.2 Air temperature

The air temperature is the most important factor that determines the precipitation phase (rain or snow), and it is strongly correlated to the snowmelt rate (Jin et al., 2006; Mote, 2006; Brown and Petkova, 2007; Kapnick and Hall, 2010). During the melting season in the mid-elevation regions of the Spanish Pyrenes, the increase in the daily snowmelt rates was correlated with the increase in the observed daily temperature (López-Moreno and Latron, 2008). In many low and mid-elevation Mediterranean mountain regions, changes in the surface air temperature had been previously identified as the major driver for the reduction in the amount of precipitation that falls as snow, the decline in the snow water equivalent, and shifts towards

earlier snowmelt (Stewart et al., 2005; Bonfils et al., 2008; Demaria et al. 2013a; Pagán et al., 2016).

Similar, to all other meteorological variables, uncertainties associated with measuring the air temperature arise from the lack of AWS in remote and high-elevation mountain areas (Raleigh et al., 2016). However, air temperature is the climatic variable that is the most often available from in situ and gridded-products. In comparison with precipitation, the in-situ measurements of temperature are much less biased and the interpolation methods are more robust. From the papers we could examine, the uncertainty on the precipitation data is generally considered as a more important issue.

2.4.1.3 Radiation and heat fluxes

In Mediterranean mountain regions, the snowpack melt energy is dominated by the radiative fluxes (shortwave and longwave) (Marks and Dozier, 1992; López-Moreno et al., 2012). The net radiative flux accounts for approximately 70-80% of the energy for snow melt in regions, such as Sierra Nevada California, Oregon Cascades, Spanish Pyrenees, and the Armenian Plateau (Marks and Dozier, 1992; Şensoy et al., 2006; Mazurkiewicz et al., 2008; López-Moreno et al., 2008; Hinkelman et al., 2015). However, this contribution varies significantly over the time and the location. For instance, the net radiation contribution to melt at three different sites in the Oregon cascades was found to range between 49 and 80% (Mazurkiewicz et al., 2008). Similar results were found in the Armenian Plateau, which indicates that the net radiation fluxes and turbulent fluxes account for 70 to 30% of the melt energy, respectively (Şensoy et al., 2006). Sensible and latent heat transfers were found to be of similar magnitude with an opposite sign, and therefore they tend to cancel each other in some sites during the now-melt season (Marks and Dozier, 1992; Jepsen et al., 2012). A significant amount of snow is lost through sublimation in Mediterranean mountains, approximately 20% of the total snowpack ablation depending on the location, and this amount increases at the end of the snow season (Beaty, 1975; Marks and Dozier, 1992; Jepsen et al., 2012). The net turbulent flux tends to increase during the melt season. Its contribution to snowmelt during the entire season was found to range between 0 to 19% in a mountain basin in Sierra Nevada California (a mean of 10% with a standard deviation of 6% over a time period of 12 years) (Jepsen et al., 2012). The contribution of the turbulent energy fluxes was found to increase under rain-on-snow events, and it accounts for up to 42% of snowmelt during such events (Mazurkiewicz et al., 2008). The contribution of turbulent fluxes (i.e., latent and sensible heat fluxes) to melt energy was found to be slightly higher in warmer Mediterranean regions (Atlas

Mountain, Iberian Peninsula and Eastern Mediterranean) (Schulz and de Jong, 2004; Herrero et al., 2009; Sade et al., 2014). Under extreme weather conditions (i.e., episodic strong low-humidity winds, clear skies, intense solar radiation, and sudden increases in temperatures), sublimation accounted for up to 40% of the total loss in snowpack in Sierra Nevada, Spain (Herrero et al., 2009), and similar results were reported for the Atlas Mountain (Schulz and de Jong, 2004) and Mount Hermon (Sade et al., 2014).

In the absence of radiation sensors (pyranometer and pyrgeometer), the incoming radiation can be estimated using (1) empirical relationships with surface air temperature and relative humidity (Jepsen et al., 2012; Lundquist et al., 2013) or (2) solar and longwave surface irradiance data from synoptic satellite products (Jepsen et al., 2012; Hinkelman et al., 2015). However, computing radiative fluxes using empirical methods can lead to overestimation errors of up to 50% in the snowmelt rates, which indicates the need for enhanced methods that combines satellite products and ground observations (e.g., Hinkelman et al., 2015). The application of such products to Mediterranean mountains should account for the fact that shortwave and longwave radiations vary significantly with elevation, terrain geometry and the forest cover (Aguilar et al., 2010; Raleigh et al., 2013, Lundquist et al., 2013).

Sensible and latent heat exchange are influenced by surface air temperature, water vapor, and wind speed (Marks and Dozier, 1992; Kim and Kang, 2007; Jepsen et al., 2012). Most of these variables exhibit high spatial variability over the complex mountainous topography (Marks and Dozier, 1992), which makes it difficult to achieve reliable estimates of the contribution of snowmelt from heat fluxes at most sites. Furthermore, while the surface air temperature is measured at most AWS, information on wind speed and humidity are often lacking, and thus, this hinders the calculation of sensible heat fluxes (Raleigh et al., 2016).

Our understanding of the energy exchange between the snowpack and the atmosphere in mountains is incomplete. The installation of more complete meteorological stations (including longwave/shortwave sensors and turbulent heat measurement systems) in mountains is needed in order to better characterize the different components of the energy balance. However, this requires solving the issue that eddy covariance systems are not considered reliable in complex terrain.

2.5 Snowpack

2.5.1 In situ observations

Historical studies on snow properties and the quantification of the waterthat falls as snow are more than 300 years old (Grew, 1673), and the importance of snow cover on climate was first highlighted by Woeikof (1885). The first published investigations of snowfall, HS, snow density, SWE and snow melt, and the first method for field sampling of snow and snow instrumentation in California can be dated to the late 19th and early 20th centuries (e.g., Church, 1913). Monthly snowfall observations in California date back to 1878 (Christy, 2012). Over the past two decades, there has been a significant increase in the number of studies that investigates HS, snow density, and SWE through manual field sampling (Bocchiola and Groppelli, 2010; Sturm et al., 2010; López-Moreno et al., 2013b; Bormann et al., 2013; Ayala et al., 2014), HS measurements using (acoustic) snow depth gauges, SWE measurements with snow pillows, and snow density measurements from HS and SWE observations (e.g., SNOTEL network) (e.g., Rice and Bales, 2010; Meromy et al., 2013; Luce et al., 2014).

The main variable of interest for snow hydrologists is the SWE, which is obtained by multiplying the snow height by the snow density. The snow height is typically measured with a calibrated snow probe and it is easier to estimate than the snow density, which requires a more elaborate field-work (e.g., Bocchiola and Groppeli, 2010; Sturm et al., 2010; López-Moreno et al., 2011b). Field measurements are usually biased with observational errors (Lundquist et al., 2015b) and uncertainty about the representativeness of in-situ snow depth and density measurements (López-Moreno et al., 2011b, 2013b). Improving the in-situ accuracy of snow courses measurements can be achieved by increasing the rate of data sampling along the snow course and minimizing human errors. Findings in the Spanish Pyrenees indicated that increasing the number of in-situ measurements (i.e., using at least five snow depth measurements at 5-10 meter intervals) could ensure a bias of less than 10% when estimating the average snow depth at plots of 100 m^2 (López-Moreno et al., 2011b). The snow density exhibits less variability than the snow depth (López-Moreno et al., 2013b), which implies the need for fewer snow density measurements along each course. Such findings support the US snow courses sampling guidelines, which indicates the need for 10 point measurements of HS, SWE, and density at 30 meter interval (over a 300 m transect) (Rice and Bales, 2010). The same applies for snow sampling approaches in other regions (e.g., Watson et al., 2006; Jost et al., 2007). However, collecting in-situ probe measurements at larger scales remains challenging. Steeps slopes and high-elevation areas (above 3000 m a.s.l) are unsafe and not easily accessible. Airborne and

terrestrial Lidar now enable the measurement of HS with a centimetric accuracy at a much higher resolution than manual surveys (Sect. 5.2.4). However, these techniques remain costly and do not provide continuous observations of HS like AWS. A terrestrial time-lapse camera is a cost-effective device used to monitor the snow cover variability in space and time, but its use is restricted to small spatial scales (less than 1 km²) (Revuelto et al., 2014). As a result, it is difficult to capture the temporal variability of the HS and SWE by field sampling. On the other hand, continuous AWS measurements of snow depth and SWE remain site specific, and most of the time, they fail to capture the spatial variability of the snowpack due to the spatial heterogeneity of the climate and terrain with respect to the network density (Bales et al., 2006; Gottardi et al., 2012; Raleigh et al., 2016).

Some regions are equipped with advanced snow observatories and the data are easily accessible (e.g., SNOTEL in the West USA) while other mountain regions, such as the Pyrenees, are well covered by ground stations but the data are to be collected from various agencies and are not always publicly distributed (e.g., Gascoin et al., 2015). The implementation of snow observatories based on the principles of open data is en route in regions such as Lebanon where snow observations are recently being collected (e.g., Fayad et al., 2017). Extending the ground-based observation networks remains crucial in mountain regions that remain under-sampled, however it is as important to share these data to foster their use by the scientific community and among water stakeholders.

2.5.2 Remote sensing of seasonal snow cover

The snow cover extent, albedo, height, and water equivalent are the main remote sensing products for snow hydrology, but they have very different levels of accuracy and resolution. Here, we only briefly present the main products that were used in our list of papers. Interested readers can refer to Dietz et al. (2012) and Frei et al. (2012) for further information on snow remote sensing.

2.5.2.1 Optical remote sensing of the snow cover

The NASA MODIS Aqua/Terra daily snow products (collection 5 MOD10A1 and MYD10A1 (Hall et al., 2002)) are the most widely used. These products have provided the binary snow-covered area (SCA) and fractional SCA (fSCA), and the snow albedo at a500 m resolution since 2000 for Terra and 2002 for Aqua. The SCA product allow the calculation of the snow cover duration (SCD), snow cover start date (SCS) and snow cover melt-out date (SCM). The SCA and fSCA allow the calculation of the snow coverage in a watershed. MODIS

snow products were tested and applied in the Sierra Nevada California (Painter et al., 2009; Molotch and Meromy, 2014), Pyrenees (Gascoin et al., 2015), Southern Alps (Dedieu et al., 2014), Moroccan Atlas (Marchane et al., 2015), Armenian Plateau (Tekeli et al., 2006), and Mount Lebanon (Telesca et al., 2014).

The main limitation of optical snow products is the obstruction by cloud cover. A cloud removal algorithm must be run to generate meaningful snow climatology from MODIS snow products (Gascoin et al., 2015; Marchane et al., 2015). There are also errors related to sensor viewing geometry and forest canopy obstruction (Dozier et al., 2008; Gao et al., 2010; Dietz et al. 2012; Raleigh et al., 2013; Kostadinov and Lookingbill, 2015).

In addition to the MOD10 family, there are more sophisticated approaches to retrieve sub-pixel fSCA, grain size, and albedo from MODIS using spectral unmixing techniques (Painter et al., 2009). The validation of the fSCA against higher resolution snow cover maps data obtained from Landsat ETM+ over the Sierra Nevada California, in particular, indicates their better accuracy compared to the MOD10A1 products (Dozier et al., 2009; Painter et al., 2009; Rittger et al., 2013). The accuracy of the fSCA is lower in forested areas, which suggests that there is a need for future research in this direction (Raleigh et al., 2013; Kostadinov and Lookingbill, 2015).

Snow cover extent and snow climatology had also been derived from AVHRR data at a spatial resolution of 1 km for the Alpine region (1985–2011) (Hüsler et al., 2014) and the Armenian Plateau (Tekeli et al., 2005a). Finally, Cortés et al., (2014) proposed and tested a sub-pixel approach for mapping snow and ice cover over the central Andes using spectral unmixing of Landsat imagery at a spatial resolution of 30 m (1986–2013).

Future improvement of snow cover representativeness from optical remote could include better cloud removal and enhanced snow cover mapping in forested regions. Daily SCA from MODIS are hindered by their spatial resolution of 500m which is too coarse to capture snow variability in heterogenous mountain slopes, in regions where snow is ephemeral, and at the end of the season when snow becomes patchy. The Sentinel-2 mission with its 20 m spatial resolution and 5 days revisit time is expected to provide better accuracy for mapping SCA in the heterogenous mountain regions.

2.5.2.2 Remote sensing of SWE

The retrieval of SWE form spaceborne passive microwave (PM) sensors involves a coarser resolution (~25 km) and limited accuracy (Dietz et al., 2012; Frei et al., 2012; Vuyovich et al., 2014; Dozier et al., 2016). PM sensors tend to underestimate SWE. For example, from

April 1st 2014 SWE estimates, the passive microwave AMSR2sensor underestimated the SWE by 40-75% compared to other SWE retrieval methods (i.e., interpolation from snow pillows and SCA, calculation using SCA and NLDAS, and modeling using SNODAS) (Dozier et al., 2016). Examples from the Mediterranean regions include the use of AMSRE/AMSR2 over the contiguous US (Vuyovich et al., 2014), California (Li et al., 2012), the Armenian Plateau (Tekeli, 2008; Şorman and Beser, 2013), and Mount Lebanon (Mhawej et al., 2014) and the use of the Scanning Multichannel Microwave Radiometer (SMMR) and Special Sensor Microwave Imagers (SSM/I) over the Andes (Foster et al., 2009).

PM sensors have limited capability in capturing the SWE in regions with ephemeral or patchy snow cover and regions with vegetation cover (Li et al., 2012; Vuyovich et al., 2014), and they exhibit an overall tendency to underestimate SWE during snowfall and melt seasons (Dozier et al., 2016). This was attributed to the high scattering in mountain regions due to relief (Li et al., 2012) and the tendency of PMs to saturate at an SWE value of 120 mm (for wavelength 18 GHz as the background signal and 37 GHz as the scattering signal) (Dietz et al. 2012).

Despite these limitations of PMs, a number of studies demonstrated that PMs are able to capture the overall seasonal variations of snow accumulation, melt timing, and season length at the macro scale, and in contrast to imaging spectrometry, they are not affected by cloud cover (Foster et al., 2009; Vuyovich et al., 2014). Coupling ground-observed data, SCA, and PM sensed SWE is being investigated as an alternative for enhancing the SWE estimation in Mediterranean regions (e.g., Vuyovich et al., 2014; Şorman and Beser, 2013).

2.5.2.3 Snow albedo

The importance of snow albedo in Mediterranean regions has been attributed to the fact that most of the snowmelt is dominated by net radiation (Sect. 4.1). A decrease in snow albedo results in an increased amount of absorbed shortwave radiation and eventually, an enhancement in the snowmelt (). Surface snow albedo changes in Mediterranean mountain regions are associated with snowpack thickness (Tekeli et al., 2006), snow grain size and surface wetness (Dozier et al., 2008, 2009), and snow impurities (mainly mineral dust and organic particles) (Lee and Liou, 2012). In California's Sierra Nevada, the reduction in the snow albedo during the melt season (March to April) is driven by the increase in surface temperature and the increase in the deposition of absorbing aerosols. Both temperature and aerosols contribute to the 61% decrease in snow albedo, and 26% of the albedo reduction was attributed to the increase

in the aerosol optical depth (Lee and Liou, 2012). Snow albedo can be calculated by observing the incoming and reflected solar radiation at AWS. Given the lack of in-situ observations, many studies have used optical remote sensing techniques. The method to derive snow albedo from imaging spectrometry is well developed in literature (e.g., Dozier and Painter, 2004; Seidel and Martinec 2004; Frei et al., 2012; Deems et al., 2013; Tedesco (ed.) 2015). In the Mediterranean context, most studies were conducted in Sierra Nevada California using MOD10A1 or MODSCAG MODIS albedo products (Painter et al., 2003; Dozier et al., 2009; Lee and Liou, 2012). In the Armenian Plateau, the MOD10A1 albedo was found to be consistent with in situ measurements in terms of magnitude and temporal variability, with a small positive bias due to differences in the acquisition time (Tekeli et al., 2006). On the contrary, in the Spanish Sierra Nevada, the coarse-resolution albedo products from MODIS and SPOT underestimated the in-situ snow albedo due to the mixing effects of snow and snow-free patches in a MODIS pixel especially during the melting periods (e.g., Pimentel et al., 2016).

Advances in airborne hyperspectral remote sensing have enabled the accurate estimation of snow surface cover, grain size and albedo at a relatively higher cost (e.g., Painter et al., 2003). Future research areas in surface snow properties can be found in Dozier et al. (2009), which indicates the need to better understand the spectral characteristics of snow from remote sensing sensors, to further investigate the consequences of dust and other impurities on snow reflectance, and to further investigate the coupling of snow properties and snowpack energy via models (e.g., Oaida et al., 2015).

2.5.2.4 High resolution airborne and ground-based remote sensing

Over the past few years, a number of studies have used ground-based terrestrial laser scanner (TLS) and airborne LiDAR to measure the snow depth at high spatial resolution with decimetric accuracy (e.g., in California (Harpold et al., 2014; Kirchner et al., 2014; Zheng et al., 2016), and the Spanish Pyrenees (Revuelto et al., 2014; López-Moreno et al., 2015). These technologies have enabled numerous fundamental advances in our knowledge of the snow depth distribution (see Sect. 5.4). They also hold potential for operational snow monitoring if their costs can be mitigated; otherwise, their application will remain restricted to relatively small areas, as noted in the scientific literature (<100 km^2). The NASA Airborne Snow Observatory (ASO) (Painter et al., 2016) is a notable exception since it is run over major water basins in the western US. ASO is composed of an imaging spectrometer and a Lidar altimeter to measure the snowpack reflectance and depth from an aircraft. The SWE maps are produced over 48 hours

using the snow reflectance as a proxy for snow density (Dozier et al. 2016). Recent alternatives were proposed to determine the snow depth at high resolution and at a lower cost: (1) an unmanned aircraft vehicle photogrammetric survey, and (2) high-resolution stereo satellites imagery (Marti et al., 2016).

2.5.3 Methods of HS and SWE regionalization

2.5.3.1 Regionalization

Spatial interpolation (regionalization) techniques are required to estimate the snowpack water equivalent at the catchment scale. Various statistical models based on the terrain characteristics were proposed to compensate for the low spatial density of snow course surveys and ground stations observations. Spatially distributed HS estimates from observations in Mediterranean mountain were represented using: linear regression models, classification trees, generalized additive models (GAMs), regression tree models (e.g., Molotch et al., 2005), and combined tree classification with GAM residuals (e.g., López-Moreno and Nogués-Bravo, 2006; López-Moreno et al., 2010). Similarly, but at much lower scale, the assimilation of snow cover area maps derived from time-lapse camera images time series was shown to give good results in small Mediterranean pilot catchments, where the snow cover is highly variable and sometimes ephemeral (Pimentel et al., 2015; Revuelto et al., 2016b).

2.5.3.2 SWE reconstruction

Dozier et al. (2016) reviewed the methods to generate spatially distributed SWE as follows: (1) spatial interpolation from ground based networks only using statistical models such as decision trees (Anderton et al., 2004); (2) constrained interpolation by remotely sensed SCA (Girotto et al., 2014); (3) SWE reconstruction using snow modeling (e.g., Raleigh and Lundquist, 2012; Guan et al. 2013b); and (4) reconstruction using data assimilation (Cortés et al., 2016) (see Sect. 6.1) and backmelt calculations (e.g., Raleigh and Lundquist, 2012), which may be combined with time-lapse photography (Revuelto et al., 2016a). The increase in the reliance of SWE reconstruction had been motivated by the assumption that knowledge of melt energy fluxes would be superior to knowledge of precipitation accumulation (Cline et al., 1998; Jepsen et al., 2012; Slater et al., 2013).

SWE reconstruction estimates the total volume of snow based on backward calculation of the amount of ablation that occurred prior to the complete removal of snow (Cline et al., 1998). The SWE reconstruction process as described by Cline et al., (1998) is performed at

each pixel by (1) determination of fSCA; (2) computation of the snowmelt energy; and (3) determination of the initial SWE at the beginning of the melt season.

Several snowpack models for SWE reconstruction are constantly being tested and enhanced for application in Mediterranean regions, and they range in complexity from (1) simple temperature index models (Daly et al., 2000; Rice et al., 2011; Biggs and Whitaker, 2012), to (2) enhanced degree day models (DDMs) that account for net radiation and snow albedo (e.g., Molotch and Bales, 2006) and tree cover (Biggs and Whitaker, 2012), and (3) modified DDMs (based on a modified SRM (Martinec, 1975) (Tekeli et al., 2005b; Şensoy and Uysal, 2012), to (4) energy balance models (Cline et al., 1998; Jepsen et al., 2012; Raleigh et al., 2016; Boudhar et al., 2016; Cornwell et al., 2016), and (5) models that perform both forward and backward reconstruction (Raleigh and Lundquist, 2012; Revuelto et al., 2016a).

SWE reconstruction models have proven to be suitable for many Mediterranean regions such as the Andes (Cornwell et al., 2016); Sierra Nevada California (Shamir and Georgakakos, 2006; Rice et al., 2011; Raleigh et al., 2016), Oregon cascades (Sproles et al., 2013); Pyrenees (Gómez-Landesa and Rango, 2002); Alps (Thirel et al., 2012); Turkey (Tekeli et al., 2005b); and the Atlas Mountains (Boudhar et al., 2016).

The uncertainty associated from SWE reconstruction arises from the probable error propagation in model forcing especially in areas where dense observing network are not available (Lundquist et al., 2015b; Dozier et al., 2016). Another source of uncertainty is attributed to the retrieval and spatial resolution of SCA and fSCA from imaging spectrometer (e.g., AVHRR and MODIS) (Sect. 5.2) and return time period (e.g., 16 days for Landsat) (Slater et al., 2013). The Sentinel-2 mission with its 5 days repeat cycle offers the prospect of improving the SWE reconstruction results in regions where the snow cover variability is high (Marti et al., 2016).

SWE reconstruction methods based on the use of depletion curves that relate fractional snow cover area to average SWE should consider that there is an hysteresis in the SWE-fSCA relationship (Luce and Tarboton, 2004; Magand et al., 2014; Gascoin et al, 2015). In fact, a given snow cover fraction generally corresponds to a smaller snow mass at the beginning of the snow season to that found at the end of the season. This is due to the snowpack evolution along the season, where snow wind redistribution and snowmelt occurring at preferential locations, tend to increase the heterogeneity in the SWE spatial distribution.

The success of the spatial interpolation techniques for the estimation of HS and SWE should encourage the implementation of regular snow surveys and automatic snow stations in less monitored mountain regions, such as the Andes, Atlas Mountains, and Mount Lebanon. In

the absence of ground measurements, methods based on SCA data assimilation into an energy balance snow model are the most promising since they rely on publicly available remote sensing and climate datasets (reanalyses) with global coverage (e.g., Kapnick and Delworth, 2013).

2.5.4 Snowpack spatial variability

2.5.4.1 Snow height spatial variability

Results from the aforementioned studies indicate that in Mediterranean mountain regions, the spatial distribution of the snow height is driven by meteorological forcing (López-Moreno 2005; Svoma, 2011; Mizukami and Smith, 2012; Bormann et al., 2013; Luce et al., 2014) and topography (elevation, slope, aspect and related radiation parameters) (e.g., Elder et al., 1998; Anderton et al., 2004; López-Moreno and Nogués-Bravo, 2006; Rice et al., 2011; Molotch and Meromy, 2014; Revuelto et al., 2014). Canopy interception (e.g., López-Moreno and Latron, 2008; Revuelto et al., 2015; Zheng et al., 2016) plays a secondary role in comparison with other snow regions because most of the snowpack accumulates above the tree line in many Mediterranean mountains. Forest regions are present at mid-altitude mountain regions (2000-2600 m a.s.l) in California (e.g., Rice and Bales, 2010; Musselman et al., 2012), Oregon (Kostadinov and Lookingbill, 2015) and the Pyrenees (e.g., Gascoin et al., 2015). Snow redistribution due to wind is probably an important process (Gascoin et al., 2013), and it is one of the less explored fields of research in Mediterranean regions. This may be due to the lack of accurate information needed to create reliable wind fields over complex topography. Snow models run using high-resolution meteorological forcing are still unable to capture wind snow redistribution, which usually occurs at the sub-pixel scale (e.g., Quéno et al., 2016). However, the wind redistribution may be less important in Mediterranean mountains than in colder regions due to the higher snowpack densification rates. Table 2.2 summarizes the contribution of climate forcing and mountain controls potentials in explaining snow distribution and depth, and the level of uncertainty in Mediterranean mountain regions.

For example, in Sierra Nevada California, Elder et al., (1998) obtained a model that could explain up to 70% of the observed variance in HS using the elevation, net radiation and slope as predictors. According to Molotch and Meromy, (2014), snow cover persistence is driven by mountain controls where elevation (the most explanatory variable) and climate controls of precipitation and temperature determined most of the snow variability. Vegetation and slope ranked second in explaining part of the snow cover variability, whereas shortwave solar radiation and the terrain aspect were of tertiary importance. Similar findings were reported

in the Spanish Pyrenees, which indicates that elevation and solar radiation explain a high percentage of the variance in HS (Anderton et al., 2004; López-Moreno and Nogués-Bravo, 2005).

Similar findings based on high-resolution airborne lidar were reported from an experiment over a micro-scale snow dominated basin (with an elevation range of 1500–3300 m) in the Sierra Nevada, California; the experiment indicated that 43% of snow-depth variability can be explained by elevation, and another 14% is related to the slope, aspect and canopy penetration fraction (Zheng et al., 2016). A ground-based terrestrial laser scanner in the Pyrenees demonstrated that the high resolution topographic position index and maximum upwind slope are more statistically significant ($\alpha<0.05$) in explaining the intra-annual snow variability compared to the elevation and slope (Revuelto et al., 2014). Snow variability at this scale is further influenced by mountain curvature, whereas the aspect and the computed incoming radiation were found to be less statistically significant when correlated with intra-annual snow variability (Revuelto et al., 2014).

Despite these encouraging results, to date, there is no accepted universal law to derive HS or SWE from a set of predictors that can be obtained anywhere. This is because the link between the terrain parameters and the snow distribution is not fully explained at the small scale (e.g., Molotch et al., 2005; López-Moreno et al., 2010, 2015; Revuelto et al., 2014; Zheng et al., 2016). This quest is hindered in particular by (1) the high inter-annual snow variability in Mediterranean regions, since most studies rely on 1-2 years of sporadic observations (e.g., Anderton et al., 2004; López-Moreno et al., 2010; Zheng et al., 2016), and (2) the increase in the scale dependency of the model results (e.g., the importance of elevation) as the grid cell size increases (López-Moreno et al., 2010).

The presence of vegetation, especially forest, adds to the ambiguity in explaining topographic control because it modifies meteorological variables, such as wind and the incoming radiation with difference intensities, which depends on the canopy density, trees trunks and crow size (e.g., Musselman et al., 2012; Harpold et al., 2014; Zheng et al., 2016). The snow depth can be significantly reduced by 20% to 80% in forested areas compared to open sites due to interception and the sublimation or melting of the intercepted snow (Revuelto et al., 2015; Szczypta et al., 2015). Information on the impact of vegetation cover on snow interception in Mediterranean mountain regions and elsewhere (Varhola et al., 2010) remains limited and warrants future research (López-Moreno and Latron, 2008; Musselman et al., 2012; Raleigh et al., 2013; Revuelto et al., 2015; Zheng et al., 2016).

Table 2.2. Main variables influencing the snow depth spatial distribution

Variable	Control Level
Elevation [1-5, 7-9]	Medium to very high
Slope [1-5, 7-9]	Low to high (micro); High (meso-macro)
Curvature [5, 8-9]	High at micro
Exposure [3-5, 7-8]	Low at micro to medium at the micro scale
Radiation [1-3, 5, 7-9]	Low to medium (micro); High (macro)
Relative elevation [2, 5, 8]	Low to very high
Upwind slope [3, 5, 7, 9]	High at micro
Canopy interception [4, 6]	Medium to high

Radiation: potential incoming solar radiation; Relative elevation (inc. topographic position index (TPI) and combined TPI); Upwind slope: maximum upwind slope.
Scale (micro 1–10^2 km^2; meso 10^2–$10^4$$km^2$; macro > $10^4$$km^2$)
Sources: [1] Elder et al., 1998; [2] López-Moreno and Nogués-Bravo, 2005, 2006; [3] Anderton et al., 2004; [4] Zheng et al., 2016; [5-6] Revuelto et al., 2014, 2015; [7] Molotch et al., 2005; [8] López-Moreno et al., 2010; and [9] López -Moreno et al., 2015.

2.5.4.2 Snowpack density

Over most parts of the maritime US, the snowpack density was found to be highly correlated with total precipitation (Svoma, 2011). The variability in snow densities is also driven by the average air temperature during days with no snowfall, the mean snowfall density, the fractional precipitation that falls as snow (Svoma, 2011) and melt-refreeze events (Bormann et al., 2013). At the slope scale, densification processes are further influenced by solar radiation, slope, vegetation cover, and wind exposure (Bormann et al., 2013, Elder et al., 1998).

However, the observed spatial variability of the snowpack density in Mediterranean regions is much lower than the spatial variability of the snow height (Mizukami and Perica, 2008; López-Moreno et al., 2013b). As a result, the number of density measurements required to derive the SWE may be lower than the number of HS measurements. This has important implications for the monitoring of the snowpack since density measurements in the field are time consuming. Similarly, year-to-year changes are significantly higher for the HS than for the snowpack density (Mizukami and Perica, 2008; Bormann et al., 2013). However, the density should be carefully measured at the start and end of each season when its intra-annual variance is maximal (Sturm et al., 2010; López-Moreno et al., 2013b; Bormann et al., 2013; Trujillo and Molotch, 2014). The low inter-annual variability of snow density also holds potentials in Mediterranean regions. Climatological values of snow density can be estimated with confidence using few years of measurements (Anderton et al., 2004; Mizukami and Perica, 2008; Meromy et al., 2013), and combined with regular HS measurements, to estimate the SWE for hydrological applications in mountains (Mizukami and Perica, 2008).

2.5.4.3 SWE

Long-term records of SWE (> 50 years) indicate that the maximum snow accumulation is higher and the snow season is shorter in the Oregon Cascades and the California Sierra Nevada than in continental mountain ranges (Trujillo and Molotch, 2014). In the western US, the April 1st SWE (a proxy of the annual peak of SWE) and the snow residence time (SRT) are highly correlated with daily temperature and precipitation (Luce et al., 2014). Hence, the observed decrease in SWE in this region was linked to the regional increase in temperature, and the results were qualitatively consistent with observed trends in temperature and precipitation at nearby stations (Mote, 2003). In southern Italian Alps, the SWE average and variances are known to a good degree of approximation if continuous information on the accumulated SWE, snow depth, and density are known (Bocchiola and Rosso, 2007). Smaller scale studies in California and Central Andes indicate a higher influence of the slope and maximum upwind slope (Molotch et al., 2005; Welch et al., 2013; Ayala et al., 2014). The influence of the theoretical incoming radiation increased during the melt season, which is in agreement with energy balance model studies (Molotch et al., 2005; Ayala et al., 2014) (Sect. 4). We do not detail the spatial variability of the SWE since it is largely inherited from the HS, as presented above.

2.6 Snowmelt hydrology and hydrogeology

Once snowmelt occurs, the snowpack water is channeled through surface outflows and streams, and it undergoes evapotranspiration, subsurface flow and groundwater recharge via deep percolation (e.g., Knowles and Cayan, 2004; Franz et al., 2010; Lundquist and Loheide, 2011; Smith et al., 2013; Manning et al., 2012; Godsey et al., 2014). Given the spatio-temporal variability of the climatic conditions that were highlighted in the previous sections, the closure of the hydrologic budget in Mediterranean snow-dominated basins remains challenging (e.g., Ralph et al., 2016). In addition, several authors point to a limited understanding of surface and sub-surface hydrologic processes in mountains (Bales et al., 2006; Smith et al., 2013).

2.6.1 Snowmelt modeling

2.6.1.1 Snow melt models

Different snowmelt models were applied in the Mediterranean context with significantly varying levels of details between the models. Following DeWalle and Rango (2008), these models can be classified under three categories: (1) statistical snowmelt-runoff methods (e.g.,

Stewart et al., 2005), (2) temperature index or degree day models (TIM/DDM) (e.g., Null et al., 2010), and (3) physically based distributed-snowmelt models or energy balance models (EBM) (e.g., Herrero et al., (2009) in the Spanish Sierra Nevada; Şensoy et al., (2006) in Karasu basin, Turkey; and Mernild et al. (2016a) in the Andes). The distinction between these boundaries seems to be fading in the literature as there is a tendency towards the use of heterogeneous modeling approaches, and a continuum now exists between the three categories. Martelloni et al., (2013) proposed and tested a modeling scheme, over the Italian Apennines that is considered as an intermediate approach between temperature index and physically based models. Sproles et al., (2016) used a modified snowmelt runoff model (SRM), which was run using MODIS SCA data, to investigate snowmelt forecasts in the data-poor regions of the Chilean Andes.

Major sources of uncertainty in snow melt simulation arise from (1) the error in the input data (particularly precipitation), (2) reliance on DDM (due to limited information on incoming and reflected radiation and fluxes), which usually translates into the lack of accounting of snow sublimation, and (3) the model parameterization regarding rain/snow separation and turbulent fluxes (Franz et al., 2010; He et al., 2011; Raleigh and Lundquist, 2012; Slater et al., 2013; Avanzi et al., 2014). Snow model inter-comparison studies in Mediterranean mountain regions (Franz et al., 2010; Slater et al., 2013) and elsewhere (Molotch and Margulis, 2008; Essery et al., 2013; Bavera et al., 2014) indicate that while very large differences can exist between models (different melt algorithms), proper simulation of snowmelt is highly associated with the proper parameterization of models (e.g., Smith et al., 2013) and the model's ability to solve SWE with high confidence (e.g., Franz et al., 2010). To the best of our knowledge the only snow-hydrological model comparison studies which includes Mediterranean catchments are the studies of Franz et al., (2010) and Valéry et al. (2014a, 2014b). We believe that there is a need for testing and comparing different snow models and carrying meaningful intercomparison exercises across different Mediterranean mountain regions. The reader is advised to look at model parameterizations and sensitivity (Clark et al., 2011; Garcia et al., 2013), the inter-comparison in forested snow regions (e.g., Essery et al., 2009; Rutter et al., 2009), the influence of soil moisture response on snow distribution and melt (Bales et al., 2011; Kerkez et al., 2012; Harpold et al., 2015), single model SRM multi-site comparison (e.g., Martinec and Rango, 1986; Seidel and Martinec, 2004; DeWalle and Rango, 2008), ensemble model simulation (e.g., Franz et al., 2010; Essery et al., 2013), and the snow model intercomparison Project (MIP) (e.g., DMIP (Smith et al., 2013) and SNOWMIP2 (Essery et al., 2009)).

2.6.1.2 Large scale land surface models and assimilation techniques

The modeling of large-scale distributed cryospheric processes had been made possible through the application of the following: (1) finer scale land surface models with snow schemes (e.g., Boone et al. 2004; Livneh et al., 2010; Brun et al., 2013; Magand et al., 2014; Singh et al., 2015); (2) physically based simulations using mesoscale WRF model (Caldwell et al., 2009; Pavelsky et al., 2011, 2012; Wayand et al., 2013; Liou et al., 2013; Franz et al., 2014; Oaida et al., 2015); (3) blending snow sensor observations and remote sensing data with snowmelt model simulations (e.g., Guan et al. 2013a; Rittger et al., 2016); and using data assimilation (e.g., Franz et al., 2014; Girotto et al., 2014) of ground and remote sensing data with Land Surface Model (Zaitchik and Rodell, 2009; Hancock et al., 2013) and Snow Data Assimilation System (SNODAS) (Guan et al., 2013a; Vuyovich et al., 2014); and (4) reanalysis of ground data (Gottardi et al., 2012; Avanzi et al., 2014), remote sensing data (Margulis et al., 2016), and land surface data (e.g., Durand et al., 2009; Vidal et al., 2010; Rousselot et al., 2012; Rutz et al., 2014).

While such techniques can capture large-scale variability in the cryospheric system, most of these techniques are still hindered by (1) limited ground data and dependence on the representativeness of the observation network (e.g., Livneh et al., 2010; Guan et al., 2013a; Balsamo et al., 2015; Dozier et al., 2016); (2) uncertainties in the quality of forcing data (surface meteorological and radiative forcing) (Livneh et al., 2010; Pavelsky et al., 2011; Gottardi et al., 2012; Liou et al., 2013; Guan et al., 2013a); (3) model parameterization and the number of model simplifications of physical phenomena (Livneh et al., 2010); (4) limitations in mountain environments (Gottardi et al., 2012; Wayand et al., 2013; Wrzesien et al., 2015), which are attributed to the downscaling of surface forcing over topographically complex areas (Livneh et al., 2010; Guan et al., 2013a); (5) fSCA data retrieval gaps due to cloud contamination (Guan et al., 2013a); (6) lack in accounting for the spatial variability snow of albedo (Livneh et al., 2010; Guan et al., 2013a); (7) accounting for canopy/forest cover (Livneh et al., 2010; Guan et al., 2013a); and (8) tendency towards reporting earlier snowmelt/depletion (Pavelsky et al., 2011; Wrzesien et al., 2015) and higher biases observed during snow depletion (Wrzesien et al., 2015) ablation seasons (Guan et al., 2013a).

2.6.2 Snowmelt contribution to runoff and groundwater

While rainfall defines most of the hydrograph shape in the mid to low mountain regions, the streamflow in higher elevation areas (typically above 2000 m a.s.l.) is dominated by

snowmelt (López-Moreno and García-Ruiz 2004; Wayand et al., 2013; Jepsen et al. 2016a). In the western US, snowmelt-dominated rivers reach their highest sustained flow during the spring melt season, whereas rain-dominated rivers achieve their highest sustained flows during the winter rainy season (Lundquist and Cayan, 2002). Streamflow was estimated to peak 2-4 weeks earlier in transitional rain–snow-dominated basins compared to snow-dominated basins (Ashfaq et al., 2013; Liu et al., 2013). Processes controlling the water transfer through overland, subsurface and groundwater flow are reasonably well understood (e.g., Jefferson et al., 2008; Tague and Grant, 2009; Smith et al., 2013; Wayand et al., 2013). However, the effect of the snowpack dynamics on those processes is one of the foremost challenges in the hydrology of Mediterranean mountains.

2.6.2.1 Snowmelt runoff

The simulation of the streamflow in snow-dominated Mediterranean regions was successfully achieved using lumped rainfall-runoff models with a snowmelt routine (e.g., Karpouzos et al., 2011; Hublart et al., 2016) distributed statistical model that combines remote sensing SCA and ground observation (e.g., Gómez-Landesa and Rango, 2002; Powell et al., 2011; Akyurek et al., 2011; Biggs and Whitaker, 2012), and a physically based distributed hydrologic model that balances both surface energy and water budgets and accounts for snowmelt using snowpack energy balance routines, such as the variable infiltration capacity (VIC) model (Maurer et al., 2007) and the Distributed Hydrology Soil Vegetation Model (DHSVM) (e.g., Wayand et al., 2013; Cristea et al., 2014). Apart from the modeling approach, the relationship between snowmelt and streamflow in Mediterranean snow-dominated regions had also been successfully addressed by the empirical analysis of streamflow data against observed SWE (Lundquist et al., 2004), and tracer tests (Liu et al., 2013).

There is a global agreement that the total annual runoff volume will decrease, in regions such as California, under a warming climate (Jepsen et al., 2016a). Changes in snow-fed streamflow volume are controlled by the (1) annual snow mass (total snowfall) and melt rates (e.g., Lundquist et al., 2005; Franz and Karsten, 2013; Morán-Tejeda et al., 2014; Godsey et al., 2014), and (2) subsurface processes (Liu et al., 2013; Jepsen et al., 2016a). Controls driven by (1) soil moisture and water holding capacity (Costa-Cabral et al., 2013), (2) vegetation cover (Biggs and Whitaker, 2012; Cristea et al., 2014), (3) evapotranspiration (Lundquist and Loheide, 2011; Goulden et al., 2012; Godsey et al., 2014), and (4) groundwater storage (Godsey et al., 2014) are usually site specific and vary depending on soil type (e.g., soil water holding

capacity) and groundwater storage capacity and flow time (e.g., low capacity and faster travel time in Karst). A study carried in a snow–rain transition mountain region in the Southern Sierra Nevada, California indicate that streamflow generation is controlled by subsurface flow (average relative contribution to streamflow discharge was greater than 60%), snowmelt runoff including rain on snow (less than 40%), and fall storm runoff (less than 7%), whereas soil water in the unsaturated zone and regional groundwater were not significant contributors to streamflow (Liu et al., 2013). In the Spanish Pyrenees, using a single multiple regression model, the contribution of snowpack to spring runoff was estimated to be a 42% for the 1955-2000 period (López-Moreno and García-Ruiz, 2004). In the Anti-Lebanon Mountain, the karst formation has a short-term influence characterized by an intra-annual patterns of fast spring discharges (Koeniger et al., 2016).

Regional long-term trends in the snowmelt-generated streamflow in California are believed to be controlled by long-term decadal changes and spring warming temperature trends (e.g., Stewart et al., 2005; Maurer et al., 2007). Whereas, the inter-annual variations of snowmelt and streamflow timing are driven by regional temperature fluctuations and precipitation anomalies (Stewart et al., 2005). It is clear that temperature and precipitation alone cannot explain the entire variability in snowmelt onset and streamflow peak timing and that changes are also influenced by elevation (Maurer et al., 2007; Biggs and Whitaker, 2012; Wayand et al., 2013) and shifts in snowfall-snowmelt patterns in regions such as California (Godsey et al. 2014), and the Spanish Sierra Nevada (Morán-Tejeda et al., 2014). In Mediterranean regions, a shift in streamflow timing would have profound implications on water management by reducing the available water resources in late spring and summer when the precipitation is low (e.g., Stewart et al., 2005; Tanaka et al., 2006; López-Moreno et al., 2008b; Vicuña et al., 2011; Fabre et al., 2015). In California, changes in snowmelt and streamflow onset timing, at the micro- and mesoscale, were found to respond non-linearly to the increase in temperature (Lundquist and Flint, 2006). Snowmelt-driven streamflow timing, at smaller scales, is strongly dominated by solar radiation and the combined effect of solar radiation exposure (a function of aspect, elevation and time of the year) and temperature (a function of elevation and shading) (Lundquist and Flint, 2006). These results highlight the need to account for solar radiation, meteorological forcing, and topography when addressing snowmelt and streamflow responses in Mediterranean-like regions (Wayand et al., 2013). Diurnal snow-dominated streamflow patterns are also sensitive to the basin size (Lundquist et al., 2005). At the micro-scale (< 30 km^2), travel times through the snowpack dominate streamflow timing, whereas in mesoscale basins (>200 km^2), streamflow peaks are more consistent, with little or

no variation, due to snowpack heterogeneity and the longer travel percolation times through deeper snowpacks and stream channels.

2.6.2.2 Snowpack control on soil moisture and evapotranspiration

The role of the soil water holding capacity in controlling soil moistures and evapotranspiration is usually site specific (Christensen et al., 2008; Maurer et al., 2010; Bales et al., 2011; Schlaepfer et al., 2012; Tague and Peng, 2013; Harpold et al., 2015; Jepsen et al., 2016a,b). The interaction between snowmelt and soil moisture is subject to soil physical properties (texture) and soil depth (Schlaepfer et al., 2012; Bales et al., 2011; Harpold, 2016).

At present, little information is available on soil water holding capacities at high elevations (e.g., Christensen et al., 2008; Bales et al., 2011; Costa-Cabral et al., 2013). Information on the soil water potential and water table depth is useful to explain the runoff generation processes (Latron and Gallart, 2008). An increase in temperature would not only reduce the snow accumulation but also increase the soil water storage and evapotranspiration in snow-dominated basins (Maurer et al., 2010; Tague and Peng, 2013; Wu et al., 2015). The acquisition of soil moisture data in snow-dominated mountain regions would aid a better understanding and forecasting snowmelt runoff (Kerkez et al., 2012).

A number of studies investigated evapotranspiration in snow-influenced Mediterranean mountains, mostly in California Sierra Nevada (Leydecker and Melack, 2000; Dettinger et al. 2004; Bales et al., 2011; Lundquist and Loheide, 2011; Tague and Peng, 2013; Costa-Cabral et al., 2013; Goulden and Bales, 2014; Jepsen et al., 2016b; Harpold, 2016); Sierra Nevada Spain (Aguilar et al., 2010) and Southern Italy (Senatore et al., 2011). The interplay between snowmelt and evapotranspiration was most of the time addressed using modeling approaches that do not explicitly account for snowpack dynamics (e.g., Aguilar et al., 2010; Lundquist and Loheide, 2011; Tague and Peng, 2013; Jepsen et al., 2016a).

In Mediterranean regions, high-elevation areas are usually snowmelt-dominated whereas lower-regions are evapotranspiration/infiltration-dominated (Lundquist and Cayan, 2002). Evapotranspiration tends to be low during the winter season through the beginning of the melt season due to the presence of the snow cover and at late summer and autumn due to soil dryness. During the melt season, the combined effect of increasing air temperatures and solar radiation tends to accelerate snowmelt, enhance water availability in soil, and increase surface temperature, which results in increased evapotranspiration (Leydecker and Melack, 2000). The inter-annual evapotranspiration is controlled by elevation and aspect, which define the amount of incoming solar radiation (Goulden et al., 2012; Lundquist and Loheide, 2011).

Evapotranspiration in mid-altitude regions is usually water-limited, i.e., controlled by the precipitation (Christensen et al., 2008; Lundquist and Loheide, 2011), whereas in higher snow-dominated regions, it is rather energy-limited, i.e., it responds more strongly to temperature variations (Christensen et al., 2008; Lundquist and Loheide, 2011; Schlaepfer et al., 2012; Godsey et al., 2014; Jepsen et al., 2016a). Based on a number of papers reported in Jepsen et al., (2016a), the evapotranspiration in Sierra Nevada California under a warming climate, has an overall tendency to increase (medium confidence) in snow-dominated regions and some regions are either susceptible to warming or expected to experience a slight decrease.

2.6.2.3 Groundwater recharge

Groundwater studies in Mediterranean mountain are most of the time presented at the basin scale and provide little information on the link between snowpack dynamics and groundwater processes. Groundwater recharge in snow-dominated regions is dominated by the timing of the snowmelt (early or late spring) and the subsurface flow (Tague and Grant, 2009). In groundwater-dominated watersheds, the aquifer storage and the slow recession can help in sustaining discharge during the summer dry periods even under a negative yearly water balance (Jefferson et al., 2008). Despite its importance, the lack of extended studies has resulted the availability of negligible information on the extent of snowpack controls on groundwater resources in most Mediterranean mountains (e.g., Palmer et al., 2007; Lowry et al., 2010, 2011; Liu et al., 2013; Valdés-Pineda et al., 2014). The separation between rain-fed and snow-fed groundwater recharge is still incomplete due to a number of factors: (1) lack of groundwater wells and monitoring networks, (2) complex geology especially in karst regions (e.g., Hartmann et al., 2014; Tobin and Schwartz, 2016), and (3) the complexity of subsurface flows in mountain regions (e.g., Knowles and Cayan, 2004; Tague and Grant, 2009; Millares et al., 2009; Godsey et al., 2014). A comprehensive review on the different groundwater mechanisms and the importance of snow in groundwater recharge under projected warming scenarios over the western USA can be found in the work of Meixner et al., (2016).

The link between snowmelt and groundwater spring discharge at the mesoscale in Mediterranean regions was addressed by using hydrochemical analysis. Studies on experimental snow-influenced micro- to mesoscale basins in Sierra Nevada California (Taylor et al., 2001; Friedman et al., 2002; Rademacher et al., 2005; Huth et al., 2004; Shaw et al., 2014), Oregon (Palmer et al., 2007), Serra da Estrela Mountain Portugal (Carreira et al., 2011), Sierra Nevada Spain (Fernández-Chacón et al., 2010), and the Southern Italian Alps (Penna et al., 2015) demonstrated the potentials of suing stable isotopic analysis for hydrograph

separation between snow-fed, rain-fed and groundwater-fed sources and to investigate flow paths (Bales et al., 2006), and the evolution of snowmelt (Taylor et al., 2001). Tracer tests were used to (1) separate between snowmelt runoff (including rain on snow) (Williams et al., 2001), subsurface flow and fall storm runoff (Liu et al., 2013; Perrot et al., 2014) and shallow evapotranspired groundwater from groundwater sources (Shaw et al., 2014), and (2) investigate meltwater-driven surface runoff and catchment transit time (e.g., McGuire and McDonnell, 2010). General chemical analyses also provided reliable information on the state of water residence time in springs (Rademacher et al., 2005). The karst aquifers are of particular relevance in the Mediterranean region since they represent a key source of freshwater supply for the people living in the Mediterranean basin (Doummar et al., 2014). The estimation of groundwater recharge from snowmelt in karst regions had been limited to mid and low latitude micro-scale snow-influenced mountainous regions with studies in southern Europe Spain (Andreo et al., 2004), Italy (Allocca et al., 2014), Greece (Novel et al., 2007), and the eastern Mediterranean regions of mount Lebanon (Bakalowicz et al., 2007). A pioneering study in the mid-altitude mountain region in Crete showed promise for simulating the contribution of snowmelt to karst hydrosystems by coupling a karstic model and an energy balance snow model (Kourgialas et al., 2010).

New opportunities for the separation between SWE, surface water reservoir storage, soil moisture, ET, and changes in groundwater storage have been made possible using the GRACE mission (Famiglietti et al., 2011; Scanlon et al., 2012) and finer-resolution land-surface models (Singh et al., 2015). The use of global position system (GPS) vertical land motion observations in the California Central Valley (Ouellette et al., 2013; Argus et al., 2014; Boniface et al., 2015) and Oregon (Fu et al., 2015) seems to show potential for estimating terrestrial water storage while accounting for snow accumulation and melt. While these studies are encouraging, they are still limited to the regional scale due to the coarse resolution of the GRACE observations (approximately 300 km).

2.7 Conclusion

The review of 620 papers published between 1913 and 2016 demonstrated that the science behind snowpack dynamics (energy and mass fluxes) and hydrological process in Mediterranean mountain regions is well developed. The number of studies that are dedicated to the snow in Mediterranean regions also reflects the societal importance of the topic in the context of climate change, economic development and population growth. The use of indicators helped in highlighting major snow hydrologic processes in Mediterranean mountains. In

specific areas, such as in identifying major drivers for snowpack dynamics, it was difficult to draw definitive conclusions given the variety of approaches (e.g., different major drivers and methods). Our classification of Mediterranean mountains encompasses a large range of geologic and physiographic conditions. Despite the fact that the theory behind hydrologic processes in mountains is well established, drawing a common conclusion remains difficult beyond the case studies because the limited number of studies in this area of research area and the variety of approaches used (e.g., different models).

Mediterranean snow-influenced regions are marked by a high inter- and intra-annual climate variability that shapes up most of the hydrologic processes. As a result, the snow depth, snow density, and snow water equivalent exhibit high inter- and intra-annual variance. In addition, the snowpack is affected by higher densification rates compared to other climate regions. The snowpack energy and mass balances are dominated by radiation fluxes, which account for most of the energy available for melt. The contribution of sensible and latent heat fluxes to ablation becomes prominent at the end of the snowmelt season. Snow sublimation is more pronounced in the high-elevation zones, whereas snowmelt dominates the warmer, low to mid-elevation regions. The role of snow metamorphism (grain size and albedo) on the melt onset is still an open field of research. There is also room for improving snow mapping in forests and assessing the impact of absorbed impurities the radiative exchange at the snow surface. In particular, the snowpack in the Mediterranean basin is exposed to the deposition of mineral dust from the surrounding desert areas in Middle East and North Africa.

In Mediterranean mountain regions snowmelt are exposed to (1) periods of low precipitation or high temperature causing “snow drought” (Cooper et al., 2016) (2) heatwaves (3) rain on snow events and (4) and dust deposition on the snowpack. Increasing air temperatures will lead to a shift in precipitation regime with elevation (i.e., rain to snow and increase in rain-on-snow events). The dust deposition tends to enhance the snow melt by increasing the radiative exchange due to the of decrease snow albedo. Understanding snowmelt sensitivity to these climate variables is of primary importance to improving our knowledge on the hydrologic processes and water resources system responses in mountain regions and downstream areas.

In situ networks are often too sparse given the aforementioned spatial variability and most of the monitoring stations only monitor few meteorological variables needed to solve the energy budget of the snowpack. The increasing availability of remote sensing data, especially in the visible domain, has enabled scientific breakthroughs, such as the reconstruction of the SWE at the mountain scale with a decametric resolution for the last 30 years (Margulis et al.,

2016). Limitations associated with passive microwave and radar are physically linked to the band width and are likely to remain in the near future. Airborne techniques (e.g., NASA's ASO, (Painter et al., 2016) are an option for acquiring high detailed and direct estimates of HS and SWE once their high operational costs are reduced.

Data assimilation portability to different regions is hindered by the reliance on larger data sets as input variables. In regions with limited ground-based observations, model outputs can be biased by an increased uncertainty (e.g., Hublart et al., 2015). Similarly, the reliance on multiple other technologies (e.g., ground-based and remote sensing observations) makes the system highly dependent on the simultaneous availability of data from all systems (Guan et al., 2013a). The results using reanalysis of remote sensing data (Margulis et al., 2016) and physically based simulations run using the mesoscale WRF model (e.g., Caldwell et al., 2009; Wayand et al., 2013) seem to provide better results of SWE in regions with limited station data. One of the promising areas for research is the development of combined products, which include ground observations and remotely sensed data through data assimilation in snowpack models.

Conducting snow measurements in less monitored regions such as Lebanon's mountains and the Atlas Mountains is required, and these investigations can make use of the extended knowledge gained from other Mediterranean regions. In the meantime, the models based on climate reanalysis and remote sensing data are more easily transferrable. Snow density and SWE spatiotemporal variability can be estimated, with an acceptable accuracy, using a few years of ground observation (e.g., Anderton et al., 2004; Mizukami and Perica, 2008). Maintaining the existing in situ network is critical for monitoring the snowpack response to climate change. Free access to open software and snow and meteorological data in the western USA has allowed an intense development of the snow science in this region that can benefit all other Mediterranean regions, which would only be possible if computation codes are made available to the research community. Although snow models, hydrological models and land surface models are increasingly distributed as open source software, data assimilation codes are less available. There is still need for more collaboration in terms of standardizing and sharing data. It is important, that snow observations, measurements and analysis are documented and archived in online snow data repositories (Kinar and Pomeroy, 2015) to serve as a source of information and provide data that can be used for research purposes and intercomparison projects.

Advancing our understanding of hydrological processes in Mediterranean mountain is partly hindered by the sparse meteorological stations and hydrological gauging networks, and the large uncertainty in key variables, such as the stream flow in headwaters catchments (Avanzi et al., 2014; Lundquist et al., 2015b; Raleigh et al., 2016). In addition, there remain challenges in taking advantage of these advances in catchment hydrology because the response of the streamflow to the snowmelt is modulated by other hydrologic processes (ET, infiltration, groundwater flow). These processes are more strongly influenced by the subsurface properties (soil, geology), and hence, they are less easily constrained by current observational networks, remote sensing and modeling technologies. Closing on the water balance in Mediterranean mountain regions seems to be only feasible when these processes are solved simultaneously. Understanding of the connections between snowmelt, streamflow, evapotranspiration, and groundwater flow in snow-dominated regions is an open field for future research (e.g., Jefferson et al., 2008; Liu et al., 2013; Godsey et al., 2014; Jepsen et al., 2016a). Furthermore, there is a need to integrate human processes, such as reservoir management and irrigation, to investigate the vulnerability of the water resources under global change scenarios (e.g., Maurer et al., 2007; López-Moreno et al., 2008b; Viviroli et al., 2011; Anghileri et al., 2016).

Snowpack response to climate variability and change remains one of the critical issues in Mediterranean mountains that motivated many of the reviewed studies (e.g., Guan et al., 2012, 2013b). Projected scenarios indicate a marked warming and increased dryness in Mediterranean regions, which will amplify the transition from a snow-dominated to a rain-dominated in mid elevation watersheds, and reduce the persistence of the seasonal SWE. These snow-related changes may have broad implications on evapotranspiration, groundwater recharge and runoff in many Mediterranean catchments. Mediterranean snow dominated basins are vulnerable to the increase in temperature and recurring dry periods. The sustainability of the water system, in the lowland regions, requires better understanding of the seasonal snow water storage and release as well as the quantification of uncertainties associated to the projected climate change, population growth, and land-use changes on the hydrologic responses of mountainous basins (e.g., Barnett et al., 2008; Morán-Tejeda et al., 2014). These challenges remain partially understood and warrant future research to anticipate their management in the coming decades.

2.8 References

Aguilar, Herrero, Polo, 2010. Topographic effects on solar radiation distribution in mountainous watersheds and their influence on reference evapotranspiration estimates at watershed scale. Hydrology and Earth System Sciences 14, 2479–2494.

Akyurek, Z., Surer, S., Beser, Ö., 2011. Investigation of the snow-cover dynamics in the Upper Euphrates Basin of Turkey using remotely sensed snow-cover products and hydrometeorological data. Hydrological Processes 25, 3637–3648.
Allocca, Manna, Vita, D., 2014. Estimating annual groundwater recharge coefficient for karst aquifers of the southern Apennines (Italy). Hydrology and Earth System Sciences.
Anderton, White, Alvera, 2004. Evaluation of spatial variability in snow water equivalent for a high mountain catchment. Hydrological Processes 18, 435–453.
Andreo, B., Liñán, C., Carrasco, F., Cisneros, C., Caballero, F., Mudry, J., 2004. Influence of rainfall quantity on the isotopic composition (18O and 2H) of water in mountainous areas. Application for groundwater research in the Yunquera-Nieves karst aquifers (S Spain). Appl Geochem 19, 561–574.
Anghileri, D., Voisin, N., Castelletti, A., Pianosi, F., Nijssen, B., Lettenmaier, D., 2016. Value of long-term streamflow forecasts to reservoir operations for water supply in snow-dominated river catchments. Water Resour Res 52, 4209–4225.
Argus, D., Fu, Y., Landerer, F., 2014. Seasonal variation in total water storage in California inferred from GPS observations of vertical land motion. Geophys Res Lett 41, 1971–1980.
Armstrong, R.L. and Brun, E., (eds.) 2008. Snow and Climate. Physical Processes, Surface Energy Exchange and Modeling. Cambridge University Press. (ISBN-13: 9780521854542) 256 pp.
Ashfaq, M., Ghosh, S., Kao, S., Bowling, L., Mote, P., Touma, D., Rauscher, S., Diffenbaugh, N., 2013. Near-term acceleration of hydroclimatic change in the western U.S. Journal of Geophysical Research: Atmospheres 118, 10,676–10,693.
Avanzi, F., Michele, C., Ghezzi, A., Jommi, C., Pepe, M., 2014. A processing–modeling routine to use SNOTEL hourly data in snowpack dynamic models. Advances in Water Resources 73, 16–29.
Ayala, McPhee, Vargas, 2014. Altitudinal gradients, midwinter melt, and wind effects on snow accumulation in semiarid midlatitude Andes under La Niña conditions. Water Resources Research 50, 3589–3594.
Bair, E., Dozier, J., Davis, R., Colee, M., Claffey, K., 2015. CUES—a study site for measuring snowpack energy balance in the Sierra Nevada. Frontiers in Earth Science 3.
Bakalowicz, M., Hakim, M., El-Hajj, A., 2007. Karst groundwater resources in the countries of eastern Mediterranean: the example of Lebanon. Environmental Geology 54, 597–604.
Bales, Hopmans, O'Geen, 2011. Soil moisture response to snowmelt and rainfall in a Sierra Nevada mixed-conifer forest.
Bales, R., Molotch, N., Painter, T., Dettinger, M., Rice, R., Dozier, J., 2006. Mountain hydrology of the western United States. Water Resources Research 42.
Balsamo, Albergel, Beljaars, Boussetta, Brun, Cloke, Dee, Dutra, Muñoz-Sabater, Pappenberger, de Rosnay, Stockdale, Vitart, 2015. ERA-Interim/Land: a global land surface reanalysis data set. Hydrology and Earth System Sciences 19, 389–407.
Barnett, Adam, Lettenmaier, 2005. Potential impacts of a warming climate on water availability in snow-dominated regions. Nature 438, 303–309.
Barnett, T., Pierce, D., Hidalgo, H., Bonfils, C., Santer, B., Das, T., Bala, G., Wood, A., Nozawa, T., Mirin, A., Cayan, D., Dettinger, M., 2008. Human-Induced Changes in the Hydrology of the Western United States. Science 319, 1080–1083.
Bavera, D, Bavay, M, Jonas, T, Lehning, M, Michele, D.C., 2014. A comparison between two statistical and a physically-based model in snow water equivalent mapping. Advances in Water Resources.
Beaty, C.B., 1975. Sublimation or Melting: Observations from the White Mountains, California and Nevada, U.S.A. Journal of Glaciology 71, 275-286.
Behrangi, A., Guan, B., Neiman, P., Schreier, M., Lambrigtsen, B., 2016. On the Quantification of Atmospheric Rivers Precipitation from Space: Composite Assessments and Case Studies over the Eastern North Pacific Ocean and the Western United States. Journal of Hydrometeorology 17, 369–382.
Beniston, M., 2003. Climatic Change in Mountain Regions- A Review of Possible Impacts.pdf. Climatic Change 59, 5–31.
Beniston, M., Stoffel, M., 2014. Assessing the impacts of climatic change on mountain water resources. Science of The Total Environment 493, 1129–1137.
Berghuijs, Woods, Hrachowitz, 2014. A precipitation shift from snow towards rain leads to a decrease in streamflow. Nature Climate Change 4, 583–586.
Bierkens, M., 2015. Global hydrology 2015: State, trends, and directions. Water Resources Research 51, 4923–4947.
Biggs, T., Whitaker, T., 2012. Critical elevation zones of snowmelt during peak discharges in a mountain river basin. Journal of Hydrology 438-439, 52–65.
Bocchiola, D., Rosso, R., 2007. The distribution of daily snow water equivalent in the central Italian Alps. Advances in Water Resources 30, 135–147.
Bocchiola, Groppelli, 2010. Spatial estimation of snow water equivalent at different dates within the Adamello Park of Italy. Cold Regions Science and Technology 63, 97–109.

Bolle, H.J. (Ed.) 2003. Mediterranean Climate: Variability and Trends. Springer, New York. pp. 5–86.
Bonfils, C., Santer, B., Pierce, D., Hidalgo, H., Bala, G., Das, T., Barnett, T., Cayan, D., Doutriaux, C., Wood, A., Mirin, A., Nozawa, T., 2008. Detection and Attribution of Temperature Changes in the Mountainous Western United States. Journal of Climate 21, 6404–6424.
Boniface, Braun, McCreight, Nievinski, 2015. Comparison of Snow Data Assimilation System with GPS reflectometry snow depth in the Western United States. Hydrological Processes 29, 2425–2437.
Boone A et al. 2004. The Rhône-aggregation land surface scheme intercomparison project: an overview. J Clim 17, 187–208.
Bormann, K., Westra, S., Evans, J., McCabe, M., 2013. Spatial and temporal variability in seasonal snow density. Journal of Hydrology 484, 63–73.
Bornmann, L., Mutz, R., 2015. Growth rates of modern science: A bibliometric analysis based on the number of publications and cited references. Journal of the Association for Information Science and Technology 66, 2215–2222.
Boudhar, A., Boulet, G., Hanich, L., Sicart, J., Chehbouni, A., 2016. Energy fluxes and melt rate of a seasonal snow cover in the Moroccan High Atlas. Hydrological Sciences Journal 1–13.
Brown, R., Mote, P., 2009. The Response of Northern Hemisphere Snow Cover to a Changing Climate. Journal of Climate 22, 2124–2145.
Brown, R., Petkova, N., 2007. Snow cover variability in Bulgarian mountainous regions, 1931–2000. International Journal of Climatology 27, 1215–1229.
Brun, E., Vionnet, V., Boone, A., Decharme, B., Peings, Y., Valette, R., Karbou, F., Morin, S., 2013. Simulation of Northern Eurasian Local Snow Depth, Mass, and Density Using a Detailed Snowpack Model and Meteorological Reanalyses. J Hydrometeorol 14, 203–219.
Buisan, S., Saz, M., López Moreno, J., 2014. Spatial and temporal variability of winter snow and precipitation days in the western and central Spanish Pyrenees. International Journal of Climatology 35, 259–274.
Burns, S., Molotch, N., Williams, M., Knowles, J., Seok, B., Monson, R., Turnipseed, A., Blanken, P., 2014. Snow Temperature Changes within a Seasonal Snowpack and Their Relationship to Turbulent Fluxes of Sensible and Latent Heat. J. Hydrometeorol. 15(1), 117–142.
Caldwell, P., Chin, H.-N., Bader, D., Bala, G., 2009. Evaluation of a WRF dynamical downscaling simulation over California. Climatic Change 95, 499–521.
Carreira, P., Marques, J., Marques, J., Chaminé, H., Fonseca, P., Santos, F., Moura, R., Carvalho, J., 2011. Defining the dynamics of groundwater in Serra da Estrela Mountain area, central Portugal: an isotopic and hydrogeochemical approach. Hydrogeology Journal 19, 117–131.
Christensen, L., Tague, C., Baron, J., 2008. Spatial patterns of simulated transpiration response to climate variability in a snow dominated mountain ecosystem. Hydrological Processes 22, 3576–3588.
Christy, J., 2012. Searching for Information in 133 Years of California Snowfall Observations. J Hydrometeorol 13, 895–912.
Church, J.E. 1913. Recent studies of snow in the United States. Quaterly Journal of the Royal Meteorological Society 39, 43-52. DOI: 10.1002/qj.49704016905
Clark, M., Hendrikx, J., Slater, A., Kavetski, D., Anderson, B., Cullen, N., Kerr, T., Hreinsson, E., Woods, R., 2011. Representing spatial variability of snow water equivalent in hydrologic and land-surface models: A review. Water Resources Research 47.
Cline, D., Bales, R., Dozier, J., 1998. Estimating the spatial distribution of snow in mountain basins using remote sensing and energy balance modeling. Water Resources Research 34, 1275–1285.
Cooper, M., Nolin, A., Safeeq, M., 2016. Testing the recent snow drought as an analog for climate warming sensitivity of Cascades snowpacks. Environmental Research Letters 11, 084–009.
Cornwell, Molotch, McPhee, 2016. Spatio-temporal variability of snow water equivalent in the extra-tropical Andes Cordillera from distributed energy balance modeling and remotely sensed snow cover. Hydrology and Earth System Sciences 20, 411–430.
Cortés, G., Girotto, M., Margulis, S., 2014. Analysis of sub-pixel snow and ice extent over the extratropical Andes using spectral unmixing of historical Landsat imagery. Remote Sens Environ 141, 64–78.
Cortés, G., Girotto, M., Margulis, S., 2016. Snow process estimation over the extratropical Andes using a data assimilation framework integrating MERRA data and Landsat imagery. Water Resour Res 52, 2582–2600.
Cortés, G., Vargas, X., McPhee, J., 2011. Climatic sensitivity of streamflow timing in the extratropical western Andes Cordillera. Journal of Hydrology 405, 93–109.
Costa-Cabral, M., Roy, S., Maurer, E., Mills, W., Chen, L., 2013. Snowpack and runoff response to climate change in Owens Valley and Mono Lake watersheds. Climatic Change 116, 97–109.
Cristea, N., Lundquist, J., Loheide, S., Lowry, C., Moore, C., 2014. Modelling how vegetation cover affects climate change impacts on streamflow timing and magnitude in the snowmelt-dominated upper Tuolumne Basin, Sierra Nevada. Hydrological Processes 28, 3896–3918.

Daly, Davis, Ochs, Pangburn, 2000. An approach to spatially distributed snow modelling of the Sacramento and San Joaquin basins, California. Hydrological Processes 14, 3257–3271.
Danielson, J.J., and Gesch, D.B., 2011. Global multi-resolution terrain elevation data 2010 (GMTED2010): U.S. Geological Survey Open-File Report 2011–1073, 26 p.
Das, Hidalgo, Pierce, Barnett, Dettinger, Cayan, Bonfils, Bala, Mirin, 2009. Structure and Detectability of Trends in Hydrological Measures over the Western United States. Journal of Hydrometeorology 10, 871–892.
Dedieu, Lessard-Fontaine, Ravazzani, Cremonese, Shalpykova, Beniston, 2014. Shifting mountain snow patterns in a changing climate from remote sensing retrieval. Science of The Total Environment 493, 1267–1279.
Deems, J., Painter, T., Finnegan, D., 2013. Lidar measurement of snow depth: a review. Journal of Glaciology 59 (13), 467–479.
Demaria, E., Maurer, E.P., Thrasher, Vicuña, Meza, F.J., 2013b. Climate change impacts on an alpine watershed in Chile: Do new model projections change the story? Journal of Hydrology 502, 128–138.
Demaria, E., Maurer, Sheffield, Bustos, Poblete, Vicuña, Meza, 2013a. Using a Gridded Global Dataset to Characterize Regional Hydroclimate in Central Chile. Journal of Hydrometeorology 14, 251–265.
Derin, Y., Anagnostou, E., Berne, A., Borga, M., Boudevillain, B., Buytaert, W., Chang, C.-H., Delrieu, G., Hong, Y., Hsu, Y., Lavado-Casimiro, W., Manz, B., Moges, S., Nikolopoulos, E., Sahlu, D., Salerno, F., Rodríguez-Sánchez, J.-P., Vergara, H., Yilmaz, K., 2016. Multiregional Satellite Precipitation Products Evaluation over Complex Terrain. Journal of Hydrometeorology 17, 1817–1836.
Dettinger, M., 2014. Climate change: Impacts in the third dimension. Nat Geosci 7, 166–167.
Dettinger, M., Redmond, K., Cayan, D., 2004. Winter orographic precipitation ratios in the Sierra Nevada-Large-scale atmospheric circulations and hydrologic consequences. Journal of Hydrometeorology.
Dettinger, M.D., Cayan, D.R., Meyer, M.K., Jeton, A.E., 2004. Simulated hydrologic responses to climate variations and change in the Merced, Carson, and American River basins, Sierra Nevada, California, 1900–2099. Climatic Change.
DeWalle, D R, Rango, A. 2008. Principles of Snow Hydrology. Cambridge Univ. Press. (ISBN-10: 0511535678) 410 pp.
Dietz, A., Kuenzer, C., Gessner, U., Dech, S., 2012. Remote sensing of snow – a review of available methods. International Journal of Remote Sensing 33, 4094–4134.
Diffenbaugh, N., Scherer, M., Ashfaq, M., 2012. Response of snow-dependent hydrologic extremes to continued global warming. Nat Clim Change 3, 379–384.
Doummar, J., Geyer, T., Baierl, M., Nödler, K., Licha, T., Sauter, M., 2014. Carbamazepine breakthrough as indicator for specific vulnerability of karst springs: Application on the Jeita spring, Lebanon. Applied Geochemistry 47, 150–156.
Dozier, J., Bair, E., Davis, R., 2016. Estimating the spatial distribution of snow water equivalent in the world's mountains. Wiley Interdisciplinary Reviews: Water 3, 461–474.
Dozier, J., Green, R., Nolin, A., Painter, T., 2009. Interpretation of snow properties from imaging spectrometry. Remote Sensing of Environment 113, S25–S37.
Dozier, J., Painter, T., 2004. MULTISPECTRAL AND HYPERSPECTRAL REMOTE SENSING OF ALPINE SNOW PROPERTIES. Annual Review of Earth and Planetary Sciences 32, 465–494.
Dozier, J., Painter, T., Rittger, K., Frew, J., 2008. Time–space continuity of daily maps of fractional snow cover and albedo from MODIS. Advances in Water Resources 31, 1515–1526.
Durand, Y., Giraud, G., Laternser, M., Etchevers, P., Mérindol, L., Lesaffre, B., 2009. Reanalysis of 47 Years of Climate in the French Alps (1958–2005): Climatology and Trends for Snow Cover. Journal of Applied Meteorology and Climatology 48, 2487–2512.
Elder, K., Rosenthal, W., Davis, R., 1998. Estimating the spatial distribution of snow water equivalence in a montane watershed. Hydrol Process 12, 1793–1808.
Essery, R., Morin, S., Lejeune, Y., Ménard, C., 2013. A comparison of 1701 snow models using observations from an alpine site. Advances in Water Resources 55, 131–148.
Essery, R., Rutter, N., Pomeroy, J., Baxter, R., Stähli, M., Gustafsson, D., Barr, A., Bartlett, P., Elder, K., 2009. SNOWMIP2: An Evaluation of Forest Snow Process Simulations. B Am Meteorol Soc 90, 1120–1135.
Estévez, Gavilán, Giráldez, 2011. Guidelines on validation procedures for meteorological data from automatic weather stations. Journal of Hydrology 402, 144–154.
Fabre, J., Ruelland, D., Dezetter, A., and Grouillet, B., 2015. Simulating past changes in the balance between water demand and availability and assessing their main drivers at the river basin scale. Hydrol. Earth Syst. Sci., 19, 1263-1285, doi:10.5194/hess-19-1263-2015.
Famiglietti, Lo, Ho, Bethune, Anderson, Syed, Swenson, de Linage, Rodell, 2011. Satellites measure recent rates of groundwater depletion in California's Central Valley. Geophysical Research Letters 38.
Favier, V., Falvey, M., Rabatel, A., Praderio, E., López, D., 2009. Interpreting discrepancies between discharge and precipitation in high-altitude area of Chile's Norte Chico region (26–32°S). Water Resources Research 45.

Fernández-Chacón, Benavente, Rubio-Campos, Kohfahl, Jiménez, Meyer, Hubberten, Pekdeger, 2010. Isotopic composition (δ18O and δD) of precipitation and groundwater in a semi-arid, mountainous area (Guadiana Menor basin, Southeast Spain). Hydrological Processes 24, 1343–1356.
Filippa, Maggioni, Zanini, Freppaz, 2014. Analysis of continuous snow temperature profiles from automatic weather stations in Aosta Valley (NW Italy): Uncertainties and applications. Cold Regions Science and Technology 104-105, 5462.
Foster, Hall, Kelly, Chiu, 2009. Seasonal snow extent and snow mass in South America using SMMR and SSM/I passive microwave data (1979–2006). Remote Sensing of Environment 113, 291–305.
Franz, K., Butcher, P., Ajami, N., 2010. Addressing snow model uncertainty for hydrologic prediction. Advances in Water Resources 33, 820832.
Franz, K., Hogue, T., Barik, M., He, M., 2014. Assessment of SWE data assimilation for ensemble streamflow predictions. Journal of Hydrology 519, 2737–2746.
Franz, K., Karsten, L., 2013. Calibration of a distributed snow model using MODIS snow covered area data. Journal of Hydrology 494, 160–175.
Frei, A., Tedesco, M., Lee, S., Foster, J., Hall, D., Kelly, R., Robinson, D., 2012. A review of global satellite-derived snow products. Advances in Space Research 50, 1007–1029.
Friedman, I., Smith, G., Johnson, C., Moscati, R., 2002. Stable isotope compositions of waters in the Great Basin, United States 2. Modern precipitation. J Geophys Res Atmospheres 1984 2012 107, ACL 15–1–ACL 15–22.
Fu, Y., Argus, D., Landerer, F., 2015. GPS as an independent measurement to estimate terrestrial water storage variations in Washington and Oregon. Journal of Geophysical Research: Solid Earth 120, 552–566.
Gao, Y., Xie, H., Yao, T., Xue, C., 2010. Integrated assessment on multi-temporal and multi-sensor combinations for reducing cloud obscuration of MODIS snow cover products of the Pacific Northwest USA. Remote Sensing of Environment 114, 1662–1675.
Garcia, E., Tague, C., Choate, J., 2013. Influence of spatial temperature estimation method in ecohydrologic modeling in the Western Oregon Cascades. Water Resources Research 49, 1611–1624.
García-Ruiz, J., López-Moreno, I., Vicente-Serrano, S., Lasanta–Martínez, T., Beguería, S., 2011. Mediterranean water resources in a global change scenario. Earth-Science Reviews 105, 121–139.
Gascoin, S., Lhermitte, S., Kinnard, C., Bortels, K., Liston, G., 2013. Wind effects on snow cover in Pascua-Lama, Dry Andes of Chile. Advances in Water Resources 55, 25–39.
Giorgi, F., 2006. Climate change hot-spots. Geophysical Research Letters 33.
Giorgi, F., Lionello, P., 2008. Climate change projections for the Mediterranean region. Global and Planetary Change 63, 90–104.
Girotto, M., Margulis, S., Durand, M., 2014. Probabilistic SWE reanalysis as a generalization of deterministic SWE reconstruction techniques. Hydrological Processes 28, 3875–3895.
Godsey, Kirchner, Tague, 2014. Effects of changes in winter snowpacks on summer low flows: case studies in the Sierra Nevada, California, USA. Hydrological Processes 28, 5048–5064.
Gómez-Landesa, Rango, 2002. Operational snowmelt runoff forecasting in the Spanish Pyrenees using the snowmelt runoff model. Hydrological Processes 16, 1583–1591.
Gottardi, F., Obled, C., Gailhard, J., Paquet, E., 2012. Statistical reanalysis of precipitation fields based on ground network data and weather patterns: Application over French mountains. Journal of Hydrology 432-433, 154–167.
Goulden, Anderson, Bales, Kelly, Meadows, Winston, 2012. Evapotranspiration along an elevation gradient in California's Sierra Nevada. Journal of Geophysical Research: Biogeosciences (2005–2012) 117.
Goulden, M., Bales, R., 2014. Mountain runoff vulnerability to increased evapotranspiration with vegetation expansion. Proceedings of the National Academy of Sciences 111, 14071–14075.
Grew, N., 1673. Some Observations Touching the Nature of Snow. Phil. Trans. 8, 5193-5196
Grouillet, B., Ruelland, D., Vaittinada Ayar, P., and Vrac, M., 2016. Sensitivity analysis of runoff modeling to statistical downscaling models in the western Mediterranean. Hydrol. Earth Syst. Sci., 20, 1031-1047, doi:10.5194/hess-20-1031-2016.
Guan, B., Molotch, N., Waliser, D., Fetzer, E., Neiman, P., 2010. Extreme snowfall events linked to atmospheric rivers and surface air temperature via satellite measurements. Geophysical Research Letters 37.
Guan, B., Molotch, N., Waliser, D., Fetzer, E., Neiman, P., 2013a. The 2010/2011 snow season in California's Sierra Nevada: Role of atmospheric rivers and modes of large-scale variability. Water Resources Research 49, 6731–6743.
Guan, B., Molotch, N., Waliser, D., Jepsen, S., Painter, T., Dozier, J., 2013b. Snow water equivalent in the Sierra Nevada: Blending snow sensor observations with snowmelt model simulations. Water Resources Research 49, 5029–5046.
Guan, B., Waliser, D., Molotch, N., Fetzer, E., Neiman, P., 2012. Does the Madden–Julian Oscillation Influence Wintertime Atmospheric Rivers and Snowpack in the Sierra Nevada? Monthly Weather Review 140, 325–342.
Guan, B., Waliser, D., Ralph, M., Fetzer, E., Neiman, P., 2016. Hydrometeorological characteristics of rain-on-snow events associated with atmospheric rivers. Geophysical Research Letters 43, 2964–2973.

Hall, D., Riggs, G., Salomonson, V., DiGirolamo, N., Bayr, K., 2002. MODIS snow-cover products. Remote Sens Environ 83, 181–194.
Hamlet, A., Mote, P., Clark, M., Lettenmaier, D., 2005. Effects of Temperature and Precipitation Variability on Snowpack Trends in the Western United States. Journal of Climate 18, 4545–4561.
Hancock, S., Baxter, R., Evans, J., Huntley, B., 2013. Evaluating global snow water equivalent products for testing land surface models. Remote Sensing of Environment 128, 107–117.
Harpold, A., 2016. Diverging sensitivity of soil water stress to changing snowmelt timing in the Western U.S. Advances in Water Resources 92, 116–129.
Harpold, A., Brooks, P., Rajagopal, S., Heidbuchel, I., Jardine, A., Stielstra, C., 2012. Changes in snowpack accumulation and ablation in the intermountain west. Water Resources Research 48.
Harpold, A., Molotch, N., 2015. Sensitivity of soil water availability to changing snowmelt timing in the western U.S. Geophysical Research Letters 42, 8011–8020.
Harpold, A., Molotch, N., Musselman, K., Bales, R., Kirchner, P., Litvak, M., Brooks, P., 2015. Soil moisture response to snowmelt timing in mixed-conifer subalpine forests. Hydrological Processes 29, 2782–2798.
Harpold, Guo, Molotch, Brooks, Bales, Fernandez-Diaz, Musselman, Swetnam, Kirchner, Meadows, Flanagan, Lucas, 2014. LiDAR-derived snowpack data sets from mixed conifer forests across the Western United States. Water Resources Research 50, 2749–2755.
Hartmann, Goldscheider, Wagener, Lange, Weiler, 2014. Karst water resources in a changing world: Review of hydrological modeling approaches. Reviews of Geophysics 52, 218–242.
He, M., Hogue, T., Franz, K., Margulis, S., Vrugt, J., 2011. Characterizing parameter sensitivity and uncertainty for a snow model across hydroclimatic regimes. Advances in Water Resources 34, 114–127.
Henn, B., Clark, M., Kavetski, D., Lundquist, J., 2015. Estimating mountain basin-mean precipitation from streamflow using Bayesian inference. Water Resources Research 51, 8012–8033.
Herrero, Polo, 2012. Parameterization of atmospheric longwave emissivity in a mountainous site for all sky conditions. Hydrology and Earth System Sciences 16, 3139–3147.
Herrero, Polo, Moñino, Losada, 2009. An energy balance snowmelt model in a Mediterranean site. Journal of Hydrology 371, 98–107.
Hinkelman, L., Lapo, K., Cristea, N., Lundquist, J., 2015. Using CERES SYN Surface Irradiance Data as Forcing for Snowmelt Simulation in Complex Terrain. Journal of Hydrometeorology 150702111346007.
Horel, J., Dong, X., 2010. An Evaluation of the Distribution of Remote Automated Weather Stations (RAWS). Journal of Applied Meteorology and Climatology 49, 1563–1578.
Howat, I., Tulaczyk, S., 2005. Climate sensitivity of spring snowpack in the Sierra Nevada. Journal of Geophysical Research: Earth Surface (2003–2012) 110.
Hrachowitz, Savenije, H.H.G., Blöschl, McDonnell, J.J., Sivapalan, Pomeroy, J.W., Arheimer, Blume, Clark, M.P., Ehret, Fenicia, Freer, J.E., Gelfan, Gupta, H.V., Hughes, D.A., Hut, R.W., Montanari, Pande, Tetzlaff, Troch, P.A., Uhlenbrook, Wagener, Winsemius, H.C., Woods, R.A., Zehe, Cudennec, 2013. A decade of Predictions in Ungauged Basins (PUB)—a review. Hydrological Sciences Journal 58, 1198–1255.
Huber, Uli M., Bugmann, Harald K.M., Reasoner, Mel A. (Eds.) 2005. Global Change and Mountain Regions. An Overview of Current Knowledge. Springer. (ISBN 978-1-4020-3508-1) 652 pp.
Hublart, P., Ruelland, D., Dezetter, A., and Jourde, H., 2015. Reducing structural uncertainty in conceptual hydrological modelling in the semi-arid Andes, Hydrol. Earth Syst. Sci., 19, 2295-2314, doi:10.5194/hess-19-2295-2015.
Hublart, P., Ruelland, D., García de Cortázar-Atauri, I., Gascoin, S., Lhermitte, S., and Ibacache, A., 2016. Reliability of lumped hydrological modeling in a semi-arid mountainous catchment facing water-use changes. Hydrol. Earth Syst. Sci., 20, 3691-3717. doi:10.5194/hess-20-3691-2016.
Hüsler, Jonas, Riffler, Musial, Wunderle, 2014. A satellite-based snow cover climatology (1985–2011) for the European Alps derived from AVHRR data. The Cryosphere 8, 73–90.
Huth, Leydecker, Sickman, Bales, 2004. A two-component hydrograph separation for three high-elevation catchments in the Sierra Nevada, California. Hydrological Processes 18, 1721–1733.
Jefferson, A., Nolin, A., Lewis, S., Tague, C., 2008. Hydrogeologic controls on streamflow sensitivity to climate variation. Hydrological Processes 22, 4371–4385.
Jepsen, S., Harmon, T., Shi, Y., 2016b. Watershed model calibration to the base flow recession curve with and without evapotranspiration effects. Water Resour Res 52, 2919–2933.
Jepsen, S., Molotch, N., Williams, M., Rittger, K., Sickman, J., 2012. Interannual variability of snowmelt in the Sierra Nevada and Rocky Mountains, United States: Examples from two alpine watersheds. Water Resources Research 48.
Jepsen, S.M., Harmon, T.C., Meadows, M.W., Hunsaker, C.T., 2016a. Hydrogeologic influence on changes in snowmelt runoff with climate warming: Numerical experiments on a mid-elevation catchment in the Sierra Nevada, USA. J Hydrol 533, 332–342.

Jin, J., Miller, N., Sorooshian, S., Gao, X., 2006. Relationship between atmospheric circulation and snowpack in the western USA. Hydrological Processes 20, 753–767.
Jong, C. (ed.), David N. Collins D.N., Ranzi, R. (eds.) 2005. Climate and Hydrology of Mountain Areas. Wiley. (ISBN: 978-0-470-85814-1) 338 pp.
Jong, C. de, Gürer, Ibrahim, Rimmer, A., Shaban, A., Williams, M., 2012. Mediterranean Mountain Environments 87–113.
Jost, G., Weiler, M., Gluns, D., Alila, Y., 2007. The influence of forest and topography on snow accumulation and melt at the watershed-scale. Journal of Hydrology 347, 101–115.
Kapnick, S., Delworth, T., 2013. Controls of Global Snow under a Changed Climate. Journal of Climate 130206114111004.
Kapnick, S., Hall, A., 2010. Observed Climate–Snowpack Relationships in California and their Implications for the Future. Journal of Climate 23, 3446–3456.
Karpouzos, Baltas, Kavalieratou, Babajimopoulos, 2011. A hydrological investigation using a lumped water balance model: the Aison River Basin case (Greece). Water and Environment Journal 25, 297–307.
Kenawy, A., Lopez-Moreno, J., McCabe, M., Vicente-Serrano, S., 2015. Evaluation of the TMPA-3B42 precipitation product using a high-density rain gauge network over complex terrain in northeastern Iberia. Global and Planetary Change 133, 188–200.
Kerkez, B., Glaser, S., Bales, R., Meadows, M., 2012. Design and performance of a wireless sensor network for catchment-scale snow and soil moisture measurements. Water Resources Research 48.
Kim, J., Kang, H.-S., 2007. The Impact of the Sierra Nevada on Low-Level Winds and Water Vapor Transport. Journal of Hydrometeorology 8, 790–804.
Kinar, Pomeroy, 2015. Measurement of the physical properties of the snowpack. Reviews of Geophysics.
Kirchner, P., Bales, R., Molotch, N., Flanagan, J., Guo, Q., 2014. LiDAR measurement of seasonal snow accumulation along an elevation gradient in the southern Sierra Nevada, California. Hydrol Earth Syst Sc 18, 4261–4275.
Knowles, N, Cayan, DR, 2004. Elevational dependence of projected hydrologic changes in the San Francisco estuary and watershed. Climatic Change.
Knowles, Dettinger, Cayan, 2006. Trends in Snowfall versus Rainfall in the Western United States 19.
Koeniger, P., Toll, M., Himmelsbach, T., 2016. Stable isotopes of precipitation and spring waters reveal an altitude effect in the Anti-Lebanon Mountains, Syria. Hydrol Process 30, 2851–2860.
Kostadinov, T., Lookingbill, T., 2015. Snow cover variability in a forest ecotone of the Oregon Cascades via MODIS Terra products. Remote Sensing of Environment 164.
Kotlarski, S., Lüthi, D., Schär, C., 2015. The elevation dependency of 21st century European climate change: an RCM ensemble perspective. International Journal of Climatology 35, 3902–3920.
Kottek, M., Grieser, J., Beck, C., Rudolf, B., Rubel, F., 2006. World Map of the Köppen-Geiger climate classification updated. Meteorologische Zeitschrift 15, 259–263.
Kourgialas, N., Karatzas, G., Nikolaidis, N., 2010. An integrated framework for the hydrologic simulation of a complex geomorphological river basin. Journal of Hydrology 381, 308–321.
Kumar, S., Zwiers, F., Dirmeyer, P., Lawrence, D., Shrestha, R., Werner, A., 2016. Terrestrial contribution to the heterogeneity in hydrological changes under global warming. Water Resources Research 52, 3127–3142.
Kyselý, J., Beguería, S., Beranová, R., Gaál, L., López-Moreno, J., 2012. Different patterns of climate change scenarios for short-term and multi-day precipitation extremes in the Mediterranean. Global and Planetary Change 98-99, 63–72.
Lapo, K., Hinkelman, L., Raleigh, M., Lundquist, J., 2015. Impact of errors in the downwelling irradiances on simulations of snow water equivalent, snow surface temperature, and the snow energy balance. Water Resources Research.
Latron, Gallart, 2008. Runoff generation processes in a small Mediterranean research catchment (Vallcebre, Eastern Pyrenees). Journal of Hydrology 358, 206–220.
Lee, W.-L., Liou, 2012. Effect of absorbing aerosols on snow albedo reduction in the Sierra Nevada. Atmospheric Environment 55, 425–430.
Lettenmaier, D., Alsdorf, D., Dozier, J., Huffman, G., Pan, M., Wood, E., 2015. Inroads of remote sensing into hydrologic science during the WRR era. Water Resources Research 51, 7309–7342.
Leydecker, Melack, 2000. Estimating evaporation in seasonally snow-covered catchments in the Sierra Nevada, California. Journal of Hydrology 236, 121–138.
Li, D., Durand, M., Margulis, S., 2012. Potential for hydrologic characterization of deep mountain snowpack via passive microwave remote sensing in the Kern River basin, Sierra Nevada, USA. Remote Sensing of Environment 125, 34–48.
Liou, Gu, Leung, Lee, Fovell, 2013. A WRF simulation of the impact of 3-D radiative transfer on surface hydrology over the Rocky Mountains and Sierra Nevada. Atmospheric Chemistry and Physics 13, 11709–11721.
Liston, G. E., 1995: Local advection of momentum, heat, and moisture during the melt of patchy snow covers. J. Appl. Meteor. 34, 1705–1715.

Liston, G., Pielke, R., Greene, E., 1999. Improving first-order snow-related deficiencies in a regional climate model. Journal of Geophysical Research: Atmospheres (1984–2012) 104, 19559–19567.
Liu, F., Hunsaker, C., Bales, R., 2013. Controls of streamflow generation in small catchments across the snow–rain transition in the Southern Sierra Nevada, California. Hydrological Processes 27, 1959–1972.
Livneh, B., Xia, Y., Mitchell, K., Ek, M., Lettenmaier, D., 2010. Noah LSM Snow Model Diagnostics and Enhancements. J Hydrometeorol 11, 721–738.
Loarie, S., Duffy, P., Hamilton, H., Asner, G., Field, C., Ackerly, D., 2009. The velocity of climate change. Nature 462, 1052–1055.
López-Moreno, JI, 2005. Recent variations of snowpack depth in the Central Spanish Pyrenees. Arctic.
López-Moreno, Beniston, García-Ruiz, 2008a. Environmental change and water management in the Pyrenees: Facts and future perspectives for Mediterranean mountains. Global and Planetary Change 61, 300–312.
López-Moreno, Fassnacht, Beguería, Latron, 2011b. Variability of snow depth at the plot scale: implications for mean depth estimation and sampling strategies. The Cryosphere 5, 617–629.
López-Moreno, Fassnacht, Heath, Musselman, Revuelto, Latron, Morán-Tejeda, Jonas, 2013a. Small scale spatial variability of snow density and depth over complex alpine terrain: Implications for estimating snow water equivalent. Advances in Water Resources 55, 40–52.
López-Moreno, García-Ruiz, J., 2004. Influence of snow accumulation and snowmelt on streamflow in the central Spanish Pyrenees / Influence de l'accumulation et de la fonte de la neige sur les écoulements dans les Pyrénées centrales espagnoles. Hydrological Sciences Journal 49.
López-Moreno, Goyette, S., Beniston, M., Alvera, B., 2008b. Sensitivity of the snow energy balance to climatic changes: prediction of snowpack in the Pyrenees in the 21st century. Climate Research 36, 203–217.
López-Moreno, J., Pomeroy, J., Revuelto, J., Vicente-Serrano, S., 2012. Response of snow processes to climate change: spatial variability in a small basin in the Spanish Pyrenees. Hydrological Processes 27, 2637–2650.
López-Moreno, J., Revuelto, J., Fassnacht, S., Azorín-Molina, C., Vicente-Serrano, S., Morán-Tejeda, E., Sexstone, G., 2015. Snowpack variability across various spatio-temporal resolutions. Hydrological Processes 29, 1213–1224.
López-Moreno, J.I., Latron, J., Lehmann, A., 2010. Effects of sample and grid size on the accuracy and stability of regression based snow interpolation methods. Hydrological Processes 24, 1914–1928.
López-Moreno, Latron, 2008. Influence of canopy density on snow distribution in a temperate mountain range. Hydrological Processes 22, 117–126.
López-Moreno, Nogués-Bravo, 2005. A generalized additive model for the spatial distribution of snowpack in the Spanish Pyrenees. Hydrological Processes 19, 3167–3176.
López-Moreno, Nogués-Bravo, 2006. Interpolating local snow depth data: an evaluation of methods. Hydrological Processes 20, 2217–2232.
López-Moreno, Vicente-Serrano, Zabalza, Beguería, Lorenzo-Lacruz, Azorin-Molina, Morán-Tejeda, 2013b. Hydrological response to climate variability at different time scales: A study in the Ebro basin. Journal of Hydrology 477, 175–188.
López-Moreno, Zabalza, Vicente-Serrano, Revuelto, Gilaberte, Azorin-Molina, Morán-Tejeda, García-Ruiz, Tague, 2014. Impact of climate and land use change on water availability and reservoir management: Scenarios in the Upper Aragón River, Spanish Pyrenees. Science of The Total Environment 493, 1222–1231.
Lowry, C., Deems, J., Steven, L., Lundquist, J., 2010. Linking snowmelt-derived fluxes and groundwater flow in a high elevation meadow system, Sierra Nevada Mountains, California. Hydrological Processes 24, 2821–2833.
Lowry, C., Loheide, S., Moore, C., Lundquist, J., 2011. Groundwater controls on vegetation composition and patterning in mountain meadows. Water Resources Research 47.
Luce, C., Lopez-Burgos, V., Holden, Z., 2014. Sensitivity of snowpack storage to precipitation and temperature using spatial and temporal analog models. Water Resour Res 50, 9447–9462.
Lundquist, Cayan, 2002. Seasonal and spatial patterns in diurnal cycles in streamflow in the western United States.
Lundquist, Flint, 2006. Onset of snowmelt and streamflow in 2004 in the western United States: How shading may affect spring streamflow timing in a warmer world.
Lundquist, J., Dettinger, M., Cayan, D., 2005. Snow-fed streamflow timing at different basin scales: Case study of the Tuolumne River above Hetch Hetchy, Yosemite, California. Water Resources Research 41.
Lundquist, J., Dickerson-Lange, S., Lutz, J., Cristea, N., 2013. Lower forest density enhances snow retention in regions with warmer winters: A global framework developed from plot-scale observations and modeling. Water Resour Res 49, 6356–6370.
Lundquist, J., Hughes, M., Henn, B., Gutmann, E., Livneh, B., Dozier, J., Neiman, P., 2015a. High-Elevation Precipitation Patterns: Using Snow Measurements to Assess Daily Gridded Datasets across the Sierra Nevada, California*. J Hydrometeorol 16, 1773–1792.
Lundquist, J., Loheide, S., 2011. How evaporative water losses vary between wet and dry water years as a function of elevation in the Sierra Nevada, California, and critical factors for modeling. Water Resources Research 47.

Lundquist, J., Minder, J., Neiman, P., Sukovich, E., 2010. Relationships between Barrier Jet Heights, Orographic Precipitation Gradients, and Streamflow in the Northern Sierra Nevada. Journal of Hydrometeorology 11, 1141–1156.
Lundquist, J., Wayand, N., Massmann, A., Clark, M., Lott, F., Cristea, N., 2015b. Diagnosis of insidious data disasters. Water Resources Research 51, 3815–3827.
Lundquist, J.D., Cayan, D.R., Dettinger, M.D., 2004. Spring Onset in the Sierra Nevada: When Is Snowmelt Independent of Elevation? Journal of Hydrometeorology 5, 327–342.
Lute, Abatzoglou, 2014. Role of extreme snowfall events in interannual variability of snowfall accumulation in the western United States. Water Resources Research 50, 2874–2888.
Magand, C., Ducharne, A., Moine, N., Gascoin, S., 2014. Introducing Hysteresis in Snow Depletion Curves to Improve the Water Budget of a Land Surface Model in an Alpine Catchment. Journal of Hydrometeorology 15, 631–649.
Manning, A., Clark, J., Diaz, S., Rademacher, L., Earman, S., Plummer, N., 2012. Evolution of groundwater age in a mountain watershed over a period of thirteen years. Journal of Hydrology 460-461, 13–28.
Marchane, Jarlan, Hanich, Boudhar, Gascoin, Tavernier, Filali, Page, L., Hagolle, Berjamy, 2015. Assessment of daily MODIS snow cover products to monitor snow cover dynamics over the Moroccan Atlas mountain range. Remote Sensing of Environment 160, 72–86.
Margulis, S., Cortés, G., Girotto, M., Durand, M., 2016. A Landsat-Era Sierra Nevada Snow Reanalysis (1985–2015). J Hydrometeorol 17, 1203–1221.
Marks, D., Dozier, J., 1992. Climate and energy exchange at the snow surface in the Alpine Region of the Sierra Nevada: 2. Snow cover energy balance. Water Resources Research 28, 3043–3054.
Marks, D., Dozier, J., Davis, R., 1992. Climate and energy exchange at the snow surface in the Alpine Region of the Sierra Nevada: 1. Meteorological measurements and monitoring. Water Resources Research 28, 3029–3042.
Martelloni, Segoni, Lagomarsino, Fanti, Catani, 2013. Snow accumulation/melting model (SAMM) for integrated use in regional scale landslide early warning systems. Hydrology and Earth System Sciences 17, 1229–1240.
Marti, Gascoin, Berthier, de Pinel, Houet, Laffly, 2016. Mapping snow depth in open alpine terrain from stereo satellite imagery. The Cryosphere Discussions 1–36.
Martinec, J., Rango, A., 1986. Parameter values for snowmelt runoff modelling. Journal of Hydrology 84, 197–219.
Martinec, J.M., 1975. Snowmelt runoff model for stream flow forecasts. Nordic Hydrology, 6 (3) 145–154.
Masiokas, M., Villalba, R., Luckman, B., Quesne, C., Aravena, J., 2006. Snowpack Variations in the Central Andes of Argentina and Chile, 1951–2005: Large-Scale Atmospheric Influences and Implications for Water Resources in the Region. Journal of Climate 19, 6334–6352.
Maurer, E., Brekke, L., Pruitt, T., 2010. Contrasting Lumped and Distributed Hydrology Models for Estimating Climate Change Impacts on California Watersheds1. JAWRA Journal of the American Water Resources Association 46, 1024–1035.
Maurer, Stewart, Bonfils, Duffy, Cayan, 2007. Detection, attribution, and sensitivity of trends toward earlier streamflow in the Sierra Nevada. Journal of Geophysical Research: Atmospheres (1984–2012) 112.
Mazurkiewicz, A., Callery, D., McDonnell, J., 2008. Assessing the controls of the snow energy balance and water available for runoff in a rain-on-snow environment. Journal of Hydrology 354, 114.
McCabe, G., Hay, L., Clark, M., 2007. Rain-on-Snow Events in the Western United States. Bulletin of the American Meteorological Society 88, 319–328.
Meixner, T., Manning, A., Stonestrom, D., Allen, D., Ajami, H., Blasch, K., Brookfield, A., Castro, C., Clark, J., Gochis, D., Flint, A., Neff, K., Niraula, R., Rodell, M., Scanlon, B., Singha, K., Walvoord, M., 2016. Implications of projected climate change for groundwater recharge in the western United States. Journal of Hydrology 534, 124–138.
Mernild, S., Liston, G., Hiemstra, C., Malmros, J., Yde, J., McPhee, J., 2016a. The Andes Cordillera. Part I: snow distribution, properties, and trends (1979–2014). International Journal of Climatology.
Mernild, S., Liston, G., Hiemstra, C., Yde, J., McPhee, J., Malmros, J., 2016b. The Andes Cordillera. Part II: Rio Olivares Basin snow conditions (1979–2014), central Chile. International Journal of Climatology.
Meromy, L., Molotch, N., Link, T., Fassnacht, S., Rice, R., 2013. Subgrid variability of snow water equivalent at operational snow stations in the western USA. Hydrological Processes 27, 2383–2400.
Mhawej, M., Faour, G., Fayad, A., Shaban, A., 2014. Towards an enhanced method to map snow cover areas and derive snow-water equivalent in Lebanon. Journal of Hydrology 513, 274–282.
Millares, Polo, Losada, 2009. The hydrological response of baseflow in fractured mountain areas. Hydrology and Earth System Sciences 13, 1261–1271.
Milly, P., Dunne, Vecchia, 2005. Global pattern of trends in streamflow and water availability in a changing climate. Nature 438, 347–50.
Mizukami, N., Perica, S., 2008. Spatiotemporal Characteristics of Snowpack Density in the Mountainous Regions of the Western United States. Journal of Hydrometeorology 9, 1416–1426.

Mizukami, N., Perica, S., Hatch, D., 2011. Regional approach for mapping climatological snow water equivalent over the mountainous regions of the western United States. Journal of Hydrology 400, 72–82.
Mizukami, N., Smith, M., 2012. Analysis of inconsistencies in multi-year gridded quantitative precipitation estimate over complex terrain and its impact on hydrologic modeling. Journal of Hydrology 428-429, 129–141.
Molotch, Fassnacht, Bales, Helfrich, 2004. Estimating the distribution of snow water equivalent and snow extent beneath cloud cover in the Salt–Verde River basin, Arizona. Hydrological Processes 18, 1595–1611.
Molotch, N., Bales, R., 2006. Comparison of ground-based and airborne snow surface albedo parameterizations in an alpine watershed: Impact on snowpack mass balance. Water Resources Research 42.
Molotch, N., Colee, M., Bales, R., Dozier, J., 2005. Estimating the spatial distribution of snow water equivalent in an alpine basin using binary regression tree models: the impact of digital elevation data and independent variable selection. Hydrol Process 19, 1459–1479.
Molotch, N., Margulis, S., 2008. Estimating the distribution of snow water equivalent using remotely sensed snow cover data and a spatially distributed snowmelt model: A multi-resolution, multi-sensor comparison. Advances in Water Resources 31, 1503–1514.
Morán-Tejeda, E., Ceballos-Barbancho, A., Llorente-Pinto, J., 2010. Hydrological response of Mediterranean headwaters to climate oscillations and land-cover changes: The mountains of Duero River basin (Central Spain). Global and Planetary Change 72, 39–49.
Morán-Tejeda, E., Lorenzo-Lacruz, J., López-Moreno, J., Rahman, K., Beniston, M., 2014. Streamflow timing of mountain rivers in Spain: Recent changes and future projections. Journal of Hydrology 517, 1114–1127.
Mote, PW, 2006. Climate-driven variability and trends in mountain snowpack in Western North America. Journal of Climate.
Mote, P., 2003. Trends in snow water equivalent in the Pacific Northwest and their climatic causes. Geophysical Research Letters 30.
Mote, P., Hamlet, A., Clark, M., Lettenmaier, D., 2005. DECLINING MOUNTAIN SNOWPACK IN WESTERN NORTH AMERICA*. Bulletin of the American Meteorological Society 86, 39–49.
Musselman, K., Molotch, N., Margulis, S., Kirchner, P., Bales, R., 2012. Influence of canopy structure and direct beam solar irradiance on snowmelt rates in a mixed conifer forest. Agricultural and Forest Meteorology 161, 46–56.
Neiman, P., Ralph, M., Moore, B., Zamora, R., 2014. The Regional Influence of an Intense Sierra Barrier Jet and Landfalling Atmospheric River on Orographic Precipitation in Northern California: A Case Study. Journal of Hydrometeorology 15, 1419–1439.
Nogués-Bravo, Araújo, Errea, Martínez-Rica, 2007. Exposure of global mountain systems to climate warming during the 21st Century. Global Environmental Change 17, 420–428.
Nohara, D., Kitoh, A., Hosaka, M., Oki, T., 2006. Impact of Climate Change on River Discharge Projected by Multimodel Ensemble. Journal of Hydrometeorology 7, 1076–1089.
Novel, J.-P., Dimadi, A., Zervopoulou, A., Bakalowicz, M., 2007. The Aggitis karst system, Eastern Macedonia, Greece: Hydrologic functioning and development of the karst structure. Journal of Hydrology 334, 477–492.
Null, S., Viers, J., Mount, J., 2010. Hydrologic Response and Watershed Sensitivity to Climate Warming in California's Sierra Nevada. PLoS ONE 5.
Núñez, Rivera, Oyarzún, Arumí, 2013. Influence of Pacific Ocean multidecadal variability on the distributional properties of hydrological variables in north-central Chile. Journal of Hydrology 501, 227–240.
Oaida, C., Xue, Y., Flanner, M., Skiles, M., Sales, F., Painter, T., 2015. Improving snow albedo processes in WRF/SSiB regional climate model to assess impact of dust and black carbon in snow on surface energy balance and hydrology over western U.S. Journal of Geophysical Research: Atmospheres 120, 3228–3248.
Ouellette, K., Linage, C., Famiglietti, J., 2013. Estimating snow water equivalent from GPS vertical site-position observations in the western United States. Water Resources Research 49, 2508–2518.
Pagán, B., Ashfaq, M., Rastogi, D., Kendall, D., Kao, S.-C., Naz, B., Mei, R., Pal, J., 2016. Extreme hydrological changes in the southwestern US drive reductions in water supply to Southern California by mid century. Environmental Research Letters 11, 094026.
Painter, T., Berisford, D., Boardman, J., Bormann, K., Deems, J., Gehrke, F., Hedrick, A., Joyce, M., Laidlaw, R., Marks, D., Mattmann, C., McGurk, B., Ramirez, P., Richardson, M., Skiles, S., Seidel, F., Winstral, A., 2016. The Airborne Snow Observatory: Fusion of scanning lidar, imaging spectrometer, and physically-based modeling for mapping snow water equivalent and snow albedo. Remote Sens Environ 184, 139–152.
Painter, T., Dozier, J., Roberts, D., Davis, R., Green, R., 2003. Retrieval of subpixel snow-covered area and grain size from imaging spectrometer data. Remote Sensing of Environment 85, 64–77.
Painter, T., Rittger, K., McKenzie, C., Slaughter, P., Davis, R., Dozier, J., 2009. Retrieval of subpixel snow covered area, grain size, and albedo from MODIS. Remote Sensing of Environment 113, 868–879.
Palmer, C., Gannett, M., Hinkle, S., 2007. Isotopic characterization of three groundwater recharge sources and inferences for selected aquifers in the upper Klamath Basin of Oregon and California, USA. Journal of Hydrology 336, 17–29.

Pavelsky, T., Kapnick, S., Hall, A., 2011. Accumulation and melt dynamics of snowpack from a multiresolution regional climate model in the central Sierra Nevada, California. Journal of Geophysical Research: Atmospheres (1984–2012) 116.

Pavelsky, T., Sobolowski, S., Kapnick, S., Barnes, J., 2012. Changes in orographic precipitation patterns caused by a shift from snow to rain. Geophysical Research Letters 39.

Penna, Meerveld, Oliviero, Zuecco, Assendelft, Fontana, D., Borga, 2015. Seasonal changes in runoff generation in a small forested mountain catchment. Hydrological Processes 29, 2027–2042.

Pepin, Bradley, Diaz, Baraer, Caceres, Forsythe, Fowler, Greenwood, Hashmi, Liu, Miller, Ning, Ohmura, Palazzi, Rangwala, Schöner, Severskiy, Shahgedanova, Wang, Williamson, Yang, 2015. Elevation-dependent warming in mountain regions of the world. Nature Climate Change 5, 424–430.

Perrot, D., Molotch, N., Williams, M., Jepsen, S., Sickman, J., 2014. Relationships between stream nitrate concentration and spatially distributed snowmelt in high-elevation catchments of the western U.S. Water Resources Research 50, 8694–8713.

Pierce, D., Barnett, T., Hidalgo, H., Das, T., Bonfils, C., Santer, B., Bala, G., Dettinger, M., Cayan, D., Mirin, A., Wood, A., Nozawa, T., 2008. Attribution of Declining Western U.S. Snowpack to Human Effects. Journal of Climate 21, 6425–6444.

Pimentel, R., Aguilar, C., Herrero, J., Pérez-Palazón, M., Polo, M., 2016. Comparison between Snow Albedo Obtained from Landsat TM, ETM+ Imagery and the SPOT VEGETATION Albedo Product in a Mediterranean Mountainous Site. Hydrology 3, 10.

Pimentel, R., Herrero, J., Zeng, Y., Su, Z., Polo, M., 2015. Study of Snow Dynamics at Subgrid Scale in Semiarid Environments Combining Terrestrial Photography and Data Assimilation Techniques. Journal of Hydrometeorology 16, 563–578.

Powell, C., Blesius, L., Davis, J., Schuetzenmeister, F., 2011. Using MODIS snow cover and precipitation data to model water runoff for the Mokelumne River Basin in the Sierra Nevada, California (2000–2009). Global and Planetary Change 77, 77–84.

Prudhomme, C., Giuntoli, I., Robinson, E., Clark, D., Arnell, N., Dankers, R., Fekete, B., Franssen, W., Gerten, D., Gosling, S., Hagemann, S., Hannah, D., Kim, H., Masaki, Y., Satoh, Y., Stacke, T., Wada, Y., Wisser, D., 2014. Hydrological droughts in the 21st century, hotspots and uncertainties from a global multimodel ensemble experiment. Proceedings of the National Academy of Sciences 111, 3262–3267.

Quéno, L., Vionnet, V., Dombrowski-Etchevers, I., Lafaysse, M., Dumont, M., Karbou, F., 2016. Snowpack modelling in the Pyrenees driven by kilometric-resolution meteorological forecasts. Cryosphere 10, 1571–1589.

Rademacher, L., Clark, J., Clow, D., Hudson, B., 2005. Old groundwater influence on stream hydrochemistry and catchment response times in a small Sierra Nevada catchment: Sagehen Creek, California. Water Resources Research 41.

Raleigh, M., Livneh, B., Lapo, K., Lundquist, J., 2016. How Does Availability of Meteorological Forcing Data Impact Physically Based Snowpack Simulations?*. Journal of Hydrometeorology 17, 99–120.

Raleigh, M., Lundquist, J., 2012. Comparing and combining SWE estimates from the SNOW-17 model using PRISM and SWE reconstruction. Water Resour Res 48.

Raleigh, M., Rittger, K., Moore, C., Henn, B., Lutz, J., Lundquist, J., 2013. Ground-based testing of MODIS fractional snow cover in subalpine meadows and forests of the Sierra Nevada. Remote Sensing of Environment 128, 44–57.

Ralph, F., Prather, K., Cayan, D., Spackman, J.R., DeMott, P., Dettinger, M., Fairall, C., Leung, R., Rosenfeld, D., Rutledge, S., Waliser, D., White, A., Cordeira, J., Martin, A., Helly, J., Intrieri, J., 2016. CalWater Field Studies Designed to Quantify the Roles of Atmospheric Rivers and Aerosols in Modulating U.S. West Coast Precipitation in a Changing Climate. B Am Meteorol Soc 97, 1209–1228.

Revuelto, J., Jonas, T., López-Moreno, J., 2016a. Backward snow depth reconstruction at high spatial resolution based on time-lapse photography. Hydrol Process 30, 2976–2990.

Revuelto, J., Vionnet, V., López-Moreno, J.-I., Lafaysse, M., Morin, S., 2016b. Combining snowpack modeling and terrestrial laser scanner observations improves the simulation of small scale snow dynamics. J Hydrol 533, 291–307.

Revuelto, López-Moreno, Azorin-Molina, Vicente-Serrano, 2014. Topographic control of snowpack distribution in a small catchment in the central Spanish Pyrenees: intra- and inter-annual persistence. The Cryosphere 8, 1989–2006.

Revuelto, López-Moreno, Azorin-Molina, Vicente-Serrano, 2015. Canopy influence on snow depth distribution in a pine stand determined from terrestrial laser data. Water Resources Research 51, 3476–3489.

Rice, R., Bales, R., 2010. Embedded-sensor network design for snow cover measurements around snow pillow and snow course sites in the Sierra Nevada of California. Water Resources Research 46.

Rice, R., Bales, R., Painter, T., Dozier, J., 2011. Snow water equivalent along elevation gradients in the Merced and Tuolumne River basins of the Sierra Nevada. Water Resources Research 47.

Rittger, K., Bair, E., Kahl, A., Dozier, J., 2016. Spatial estimates of snow water equivalent from reconstruction. Advances in Water Resources 94, 345–363.

Rittger, K., Painter, T., Dozier, J., 2013. Assessment of methods for mapping snow cover from MODIS. Advances in Water Resources 51, 367–380.
Rousselot, Durand, Giraud, Mérindol, Dombrowski-Etchevers, Déqué, Castebrunet, 2012. Statistical adaptation of ALADIN RCM outputs over the French Alps – application to future climate and snow cover. The Cryosphere 6, 785–805.
Rutter, N., Essery, R., Pomeroy, J., Altimir, N., Andreadis, K., Baker, I., Barr, A., Bartlett, P., Boone, A., Deng, H., Douville, H., Dutra, E., Elder, K., Ellis, C., Feng, X., Gelfan, A., Goodbody, A., Gusev, Y., Gustafsson, D., Hellström, R., Hirabayashi, Y., Hirota, T., Jonas, T., Koren, V., Kuragina, A., Lettenmaier, D., Li, W.-P., Luce, C., Martin, E., Nasonova, O., Pumpanen, J., Pyles, D., Samuelsson, P., Sandells, M., Schädler, G., Shmakin, A., Smirnova, T., Stähli, M., Stöckli, R., Strasser, U., Su, H., Suzuki, K., Takata, K., Tanaka, K., Thompson, E., Vesala, T., Viterbo, P., Wiltshire, A., Xia, K., Xue, Y., Yamazaki, T., 2009. Evaluation of forest snow processes models (SnowMIP2). Journal of Geophysical Research 114.
Rutz, J., Steenburgh, J., Ralph, M., 2014. Climatological Characteristics of Atmospheric Rivers and Their Inland Penetration over the Western United States. Monthly Weather Review 142, 905–921.
Sade, R., Rimmer, A., Litaor, I., Shamir, E., Furman, A., 2014. Snow surface energy and mass balance in a warm temperate climate mountain. Journal of Hydrology 519, 848–862.
Scanlon, B., Longuevergne, L., Long, D., 2012. Ground referencing GRACE satellite estimates of groundwater storage changes in the California Central Valley, USA. Water Resour Res 48, n/a–n/a.
Schlaepfer, D., Lauenroth, W., Bradford, J., 2012. Consequences of declining snow accumulation for water balance of mid-latitude dry regions. Global Change Biology 18, 1988–1997.
Schulz, O., Jong, C. de, 2004. Snowmelt and sublimation: field experiments and modelling in the High Atlas Mountains of Morocco. Hydrology and Earth System Sciences 8, 1076–1089.
Seidel, K. and Martinec, J., 2004. Remote Sensing in Snow Hydrology. Runoff Modelling, Effect of Climate Change. (ISBN: 978-3-540-40880-2) 150 pp.
Senatore, A., Mendicino, G., Smiatek, G., Kunstmann, H., 2011. Regional climate change projections and hydrological impact analysis for a Mediterranean basin in Southern Italy. Journal of Hydrology 399, 70–92.
Şensoy, A., Uysal, G., 2012. The Value of Snow Depletion Forecasting Methods Towards Operational Snowmelt Runoff Estimation Using MODIS and Numerical Weather Prediction Data. Water Resources Management 26, 3415–3440.
Şensoy, Şorman, Tekeli, Şorman, Ü., Garen, 2006. Point-scale energy and mass balance snowpack simulations in the upper Karasu basin, Turkey. Hydrological Processes 20, 899–922.
Shamir, E., Georgakakos, K., 2006. Distributed snow accumulation and ablation modeling in the American River basin. Advances in Water Resources 29, 558–570.
Shaw, G., Conklin, M., Nimz, G., Liu, F., 2014. Groundwater and surface water flow to the Merced River, Yosemite Valley, California: 36Cl and Cl− evidence. Water Resources Research 50, 1943–1959.
Singh, Reager, Miller, Famiglietti, 2015. Toward hyper-resolution land-surface modeling: The effects of fine-scale topography and soil texture on CLM4.0 simulations over the Southwestern U.S. Water Resources Research 51, 2648–2667.
Slater, Barrett, Clark, Lundquist, Raleigh, 2013. Uncertainty in seasonal snow reconstruction: Relative impacts of model forcing and image availability. Advances in Water Resources 55, 165–177.
Smith, M., Koren, V., Zhang, Z., Moreda, F., Cui, Z., Cosgrove, B., Mizukami, N., Kitzmiller, D., Ding, F., Reed, S., Anderson, E., Schaake, J., Zhang, Y., Andréassian, V., Perrin, C., Coron, L., Valéry, A., Khakbaz, B., Sorooshian, S., Behrangi, A., Imam, B., Hsu, K.-L., Todini, E., Coccia, G., Mazzetti, C., Andres, E., Francés, F., Orozco, I., Hartman, R., Henkel, A., Fickenscher, P., Staggs, S., 2013. The distributed model intercomparison project – Phase 2: Experiment design and summary results of the western basin experiments. Journal of Hydrology 507, 300–329.
Şorman, A., Şensoy, Tekeli, Şorman, Ü., Akyürek, 2009. Modelling and forecasting snowmelt runoff process using the HBV model in the eastern part of Turkey. Hydrological Processes 23, 1031–1040.
Sorman, U., Beser, O., 2013. Determination of snow water equivalent over the eastern part of Turkey using passive microwave data. Hydrological Processes 27, 1945–1958.
Sproles, E., Kerr, T., Nelson, C., Aspe, D., 2016. Developing a Snowmelt Forecast Model in the Absence of Field Data. Water Resources Management 30, 2581–2590.
Sproles, Nolin, Rittger, Painter, 2013. Climate change impacts on maritime mountain snowpack in the Oregon Cascades. Hydrology and Earth System Sciences 17, 2581–2597.
Stewart, IT, Cayan, DR, Dettinger, MD, 2005. Changes toward earlier streamflow timing across western North America. Journal of climate.
Stewart, I., 2009. Changes in snowpack and snowmelt runoff for key mountain regions. Hydrological Processes 23, 78–94.
Stewart, I., 2013. Connecting physical watershed characteristics to climate sensitivity for California mountain streams. Climatic Change 116, 133–148.

Storck, P., Lettenmaier, D., Bolton, S., 2002. Measurement of snow interception and canopy effects on snow accumulation and melt in a mountainous maritime climate, Oregon, United States. Water Resources Research 38, 5–1–5–16.
Sturm, M., 2015. White water: Fifty years of snow research in WRR and the outlook for the future. Water Resources Research.
Sturm, M., Holmgren, J., Liston, G.E., 1995. A Seasonal Snow Cover Classification System for Local to Global Applications. J. Climate, 8, 1261–1283.
Sturm, M., Taras, B., Liston, G., Derksen, C., Jonas, T., Lea, J., 2010. Estimating Snow Water Equivalent Using Snow Depth Data and Climate Classes. Journal of Hydrometeorology 11, 1380–1394.
Surfleet, C., Tullos, D., 2013. Variability in effect of climate change on rain-on-snow peak flow events in a temperate climate. Journal of Hydrology 479, 24–34.
Svoma, B., 2011. Winter Climatic Controls on Spring Snowpack Density in the Western United States. Arct Antarct Alp Res 46, 118–126.
Szczypta, Gascoin, Houet, Hagolle, Dejoux, -F, Vigneau, Fanise, 2015. Impact of climate and land cover changes on snow cover in a small Pyrenean catchment. Journal of Hydrology 521, 84–99.
Tague, C., Grant, G., 2009. Groundwater dynamics mediate low-flow response to global warming in snow-dominated alpine regions. Water Resources Research 45.
Tague, C., Peng, H., 2013. The sensitivity of forest water use to the timing of precipitation and snowmelt recharge in the California Sierra: Implications for a warming climate. Journal of Geophysical Research: Biogeosciences 118, 875–887.
Tanaka, S., Zhu, T., Lund, J., Howitt, R., Jenkins, M., Pulido, M., Tauber, M., Ritzema, R., Ferreira, I., 2006. Climate Warming and Water Management Adaptation for California. Climatic Change 76, 361–387.
Taylor, S., Feng, X., Kirchner, J., Osterhuber, R., Klaue, B., Renshaw, C., 2001. Isotopic evolution of a seasonal snowpack and its melt. Water Resources Research 37, 759–769.
Tedesco M (ed.) 2015. Remote Sensing of the Cryosphere. Wiley. (ISBN: 978-1-118-36885-5) 432 pp.
Tekeli, A., Şensoy, A., Şorman, A., Akyürek, Z., Şorman, Ü., 2006. Accuracy assessment of MODIS daily snow albedo retrievals with in situ measurements in Karasu basin, Turkey. Hydrological Processes 20, 705–721.
Tekeli, E., 2008. Early findings in comparison of AMSR-E/Aqua L3 global snow water equivalent EASE-grids data with in situ observations for Eastern Turkey. Hydrological Processes 22, 2737–2747.
Tekeli, E., Akyürek, Z., Şensoy, A., Şorman, A., Şorman, Ü., 2005a. Modelling the temporal variation in snow-covered area derived from satellite images for simulating/forecasting of snowmelt runoff in Turkey/Modélisation de la variation temporelle de la surface enneigée à partir d'images satellitaires pour la simulation/prévision de l'écoulement de fonte nivale en Turquie. Hydrological Sciences Journal 50.
Tekeli, E., Akyürek, Z., Şorman, A., Şensoy, A., Şorman, Ü., 2005b. Using MODIS snow cover maps in modeling snowmelt runoff process in the eastern part of Turkey. Remote Sensing of Environment 97, 216–230.
Telesca, L., Shaban, A., Gascoin, S., Darwich, T., Drapeau, L., Hage, M., Faour, G., 2014. Characterization of the time dynamics of monthly satellite snow cover data on Mountain Chains in Lebanon. Journal of Hydrology 519, 3214–3222.
Thirel, Notarnicola, Kalas, Zebisch, Schellenberger, Tetzlaff, Duguay, Mölg, Burek, de Roo, 2012. Assessing the quality of a real-time Snow Cover Area product for hydrological applications. Remote Sens Environ 127, 271–287.
Tobin, B., Schwartz, B., 2016. Using periodic hydrologic and geochemical sampling with limited continuous monitoring to characterize remote karst aquifers in the Kaweah River Basin, California, USA. Hydrol Process 30, 3361–3372.
Trujillo, E., Molotch, N., 2014. Snowpack regimes of the Western United States. Water Resources Research 50, 5611–5623.
Trujillo, E., Molotch, N., Goulden, M., Kelly, A., Bales, R., 2012. Elevation-dependent influence of snow accumulation on forest greening. Nature Geoscience 5, 705–709.
Valdés-Pineda, R., Pizarro, R., García-Chevesich, P., Valdés, J., Olivares, C., Vera, M., Balocchi, F., Pérez, F., Vallejos, C., Fuentes, R., Abarza, A., Helwig, B., 2014. Water governance in Chile: Availability, management and climate change. Journal of Hydrology 519, 2538–2567.
Vano, J., Nijssen, B., Lettenmaier, D., 2015. Seasonal hydrologic responses to climate change in the Pacific Northwest. Water Resources Research 51, 1959–1976.
Varhola, A., Wawerla, J., Weiler, M., Coops, N., Bewley, D., Alila, Y., 2010. A New Low-Cost, Stand-Alone Sensor System for Snow Monitoring. Journal of Atmospheric and Oceanic Technology 27, 1973–1978.
Vicuna, Dracup, 2007. The evolution of climate change impact studies on hydrology and water resources in California. Climatic Change 82, 327–350.
Vicuña, S., Garreaud, R., McPhee, J., 2011. Climate change impacts on the hydrology of a snowmelt driven basin in semiarid Chile. Climatic Change 105, 469–488.

Vidal, J., Martin, E., Franchistéguy, L., Baillon, M., Soubeyroux, J., 2010. A 50-year high-resolution atmospheric reanalysis over France with the Safran system. International Journal of Climatology 30, 1627–1644.
Viviroli, Archer, Buytaert, Fowler, Greenwood, Hamlet, Huang, Koboltschnig, Litaor, López-Moreno, Lorentz, Schädler, Schreier, Schwaiger, Vuille, Woods, 2011. Climate change and mountain water resources: overview and recommendations for research, management and policy. Hydrology and Earth System Sciences 15, 471–504.
Viviroli, D., Dürr, H., Messerli, B., Meybeck, M., Weingartner, R., 2007. Mountains of the world, water towers for humanity: Typology, mapping, and global significance. Water Resources Research 43.
Vuyovich, C., Jacobs, J., Daly, S., 2014. Comparison of passive microwave and modeled estimates of total watershed SWE in the continental United States. Water Resources Research 50, 9088–9102.
Watson, F., Anderson, T., Newman, W., Alexander, S., Garrott, R., 2006. Optimal sampling schemes for estimating mean snow water equivalents in stratified heterogeneous landscapes. Journal of Hydrology 328, 432–452.
Wayand, N., Hamlet, A., Hughes, M., Feld, S., Lundquist, J., 2013. Intercomparison of Meteorological Forcing Data from Empirical and Mesoscale Model Sources in the North Fork American River Basin in Northern Sierra Nevada, California*. Journal of Hydrometeorology 14, 677–699.
Wayand, N., Lundquist, J., Clark, M., 2015. Modeling the influence of hypsometry, vegetation, and storm energy on snowmelt contributions to basins during rain-on-snow floods. Water Resources Research 51, 8551–8569.
Welch, S., Kerkez, B., Bales, R., Glaser, S., Rittger, K., Rice, R., 2013. Sensor placement strategies for snow water equivalent (SWE) estimation in the American River basin. Water Resources Research 49, 891–903.
Williams, M., Leydecker, A., Brown, A., Melack, J., 2001. Processes regulating the solute concentrations of snowmelt runoff in two subalpine catchments of the Sierra Nevada, California. Water Resources Research 37, 1993–2008.
Woeikof, A., 1885. On the influence of accumulations of snow on climate. Quaterly Journal of the Royal Meteorological Society, 299-309.
Wrzesien, M., Pavelsky, T., Kapnick, S., Durand, M., Painter, T., 2015. Evaluation of snow cover fraction for regional climate simulations in the Sierra Nevada. International Journal of Climatology.
Wu, W., Lan, C., Lo, M., Reager, J., Famiglietti, J., 2015. Increases in the annual range of soil water storage at northern middle and high latitudes under global warming. Geophysical Research Letters 42, 3903–3910.
Zaitchik, B., Rodell, M., 2009. Forward-Looking Assimilation of MODIS-Derived Snow-Covered Area into a Land Surface Model. Journal of Hydrometeorology 10, 130–148.
Zampieri, M., Scoccimarro, E., Gualdi, S., Navarra, A., 2015. Observed shift towards earlier spring discharge in the main Alpine rivers. Science of The Total Environment 503-504, 222232.
Zheng, Z., Kirchner, P., Bales, R., 2016. Topographic and vegetation effects on snow accumulation in the southern Sierra Nevada: a statistical summary from lidar data. Cryosphere 10, 257–269.

Summary of Chapter: "Snow observation on Mount-Lebanon"

This chapter in its current form is published in the journal Earth System Science Data: Fayad, A., Gascoin, S., Faour, G., Fanise, P., Drapeau, L., Somma, J., Fadel, A., Al Bitar, A., Escadafal, R.: Snow observations in Mount-Lebanon (2011–2016), Earth Syst. Sci. Data, doi:10.5194/essd-2017-3. The spatio-temporal variability of snow was presented in the second INARCH workshop held at the Laboratoire de Glaciologie et de Géophysique de l'Environnement (LGGE) in Grenoble (17-19 October 2016) (http://www.usask.ca/inarch/wkshp2_report.php).

The main objective of this chapter is to address the spatio-temporal variability of snow depth, snow density, and SWE in the snow dominated regions of Mount-Lebanon (1300-2900 m a.s.l.). The study region covers the recharge area of three karstic river basins (total area of 1092 km^2), up to 3088 m in elevation.

In this chapter, we present a snow meteorological dataset for the first time in Lebanon (2011-2016). The dataset builds from previous joint efforts of CESBIO/CNRS-L/USJ and includes observations from three high elevation automatic weather stations (1840-2834 m a.s.l.). Continuous meteorological observations at 30 minute intervals for the snow seasons (November – June) between 2011 and 2016 include surface air temperature and humidity, precipitation, wind speed and direction, incoming and reflected shortwave irradiance, and snow height. Observations of snow height (HS), snow water equivalent, and snow density were collected at 30 snow courses located at elevations between 1300 and 2900 m a.s.l. during two snow seasons 2014–2016 with an average revisit time of 11 days. Daily gap-free snow cover extent (SCA) and snow cover duration (SCD) derived from MODIS snow products are provided for the same period (2011–2016).

We used the dataset to (1) describe the climatology of the winter seasons 2013-2016 from AWS observations and to characterize (2) mean snow height, and (3) SWE and density across different elevation gradients for the first time in Mount-Lebanon. We found that snow is characterized with large snow height and SWE variances and a high-density mean (equal to 467 kg m^{-3}). We used a model to investigate the link between snow density and HS. The model explained 34% of the variability in the entire dataset (all regions between 1300 and 2900 m a.s.l.) and 61% for high mountain regions (elevation 2200–2900 m a.s.l.).

Finally, this dataset was made to be fully compatible with the application of distributed energy-balance snowpack models. Therefore, this data set holds the potential to greatly improve the quantification of snowmelt and mountain hydrometeorological processes in this data-scarce region of the Mont-Lebanon. The dataset was deposited in the public domain to foster its application beyond this work.

3 SNOW OBSERVATION ON MOUNT LEBANON

Abstract

We present a unique meteorological and snow observational dataset in Mount Lebanon, a mountainous region with a Mediterranean climate, where snowmelt is an essential water resource. The study region covers the recharge area of three karstic river basins (total area of 1092 km2 and an elevation up to 3088 m). The dataset consists of (1) continuous meteorological and snow height observations, (2) snowpack field measurements, and (3) medium-resolution satellite snow cover data. The continuous meteorological measurements at three automatic weather stations (MZA 2296 m; LAQ 1840 m; and CED 2834 m a.s.l.) include surface air temperature and humidity, precipitation, wind speed and direction, incoming and reflected shortwave irradiance, and snow height, at 30 minute intervals for the snow seasons (November – June) between 2011 and 2016 for MZA and between 2014 and 2016 for CED and LAQ. Precipitation data were filtered and corrected for Geonor undercatch. Observations of snow height (HS), snow water equivalent, and snow density were collected at 30 snow courses located at elevations between 1300 and 2900 m a.s.l. during the two snow seasons 2014–2016 with an average revisit time of 11 days. Daily gap-free snow cover extent (SCA) and snow cover duration (SCD) maps derived from MODIS snow products are provided for the same period (2011–2016). We used the dataset to characterize mean snow height, snow water equivalent (SWE), and density for the first time in Mount Lebanon. Snow seasonal variability was characterized with high HS and SWE variance and a relatively high snow density mean equal to 467 kg m-3. We find that the relationship between snow depth and snow density is specific to the Mediterranean climate. The current model explained 34% of the variability in the entire dataset (all regions between 1300 and 2900 m a.s.l.) and 62% for high mountain regions (elevation 2200–2900 m a.s.l.). The dataset is suitable for the investigation of snow dynamics and for the forcing and validation of energy balance models. Therefore, this dataset bears the potential to greatly improve the quantification of snowmelt and mountain hydrometeorological processes in this data-scarce region of the eastern Mediterranean. The DOI for the data is https://doi.org/10.5281/zenodo.583733.

Keywords: Snow observations; Snow water equivalent; Automatic weather station; Mountain hydrology; Water resources; Mediterranean climate

3.1 Introduction

Water scarcity is a growing concern in Lebanon due to the unsustainable water resource management, the limited accessibility to the water sources, increasing water demand by all sectors, increasing water pollution, and sea water intrusion (MOEW, 2010; UNDP, 2014; Kalaoun et al. 2015). Lebanon receives on average 830 mm of precipitation per water year (September–August) (MOEW, 2010). Most precipitation falls during the winter season

(December–March). The two Lebanese mountain chains, the Mount Lebanon and Anti Lebanon, receive between 50 and 67% of the total annual precipitation as snow (UNDP, 2014). This is mainly due to the orographic enhancement of the precipitation on the western slope of the mountain chains. The Mount Lebanon range has an average elevation above 2200 m and stretches over a distance of 150 km parallel to the Mediterranean coast, therefore causing enhanced orographic uplift of moist air masses. Due to the influence of the Mediterranean climate (wet winter, dry summer) most of the precipitation above 1200 m a.s.l. falls as snow on Mount Lebanon (Shaban et al., 2004; Aouad-Rizk et al., 2005; Mhawej et al., 2014; UNDP, 2014). The average contribution of snowmelt to spring and river discharge in Mount Lebanon was estimated at 30% by Telesca et al. (2015). Snowmelt contributes to the recharge of karstic aquifers and springs of all the watersheds located in the windward regions of Mount Lebanon (Fig. 3.1) (e.g., Bakalowicz et al., 2008; Doummar et al., 2014). This snow contribution to groundwater recharge can reach up to 75% in the upper mountainous aquifers where the groundwater recharge was estimated at 81% from precipitation in the snow-dominated regions of the El Kelb Basin (Margane et al., 2013; Königer and Margane, 2014). The snowmelt contribution from high-elevation regions (above 1800 m a.s.l.) was estimated to contribute to around 56% of the major spring discharge at the lowland regions (Margane et al., 2013). The coastal watersheds, such as the EL Kelb Basin, are the major sources of water for the coastal population, where most of the Lebanese population is located.

Although snow is recognized as a major component of the hydrologic system in Mount Lebanon (Shaban et al., 2004; Aouad-Rizk et al., 2005; Bakalowicz et al. 2008; Mhawej et al., 2014; Königer and Margane 2014), the link between snowmelt and the hydrological processes remains poorly characterized on the basin scale. This can be attributed to the (1) lack of an operational snow observation network in Lebanon and (2) limited number of published basin-scale hydrometeorological datasets. Meteorological stations operated by the department of civil aviation are usually located below the snowline (maximum elevation at 1220 m a.s.l.) and the few stations located in the mountainous regions (elevation range 1510–1890 m a.s.l.) are not equipped to measure snowfall. Furthermore, only a few datasets on precipitation, temperature, snow, groundwater recharge and streamflow are available for basin-scale studies (e.g., Königer and Margane 2014). Existing datasets, available through published material, are usually limited to (1) national-scale studies with monthly or yearly means (Shaban et al. 2004; Corbane et al., 2005; Mhawej et al., 2014; Telesca et al., 2014), (2) multi-year daily spring discharge and precipitation time series (e.g., Hreiche et al., 2007), (3) seasonal observations collected for mesoscale catchment studies (Bernier et al. 2003; Aouad-Rizk et al., 2005; Doummar et al.

2014), and (4) local-scale snowpack observations (e.g., Somma et al., 2006, 2014). In most cases the research datasets are not made publicly available.

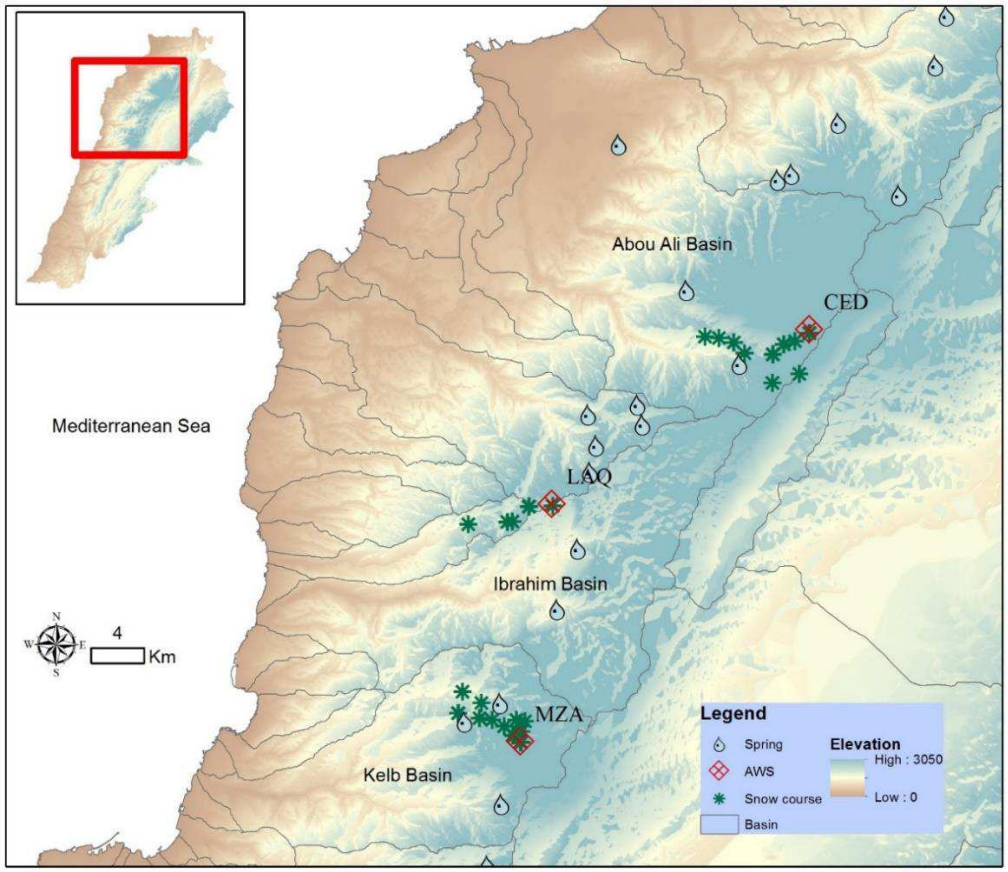

Fig. 3.1. Location of the three study river basins in Mount Lebanon and the location of the three automatic weather stations (AWSs). Points indicates the location of the snow courses. Snow height HS, snow density, and snow water equivalent (SWE) were measured at 30 snow courses for the two snow years (2014–2016): 9 snow courses at Cedars have an elevation range between 1800 and 2900 m a.s.l., 15 snow courses between Faraya and Mzar (elevation between 1350 and 2350 m), and 6 snow courses between Ehmej and Laqlouq (elevation range 1350-1850 m a.s.l.).

In this paper, we present a dataset targeted at the study of the mountain and snow hydrology in three mesoscale basins (area 256–513 km^3) located on the west slope of Mount Lebanon (Fig. 3.1). The dataset consists of, (1) continuous meteorological and snow height observations collected at three automatic weather stations (AWSs) (2011–2016), (2) snowpack field measurements collected during two snow seasons (2014–2016), and (3) medium-resolution satellite observations of the snow cover extent at a daily time step (MODIS). We use these data to characterize the variability in key snowpack properties. The dataset presented in this paper is unique because it is the only dataset that includes a range of continuous snow and meteorological measurements in the mountain region of Lebanon at the elevation regions

between 1300 and 2900 m a.s.l. The data presented are readily suitable for the forcing and validation of a snowpack energy and mass balance model. The data also can be useful for further hydro-meteorological studies such as climate model downscaling or hydrological modeling for water resource management.

The study area is described in section 3.2. Meteorological observations and post processing methods, snow course measurement protocols, and MODIS data processing are presented in section 3.3. Section 3.4 provides a summary of the observations and an example application on using the datasets to derive the relationships between HS, snow water equivalent (SWE) and snow density. Data accessibility and conclusions are presented in sections 3.5 and 3.6 respectively.

3.2 Study area

This study's measurements were collected in the upper area of three mesoscale snow-dominated mountain basins located in Mount Lebanon with an average centroid located at 34.10° N and 35.90° E and covering a total area of 1092 km^2 (Fig. 3.1). These basins belong to the "coastal watersheds", which supply fresh water to major Lebanese cities including Beirut. Due to the influence of the Mediterranean climate, most precipitation falls between November and April. Winter precipitation (December–March) accounts for 84 % of the total annual precipitation. Most precipitation above 1600 m a.s.l. falls as snow. The topography of the mid-elevation regions (1600–2200 m a.s.l.) is usually rugged terrain (Fig. 3.2). The mid-elevation and high-elevation plateau are found at elevation ranges between 2300 and 2500 m and between 2700 and 3000, respectively (Fig. 3.2). The treeline is located at 1550 m a.s.l., where sparse scrublands dominate most of the land cover. The retreat of the natural tree line is due to the increased deforestation and urbanization. The natural tree line which can be still found in sparse, small, forested regions extends up to 2450 m in Abou Ali and 1900 m in Ibrahim and El Kelb basins. Most snow-fed karstic springs are located at altitudes between 300 and 2280 m a.s.l. The physical attributes of the three study basins are shown in Table 3.1.

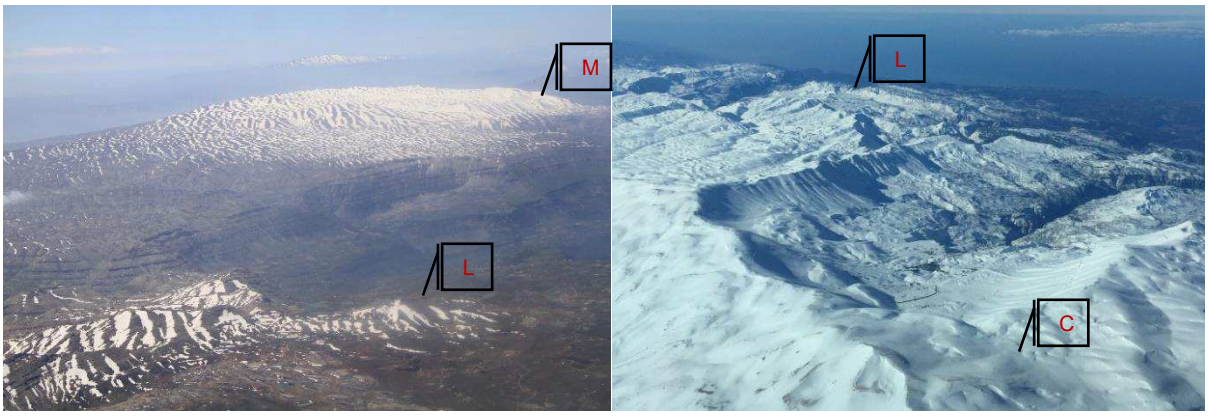

Fig. 3.2. Overview of the mountain topography at (a) Laqlouq and Mzar, and (b) Cedars, Mount Lebanon. The images were captured on 6 May 2011 (a) and 21 February 2015 (b) (courtesy of the author). The locations of the AWSs are shown approximately on the images where the letters M, L, and C represent the stations at MZA, LAQ, and CED, respectively (see Table 3.1). The topography near Laqlouq (LAQ) is a relatively low plain (elevation between 1600 and 1800 m a.s.l.) and low-elevation mountains (1900 – 2100 m a.s.l.). The region near Mzar (MZA) is characterized by rugged terrain (1600 – 2200 m a.s.l.) and mid-elevation plateau (elevation range 2300 – 2500 m). The high-elevation plateau (shown partially in (b) near Cedars (CED)) have an elevation range between 2700 and 3000 m a.s.l. Snow presists until the end of May in the mid-elevation mountain regions (plateau and rugged terrain region above 2300 m a.s.l.). The low-elevation and mid-elevation regions (1300 – 2000 m a.s.l.) are usually snow-free by mid-March to mid-April.

Table 3.1. Attributes of the three snow-dominated basins in Mount Lebanon described in this study.

Basin[a]	Area (km^2)	Elevation range (average)[b], m a.s.l.	Dominant land cover[c] (%)	AWS Elevation, m a.s.l. (year installed)[d]	Snow course count (elevation range[e]
1	513	0–3088 (1202)	Clear grassland (20%)	2834 (2013)	9 (1650–2900)
2	323	0–2681 (1547)	Clear grassland (30%)	1840 (2014)	6 (1300–1850)
3	256	0–2619 (1381)	Clear grassland (16%)	2296 (2011)	15 (1300–2300)

[a]Basins are Abou Ali (1), Ibrahim (2), and El Kelb (3) (Fig. 3.1). [b]Values are derived for the national 10 meter DEM (NCRS). [c]Source: Landuse land cover map of Lebanon (NCRS, 2015). [d]Source: Institut de recherche pour le développement (IRD) (Tabel 3.2). [e]Snow courses observations were conducted between December and May over two snow years (2014–2016) (Fig. 3. 1).

3.3 Snow and Meteorological Data

3.3.1 Meteorological data

The three AWSs were installed in Mount Lebanon above the winter snowline (approximately 1550 m a.s.l.) with the primary objective to monitor the meteorological variables that drive seasonal snowpack evolution on Mount Lebanon (Fig. 3.1 and Fig. 3.2). The Laqlouq AWS (LAQ) is located in a monastery at 1840 m a.s.l., the Mzar station (MZA) is located in a ski resort domain at 2296 m a.s.l., and the Cedars AWS (CED) (2834 m a.s.l.) is located on the higher plateau below the mountain's peak at Qornet El Sawda, 3088 m a.s.l. (Fig. 3.1, Table 3.2). The LAQ station is in a relatively flat plain area with fruit trees, bare rocks, and

sparse, short grasslands. The MZA station is located on one of the medium-elevation peaks in a mountainous region with rugged terrain (maximum elevation in the area is ~2600 m a.s.l.) with dominant bare soils and sparse speargrass grassland. The CED AWS is located on a higher plateau with dominant bare rocks and sparse shrubs and grasslands at lower elevations (1600–2200 m a.s.l.). Wind effects on snow cover are more noticeable in MZA due to the combined effect of topography and higher wind velocities. The three stations are operated under a joint program for establishing a network for snow observation (NSO). The program, established in 2010, is a collaboration between the Institut de Recherche pour le Développement (IRD, France), the Centre d'Etudes Spatiales de la Biosphere (CESBIO, France), the National Council for Scientific Research – Remote Sensing Center (CNRS/NCRS, Lebanon), and the University of Saint Joseph (USJ, Lebanon).

Table 3.2. Meteorological stations.

Station[a]	Location	Elevation, m a.s.l.	Record period (30 min averages) [b]	Coordinates (WGS84)
CED	Cedars	2834	2013–2016	34.27° N, 36.09° E
LAQ	Laqlouq	1840	2014–2016	34.14° N, 35.88° E
MZA	Mzar	2296	2011–2016	33.98° N, 35.86° E

[a]See Table 3. 3 for sensors description. [b] The time period cover the snow season between 1 November and 30 June.

Meteorological data are available starting from snow season (December–June) 2011 for Mzar AWS and the monitoring network became fully operational in snow season 2014–2015 with the installation of the third AWS (LAQ) at Laqlouq (Table 3.2). Meteorological data– including snow height, temperature, relative humidity, incoming and reflected shortwave solar radiation, wind speed and direction, and atmospheric pressure – are collected at the three sites using sensors mounted on towers (Fig. 3.3). Longwave radiation, which is, an important component of the energy balance in Mediterranean regions (Herrero and José Polo 2016), is not measured. However, incoming longwave radiation can be estimated from air temperature and humidity measurements at the stations (Brutsaert 2013). Incoming solar radiation can also be used to better constrain the cloud fraction in the computation of the longwave radiation. Each station consists of a data logger (CR1000; Campbell Scientific Inc., Utah, USA) and a precipitation gauge (T-200B; Geonor Inc., Eiksmarka, Norway), a snow depth sensor (SR50A; Campbell Scientific Inc., Utah, USA), an air temperature and humidity sensor (CS215; Campbell Scientific Inc., Utah, USA), an incoming and reflected shortwave solar radiation sensor (SP LITE 2 pyranometer; Kipp & Zonen, Netherlands), and a wind speed and direction

sensor (Alpine v05103–45L, Young, USA). Data are transmitted via a GPRS modem every 8 hours. Observations from the three AWSs are collected at 30 sec and then aggregated into 30 min averages. Temperature and humidity sensor are installed at 2.4 m in MZA, 3.9 m in LAQ, and 4.2 m in CED. Wind speed sensors are installed at 2.6 m in MZA, 4.2 m in LAQ, and 4.9 m in CED. Snow height observations were recorded automatically at each station using an acoustic snow gauge installed at 2.0 m in MZA and at 4.0 m in CED and LAQ. Precipitation data are recorded at a snow gauge placed in the proximity of the station (Fig. 3.3). Precipitation has been observed since 2012 at MZA (2012–2016) and since 2014 at LAQ (2014–2016). The CED station was equipped with a Geonor in December 2016. Data for precipitation were missing during the first year (2011–2012) at MZA and shortwave solar radiation measurements began in snow season 2014. CED AWS data between 24 April and 30 June 2015 were removed due to station rotation. The wind speed data located at CED were discarded after 15 January 2016 due to sensor malfunction. Missing data were less than 10% for all stations after the network became fully operational (2014–2016).

Raw data collected at the stations underwent basic quality control, including checks for missing data and boundary values. We performed further quality control for the 30 min and daily average observations by screening outliers and erroneous data following rules given by Serreze et al., (1999), Shafer et al., (2000), and Estévez et al., (2011). Humidity, pyranometers, and wind sensors were unheated and thus may be subject to error when covered by frost (Malek, 2008). The temperature sensors are protected against solar radiation (Huwald et al., 2009) using radiation shield and are naturally ventilated. The accumulation of frost on the sensor was observed during multiple field visits at MZA and CED. These events usually coincide with the week following storm events.

For precipitation (P), air temperature (T), snow height (HS), and humidity (RH), we used running step tests to detect abrupt jumps in means, especially during storm events (Table 3.3). Incoming and reflected shortwave solar radiation (SR) measurements were screened using snow half-hourly albedo, by eliminating data that do not give a positive albedo ($0 \leq$ albedo ≤ 1). We used a positive snow height (HS) to detect the presence or absence of snow. Data ranges were used for P (0–240 mm h^{-1}), T (–30 to +40 °C), RH (0–100%), HS (0–4.5 m), and SR (0–1500 W/m^2). For the two snow seasons 2015–2016 (November–June) data record retained at the three stations were 71.1, 95.4, and 94.3% of the total datasets for CED, LAQ, and MZA, respectively. An example of the semi-hourly precipitation and temperature observations at Laqlouq for the snow seasons (2014-2016) is shown in Figure 3.4.

Fig. 3.3. Automatic weather station at Mzar (MZA) (2296 m a.s.l.) where all sensors are located on the tower and the precipitation gauge is located to the right of the station. Image captured on March 5th, 2015 (courtesy of the author).

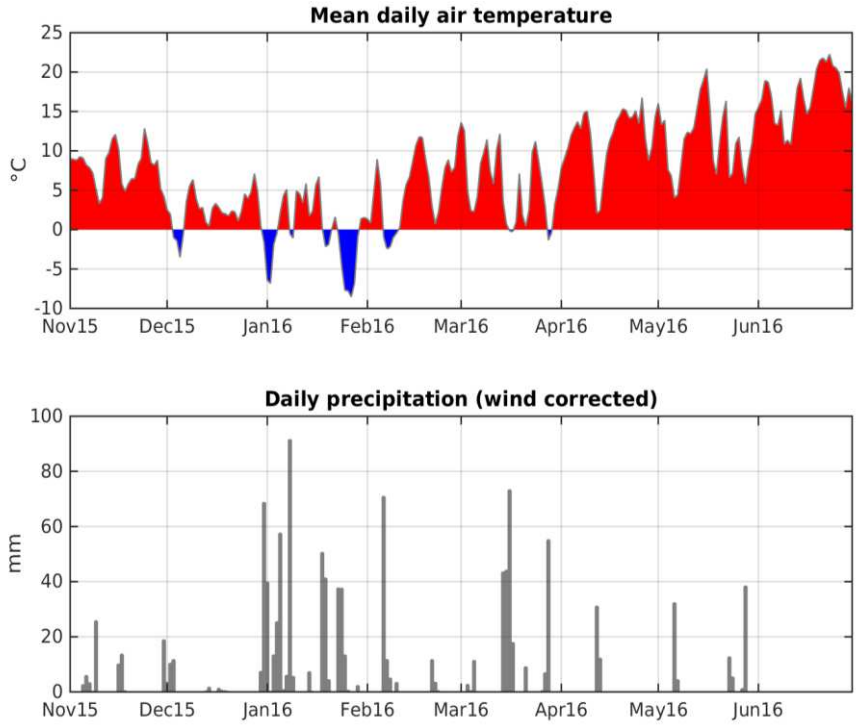

Fig. 3.4. Example of daily precipitation and temperature observations at Laqlouq (1840 m a.s.l.) during snow season 2015-2016 (November–June).

Table 3.3. Sensor specifications and quality control checks for hourly and daily data – modified after Estévez et al. (2011) and WMO (2008).

Sensor	Variable	Accuracy (Sensitivity)	Range test	Step test	Cross–validation test
T–200B (1000mm at MZA and LAQ) and 1500mm at CED[†])	Precipitation (mm)	0.1% Full scale (0.075 – 0.1)	$0 \leq P_{sh} \leq 120$ $0 \leq P \leq 508$	$0 \leq P_{sh}$; $P(0-6h) \leq P(0-24h)$;	$RH_{sh} > 80\%$
SR50	Snow height (cm)	±1 (0.25)	$0 \leq HS_{sh} \leq 450$		Maximum HS(0–24h) < 0.15*P(0–24h)
CS215	Temperature (°C)	±0.4	$-30 < T < 50$	$\lvert T_{sh} - T_{sh-1} \rvert < 3$	$T_{sh} \neq T_{sh-1} \neq T_{sh-2} \neq T_{sh-4}$
SP LITE 2	Incoming Radiation		$-1 < SwI_{sh} < 1500$	$0 \leq \lvert SwIsh - SwR_{sh-1} \rvert \leq 555$	For $SwI_{sh} > 0$ & $SwR_{sh} > 0$ [0 < Albedo (SwR/SwI) < 0.95]
	Reflected Radiation		$-1 < SwR_{sh} < 1500$	$0 \leq SwR_{sh} - SwR_{sh-1} \leq 550$	
CS215	Relative Humidity (%)	±0.2	$0.8 < RH < 103$	$\lvert RH_{sh} - RH_{sh-1} \rvert \leq 45$	
Young 05103 – Alpine	Wind Speed (m s^{-1})	±0.3	$0 < Ws < 60$		$Ws_{sh} = 0$ & $Wds_h = 0$; $Ws_{sh} \neq Ws_{sh-1}$ $Ws_{sh} \neq Ws_{sh-2} \neq Ws_{sh-4}$; $Wd_{sh} \neq Wd_{sh-1}$ $Wd_{sh} \neq Wd_{sh-2} \neq Wd_{sh-4}$
	Wind direction (deg)	±3	$0 \leq Wd \leq 360$		

Where: P and Psh = daily and semi-hourly precipitation; SD and SDsh = daily and semi-hourly snow depth; T = mean air temperature respectively; Tsh = semi-hourly air temperature; SwI and SwR = incoming and reflected solar radiation respectively (sh denotes semi-hourly); RH and RHsh = daily mean and semi-hourly relative humidity; W_S and Wd = mean wind speed and mean wind direction respectively (sh denotes semi-hourly); For SD we used visual interpretation to account for snow depth following snowfall, or when SR50 measurement are lost, assuming the difference in SD over a single day is less than total daily precipitation multiplied by an average fresh snow density of 0.15 g cm^{-1}. The sensor's field life cycle is ~ 3 years. †The snow gauge (model T–200B, 1500mm) was installed in October 2016 and measurements will be available staring snow year 2016–2017.

3.3.2 Correcting for Geonor undercatch

The output data from the Geonor accumulating gauge were post-processed in order to identify and correct biased observations, to determine the precipitation type, and to correct the Geonor precipitation undercatch. Three types of biases are found in the Geonor observations similarly to previous studies (Harder and Pomeroy 2013; and Pan et al. 2016): (1) erroneous readings associated with the Geonor field servicing (i.e., emptying and/or adding of antifreeze and oil to the Geonor bucket); (2) jitters and diurnal noise due to wind speed (e.g., MZA) and changes in temperature are similar to those found in sites with strong diurnal changes in temperature, radiation, and wind speed (e.g., Harder and Pomeroy 2013; and Pan et al. 2016); and (3) long-term drift results from evaporation within the bucket, which occurs at the end of snow season when air temperature is high. We post-processed the raw precipitation data using

a supervised correction similar to the one described in Harder and Pomeroy, (2013) by performing the following steps: (1) The Geonor raw data were adjusted to account for when the gauge is emptied and/or filled with oil and antifreeze. (2) We used the predefined values for range test and cross validation tests (Table 3) to automatically flag and remove erroneous peaks (e.g., $P_{sh} > 120$ mm). (3) All erroneous changes in the calculated raw cumulative precipitation (raw Psh < –20 mm and > 20 mm) were removed. (4) We flagged and removed all accumulated precipitation greater than 1000 mm (equal to the maximum capacity of the Geonor bucket), and the precipitation data for the same time period is set to "no data" in the final dataset. (5) All missing cumulative precipitation observations were assumed to be equal to the previous observed observation for running the filter. (6) We used a supervised rolling maximum filter (Harder and Pomeroy, 2013) to remove the biased precipitation observation. The filter was run sequentially on the time series of the cumulated precipitation: the precipitation observation was retained if it was greater than the previous maximum.

The rolling maximum filter preserves the cumulative change in precipitation and the timing of precipitation events (Harder and Pomeroy, 2013) (Fig. 3.5). However, a visual check is needed to flag potential errors. We visually compared the auto-filtered data versus the raw data to (1) check for erroneous departures between the auto-filtered and raw data; (2) check whether the filter captured the start of a precipitation event and whether the calculated Psh occurred when humidity was greater than 80% (Psh with low humidity values were removed); and (3) check and correct errors attributed to gauge drift events, which are associated with evaporation effects, that are not captured by the filter (Fig. 3.5a). We corrected these errors by manually replacing the filtered accumulated precipitation data to fit the actual change from the raw precipitation data (Fig. 3.5a). We made sure that the total sum of the replaced precipitation was equal to the cumulative observed precipitation which was assumed to be correct over the same time period. We also checked that the precise start and timing of precipitation events was preserved and that the long-term drift due to evaporation was eliminated (Fig. 3.5a).

Fig. 3.5. Examples of the jitters and diurnal noise filtering for Geonor T-200B weighing gauge (Praw: raw data; Padj: filtered data). (a) Significant evaporation occurred during winter season 2014 (e.g., MZA: 12 – 29 December 2013) and required manual correction (28 – 29 December). No correction for the accumulation of raw precipitation between 22 – and 23 December was made because the observed average humidity was below 15%. (b) Filtering of jitters and diurnal noise (no manual correction) (e.g., MZA: 23 March – 11 April, 2015).

The collection efficiency of precipitation gauges is influenced by the wind speed and a bias adjustment for solid precipitation is needed under windy conditions (Rasmussen et al., 2012; Buisan et al., 2017; Smith et al., 2017; Pan et al., 2016). Measurement errors due to gauge undercatch frequently range between 20% and 50% (Rasmussen et al., 2012). The catch efficiency for the Geonor with a single Alter shield decreases linearly to approximately 60% at wind speed 5 m s^{-1} (Thériault et al., 2012). The bias adjustment for precipitation undercatch is achieved by estimating the catch efficiency (CE) (wind speed relationship) of the precipitation gauge. The determination of CE requires the determination of precipitation type and that the wind speed is measured at gauge height (Rasmussen et al., 2012). The need for precipitation type separation is important because the influence of wind is much more pronounced for solid precipitation than for liquid precipitation (Rasmussen et al., 2012). In this study, we applied bias correction for the filtered precipitation data (P_{adj}). For solid precipitation, we used the

empirical relationship between catch efficiency and wind speed derived by Thériault et al., (2012) after Yang et al., (1998) and Rasmussen et al., (2001):

$$P_{cor} = P_{adj}/CE$$

$$CE = \frac{100 + Ws * C}{100}$$

where P_{cor} (mm) is the corrected precipitation, P_{adj} (mm) is the measured precipitation after filtering, CE is the catch efficiency of the Geonor, Ws (m s^{-1}) is the hourly mean wind speed at the gauge height, and C is a constant and represents the gauge configuration parameter and is equal to – 7.1 (C= – 7.1) for the single Alter shield Geonor (Thériault et al., 2012). Over-correction is possible for snowfall events and occurs under the impact of blowing snow at high wind speeds (Pan et al. 2016). To limit overcorrection, we used a threshold for maximum wind speed. Thus, the CE was set to 0.44 (CE for 8 m s^{-1}). We used this threshold since the median collection efficiency of the Geonor in the single Alter shield seemed to saturate at wind speeds greater than 8 m s^{-1} for a test site in Colorado (Thériault et al., 2012). The median wind speed recorded during precipitation events over the winter seasons of 2014-2016 ranged between 3.3 and 3.7 m s^{-1} for LAQ and 8.8 and 9 m s^{-1} for MZA with maximum recorded wind speed at 10 and 20.1 m s^{-1} for LAQ and MZA, respectively. We adjusted all rainfall measurements using the constant average catch efficiency for the single Alter shield Geonor estimated at 95% (CE = 0.953) (Devine and Mekis, 2008).

Wind speed at gauge height is required for the estimation of CE. We used the logarithmic wind profile to estimate the wind speed at the height of the Geonor gauge (Yang et al. 1998):

$$W_s(h) = W_s(H)\left[\frac{\ln(h/z_0)}{\ln(H/z_0)}\right]$$

where Ws(h) is the estimated hourly wind speed (m s^{-1}) at the gauge height, Ws(H) is the measured mean hourly wind speed at the anemometer height, h and H are the heights (m) of the Geonor gauge and the anemometer, respectively, and z_0 is the roughness parameter (m), set to 0.01 m for the winter snow surface and 0.03 m for short grass in the warm period (Yang et al. 1998). For this study, we set $z_0 = 0.01$ for the time period between December and March and $z_0 = 0.03$ for the rest.

Different approaches for precipitation phase determination have been summarized in Harpold et al., (2017). Most common methods rely on the use of mean air temperature (Ta)

thresholds (e.g., Marks et al., 2013). In this study, we use a static Ta threshold at 0°C (Marks et al., 2013) to distinguish between snowfall and rainfall. All precipitation below or above the threshold are partitioned as snow or rain, respectively. This method was found to produced reliable snow volume predictions in Idaho when cloud levels are at or close to the surface during storms and the RH is at or close to saturation (Marks et al., 2013). The Mount Lebanon meteorological conditions during storm events are similar and are usually characterized by RH saturation and cloud levels are near the surface.

3.3.3 Snow course data

We identified 30 different snow courses with lengths varying between 75 and 400 m, within the upper area of the three basins (Fig. 3.1). The locations of the snow courses were selected based on accessibility, representativeness of the snow cover within the region (suggesting, whenever possible, one snow course for relatively flat and low slope regions and two snow courses representing the maximum and minimum snow depth transects in rough topographic regions). Snow courses were spaced at ~100 m vertical elevation. All snow courses had a slope of less than 30%. Field measurements of snow depth, snow density, and SWE were carried out over two snow seasons (2014–2016) with an average revisit time of 11.4 days for each snow course. A total of 649 snow course measurements are reported and can be found at (https://doi.org/10.5281/zenodo.583733). Snow depth was measured manually, to the nearest 1 cm, using a 3 m snow probe, at 5 meter intervals along each snow course. Snow density was measured using a federal snow sampler (snow cutter inner diameter at 3.772 cm) along each snow course at 25 meter intervals for snow courses shorter than 100 m and at 50 m intervals for longer snow courses so at least 3–5 snow density measurements were recorded at each snow course site. Snow density and SWE protocol consisted of weighing the empty tube. The snow tube was then plunged into the snowpack and the snow depth marker on the tube was recorded. Once the core was removed the snow depth of the snowpack was checked to make sure that at least 80% of the snowpack has been cored (Dixon and Boon, 2012). We also measured the snowpack HS using a marked snow probe (1 cm) to make sure no snow was left unsampled. Any amount of soil entering the snow cutter, especially during the melt season, was removed and reported alongside the HS measurements. The combined weight of the tube and core was recorded. Each snow sample was weighed three times (five times under windy conditions) and the average snow weight was registered. Under windy conditions maximum and minimum weights were removed and the weight was averaged for the three measurements. The mass of

the snow core sample was calculated by subtracting the empty tube mass from the combined tube and snow core mass. Snow courses with an HS of less than 30 cm and where the snow cover was less than 50 % (based on visual interpretation) were sampled by taking bulk density measurements. Bulk density measurement consisted on taking four snow core samples at a single location and weighing the total mass for the combined four samples, the average density is then reported for this point-location. Weighing scales were validated under normal weather conditions by taking 50 measure s of the empty snow tube and thus suggesting an accuracy of 98.75% when using a 2 m snow tube. Snow density and snow water equivalent were calculated using:

$$\rho_s = \frac{m_{sample}}{\pi r^2 \times HS}$$

$$SWE = HS\frac{\rho_s}{\rho_w}$$

where ρ_s is the density of the snow core sample (g cm^{-3}), ρ_w is the density of water (1 g cm^{-3}), m_{sample} is the mass of the snow core sample, r is the inside radius of the snow tube cutter (3.772 cm), and HS is snow height (cm).

3.3.4 Snow cover extent and snow cover data

Daily maps of the snow cover extent at 500 m spatial resolution were generated for the three watersheds from the MODIS snow products. We used the "binary" snow cover area sub-dataset from MOD10A1 (Terra) and MYD10A1 (Aqua) collection 5 products from the National Snow and Ice Data Center (Hall et al., 2006). Mount Lebanon falls between MODIS grid tiles h20v05 and h21v05. All available tiles from 01 September 2011 to 31 August 2016 were assembled and resampled to 500 m with a nearest-neighbor method in UTM 36N using the MODIS reprojection tool over a rectangular spatial subset (upper left x = 730 km, y = 3830 km ; lower right x = 850 km, y = 3680 km). Then we ran a gap-filling code which is fully described in (Gascoin et al., 2015) to interpolate the missing information mostly caused by cloud cover. The algorithm utilizes the topographic information (elevation and aspect) from the ASTER global digital elevation map, which was resampled to the same resolution. The output is a series of daily, gap-free, raster maps of the snow presence or absence for every pixel. These data were then used to compute the daily snow cover area in each watershed and the mean annual snow cover duration per pixel (SCD), i.e., the mean number of snow days per year. The dataset is available at https://doi.org/10.5281/zenodo.583733.

3.4 Results and discussion

In this section, we limited the data analysis to two snow seasons (2014–2016) because (1) the AWS network became fully operational with the installation of the third station in 2014 and (2) snow field observations were collected starting in snow season 2014–2015.

3.4.1 Meteorology

The observed average seasonal (average 30–min from 01 November to 30 June) surface air temperature for the two snow seasons (2014–2016) was 6.9, 4.3, and –1.4 °C for LAQ (monthly range: –0.3–17.1 °C), MZA (–2.9–14.3 °C), and CED (–7.1–8.4 °C), respectively. There is a strong positive correlation in the 30 min surface air temperature records from the three stations (r = 92.7–97.9). Total annual precipitation ranged between 732 and 1125 mm during 2014–2015 and 1592 to 1880 mm for 2015–2016, representing precipitation data recorded at the LAQ and MZA stations, respectively (1840–2294 m a.s.l.). Average wind speeds for the same time period (2014–2016) were 2.4 m s^{-1} (monthly range: 1.5–3.3), 5.4 (4.1–8.0), and 4.7 m s^{-1} (3.6–5.5) for LAQ, MZA, and CED, respectively. Strong winds seldom exceed 10 m s^{-1} at LAQ, 20 m s^{-1} at MZA, and 25 m s^{-1} at CED except during storm events, where maximum wind gusts recorded reached up to 40.1 m s^{-1} at CED. Seasonal incoming solar shortwave radiation averages (30–min averages) ranged between 156 and 219 W m^{-2} for the three stations (2014–2016).

3.4.2 Snow depth, snow density and SWE

SWE peaks in mid-February at low and mid-altitude regions and in mid-March high mountainous regions. Snowmelt varies depending on elevation, beginning late February at lower altitudes and by mid-March at higher altitudes and extending into late April. Rain on snow events are common during winter season and usually occur at elevations below 1800 m amsl. Snow patches can persist until June in areas above 2700 m a.s.l. The median HS, SWE, and density obtained from snow courses (1300–2900 m a.s.l.) between 2014 and 2016 are shown in Fig. 3.6. The median HS, SWE, and density across different region and mountain elevation are illustrated in (Fig. 3.7). High regions like CED (1650–2900) and MZA (1300–2300) have higher mean HS and SWE when compared to mid- and low mountainous regions like LAQ (1300–1850). Median seasonal HS values at high elevations (i.e. mean for all CED and MZA snow courses; Fig. 3.7a,d) were very close which reflects similar snowfall patterns.

CED seasonal HS medians were 77 and 79 cm representing snow years 2014–2015 and 2015–2016, respectively, and similar values were found in MZA (71 and 76 cm). Meanwhile, HS medians at LAQ were 53 and 54 cm over the same time period. The high mountainous regions above 2200 (e.g., CED) have a higher 75th quantile range and this is attributed to the extend snow persistence. The higher maximum HS observed in MZA can be attributed to the rough topography of the region whereas the high region in CED above 2700 m a.s.l. is presented as a plateau with less variance in HS and SWE when compared to high regions in MZA (2100–2500).

Peak SWE values for the two winter seasons (2014–2015; 2015–2016) were 103 and 83 cm w.e. for CED, 127 and 158 cm w.e. for MZA, and 59 and 36 cm w.e. for LAQ. The peaks for SWE, and similarly for HS, observed at MZA (Fig. 3.7) are attributed to the topography of the region where wind-blown snow was more noticeable. Despite MZA bieng characterized by higher variability in the SWE and HS, observations at CED show higher seasonal medians for both variables, which is expected since CED is higher and the snow season extends longer than the one observed at MZA. SWE remains relatively constant during winter season and starts to melt starting mid-March or early April at regions above 2100 m a.s.l. Snowmelt at lower elevation 1600–2100 m a.s.l. started earlier by mid–February and early March. Regions between 1300 and 2000 m a.s.l. are subject to rain on snow, which influences snowmelt processes during the entire snow season especially in warm years. The higher variance and inter-seasonal variability in the observed SWE across the different regions (Fig 3.5) illustrate the importance for monitoring snowpack dynamics in Mount Lebanon as it is the major contributor to the water resource system.

The median seasonal snow density for all snow courses over the 2-year period (2014–2016) (Fig. 3.6) was 476 km m^{-3} and ranged between 431 and 522 kg m^{-3}, representing the 25th and 75th percentiles. Mean snow density for the three regions (Fig. 3.7c, f) over the two snow seasons (2014–2016) ranged between 440 and 489 kg m^{-3}. These high seasonal density values are common in Mediterranean regions (e.g., Rice and Bales, 2010; López–Moreno et al., 2013). Although close median values can be observed for snow density across the different regions, it is worth noting that different snow metamorphism, compaction, or melting differences exist between regions. During the months of January and February the mid-altitude regions (e.g., LAQ) snow is usually wetter and less compacted when compared to high-elevation regions (e.g., CED), where snow is usually wind-compacted, highly supportable, and dry.

Snow year 2015–2016 was characterized by rain-on-snow events, when most of the precipitation occurring few days after the first major snowfall event (mid-January) fell as rain

in mid-altitude regions (1300–2300 m a.s.l.). Rain on snow resulted in the disappearance of the snowpack below 1800 m a.s.l and accelerated the snow densification at elevations between 1800 and 2300 m a.s.l. Observed snow densities for the same date were 1.4–1.6 times higher than those observed during the same time period in the previous year (2014–2015).

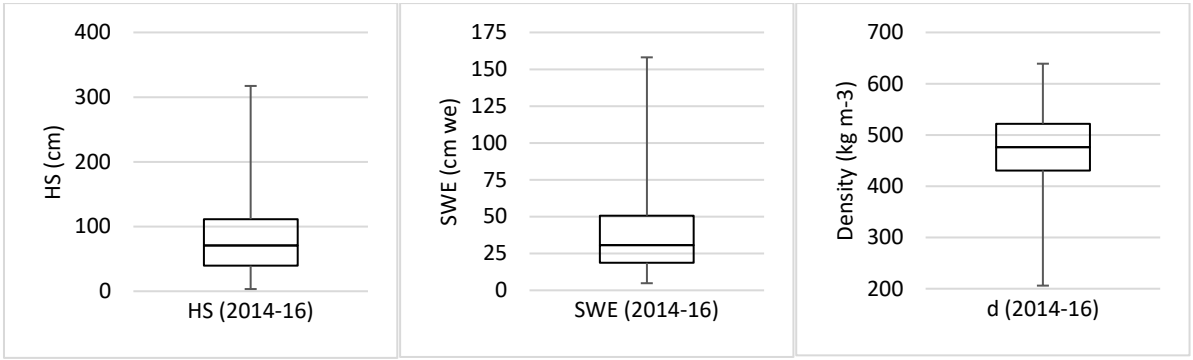

Fig. 3. 6. Box-and-whisker plots for nonzero data : (a) snow height, (b) SWE, and (c) snow density over the two snow seasons of 2014–2016 using data from 30 snow courses located at elevations between 1300 and 2900 m a.s.l (n = 649). The box brackets represent 25% and 75% of the data (lower and upper boxes, respectively). The whiskers are at minimum and maximum values.

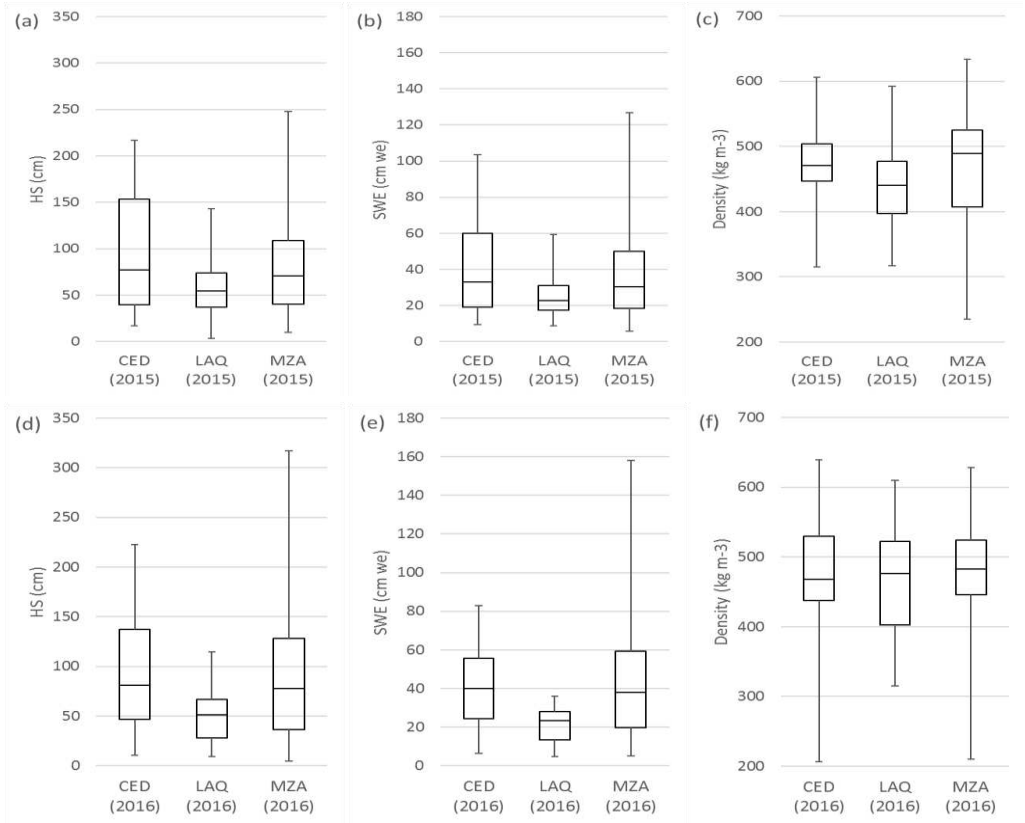

Fig. 3.7. Box-and-whisker plots for nonzero data: (a) snow height, (b) SWE, and (c) snow density over two snow season 2014–2015 (n = 311) and (d) snow height, (e) SWE, and (f) snow density over snow season 2015–2016 (n = 371) distributed by region where CED (elevation range, 1650–2900 m), LAQ (1300 – 1850 m), and MZA (1350 – 2350 m). The box brackets represent 25% and 75% of the data (lower and upper boxes, respectively). The whiskers are at minimum and maximum values.

3.4.3 Modeling snow bulk density

Establishing the relationship between distributed snow depth and SWE is among the used approaches to quantify SWE from snow depth measurements (e.g., Jonas et al., 2009). Figure 3.8. shows the general relationship between SWE vs. HS (Fig. 3.8a) and density vs. HS (Fig. 3.8b). The higher densities (Fig. 8b) are typical with Mediterranean, warm maritime, and alpine regions (e.g., Sturm et al. 2010). In contrast, the observed scatter between snow density and HS (Fig. 8b) cannot be explained using linear estimators. While SWE can be estimated linearly from HS, it is recommended to model the bulk density from HS and then derive SWE (Sturm et al. 2010). Such an approach is justified by the fact that (1) depth varies over a range that is many times greater than that of bulk density and (2) because estimates derived from measured depths and modeled densities are usually very close to measured values of SWE. The snow density can be estimated from HS using a linear function. However, a better representation of snow density from snow depth measurement can be achieved using nonlinear function that include HS and account for the effect of snow aging (represented in terms of day of the year, DOY) (Sturm et al. 2010). Distinct classes for different climate regions are used to account, indirectly, for the effects of meteorological condition (i.e. temperature and wind) (Sturm et al., 2010). The general equation is a nonlinear function asymptotic to the maximum seasonal density (Sturm et al. 2010):

$$\rho_{h_i,DOY_i} = (\rho_{max} - \rho_0)\left[1 - e^{(-k_1 \times h_i - k_2 \times DOY_i)}\right] + \rho_0$$

where ρ_{max} and ρ_0 are maximum and minimum bulk density, k_1 and k_2 are densification parameters, and h_i is snow depth at the i^{th} observation. ρ_{max}, ρ_0, k_1, and k_2 vary with climate region and the model parameters for the major snow class are found in Sturm et al. (2010) Table 3.4. The equation was applied to the ensemble points, presented in Figure 3.8b, using snow depth and DOY as predictor variables and snow depth as predictand. The model parameters were ρ_{max} = 0.553, ρ_0 = 0.0345, k_1 = 0.0000, and k_2 = 0.0167 for the entire dataset with the model explaining 34% (coefficient of determination r^2 = 0.344) of the snow density variability (Table 3.4). We believe that some of the observed differences between the current Mediterranean and the maritime and alpine regions in general can be attributed to the shorter snow season, warmer temperature, and higher densification rates, especially in the mid-elevation zone (1300–1900 m a.s.l.). During February field visits, most of the observed snow at this mid-elevation zone was wetter and characterized by higher densities when compared to high-elevation regions (e.g., above 2200 m a.s.l., where the snow was usually dry). A better snow density fit was achieved using elevation bands with a better fit for elevation above 2200

m (Table 3.4). The model was not able to explain the variability in snow densities to snow elevation in low mountain regions (1300–1800 m a.s.l.) namely because this region is subject to rain-on-snow events and multiple instances of snow accumulation and melt during a single snow season.

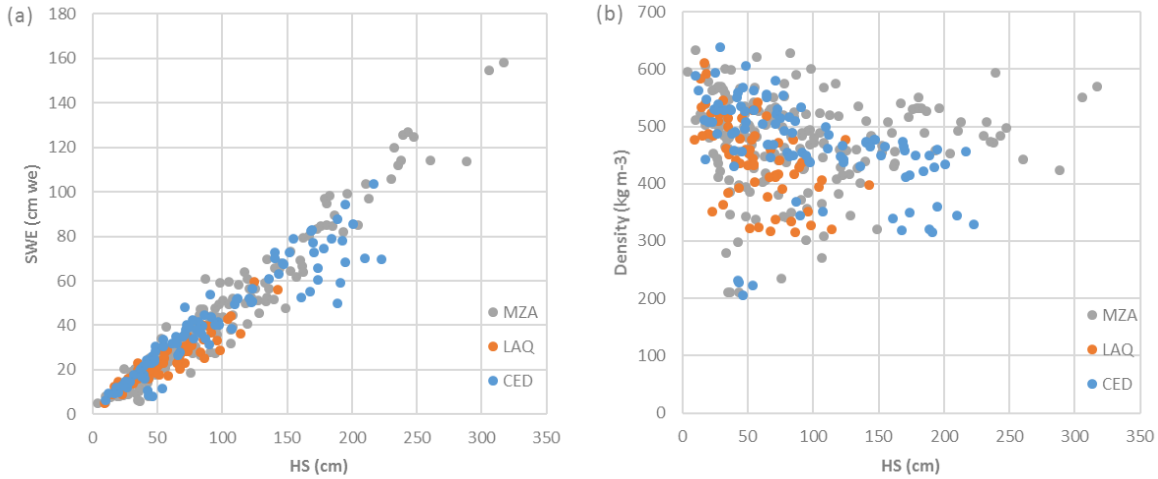

Fig. 3.8. (a) SWE vs. snow height (HS) and (b) density vs HS for all snow course data (observed during two snow seasons of 2014–2016 at elevations between 1300 and 2900 m a.s.l) (n = 649).

Table 3.4. Model parameters by elevation bands for nonzero data.

Elevation range (m a.s.l.)	**ρ_{max}**	**ρ_0**	**k_1**	**k_2**	**r^2**
2200–2900 (n = 136)	0.582	0.229	0.0004	0.0139	0.616
1300–2900 (n = 353)	0.553	0.345	0.0000	0.0167	0.344

3.4.4 Remote sensing snow cover data

MODIS data indicate that snow storm events occurred between November and March. The snow cover area peaked between January and February. Maximum snow cover duration (SCD) was 160 days at higher altitudes (above 2700 m a.s.l.). SCD in medium-elevation mountain regions (2200–2600 m a.s.l.) ranged between 100 and 140 days per average year. The percent of snow-covered area (SCA) of the basins during winter months (December–March), for the years between 2011 and 2016, ranged between 28 and46% (Abou Ali), 36 and 66% (Ibrahim), and 27 and 50% (El Kelb) (Fig. 3.9).

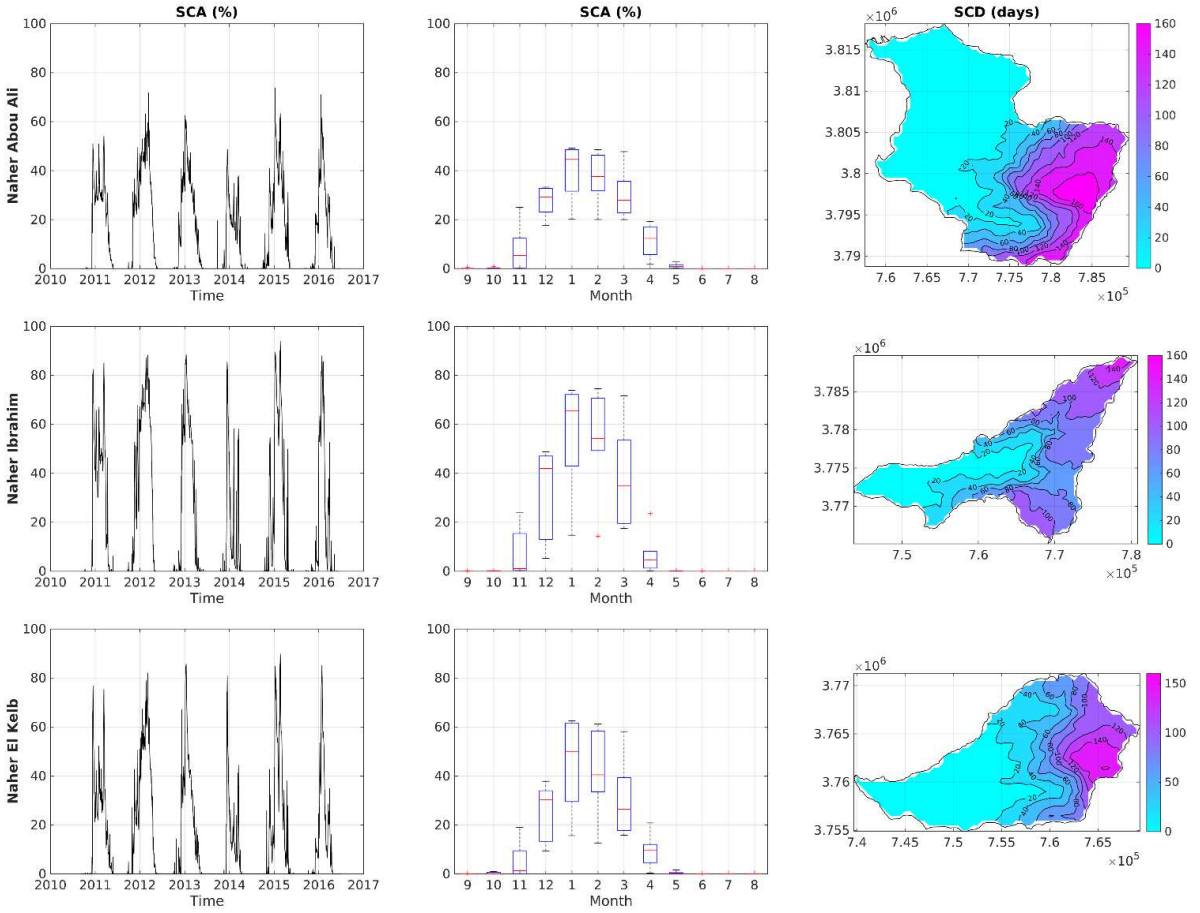

Fig. 3.9. From left to right: time series of the snow cover area (SCA, percentage of the basin area), box plot of mean monthly SCA, and snow cover duration (SCD) for (from top to bottom) the Abou Ali, Ibrahim, and El Kelb River basins.

3.5 Data availability

All data described in this paper are made publicly available at Zenodo ((Fayad et al., 2017). Included are comma-separated files (.csv) for AWSs listing the three stations and snow course observation, as well as a compressed file for processed daily MODIS SCA and SCD.

3.6 Conclusions

This paper presents the first dataset of snow and meteorological conditions in Mount Lebanon. The observations focused on three major basins of the coastal region of Lebanon and cover the snow seasons between 2011 and 2016 (for MZA AWS located at 2300 m a.s.l.). The observation network became fully operational in 2014. The network includes three automatic stations covering the range of snow-dominated areas between 1840 and 2834 m a.s.l. Distributed in situ HS and SWE measurements were also collected during two snow seasons (2014–2016) at 30 different snow courses located between 1300 and 2900 m a.s.l. MODIS snow products were processed to compute SCA and SCD at the basin scale. These observations are the result of an ongoing joint collaboration between IRD (France), CESBIO (France),

CNRS/NCRS (Lebanon), and USJ (Lebanon). The observatory is currently being funded for 2 years (2016–2018) via grants from CNRS/NCRS, IRD and USJ.

Additional unpublished data observations may also be available to complete this dataset, including meteorological data collected by the meteorological services at the department of civil aviation and the Lebanese Agricultural Research Institute (LARI), and river and spring discharges monitored by the Litani River Authority (LRA) as well as meteorological and hydrological data combined by the early warning system at the National Center for Remote Sensing (NCRS) and the observational datasets at the Centre d'Information et de Formation aux Métiers de l'Eau (CIFME) at the Ministry of Energy and Water (MOEW).

We provided mean and seasonal snow properties over two snow seasons (2014–2016) and provided an example on how SWE and snow density can be obtained using only HS measurements. This time span is insufficient to characterize the temporal variability in the snow cover. However, it already provides consistent information on the snow spatial variability. The combination of the meteorological station, snow courses, and remote sensing data through the application of a snowpack model will enable a multi-year evaluation of the snow resources at the basin scales.

The accurate representation of the spatial distribution of HS, SWE, and snow density is crucial for hydrological applications. In particular, we are using the AWS data for running a distributed energy balance model. The snow observations also hold potential for the characterization of the spatial distribution of snow across different gradients. SCA and SCD data can be used for model validation or as an operational tool for water resource management (e.g., Sproles et al. 2016). The AWS data may also support the validation and downscaling of regional climate models for various applications beyond the study of snow hydrology and the use of water resources.

3.7 References

Aouad–Rizk, A., Job, J.–O., Khalil, S., Touma, T., Bitar, C., Boqcuillon, C. and Najem, W.: Snow in Lebanon: a preliminary study of snow cover over Mount Lebanon and a simple snowmelt model / Etude préliminaire du couvert neigeux et modèle de fonte des neige pour le Mont Liban, Hydrological Sciences Journal, 50(3), 555–569, doi:10.1623/hysj.50.3.555.65023, 2005.

Bakalowicz, M., Hakim, M. and El–Hajj, A.: Karst groundwater resources in the countries of eastern Mediterranean: the example of Lebanon, Environmental Geology, 54(3), 597–604, doi:10.1007/s00254–007–0854–z, 2008.

Bernier, M., Fortin, J.P., Gauthier, Y., Corbane, C., Somma, J., and Dedieu. J.P.: Intégration de données satellitaires à la modélisation hydrologique du Mont Liban. Hydrological Sciences Journal, 48(6), 999–1012, DOI: 10.1623/hysj.48.6.999.51428, 2003.

Brutsaert, W.: Evaporation into the atmosphere: theory, history and applications (Vol. 1), Springer Science & Business Media, https://doi.org/10.1007/978-94-017-1497-6, 2013.Buisán, S. T., Earle, M. E., Collado, J. L., Kochendorfer, J., Alastrué, J., Wolff, M., Smith, C. D., and López-Moreno, J. I.: Assessment of snowfall accumulation underestimation by tipping bucket gauges in the Spanish operational network, Atmos. Meas. Tech., 10, 1079–1091, https://doi.org/10.5194/amt-10-1079-2017, 2017. Corbane, C., Somma, J., Bernier, M., Fortin, J.P., Gauthier y., and Dedieu, J.P.: Estimation de L'équivalent en Eau du Couvert Nival en Montagne Libanaise à Partir des Images RADARSAT–1/Estimation of Water Equivalent of the Snow Cover in Lebanese Mountains by Means of RADARSAT–1 Images, Hydrological Sci J, 50(2), 355–370, doi:10.1623/hysj.50.2.355.61802, 2005.

Devine, K. A. and Mekis, É.: Field accuracy of Canadian rain measurements, Atmos.-Ocean., 46, 213–227, doi:10.3137/ao.460202, 2008.

Dixon, D. and Boon, S.: Comparison of the SnowHydro snow sampler with existing snow tube designs, Hydrol Process, 26(17), 2555–2562, doi:10.1002/hyp.9317, 2012.

Doummar, J., Geyer, T., Baierl, M., Nödler, K., Licha, T. and Sauter, M.: Carbamazepine breakthrough as indicator for specific vulnerability of karst springs: Application on the Jeita spring, Lebanon, Applied Geochemistry, 47, 150156, doi:10.1016/j.apgeochem.2014.06.004, 2014.

Estévez, J., Gavilán, P., and Giráldez, J. V.: Guidelines on validation procedures for meteorological data from automatic weather stations, J Hydrol, 402(1–2), 144–154, doi:10.1016/j.jhydrol.2011.02.031, 2011.

Fayad, A., Gascoin, S., Faour, G., Fanise, P., and Drapeau, L.: Snow dataset for Mount-Lebanon (2011–2016), https://doi.org/10.5281/zenodo.583733, 2017.

Gascoin, S., Hagolle, O., Huc, M., Jarlan, L., Dejoux, J.–F., Szczypta, C., Marti, R., and Sánchez, R.: A snow cover climatology for the Pyrenees from MODIS snow products, Hydrology and Earth System Sciences, 19(5), 2337–2351, doi:10.5194/hess–19–2337–2015, 2015.

Hall, D. K., G. A. Riggs, and V. V. Salomonson: MODIS/Terra Snow Cover 5–Min L2 Swath 500m. Version 5. Boulder, Colorado USA: NASA National Snow and Ice Data Center Distributed Active Archive Center. http://dx.doi.org/10.5067/ACYTYZB9BEOS, 2006.

Harder, P., and Pomeroy, J.: Estimating precipitation phase using a phycrometric energy balance method. Hydrol. Processes, 27, 1901–1914, 2013, doi:10.1002/hyp.9799.

Harpold, A. A., Kaplan, M. L., Klos, P. Z., Link, T., McNamara, J. P., Rajagopal, S., Schumer, R., and Steele, C. M.: Rain or snow: hydrologic processes, observations, prediction, and research needs, Hydrol. Earth Syst. Sci., 21, 1-22, doi:10.5194/hess-21-1-2017, 2017.

Herrero, J. and Polo, M. J.: Evaposublimation from the snow in the Mediterranean mountains of Sierra Nevada (Spain), The Cryosphere, 10, 2981–2998, https://doi.org/10.5194/tc-10-2981-2016, 2016.

Hreiche, A., Najem, W. and Bocquillon, C.: Hydrological impact simulations of climate change on Lebanese coastal rivers /Simulations des impacts hydrologiques du changement climatique sur les fleuves côtiers Libanais, Hydrological Sciences Journal, 52(6), 11191133, doi:10.1623/hysj.52.6.1119, 2007.

Huwald, H., C. W. Higgins, M.-O. Boldi, E. Bou-Zeid, M. Lehning, and M. B. Parlange (2009), Albedo effect on radiative errors in air temperature measurements, Water Resour. Res., 45(8), W08431, doi:10.1029/2008WR007600.

Jonas, T., Marty, C., and Magnusson, J.: Estimating the snow water equivalent from snow depth measurements in the Swiss Alps, Journal of Hydrology, 378(1–2), 161–167, doi:10.1016/j.jhydrol.2009.09.021, 2009.

Kalaoun, O., Al Bitar, A., Gastellu-Etchegorry, J.-P.; Jazar M. : Impact of Demographic Growth on Seawater Intrusion: Case of the Tripoli Aquifer, Lebanon, Water, 8, 104, https://doi.org/10.3390/w8030104, 2016. Königer, P., Margane, A.: Stable Isotope Investigations in the Jeita Spring catchment, Technical Cooperation Project Protection of Jeita Spring, BGR Technical Report No. 12. 56 pp. Hannover, Germany, 2014.

López–Moreno, J.I., Fassnacht, S.R., Heath, J.T., Musselman, K.N., Revuelto, J., Latron, J., Morán–Tejeda, E., and Jonas, T.: Small scale spatial variability of snow density and depth over complex alpine terrain: Implications for estimating snow water equivalent, Advances in Water Resources, 55, 4052, doi:10.1016/j.advwatres.2012.08.010, 2013.

Malek, E: The daily and annual effects of dew, frost, and snow on a non–ventilated net radiometer, Atmos. Res., 89(3), 243–251, doi:10.1016/j.atmosres.2008.02.006, 2008.

Margane, A., Schuler, P., Königer, P., Abi Rizk, J., Stoeckl, L., and Raad, R.: Hydrogeology of the Groundwater Contribution Zone of Jeita Spring. Technical Cooperation Project Protection of Jeita Spring, BGR Technical Report No. 5, 317pp. Raifoun, Lebanon, 2013.

Marks, D., Winstral, A., Reba, M., Pomeroy, J., and Kumar, M.: An evaluation of methods for determining during-storm precipitation phase and the rain/snow transition elevation at the surface in a mountain basin, Adv. Water Resour., 55, 98–110, 2013.

Mhawej, M., Faour, G., Fayad, A. and Shaban, A.: Towards an enhanced method to map snow cover areas and derive snow–water equivalent in Lebanon, Journal of Hydrology, 513, 274282, doi:10.1016/j.jhydrol.2014.03.058, 2014.

Ministry of Energy and Water (MOEW): National Water Sector Strategy (NWSS) Report, Beirut, Lebanon, 2010.

National Council for Scientific Research (NCRS): Land-use land cover map of Lebanon, Beirut, Lebanon, available at: http://www.cnrs.edu.lb/ (last access: 9 January 2017), 2015.

Pan, X., Yang, D., Li, Y., Barr, A., Helgason, W., Hayashi, M., Marsh, P., Pomeroy, J., and Janowicz, R. J.: Bias corrections of precipitation measurements across experimental sites in different ecoclimatic regions of western Canada, The Cryosphere, 10, 2347-2360, doi:10.5194/tc-10-2347-2016, 2016.

Rasmussen, R., Baker, B., Kochendorfer, J., Meyers, T., Landolt, S., Fischer, A., Black, J., Thériault, J., Kucera, P., Gochis, D., Smith, C., Nitu, R., Hall, M., Ikeda, K. and Gutmann, E.: How Well Are We Measuring Snow: The NOAA/FAA/NCAR Winter Precipitation Test Bed, B Am Meteorol Soc, 93(6), 811–829, doi:10.1175/BAMS–D–11–00052.1, 2012.

Rasmussen, R., Dixon, M., Hage, F., Cole, J., Wade, C., Tuttle, L., McGettigan, S., Carty, T., Stevenson, L., Fellner, W., Knight, S., Karplus, E., and Rehak, N.: Weather support to deicing decision making (WSDDM): A winter weather nowcasting system, Bull. Am. Meteorol. Soc., 82, 579–595, 2001.

Rice, R. and Bales, R.: Embedded-sensor network design for snow cover measurements around snow pillow and snow course sites in the Sierra Nevada of California, Water Resources Research, 46(3), W03537, doi:10.1029/2008wr007318, 2010.

Serreze, M., Clark, M., Armstrong, R., McGinnis, D. and Pulwarty, R.: Characteristics of the western United States snowpack from snowpack telemetry (SNOTEL) data, Water Resources Research, 35(7), 2145–2160, doi:10.1029/1999wr900090, 1999.

Shaban, A., Faour, G., Khawlie, M. and Abdallah, C.: Remote sensing application to estimate the volume of water in the form of snow on Mount Lebanon / Application de la télédétection à l'estimation du volume d'eau sous forme de neige sur le Mont Liban, Hydrological Sciences Journal, 49(4), 643–653, doi:10.1623/hysj.49.4.643.54432, 2004.

Shafer, M., Fiebrich, C., Arndt, D., Fredrickson, S. and Hughes, T.: Quality Assurance Procedures in the Oklahoma Mesonetwork, J Atmos Ocean Tech, 17(4), 474–494, doi:10.1175/1520–0426(2000)017<0474:QAPITO>2.0.CO;2, 2000.

Smith, C. D., Kontu, A., Laffin, R., and Pomeroy, J. W.: An assessment of two automated snow water equivalent instruments during the WMO Solid Precipitation Intercomparison Experiment, The Cryosphere, 11, 101–116, https://doi.org/10.5194/tc-11-101-2017, 2017. Somma, J., Luxey, P., and Dhont, D.: Snow Volumes 3D Modeling on the Karstic Plateau of Mount Lebanon (Lebanon), AGU, Fall Meeting 2006, 11–15 December 2006, San Francisco, CA, USA, abstract # H11B–1260, 2006.

Somma, J., Drapeau, L., Abou Chakra, C., and El-Ali, T.: Geomatics contributions to key indicators for estimation and monitoring of snow cover input to hydrogeological resources, AGU, Fall Meeting 2014, 15–19 December 2014, San Francisco, CA, USA, abstract # C43C–0404, 2014.

Sproles, E.A., Kerr, T., Orrego Nelson, C., and Lopez Aspe, D.: Developing a Snowmelt Forecast Model in the Absence of Field Data, Water Resour Manage 30(7): 2581–2590. doi:10.1007/s11269–016–1271–4, 2016

Sturm, M., Taras, B., Liston, G., Derksen, C., Jonas, T., Lea, J.: Estimating Snow Water Equivalent Using Snow Depth Data and Climate Classes, Journal of Hydrometeorology , 11, 1380–1394, 2010.

Telesca, L., Shaban, A., Gascoin, S., Darwich, T., Drapeau, L., Hage, M. and Faour, G.: Characterization of the time dynamics of monthly satellite snow cover data on Mountain Chains in Lebanon, Journal of Hydrology, 519, 32143222, doi:10.1016/j.jhydrol.2014.10.037, 2014.

Thériault, J. M., Rasmussen, R., Ikeda, K., and Landolt, S.: Dependence of Snow Gauge Collection Efficiency on Snowflake Characteristics, J. Appl. Meteorol. Climatol., 51, 745–762, 2012.

UN Development Programme (UNDP): Assessment of Groundwater Resources of Lebanon, Beirut, available at: http://www.lb.undp.org/content/lebanon/en/home/library/environment_energy/assessment-of-groundwater-resources-of-lebanon.html (lastaccess: 7 August 2017), 2014 World Meteorological Organization (WMO): Guide to Meteorological Instruments and Methods of Observations, WMO–No.8, Geneva, Switzerland, 2008.

Yang, D., B. E. Goodison, C. S. Benson, and S. Ishda, Adjustment of daily precipitation at 10 climate stations in Alaska: Application of the World Meteorological Organization intercomparison results, Water Resour. Res., 34(2), 241–256, 1998.

Summary of chapter: "Modeling the daily distribution of SWE, snow depth, and SCA in Mount-Lebanon"

This chapter is in preparation for submission to Water Resources Research.

This chapter's main objective is to address the spatial distribution of the SWE and the contribution of snowmelt to the hydrologic budget in the three major basins of Mount-Lebanon.

We used the meteorological dataset presented in Chapter 3 as forcing data for the energy balance SnowModel (Liston and Elder, 2006) to simulate the spatial distribution of the SWE and snowmelt for the first time in three major catchments in coastal Lebanon. We ran the model at 30-min time step over snow seasons (2013-2016) with a spatial resolution of 100 m over a domain of 150x120 km but we focused on the windward slope of Mount Lebanon for the validation. The model was evaluated against continuous snow depth observations at the AWS, snow courses measurements, and MODIS snow cover area.

Model derived daily SCA (based on modeled SWE) showed good correlation (r=0.87) against MODIS SCA (MOD10A1). The model was able to capture most of the variability in observed snow height (HS), snow density and SWE. However, the model had a tendency to underestimate snowmelt during spring season at higher elevations. This can be attributed to an overestimation in precipitation distribution and snow to rain partitioning.

We found that SWE peaked between late-February early-March for the three basins over the simulation period. Over the three snow years between 2013 and 2013 the April 1st snow water equivalent (SWE) ranged between 173 mm and 421 mm w.e. (Abou Ali), 24-198 mm w.e. (Ibrahim), and 54-193 mm w.e. (Kelb) (average calculated for the snow dominated watersheds with elevations above 1200 m a.s.l.). The simulated snowmelt is concentrated between February and April but significant melt occurred throughout the entire snow season. The length of the snowmelt season can vary by more than one month depending on the year.

These results are important for understanding the link between snowmelt and groundwater recharge in Mount-Lebanon and provide the basis for further studies over longer periods using climate reanalysis data and future climate scenarios. The need for better separation between rain and snowfall is important especially in mid-elevation regions and given the specificity of the warm Mediterranean climate and the projected warming, we believe this specific area of research warrants future investigations. Understanding the evolution of snow density and the potential impact of rain on snow is a potential field for future research.

4 MODELING THE DAILY DISTRIBUTION OF SWE, SNOW DEPTH, AND SCA IN MOUNT-LEBANON

Abstract

The seasonal snowpack is an essential component of the national water budget in Lebanon. In particular, snowmelt from the high-elevation plateau of Mount-Lebanon recharges a system of karst aquifers, which supply key water resources to the coastal plain of Lebanon where most of the Lebanese population lives. To date, the estimation of the snow water equivalent (SWE) and snow melt was limited by the lack of meteorological and snow observations in the high-elevation mountain areas. In this study, we used new measurements from three automatic weather stations (AWS) located in the snow-dominated regions of Mount-Lebanon (elevation range 1840-2834 m a.s.l.) to compute the spatial distribution of the SWE and snowmelt for the first time in three major basins of the coastal Lebanon. We ran a spatially-distributed snowpack evolution model at a 100 m resolution grid forced by 30-min meteorological data over three snow seasons (2013-2016). The model was evaluated against continuous snow depth observations at the AWS, snow courses measurements, and MODIS snow cover area. Results showed the model ability to capture most of the variability in observed snow height (HS), snow density and SWE. However, the model had a tendency to underestimate snowmelt during spring season at higher elevations, and this was attributed to an overestimation in precipitation distribution and snow to rain partitioning. SWE peaked between late-February early-March for the three basins over the simulation period. Over the three snow years between 2013 and 2013 the April 1st snow water equivalent (SWE) ranged between 173 mm and 421 mm w.e. (Abou Ali), 24-198 mm w.e. (Ibrahim), 54-193 mm w.e. (Kelb) (average calculated for the snow dominated watersheds with elevation above 1200 m a.s.l.). The simulated snowmelt is concentrated between February and April but significant melt occurred throughout the entire snow season. The length of the snowmelt season can vary by more than one month depending on the year. These results are important for understanding the link between snowmelt and groundwater recharge in Mount-Lebanon and provide the basis for further studies over longer periods using climate reanalysis data and future climate scenarios.

Keywords: Snow; Snow water equivalent; Snowmelt; Snow hydrology; Lebanon; Mediterranean climate

4.1 Introduction

The Mount-Lebanon mountains is a major water tower for Lebanon. The hydrology of the snow dominated basins in Mount-Lebanon are influenced by the Mediterranean climate which limits precipitation to the winter season (December- March). Snow, which usually falls above 1200 m a.s.l., play a key role in defining the availability of water resources by releasing the stored water during dry months (April-June). Snowmelt is the main contributor to the karst groundwater recharge (Margane et al., 2013; UNDP, 2014) and help in sustaining spring flow during dry months (April to August with flow peaks in May-June).

Despite the importance snowpack to the hydrologic budget in Lebanon (Shaban et al., 2004; Corbane et al., 2005; Aouad-Rizk et al., 2005; Bakalowicz et al., 2007; Somma et al.,

2014; Mhawej et al., 2014; Koeniger and Margane, 2014; Telesca et al., 2014), little is known on the spatio-temporal variability of snow water equivalent (SWE) nor on the timing and release of snow water into the hydrologic system. So far, most estimates are either available at the experimental scale (point scale and small catchments) (e.g., Aouad-Rizk et al., 2005; Hreiche et al., 2007) or spatially derived as monthly or yearly averages (Bernier et al., 2003; Mhawej et al., 2014; Telesca et al., 2014; UNDP, 2014).

The annual SWE over the past decade was assessed using index based models combining average snow density observations with remote sensing SCA (e.g., Shaban et al., 2004; Mhawej et al., 2014; Telesca et al., 2014). The average annual SWE, from multiple studies conducted over different time frames between 2000 and 2012, was estimated to range between 1.7 and 2.8 billion m^3 yr^{-1} for both Mount- and Anti Lebanon (Mhawej et al., 2014; UNDP, 2014). The average annual SWE was estimated to 2.42 billion m^3 yr^{-1} (2002-2011) (Mhawej et al., 2014). Early annual SWE estimates over mount-Lebanon for the water year 2000-2001 was estimated to 1.1 billion m^3 yr^{-1} (425 mm equivalent) (Shaban et al., 2004). Meanwhile, the long-term average over Mount-Lebanon was estimated to 0.77 billion m^3 yr^{-1} (water years between 2000 and 2013) (Telesca et al., 2014).

The temporal viability of SWE was addressed using degree day methods and energy balance models run at the point scale (e.g., Aouad-Rizk et al., 2005) or by coupling hydrological models with a DDM module to investigate runoff (e.g., Hreiche et al., 2007) and groundwater recharge (e.g., Koeniger and Margane, 2014) in snow-dominated basins. hese experimental studies highlighted the need to account for the variation of SWE and snow density along with elevation (Aouad-Rizk et al., 2005). One of main limitation highlighted by these studies was the lack of meteorological and snow data needed for model forcing and validation.

Snowmelt contribution to surface runoff in the Mount-Lebanon was estimated to 30% based on sparse in situ SWE samples (2000-2012) (Telesca et al., 2014). Meanwhile, the snow contribution to groundwater recharge was estimated at 75% in the snow dominated regions (above 1600 m a.s.l.) of the El Kelb Basin (Fig 4.1.) (Margane et al., 2013; Königer and Margane, 2014). The snowmelt contribution from high elevation regions (above 1800 m a.s.l.) was estimated to 56% of the major spring discharge at the Jeita spring (outlet at 60 m a.s.l.) which is the major spring feeding Beirut the capital (Jeita contributes to 75% of the total potable water supplied for Beirut) (Margane et al., 2013). One of the major aspect related to snowmelt-hydrology is the fast spring response to precipitation. In the snow-dominated basin El Kelb the spring response can be seen within 24-48h after precipitation events and usually depends on the

distribution and type of precipitation (rainfall or snowfall) (Margane et al., 2013; Koeniger and Margane, 2014).

The and snowmelt contribution to surface runoff and groundwater recharge remains poorly known (UNDP, 2014). The deficiency in the estimation of spatio-temporal SWE can be attributed to the scarcity of snow measurements and the lack of meteorological observations in mountainous areas; and the limited number of ground observations used to validate model estimates. These deficiencies in the proper representation of the spatial-temporal distribution of SWE had thus resulted in that the link between snowmelt and other hydrological processes remains largely unknown.

These data allow us to spatially simulate the temporal variability of SWE and snowmelt in three major snow dominated basins located in the windward side of Mount-Lebanon (total area 1092 km^2; elevation range 0-3080 m a.s.l.) (Fig. 4.1). For that purpose, we used the distributed snow energy model SnowModel (Liston and Elder, 2006a, 2006b). The model had been used for modeling snow in different climate regions (e.g. semi-arid, alpine, and arctic) (e.g., Hiemstra et al. 2006; Sturm and Wagner 2010; Gascoin et al. 2013; Mernild et al. 2016).

The model is run over a domain area extending over the three snow dominated basins of Mount Lebanon (Fig. 4.1). As model forcing we use 30-min meteorological observations from the three automatic weather stations over the period 2013-2016. SnowModel is used to (1) generate spatially distributed meteorological forcing data over the study domain (MicroMet submodel, Liston and Elder, 2006a, 2006b); (2) solve the snowpack energy balance (EnBal submodel, Liston 1995; Liston et al. 1999); (3) simulate the snow depth evolution (SnowPack-ML, Liston and Mernild, 2012); and (4) simulate the wind effects on snow distribution (SnowTran-3D, Liston and Sturm, 1998, 2002; Liston et al., 2007).

The model outputs are validated against (1) daily averages of observed albedo and HS at the three AWS, (2) bi-weekly snow course measurements of the SWE and snow density, and (3) daily maps of the snow cover extent from MODIS. The model outputs are then used to quantify the daily evolution of the SWE and snowmelt across the three snow seasons in the three study catchments.

The study area is described in section 4.2. The methodology and data used are described in section 4.3. Section 4.4 shows the results and discusses model uncertainty. The conclusions are presented in section 4.5.

4.2 Study area

The Mount-Lebanon (35.98E, 34.14N) and Anti-Lebanon Mountains (36.25E, 33.8N) are located on the eastern part of the Mediterranean Sea and extend parallel to the coastline over 145 and 150 km respectively (Fig. 4.1). The mountains are classified mid- to high-altitude ranges with rugged topography and high plateaus (based on a classification adopted after Viviroli et al. (2007). Elevation ranges between 500 and 3000 m msl for Mount-Lebanon which peaks at Qurnet El Sawda (3088 m a.s.l.) and 500 to 2500 for Anti-Lebanon (peaks at Mount Hermon, 2814 m a.s.l.). The land cover is mainly bare rocks and soils, low scrublands, and speargrass.

The climate is typical Mediterranean with precipitation occurring between mid-November to late April and peaks during winter season (January to March). The mountain regions (above 1200 m a.s.l.) receive between 50 to 67% of their total annual precipitation as snow (Shaban et al., 2004; Aouad-Rizk et al., 2005). Annual average precipitation for four hydrological years between 2008 and 2012 was estimated at 7.41 billion m^3 (946 mm yr^{-1} equivalent) (± 1222 standard deviation, equivalent to ±143 mm yr^{-1}). The estimated snowpack volume for the same time period, based on monthly averages, was 2.3 billion m^3 yr^{-1} (294 mm yr-1) (±0.294 standard deviation, equivalent to 29 mm yr^{-1}) the monthly snowfall to precipitation ratio (S/P) was estimated at 0.31 (±0.24) (UNDP, 2014).

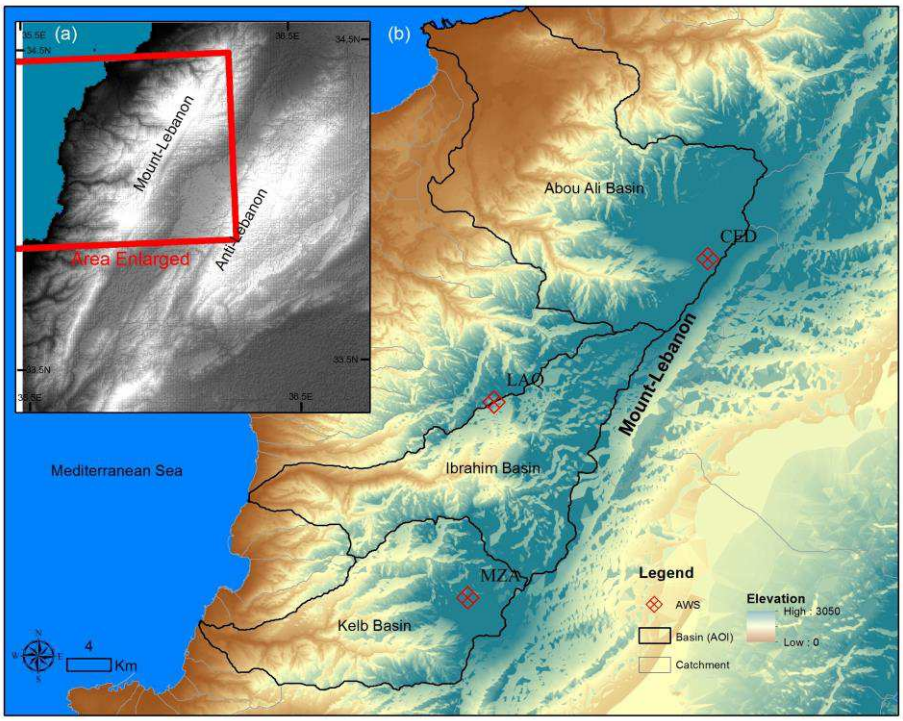

Fig. 4.1. (a) Mount- and Anti-Lebanon mountains (b) topography with the same extent as the simulation domain (200-m contour interval) with snowline shown in blue and the location of the three automatic weather stations.

4.3 Methods

4.3.1 Model description

The SnowModel (Liston and Elder, 2006a, 2006b) model is a spatially distributed snow model that account for meteorological forcing, topography and vegetation cover. SnowModel combines six submodels: MicroMet (Liston and Elder, 2006a, 2006b) is a spatially distributed meteorological forcing conditions from AWS observations. EnBal is a distributed energy balance model which simulates energy and water fluxes from the MicroMet outputs (Liston 1995; Liston et al. 1999); SnowPack simulates snow depth, snow desnity, and snow water equivalent (Liston and Mernild, 2012). SnowTran-3D simulates blowing snow and snow redistribution by wind (Liston and Sturm 1998, 2002; Liston et al. 2007), SnowAssim (Liston and Hiemstra, 2008) assimilates field and remote sensing data (not used in this study), and Hydrofow is a runoff routing model (Liston and Mernild, 2012) (not used in this study). SnowModel requires temporally varying meteorological forcing data (at least surface air temperature, relative humidity, wind speed, wind direction, and snow precipitation) and spatially distributed grids of topography and land-cover types (Liston and Elder, 2006a). The model can be configured to run at different temporal (sub-hourly-1day) and spatial scales (meter to multi-kilometer grids). The SnowModel sub-models are run simultaneously to generate spatially distribute meteorological forcing grids (MicroMet) over the entire domain, the model then solves the mass balance (EnBal) whith the option of accounting for snow transports (SnowTran-3D) at each time step. Snowpack then simulates HS and SWE at each grid cell. A complete description of SnowModel and sub-models can be found in Liston and Elder (2006a, 2006b).

4.3.2 Simulation domain

The model simulation domain includes both mountain regions and lowland areas (Fig. 4.1a). The domain covered an area of 120 x 150 km (180,000 km^2) centered at x = 790,000 and y = 3,755,000 (UTM Zone 36N) with 100-meter pixel resolution. Elevation ranged between 0 m mean seal level to 3050 m a.s.l. (mean elevation of 998 ± 597 m a.s.l) (Fig. 4.1b). Model forcing is made from three AWS located on the windward side of Mount-Lebanon (Fig. 4.1b). The three automatic weather stations are located at 2296 (MZA), 1830 (LAQ), and 2834 (CED) m a.s.l.. Model validation was evaluated at three snow dominated basins located within the same domain of the weather stations (Fig 4.1b; Table 4.1). The three AWS are all located above the winter snowline (approximately 1550 m a.s.l.) (Fig. 4.1b). The LAQ station (1830 m a.s.l.)

is located in the Ibrahim Basin in a relatively flat plain area with fruit trees, bare rocks, and sparse short-grasslands. The Mzar (MZA) station (2296 m a.s.l.) is located in the El Keleb Basin, in a rugged terrain mountainous region at one of the medium elevation peaks (maximum elevation in the area is ~2600 m a.s.l.) with dominant bare soils and some sparse speargrass grassland. The Cedars (CED) AWS (2834 m a.s.l.) is located Abou Ali Bain, at a higher plateau with dominant bare rocks (Fig. 4.1., Table 4.1). The validation domain covers a total area of 1092 km^2 (elevation range 0-3088 m a.s.l..

The elevation grid for the simulation domain was obtained from ASTER GDM V2 (reference). The original ASTER 1 acrsecond horizontal (30 meter at the equator) with a vertical accuracy of 10-25 meters (RMSE) dataset was rescaled into 100 m horizontal grid (Fig. 4.1b). The land cover distribution grid was obtained by aggregating the land cover land use (LULC) map of Lebanon produced at a spatial resolution of 25 m (CNRS, 2015) into 100 m using maximum pixel count. Land classes were aggregated into 9 classes after Liston and Elder (2006a): Bare soils and rocks (59%), Shrubland/Playa (12%), Ocean/Sea (8%), Crops (7%), Grassland (4%), Clear-cut conifer (4%), Urban (3%), Coniferous, Deciduous and mixed forests (<3%), and Water (<1%). The different land classes are needed to account for the snow holding capacities and LAI (see Liston and Elder, 2006a).

Table 4.1. Attributes of the three snow-dominated basins in Mount-Lebanon described in this study.

asin[a]	Area (km^2)	Elevation range (average)[b], m a.s.l.	Dominant land cover[c] (%)	AWS Elevation, m a.s.l. (year installed)[d]	Snow courses count (elevation range[e]
1	513	0-3088 (1202)	Clear grassland (20%)	2834 (2013)	9 (1650-2900)
2	323	0-2681 (1547)	Clear grassland (30%)	1840 (2014)	6 (1300-1850)
3	256	0-2619 (1381)	Clear grassland (16%)	2296 (2011)	15 (1300-2300)

[a]Basins are Abouali (1), Ibrahim (2), and Kelb (3) (Fig. 4.1)
[b]Values are derived for the national 10 meter DEM (NCRS)
[c]Source: Landuse land cover map of Lebanon (NCRS, 2015)
[d]Source: Institut de recherche pour le développement (IRD)
[e]Snow courses observations were conducted between December and May over two snow years (2014-2016) (Fayad et al., 2017b).

4.3.3 Meteorological forcing

The model was forced by 6 meteorological variables including, precipitation (not observed at CED AWS), temperature, relative humidity, incoming solar radiation, wind speed and direction, and atmospheric pressure, collected at three AWS. No observations were

available for LAQ AWS during snow season (2013-2014). Model simulations were run at 30-min time step for three snow seasons between 2013 and 2016 (1 November to 30 June).

Fig. 4.2 illustrates the major climate and atmospheric forcing variables at the three AWS. Highlighted are air temperatures (temperature above 0°C contributes to snowmelt) and precipitation (temperature and precipitation are the two major drivers for snow accumulation and melt in Mediterranean like regions (e.g., see Chapter 2; Fayad et al. 2017a; Molotch et al., 2014). Wind speeds are another important factor since greater than 5 m s^{-1} contributes to snow transport (e.g., Pomeroy and Burn 2001; Mernild et al., 2006). Incoming shortwave solar radiation (not shown) are also important as they are one of the major drivers for snowmelt (e.g., see Chapter 2; Molotch et al. 2014).

The observed average seasonal (average 30-min from 01 November to 30 June) surface air temperature for the three snow seasons (2013-2016) was 6.93, 4.26, -1.36 °C for LAQ, MZA, and CED respectively. The months with temperature below zero varies by station (different elevations) and the time of year. The coldest months were January and February (Fig. 4.2). In LAQ and MZA (elevation 1840-2296 m) it is common to have temperature above 5°C during winter season. By early April temperature is almost always positive. CED temperature (elevation 2834 m) is negative most of the winter and above zero temperature are only observed starting April. There is a strong positive correlation in the 30-min surface air temperature records from the three stations (r 92.7-97.9). Such correlation, indicates strong orographic effects and can be used for calculating monthly temperature lapse as model parameterization input for MicroMet. Total annual precipitation ranged between 546 and 1025 mm during 2014-2015 and 1018 to 1288 mm for 2015-2016 representing precipitation data recorder at stations LAQ and MZA respectively (1840-2294 m a.s.l.).

Average wind speed for the three seasons (2013-2016) were 2.17 m s^{-1} (range 2.25, 2.09), 4.44 (4.76-4.11), and 4.40 (4.31, 4.49) m s^{-1} for LAQ (2014-2016), MZA, and CED respectively (Fig 2). Dominant wind directions were N to E for LAQ, S and SW for MZA, and S to NW for CED (Not shown). Strong winds typically do not exceed the 15 m s^{-1} barrier (LAQ, CED) and 20 m s^{-1} (MZA) except during storm events were maximum wind gusts reached up to 40.1 m s^{-1} (2014-2016). Wind effects on snow erosion is more noticeable in MZA (notes from field visits) due to the combined effect of topography and higher wind velocities. Seasonal incoming solar shortwave radiation averages (30-min averages) ranged between 156 and 219 W m^{-2} for the three stations (2014-2016).

These thee years when compared to the long time average at Beirut AWS (operated by the national civil aviation service) (20 m a.s.l.) for the time period (1930-2016) suggest a very

dry year (2013-2014), average year (2014-2015), and an average warm year (2015-2016) (Table 4.2). The snow starts to fall by mid-November in altitudes above 2700 m and snow patches in sheltered places remain till end of August in regions above 2900 m a.s.l.. Snowpack season starts by mid-late December and heavy snow usually fall between late November and late March. Snowmelt starts by early to mid-March in lower mountain regions 1600-2000 m a.s.l. and by late March to late April in medium to high altitude regions (2200-2800 m a.s.l.).

Table 4.2. Snow season (November –June) median air temperature, precipitation, solar radiation, wind speed, and humidity calculated from half-hourly data (2013-2016). Long-term averages (1930-2016) for the same months are provided for the Beirut (BEY) station (24 m a.s.l.).

Year (Nov-June)	Air temperature average (°C yr-1)				Precipitation total (cm yr-1)				Humidity (%)			
	BEY	LAQ†	MZA	CED‡	BEY	LAQ†	MZA	CED	BEY	LAQ†	MZA	CED
2013-2014		NA				NA		NA		NA		
2014-2015		5.78	3.79	-2.62		54.6*	101.8	NA		68.9	66.18	79.4
2015-2016		7.25	4.14	-0.36		102.5	130	NA		60.2	56.9	63.0

† LAQ observations for 2013-2014 are not available ‡ CED AWS data between April 24th and June 30th 2015 were removed due to station rotation.

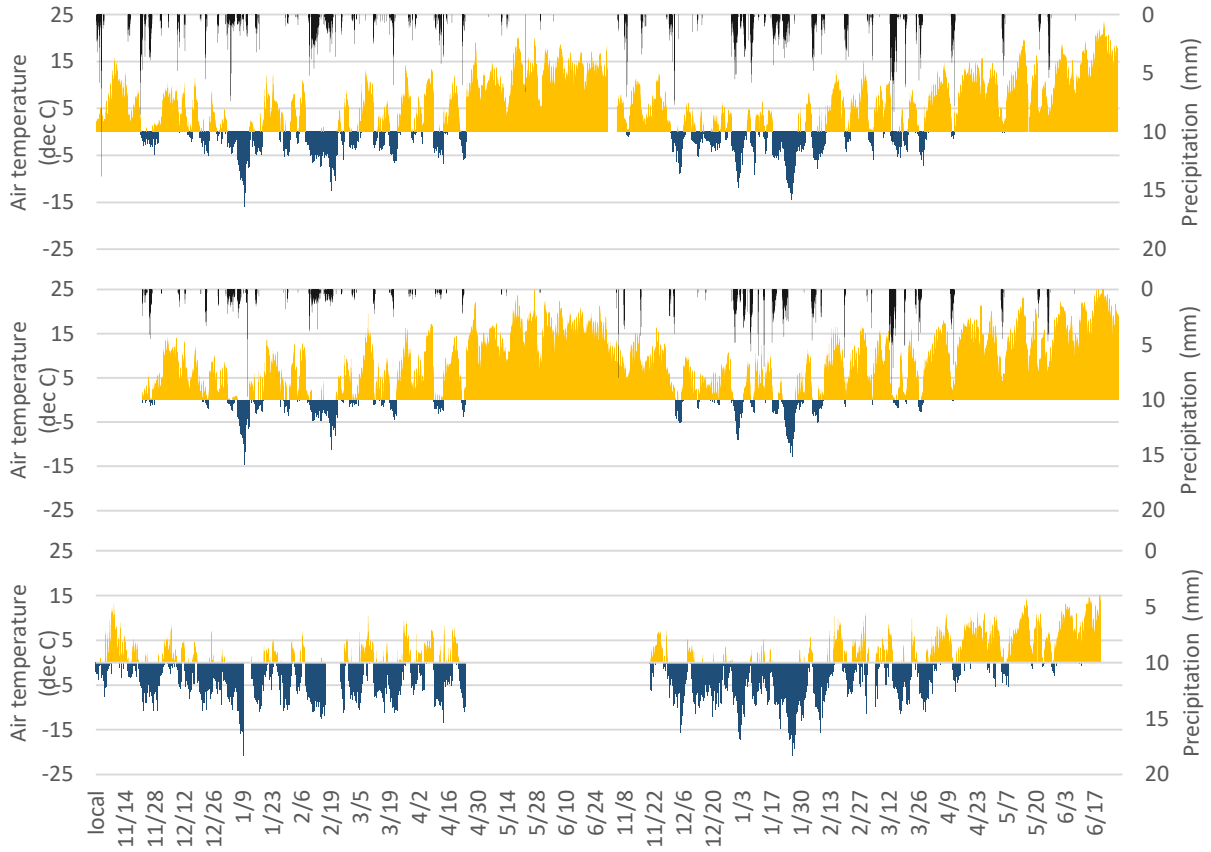

Fig. 4.2. Sub-hourly climate forcing variables of precipitation and surface air temperature at the three AWS for the winter seasons (1 November to 30 June) (2014-2016).

4.3.4 Evaluation datasets

The validation dataset includes sub-hourly snow height (HS) and snow albedo collected at the three AWS (2013-2016), bi-weekly snow course measurement of snow density, SWE, and HS collected over two winter seasons (2014-2016) at 30 different snow courses (elevation range 1300-2900 m a.s.l.), and daily MODIS snow cover area (2013-2016) observations. Observed snow height (HS) was recorded at 30 min interval for LAQ (2014 to 2016) and MZA and CED (2013-2016) and we computed the daily snow albedo by integrating 30-min incoming and reflected shortwave radiation (Table 4.2). The snow course observations are used in order to verify the model outputs of HS, SWE and snow density in three basins with different elevation ranges. We used the MODIS snow product MOD10A1 to generate daily cloud-free maps of the snow presence and absence at 500 m resolution. All these data are fully described in Chapter 3 (Fayad et al., 2017b) and are available as open data in a public repository (Fayad et al. 2017c).

4.3.5 Model configuration (Model setup/ Model simulation)

SnowModel was run using three configurations: (1) The model was first run using default configuration and standard lapse rates for temperature, precipitation and humidity and standard snow albedo ranges (for dry and melting snow albedo) and snow density parameter for Snowtrans-3D initialization (Liston and Elder 2006a, 2006b) (Tabel 4.3). The second run (2) a modified model configuration by setting the precipitation lapse rate to zero in an attempt to remove the dependency of precipitation to elevation. This was based on the lack of distributed rain and snow gauges in the study area and the plateau geomorphology of Mount-Lebanon. For the third configuration (3) we used a modified model configuration based on different precipitation partitioning between rain and snow. The SnowModel is configured to separate between snow and rain using the air temperature threshold of +2.0 after Auer (1974). We set the temperature threshold for snow at zero (Tsnow = 0) after (Harpold et al. 2017) (Table 4.3). Model runs were validated against AWS observations, snow course measurements and MODSI SCA.

Table 4.3. List of user-defined variables used in model parameterization and simulations (2013-2016) (see Liston and Elder, (2006a, 2006b) for a detailed description for parameter definitions).

Variable	Value (Range)			Description
	Run 1 (Default)	Run 2 (Optimized)	Run 3 (Optimized)	
Snow melting albedo	0.6	0.6	0.6	Albedo for snow melting (clearing) (unitless)
Albedo (dry snow)	0.8	0.8	0.8	Albedo for dry snow (non melting) (unitless)
Tlapse	5.5 4.7 4.4 5.9 7.1 7.8 8.1 8.2	5.5 4.7 4.4 5.9 7.1 7.8 8.1 8.2	5.5 4.7 4.4 5.9 7.1 7.8 8.1 8.2	Temperature monthly lapse Nov-June (deg C km^{-1}); Default run 1 are based on (Liston and Elder 2006a); Optimized run 2 are medians (2014-2016)
Plapse	Default	Zero	Zero	Precipitation adjustment factor (km^{-1})
Separation between rain and snow	Default (+2 C°)	Default (+2 C°)	Optimized (0 C°)	Default: based on Auer (1974) Optimized: modified after Harpold et al. (2017)
Snow density (ro_snow)	300	300	300	Snow density (kg m^{-3})
Snow layer	1	1	1	Number of snow layer; 1 = Single layer snow
Time step	30	30	30	Sub-hourly time step
Vegetation	11	11	11	Land use classes (unitless) based on Liston and Elder (2006).
Elevation	0-3062	0-3062	0-3062	Grid (meter a.s.l.), same as MODIS Grid
Grid resolution (dx, dy)	100	100	100	Grid (cell size in meter), same as MODIS Grid
Model and sub-routines	Activated	Activated	Activated	
SnowTran-3D	Yes	Yes	Yes	Simulates gridded meteorological forcing
EnBal	Yes	Yes	Yes	Simulate snow energy balance
SnowPack	Yes	Yes	Yes	Simulate snow depth
SnowTran-3D	Yes	Yes	Yes	Simulates wind-effects on snow distribution

4.4 Results and discussion

4.4.1 Model validation

4.4.1.1 Simulated vs. observed AWS snow height (HS)

Median snow height recorded for snow seasons 2014-2016 were 70 and 66 cm (std dev 37, 36) at LAQ, 25 and 30 cm (std dev 37-23) at MZA, and 114 and 99 cm (std dev 56, 44) at CED. We extracted the simulated snow height for three pixels representing the location of the three AWS (i.e. CED, LAQ, and MZA) (Table 4.1). The correlation between daily modeled and observed HS at the AWS was good ranged between 0.41 for MZA and 0.72 for LAQ and 0.73 for CED (Fig. 4.3). The bias was 0.48 for MZA, -0.06 for LAQ and 0.46 for CED. We noted

good agreement for the CED and LAW stations which are in relatively flat mountain regions. The underestimated HS values for snow season (2014-2015) in LAQ may be attributed to the underestimated snowfall in the station for this year. The model overestimation at MZA is attributed to the topography which result in high snow erosion with few tens of meters near the station. HS at MZA were not representative for the melting season due to blowing wind conditions and rough topography which resulted in the removal of snow from the station domain. The combined effect of wind and topography resulted in that the MZA AWS was indicating lower HS observations and this is due to the high snow variability in this region as can be seen in Fig. 4.4. The model overestimation in CED may be attributed to the lack of precipitation from the AWS (2834 m a.s.l.). With the start of snowfall observation in CED starting snow-season (2016-2017) future simulation may help in addressing this issue.

4.4.1.2 Simulated vs. snow course observed snow density and SWE

We compared the modeled snow density and SWE against observed snow course data for the three snow courses located near the three AWS stations for two snow seasons (01 November –30 June) between 2014-2016) (Fig. 4.5 and 4.6 respectively). The model showed good potentials in capturing snow density at the different elevations (range 1850-2850 m a.s.l.) (Fig. 4.5a). Better snow density estimates were reported at the CED snow course (elevation 2850 m a.s.l.). Good fit between simulated and observed snow densities were found during snow season 2015-2016. The model underestimate of snow densities at the beginning of season 2015-2016 (Fig. 4.5a) and may be attributed to the rain on snow event which resulted the high densification of snow at higher elevations (1700-2400 a.s.l.). The model also showed good potentials in capturing SWE (Fig. 4.5b) with a tendency to overestimate SWE at the end of season. The overestimation of SWE at LAQ during winter 2014-215 may be attributed to snowfall undercatch at the station.

Snow density observations over the time period (2014-2016) showed that maximum snow densification can be reached within 2-3 weeks following the major first snow events and 1-2 weeks following secondary and tertiary snowfall events. The snow density range for the three basins is presented in Fig. (4.6a).

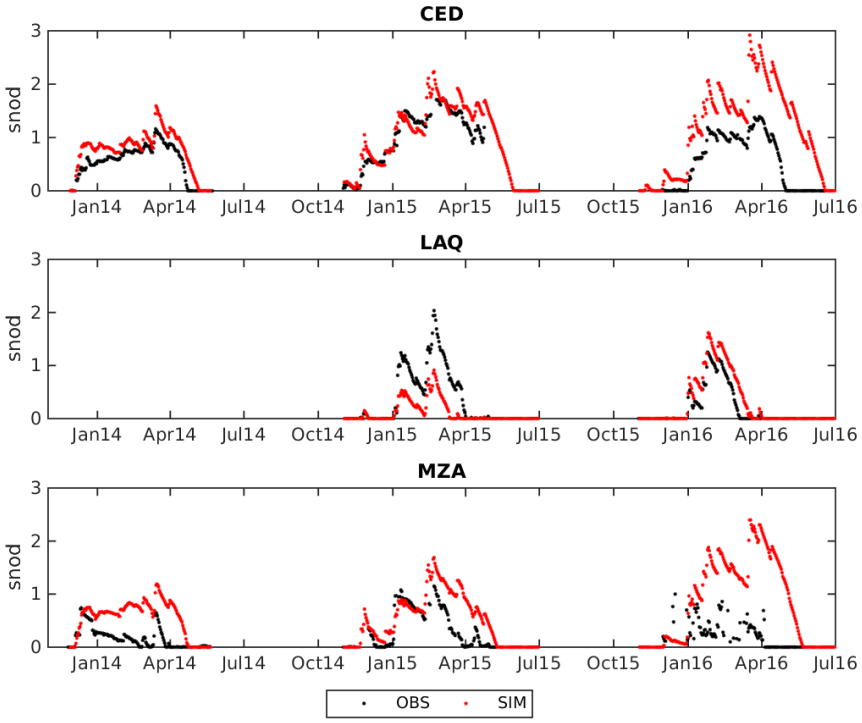

Fig. 4.3. Comparison between observed and simulated HS at the three stations - snow seasons (01 November –30 June) (2013-2016).

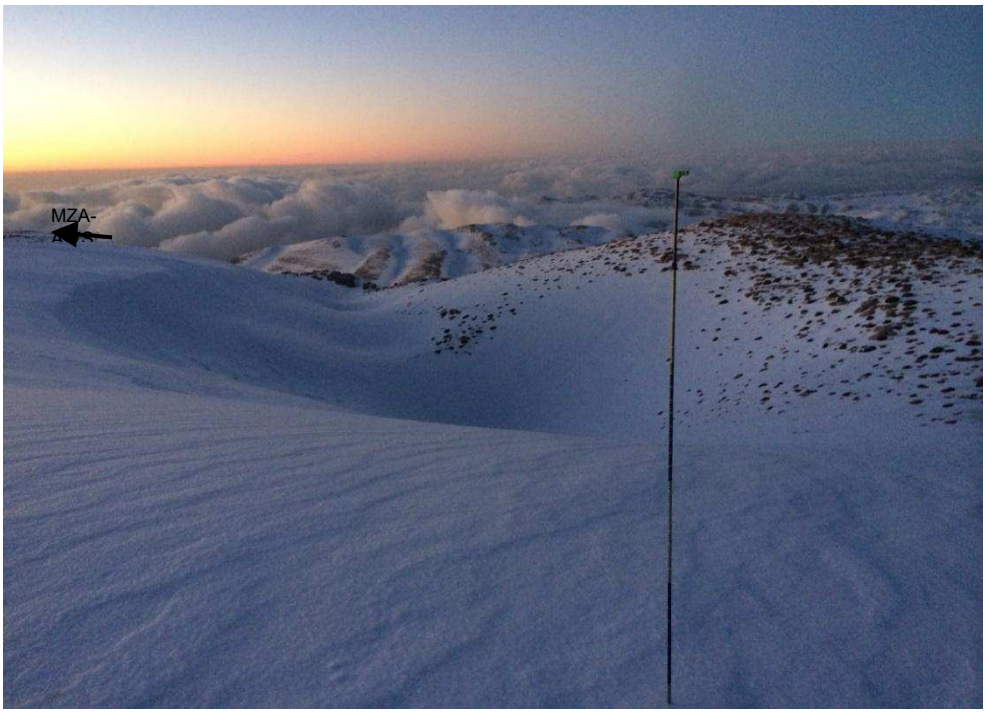

Fig. 4.4. Snow redistribution following major snowfall event at 2310 m a.s.l. and 200 m away from the MZA AWS (located at 50 m to the left of the image). Image taken on January 15th, 2016 at 2310 m a.s.l. Snow depth readings at the station was 7.5 cm.

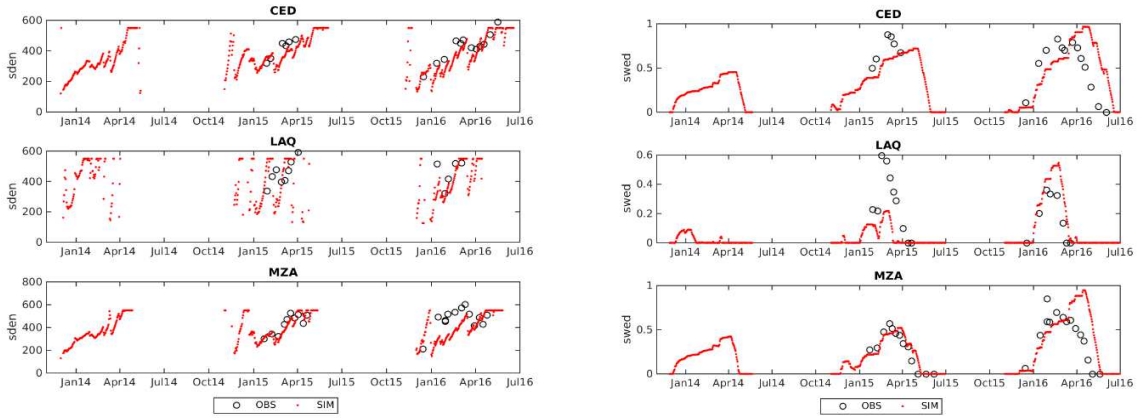

Fig. 4.5. Comparison between observed and simulated snow density collected at the three snow courses located near the three AWS stations - snow seasons (01 November –30 June) (2014-2016).

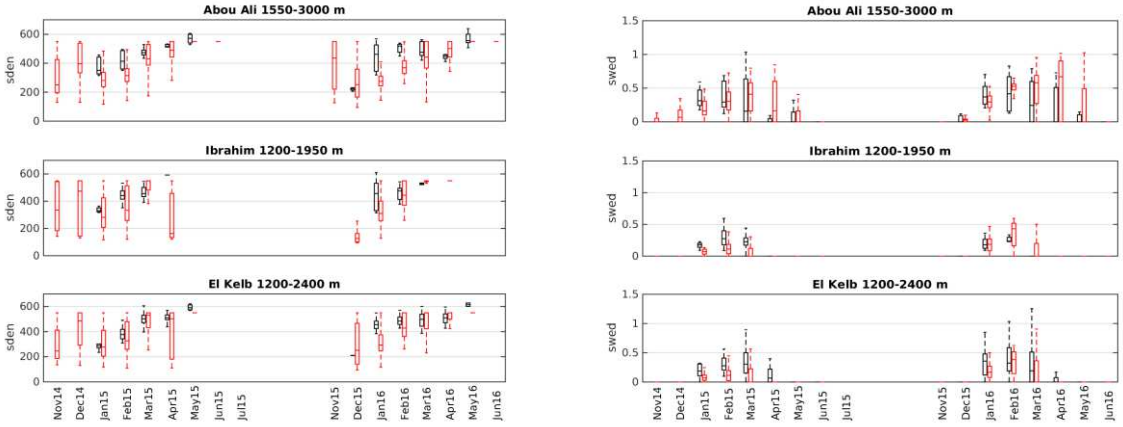

Fig. 4.6. Boxplots comparison between observed and simulated (a) snow density and (b) SWE (m w.e.) variability by basin representing the different elevation ranges in Mount-Lebanon - snow seasons (01 November –30 June) (2013-2016).

4.4.1.3 Modeled vs. MODIS SCA

The model was validated against daily MODIS SCA over the large domain area (120x150 km) (Fig. 4.1). Since SnowModel does not simulate SCA we used the modeled SWE with a detection threshold equal to 40mm water equivalent (w.e.) (Gascoin et al., 2015). The model derived SCA dataset was then resampled from the 100-m grid size to match the MODIS 500 m grid using a cubic interpolation. We compared the results over all model runs (Table 4.2). The model had an overall tendency to overestimate SCA especially over the Anti-Lebanon area (which is not covered by AWS) (Fig. 4.7). The correlation between MODIS and modeled SCA ranged between 0.83-0.9 under model runs. The optimized model configuration which is used for the analysis of SWE and snowmelt was 0.871 (Fig. 4.7c). When using single station (i.e. MZA) for model forcing the estimate correlation dropped to 0.79 but was still within good agreement. The model showed better correlation when compared to the MODIS SCA at the

basin scale (Fig. 4.8). This higher correlation is expected since the model was forced which meteorological data form the 3 AWS located within these basins. The good fit between the modeled and observed SCA confirms the model ability to simulate SCA with high accuracy when the climatological forcing are within the study domain. We noted a slight model tendency to overestimate SCA at higher-elevations, this can be seen in Abou Ali (elevation range 0-3088 m a.s.l.) (Fig. 4.8). We think this is linked to the lack of precipitation data at the CED stations (2834 m a.s.l.). The overestimation in the Ibrahim and El Kelb during snow season 2015-2016 may be attributed to the rain on snow events which resulted in the disappeared of snow at lower elevations (mostly below 1600 m a.s.l.) and the high densification of snow at higher elevations (1700-2400 a.s.l.).

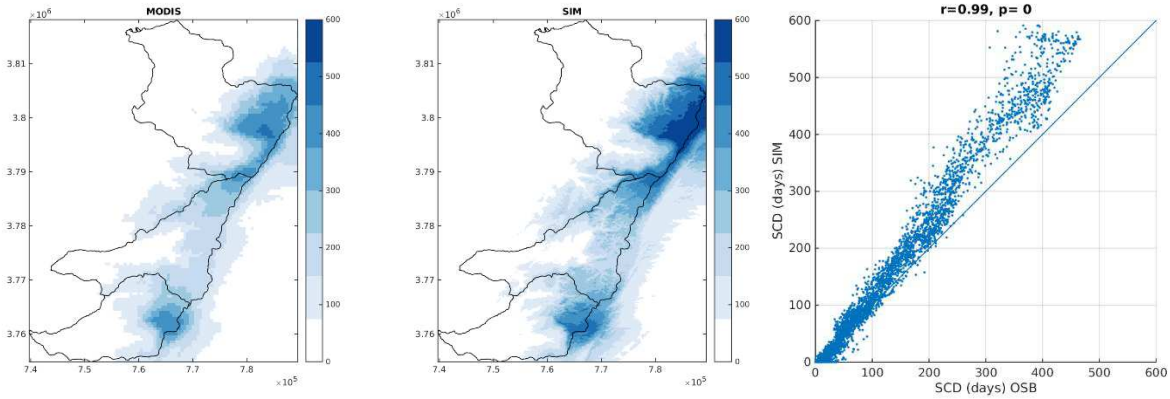

Fig. 4.7. Comparison between daily MODIS and model derived snow cover day (SCD) over the snow seasons (01 November –30 June) (2013-2016); where (a) total MODIS SCD, (b) average model derived SCD, and (c) scatter plot between MODIS and modeled SCD.

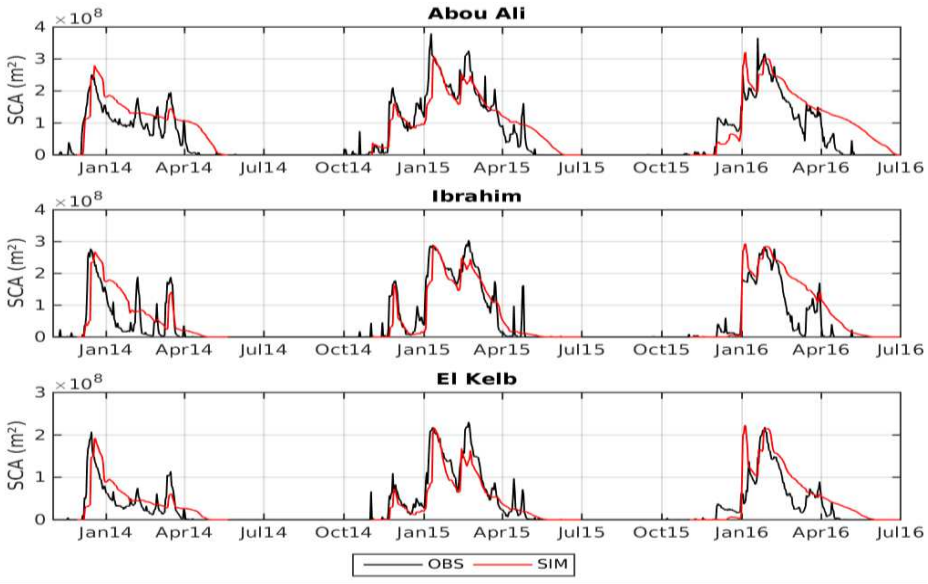

Fig. 4.8. Comparison between daily MODIS and model derived SCA over the three basins - snow seasons (01 November –30 June) (2013-2016).

4.4.2 SWE estimation and snowmelt by basin

Snow water equivalent monthly medians for the three basin is presented in Fig. 4.6b for the two snow seasons 2014-2016 along with observed snow courses data. The maximum observed SWE storage based on snow course data was during February. The modeled results reveal a higher difference which is expected given the model was run at daily time step and has a better representation of all snow cover within the catchment area. Fig. 4.9 portrays the spatial distribution of the April 1st snow in the three basins. Fig 4.10. Illustrates the average daily SWE evolution in the three Basins. Here we can see that the SWE peaked during mid-late February in the El Kelb and the Ibrahim basin over the snow seasons between 2014 and 2016. The SWE is more consistent in the Abou Ali basin where snow melts at lower rates over the time period between late-February and early-April. The snow year 2013-2014 was very dry and this can be seen with the relatively low SWE when compared to snow seasons 2014-2016 (Fig. 4.10).

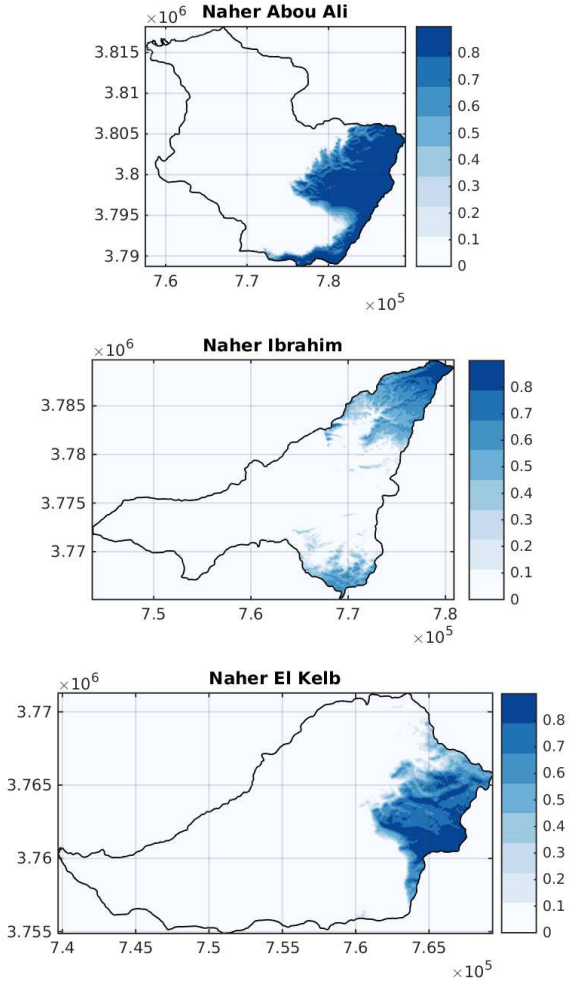

Fig. 4.9. Spatial distribution of April 1st SWE for the three major basins in Mount-Lebanon averaged over three snow seasons (01 November –30 June) (2013-2016).

The estimated April 1st SWE for the snow dominated regions (above 1200 m) for the three basins (2013-2016) were 173 -421 mm w.e. (Abou Ali), 24-198 mm w.e. (Ibrahim), and 54-193 mm w.e. (Kelb) (Fig. 4.10). The maximum SWE for was observed between 11 and 23 February for the snow seasons (2014-2016). Maximum SWE for the three basins over the three seasons (2013-2016) ranged between 181 and 451 mm w.e. (Abou Ali), 94-429 mm w.e. (Ibrahim), and 96-370 mm w.e. (Kelb) (Fig 4.10).

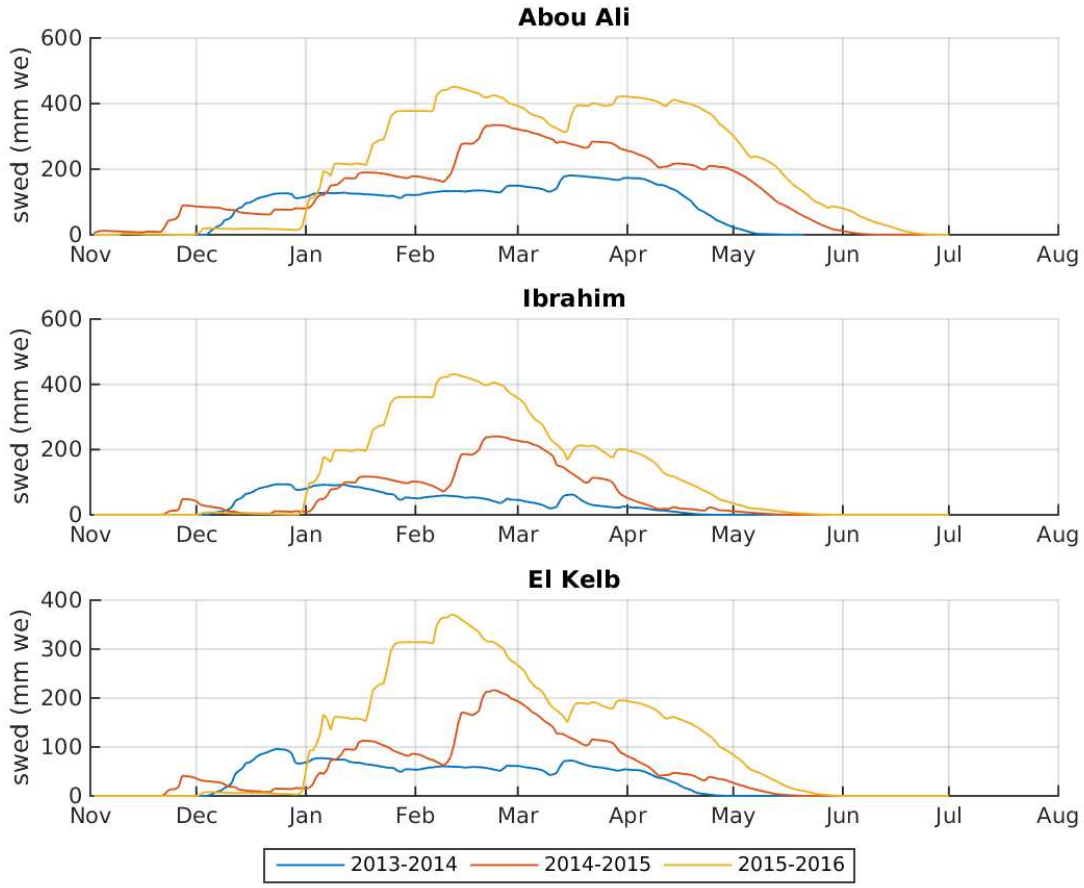

Fig. 4.10. Temporal evolution of daily SWE (m w.e.) at the snow dominated regions (elevation > 1200 m a.s.l.) of the three basin for the snow seasons between 2013 and 2016 (01 November –30 June).

4.5 Conclusions

This study represents the first simulation of the daily SWE on Mount-Lebanon (2013-2016). This was made possible with the availability of sub-hourly meteorological AWS observations in the high elevation areas (1840-2834 m a.s.l.). The results indicate that over the simulation period 2013-2016 the maximum SWE is reached between February and March and can change significantly from year to year in the three major snow basins in Mount-Lebanon

(i.e. Abou Ali, Ibrahim, El Kelb). The snowmelt occurred from Mid-February to Mid-April and Early-May in the basins Ibrahim and El Kelb.

Despite the importance of these findings it is good to note that the stations used have a short record to study long term snowmelt dynamics. Future work could focus on the application of reanalysis data (e.g. Grouillet et al., 2016) to extend the study period. Applying hydrological models with snow module could be used to assess water resources availability (e.g., Hublart et al., 2016). Longer SWE time series would also allow the coupling with a hydrogeological model of the karst to improve our knowledge on the snowpack dynamics in the regional water cycle.

4.6 References

Aouad–Rizk, A., Job, J.–O., Khalil, S., Touma, T., Bitar, C., Boqcuillon, C. and Najem, W., 2005. Snow in Lebanon: a preliminary study of snow cover over Mount Lebanon and a simple snowmelt model / Etude préliminaire du couvert neigeux et modèle de fonte des neige pour le Mont Liban. Hydrological Sciences Journal, 50(3), doi:10.1623/hysj.50.3.555.65023.

Bakalowicz, M., Hakim, M. and El–Hajj, A. 2007. Karst groundwater resources in the countries of eastern Mediterranean: the example of Lebanon, Environmental Geology, 54(3), 597–604, doi:10.1007/s00254–007–0854–z.

Bernier, M., Fortin, J.P., Gauthier, Y., Corbane, C., Somma, J., and Dedieu. J.P, 2003. Intégration de données satellitaires à la modélisation hydrologique du Mont Liban. Hydrological Sciences Journal, 48(6), 999–1012, DOI: 10.1623/hysj.48.6.999.51428.

Corbane, C., Somma, J., Bernier, M., Fortin, J.P., Gauthier y., and Dedieu, J.P. 2005. Estimation de L'équivalent en Eau du Couvert Nival en Montagne Libanaise à Partir des Images RADARSAT–1/Estimation of Water Equivalent of the Snow Cover in Lebanese Mountains by Means of RADARSAT–1 Images. Hydrological Sci J, 50(2), doi:10.1623/hysj.50.2.355.61802.

Fayad, A., Gascoin, S., Faour, G., López-Moreno J. I., Drapeau L., Le Page M., Escadafal, R., 2017a: Snow hydrology in Mediterranean mountain regions: a review, J. Hydrol. doi:10.1016/j.jhydrol.2017.05.063

Fayad, A., Gascoin, S., Faour, G., Fanise, P., Drapeau, L., Somma, J., Fadel, A., Al Bitar, A., Escadafal, R., 2017b. Snow observations in Mount-Lebanon (2011–2016), Earth Syst. Sci. Data, doi:10.5194/essd-2017-3.

Fayad, A., Gascoin, S., Faour, G., Fanise, P., and Drapeau, L., 2017c. Snow dataset for Mount-Lebanon (2011–2016), https://doi.org/10.5281/zenodo.583733

Gascoin, S., Hagolle, O., Huc, M., Jarlan, L., Dejoux, J.-F., Szczypta, C., Marti, R., and Sánchez, R., 2015. A snow cover climatology for the Pyrenees from MODIS snow products, Hydrol. Earth Syst. Sci., 19, 2337–2351, doi:10.5194/hess-19-2337- 2015.

Gascoin, S., Lhermitte, S., Kinnard, C., Bortels, K., Liston, G., 2013. Wind effects on snow cover in Pascua-Lama, Dry Andes of Chile. Advances in Water Resources 55, 25–39.

Grouillet, B., Ruelland, D., Vaittinada Ayar, P., and Vrac, M., 2016. Sensitivity analysis of runoff modeling to statistical downscaling models in the western Mediterranean. Hydrol. Earth Syst. Sci., 20, 1031-1047, doi:10.5194/hess-20-1031-2016.

Harpold, A. A., Kaplan, M. L., Klos, P. Z., Link, T., McNamara, J. P., Rajagopal, S., Schumer, R., and Steele, C. M, 2017. Rain or snow: hydrologic processes, observations, prediction, and research needs, Hydrol. Earth Syst. Sci., 21, 1-22, doi:10.5194/hess-21-1-2017.

Hiemstra, C.A., G.E. Liston and W.A. Reiners. 2006. Observing, modelling, and validating snow redistribution by wind in a Wyoming upper treeline landscape. Ecol. Model. 197(1–2), 35–51.

Hreiche, A., Najem, W. and Bocquillon, C., 2007. Hydrological impact simulations of climate change on Lebanese coastal rivers /Simulations des impacts hydrologiques du changement climatique sur les fleuves côtiers Libanais. Hydrological Sciences Journal, 52(6), 11191133, doi:10.1623/hysj.52.6.1119.

Hublart, P., Ruelland, D., García de Cortázar-Atauri, I., Gascoin, S., Lhermitte, S., and Ibacache, A., 2016. Reliability of lumped hydrological modeling in a semi-arid mountainous catchment facing water-use changes. Hydrol. Earth Syst. Sci., 20, 3691-3717. doi:10.5194/hess-20-3691-2016.

Köeniger, P., Margane, A., 2014. Stable Isotope Investigations in the Jeita Spring catchment, Technical Cooperation Project Protection of Jeita Spring, BGR Technical Report No. 12. 56 pp.

Liston GE, Haehnel RB, Sturm M, Hiemstra CA, Berezovskaya S, Tabler RD. 2007. Simulating complex snow distributions in windy environments using SnowTran-3D. J. Glaciol. 53: 241–256.
Liston GE, Hiemstra CA. 2008. A simple data assimilation system for complex snow distributions (SnowAssim). J. Hydrometeorol. 9: 989–1004, doi: 10.1175/2008JHM871.1.
Liston GE, Mernild SH. 2012. Greenland freshwater runoff. Part I: a runoff routing model for glaciated and non-glaciated landscapes (HydroFlow). J. Clim. 25(17): 5997–6014.
Liston GE, Sturm M. 1998. A snow-transport model for complex terrain. J. Glaciol. 44: 498–516.
Liston GE, Sturm M. 2002.Winter precipitation patterns in Arctic Alaska determined from a blowing-snow model and snow depth observations. J. Hydrometeorol. 3: 646–659.
Liston GE, Winther J-G, Bruland O, Elvehøy H, Sand K. 1999. Below surface ice melt on the coastal Antarctic ice sheet. J. Glaciol. 45: 273–285, doi: 10.3189/002214399793377130.
Liston GE. 1995. Local advection of momentum, heat, and moisture during the melt of patchy snow covers. J. Appl.Meteorol. 34: 1705–1715, doi: 10.1175/1520-0450-34.7.1705.
Liston, G.E. and K. Elder. 2006a. A distributed snow-evolution modeling system (SnowModel). J. Hydromet., 7(6), 1259–1276.
Liston, G.E. and K. Elder. 2006b. A meteorological distribution system for high-resolution terrestrial modeling (MicroMet). J. Hydromet., 7(2), 217–234.
Margane, A., Schuler, P., Königer, P., Abi Rizk, J., Stoeckl, L., and Raad, R., 2013. Hydrogeology of the Groundwater Contribution Zone of Jeita Spring. Technical Cooperation Project Protection of Jeita Spring, BGR Technical Report No. 5, 317pp. Raifoun, Lebanon.
Mernild SH, Liston GE, Hasholt B, Knudsen NT. 2006. Snow distribution and melt modeling for Mittivakkat Glacier, Ammassalik Island, Southeast Greenland. J. Hydrometeorol. 7: 808–824, doi: 10.1175/JHM522.1.
Mernild, S., Liston, G., Hiemstra, C., Malmros, J., Yde, J., McPhee, J., 2016. The Andes Cordillera. Part I: snow distribution, properties, and trends (1979–2014). International Journal of Climatology.
Mhawej, M., Faour, G., Fayad, A., Shaban, A., 2014. Towards an enhanced method to map snow cover areas and derive snow-water equivalent in Lebanon. Journal of Hydrology 513, 274–282.
Molotch, N. P., and Meromy, L. 2014. Physiographic and climatic controls on snow cover persistence in the Sierra Nevada Mountains, Hydrological Processes, 28, 4573-4586.
National Council for Scientific Research (NCRS): Land-use land cover map of Lebanon, Beirut, Lebanon, available at: http://www.cnrs.edu.lb/ (last access: 9 January 2017), 2015.
Pomeroy, J.W. and Brun, E. 2001. Physical Properties of Snow. In: Snow Ecology. (Eds.) Jones, H.G., Pomeroy, J.W., Walker, D.A. and Hoham, R.W. 378 pp. Cambridge University Press.
Shaban, A., Faour, G., Khawlie, M. and Abdallah, C., 2004. Remote sensing application to estimate the volume of water in the form of snow on Mount Lebanon / Application de la télédétection à l'estimation du volume d'eau sous forme de neige sur le Mont Liban. Hydrological Sciences Journal, 49(4), doi:10.1623/hysj.49.4.643.54432.
Somma, J.; Drapeau, L.; Abou Chakra, C.; and El–Ali, T., 2014. Geomatics contributions to key indicators for estimation and monitoring of snow cover input to hydrogeological resources. AGU, Fall Meeting 2014, abstract #C43C–0404.
Sturm, M. and Wagner, A. M., 2010. Using repeated patterns in snow distribution modeling: An Arctic example, Water Resour. Res.,46, W12549, doi:10.1029/2010WR009434.
Telesca, L., Shaban, A., Gascoin, S., Darwich, T., Drapeau, L., Hage, M., Faour, G., 2014. Characterization of the time dynamics of monthly satellite snow cover data on Mountain Chains in Lebanon. Journal of Hydrology 519, 3214–3222.
UN Development Programme (UNDP), 2014. Assessment of Groundwater Resources of Lebanon. Beirut. www.lb.undp.org/ content/lebanon.
Viviroli, D., Dürr, H., Messerli, B., Meybeck, M., Weingartner, R., 2007. Mountains of the world, water towers for humanity: Typology, mapping, and global significance. Water Resources Research 43.

5 CONCLUSION AND FUTURE WORK

This work is motivated by the importance of snowmelt as an essential source of surface water and groundwater recharge in Lebanon. This thesis made use of an integrated approach by combining field measurements, automatic weather station observations, and energy balance modeling in order to understand the evolution of SWE and snowmelt in Mount-Lebanon. Solving the snow balance is the first step towards understanding the link between snowpack and groundwater recharge in Lebanon. In this thesis we tried to address the different science questions by (1) reviewing the major drivers controlling snow hydrologic processes in Mediterranean-like mountain regions (2) by quantitatively investigating the snowpack properties in the field, and (3) computing melt in three major basins of the windward snow dominated regions of Mount-Lebanon.

5.1 Conclusion

In chapter 2 we tried to address the first question related to "What are the major meteorological and physiographic factors controlling the snow processes in Mediterranean like regions and what is the fate of snowmelt in the hydrologic system of these regions?" we found that the snow distribution in Mediterranean mountain are characterized with high densification rates and intra-annual variability. Such variability is good as it allows the estimation of snow density and SWE with confidence using few years of HS and SWE measurements. Snow cover persistence is mainly controlled by precipitation and elevation and snowmelt is driven by radiative fluxes and heat flux contribution tend to increase during the melt season and during heat waves and rain-on-snow events. Despite snow importance in Mediterranean like mountain regions the proper investigation of snow dynamics and SWE is still hindered by the lack consistent ground observation especially in high-elevation regions. The spatial representation of SCA and SCD can be well achieved using remotely sensed snow data. Meanwhile the reconstruction of the SWE from SCA and melt models provides reasonable information that is suitable for hydrological applications. There is still a need to further collect snow data and finer and more accurate climate forcing dataset in Mediterranean snow-dominated with the notable exception of the Sierra Nevada in the USA, where the NASA's Airborne Snow Observatory now provides routinely SWE maps every two weeks in key watersheds. Finally, while the theory on the snowpack energy and mass balance is now well established the connections

between the snowpack and the water pathways in the critical zone (soil, groundwater) require further investigation.

In Chapter 3 we tried in answer the second question "What is the spatio-temporal variability of snow depth, snow density, and SWE at different elevation range (1300-2900 m a.s.l.), in the snow dominated regions of Mount-Lebanon?" In this chapter we presented a snow meteorological dataset for the first time in Lebanon (2011-2016). The dataset builds from previous joint efforts of CESBIO/CNRS-L/USJ and includes observations from three high elevation automatic weather stations (1840-2834 m a.s.l.). It was completed by snow course measurements conducted during this thesis, and post-processed MODIS snow products. The meteorological and snow observations include 30-min data of precipitation, temperature, humidity, wind speed and direction, shortwave solar radiation, snow depth, and snow albedo spanning over snow seasons between 2011 and 2016 (November-June). Snow course measurements includes SWE, HS, and snow density conducted over 30 different snow courses (1300-2900 m a.s.l.) and were collected over two snow seasons (2014-2016) with an average revisit time of 11.4 days. We found that snow is characterized with large snow height and SWE variances and a high density values. This suggests the importance of conducting field measurements with a bi-weekly revisit time. The variability of snow across different elevation ranges is also important given the different forcing variables affecting snow especially at mid-elevation altitudes. We also found that the relationship between snow height and snow density is specific to warm climate and may be classified as warm Mediterranean. Finally, this dataset was made to be fully compatible with the application of distributed energy-balance snowpack models. The dataset was deposited in the public domain to foster its application beyond this work.

In Chapter 4 we tried to quantify "To which extent can we accurately estimate the spatial distribution of the SWE at the daily timestep? and what is the contribution of snowmelt to the hydrologic budget in the three major basins of Mount-Lebanon?". We used the meteorological dataset presented in Chapter 3 as forcing for the energy balance SnowModel (Liston and Elder, 2006). The model was validated using the snow observations from AWS, snow course data and MODIS SCA. The model was run at 30-min time step over snow seasons (2013-2016) with a spatial resolution of 100 m over a domain of 150x120 km but we focused on the windward slope of Mount Lebanon for the validation. Model derived daily SCA (based on modeled SWE) showed good correlation (r=0.87) against MODIS SCA (MOD10A1). The correlation between

modeled HS and AWS HS showed good correlation (range for 3 stations) with an bias of !cm.day). The validation of modeled SWE, HS, and snow density against snow course data showed good correlation at point the scale. A good correlation was also found when comparing model averages across different elevation ranges (1300-2900 ma.s.l.). The estimated April 1st SWE for the snow dominated regions (above 1200 m) for the three basins (2013-2016) were 173 -421 mm w.e. (Abou Ali), 24-198 mm w.e. (Ibrahim), and 54-193 mm w.e. (Kelb). While the modeled values correlated better during season 2014-2015 the model underestimated snow density values in winter season 2015-2016 could be attributed to the rain on snow events which was not captured by the model. Understanding the evolution of snow density and the potential impact of rain on snow a potential field for future research. The comparison of modeled and observed snow albedo is also another potential field for future investigation given the difference in modeled albedo (entire snowpack) and bias related to the pyranometer representativeness of snow area as well as the dust on snow deposition not accounted by the model. While the model had an overall tendency to overestimate SWE and HS we suspect this is attributed to model precipitation forcing and the separation between rain and snow. The need for better separation between rain and snowfall is important especially in mid-elevation regions and given the specificity of the warm Mediterranean climate and the projected warming we believe this specific area of research is warranted future investigations.

5.2 Major contribution

The thesis as a whole represent a first attempt in (1) summarizing major climate forcing and snow hydrological processes in Mediterranean like regions and (2) to quantitatively assess snow hydrology and SWE evolution in the warm Mediterranean regions of Mount-Lebanon.

- This research provided a synthesis on snow hydrology in Mediterranean like climate region with emphasis on major climate forcing and topographic controls on the persistence of snowpack in in these regions.
- This thesis highlighted the importance of operational snow observation network and snow measurements and meteorological observations in the data-scarce snow dominated mountain basins with emphasis on the major windward basins of Mount-Lebanon.
- This work provided information on the seasonal spatial variability of HS, SWE, and snow density in the snow dominated region of Mount-Lebanon (elevation range 1300-2900 m a.s.l.). The publishing of AWS observations and snow course field

measurements is the first step towards operational snow hydrologic monitoring in this data scarce region.

- This work contributed to the knowledge on snow hydrology in the Mount-Lebanon by providing spatially distributed SWE estimates (at 100m pixel resolution) at 30-min temporal resolution. In contrast to existing knowledge these estimates are both spatially and temporally distributed. The developed model is also the first step towards linking snowmelt to groundwater karst system. Information on the SWE spatio-temporal variability will allow for the estimation of water availability during dry months.

5.3 Perspectives

- While the two years field measurements provide sound information on the snow variability across elevation gradient it is recommended that operational snow course measurement are carried on yearly basis to meet the recommended standard of 5-10 years (e.g., Mizukami and Perica, 2008). Despite their relatively high operational cost whether for the AWS maintenance or the operational cost for conducting field measurements they are of particular interest for Lebanon given the persistence in water shortage during summer time period and the projected impact of global warming on the mechanism of snow accumulation and melt. Long-term snow observatories are the focus of the International Network for Alpine Research Catchment Hydrology (INARCH). INARCH is a collaborative effort to provide measurement strategies, sharing data and tools to improve the understanding of hydrometeorological processes in mountains. As such, we suggest that our (albeit recent) Lebanese netwerok for snow observatoions (NSO) joins INARCH to increase its visibility and benefit from the most recent developments in future climate downscaling for example.

- Snow cover is one of the most sensitive variables of the hydrological cycle to air temperature, projected climate warming for the next decades are likely to have profound implications on the regional water resources, which are already under stress. The validated model provides a starting point for the use of reanalysis data and the the potential investigation of projected climate change scenarios on both snowpack dynamics and their induced impact on the hydrologic system of major river basins in Lebanon.

- One the main remaining challenge is to find an adequate method to simulate the water pathways from the snowmelt to the discharge at the karst outlets. . A first approach could be to feed a simple karst model such as KARSTMOD (Jourde et al., 2015) with our simulated snowmelt. There remains a long way (maybe another thesis?) to address this question with a proper quantification of the uncertainties given the complexity of the karst system.

5.4 References

Jourde, H., Mazzilli, N., Lecoq, N., Arfib, B., Bertin, D. 2015. KARSTMOD: A generic modular reservoir model dedicated to spring discharge modeling and hydrodynamic analysis in karst. In book: Hydrogeological and Environmental Investigations in Karst Systems, Publisher: Springer Berlin Heidelberg, Eds: Bartolomé A. and Carrasco, F., Durán, J.J. and Jiménez, P., and LaMoreaux, J.W., pp.339-344. DOI: 10.1007/978-3-642-17435-3_38.

Mizukami, N., Perica, S., 2008. Spatiotemporal Characteristics of Snowpack Density in the Mountainous Regions of the Western United States. Journal of Hydrometeorology 9, 1416–1426.

5.5 CONCLUSION ET PERSPECTIVES (VERSION FRANÇAISE)

V. 1. Conclusion

Ce travail de recherche est motivé par l'importance de la fonte des neiges pour la recharge des eaux souterraines au Liban. Cette thèse a fait appel à une approche intégrée en combinant les mesures de terrain, les observations automatiques de stations météorologiques et la modélisation afin de comprendre l'évolution du SWE et de la fonte des neiges sur le flanc ouest du Mont-Liban. Cela est une première étape vers la compréhension du lien entre le manteau neigeux et la production d'eau souterraine au Liban.

Dans le chapitre 2, nous avons tenté de répondre à la première question: 1- Quels sont les principaux facteurs météorologiques et physiographiques qui contrôlent les processus nivaux dans les régions méditerranéennes et quel est le rôle de la fonte des neiges dans l'hydrologie de ces régions?

La revue de la littérature suggère que le manteau neigeux méditerranéen se caractérise par des taux de densification élevés et une forte variabilité intra-annuelle. Une telle variabilité est permet l'estimation de la densité a partir de la profondeur de neige avec confiance en utilisant quelques années de mesures seulement. La persistance de la couverture neigeuse est principalement contrôlée par les précipitations et l'altitude tandis que la fonte est contrôlée par les flux radiatifs. La contribution du flux de chaleur sensible tend à augmenter pendant la saison de fonte et pendant les vagues de chaleur. Les événements pluie-sur-neige sont importants dans la dynamique de fonte. Malgré l'importance de la neige dans les régions méditerranéennes montagneuses, la caractérisation du SWE est encore entravée par l'absence d'observations in situ, en particulier dans les régions de haute-altitude. Si la représentation spatiale de la surface enneigée ou SCA est bien acquise par télédétection optique, le SWE reste inatteignable par télédétection satellite seulement. Pour cela, il est recommandé de combiner modélisation, SCA satellite et données in situ. Il est encore nécessaire de recueillir davantage de données climatiques dans les régions méditerranéennes de montagne, à

l'exception notable de la Sierra Nevada aux États-Unis, où l'observatoire aéroporté de la neige de la NASA fournit désormais des cartes SWE toutes les deux semaines de façon quasi opérationnelle pour les principaux bassins versants. Enfin, la théorie du bilan de masse et d'énergie est maintenant bien établie, mais les connexions entre le manteau neigeux et les chemins de l'eau dans la zone critique (sol, eaux souterraines) sont encore méconnus.

Dans le chapitre 3, nous avons essayé de répondre à la deuxième question: "2- Quelle est la variabilité spatio-temporelle du manteau neigeux à différentes altitude (1300-2900 m a.s.l.) sur le versant ouest du Mont-Liban?" Dans ce chapitre, nous avons présenté pour la première fois un ensemble de données météorologiques pour l'étude de la neige au Liban (2011-2016). L'ensemble de données est le résultat des efforts conjugués du CESBIO / CNRS-L / USJ et comprend les données de trois stations météorologiques automatiques d'altitude (1840-2834 m a.s.l.). Elle a été complétée par des parcours nivométriques effectuées au cours de cette thèse, et les données de SCA MODIS. Les données des stations sont des données au pas de temps 30 minutes des précipitations, température et humidité de l'air, vitesse et la direction du vent, rayonnement solaire, hauteur de neige et albédo pour les saisons nivales entre 2011 et 2016 (novembre-juin), mais il y a beaucoup de lacunes avant 2013. Les mesures de parcours nivométrique incluent le SWE, HS et densité sur 30 parcours différents (1300-2900 m a.s.l.) pendant deux saisons (2014-2016) avec un temps moyen de revisite de 11,4 jours. Nous avons constaté une grande variabilité temporelle dans la hauteur de neige et le SWE et des valeurs élevées densité. Cela montre l'importance de procéder à des mesures de terrain avec une périodicité bi-hebdomadaire. La variabilité spatiale de ces mesures entre les différentes tranches d'altitude est également importante. Nous avons constaté une corrélation entre la hauteur de neige et la densité caractéristique d'un climat méditerranéen chaud. Enfin, ce jeu de données a été conçu pour être pleinement compatible avec l'application des modèles distribués de bilan d'énergie du manteau neigeux. L'ensemble de données a été déposé dans le domaine public pour favoriser sa diffusion au-delà de ce travail.

Dans le chapitre 4, nous avons essayé de répondre à: “Dans quelle mesure pouvons-nous estimer avec précision la répartition spatiale du SWE au pas de temps journalier à une résolution spatiale fine (100 m)?”. Nous avons utilisé l'ensemble de données météorologiques présentées au chapitre 3 pour forcer le modèle de bilan énergétique et d’évolution du manteau neigeux SnowModel (Liston et Elder, 2006). Le modèle a été validé à l'aide des observations continues de hauteur de neige aux stations, des données des parcours nivométriques, et de SCA MODIS. Le modèle a été exécuté au pas de temps de 30 minutes sur les saisons de neige 2013-2016 à une résolution spatiale de 100 m sur un domaine de 150x120 km, mais nous nous sommes concentrés pour la validation sur la partie ouest du Mont-Liban qui nous intéresse. La surface enneigée simulée est bien corrélée avec les observations MODIS ($r = 0.87$). La comparaison de HS modélisé et HS observé aux stations est globalement satisfaisante. Les simulations de SWE, HS et densité dans les secteurs couverts par les parcours nivométriques est également encourageante. Nous avons estimé que le SWE du premier avril variait entre 173 et 421 mm w.e. (Abou Ali), 24-198 mm w.e. (Ibrahim), and 54-193 mm w.e. (Kelb). Les simulations sont meilleures pendant la saison 2014-2015. Le modèle sous-estime la densité de neige pendant la saison hivernale 2015-2016, ce qui peut être attribué à un événement de pluie sur neige qui n'a pas été capturé par le modèle.

V. 2. Résumé des contributions de ce travail

Cette thèse a fourni une synthèse sur l'hydrologie nivale sous climat méditerranéen, en mettant l'accent sur les facteurs climatiques et topographiques.

Nous avons décrit et mis en évidence l'importance d’un réseau d'observation de la neige et des conditions météorologiques dans les bassins montagneux du Mont-Liban où les données sont rares (altitude entre 1300-2900 m a.s.l.). La publication des données est la première étape vers une recherche plus poussée et un suivi plus opérationnel de la ressource nivale.

Enfin nous avons simulé pour la première fois le SWE sur le Mont-Liban. Contrairement aux études précédentes, ces estimations sont spatialement et temporellement distribuées. Le modèle développé est une première étape vers une représentation intégrée du système hydrologique depuis le manteau neigeux jusqu'au système karstique des eaux souterraines qui permettra de mieux connaitre la disponibilité de l'eau pendant les mois secs en temps présent et sous climat futur.

V. 3. Perspectives

Il est recommandé de poursuivre les mesures afin de respecter la norme recommandée de 5 à 10 ans (Mizukami et Perica, 2008 Meromy et al., 2013). Malgré leur coût relativement élevé, les stations ou les mesures sur le terrain présentent un intérêt particulier pour le Liban étant donné la persistance de la pénurie d'eau pendant la période estivale et l'impact du réchauffement climatique attendu sur l'accumulation et la fonte. Mieux comprendre l'effet de la pluie sur l'évolution de la densité de la neige est un sujet de recherche futur important. Une évaluation plus poussée de l'albédo modélisé est également une voie de recherche importante car le dépôt de poussières n'a pas été pris en compte ; mais il faudra faire attention aux biais d'observations liés à la position du pyranomètre. Enfin, une meilleure séparation entre la pluie et les chutes de neige est importante, surtout dans les régions de moyenne altitude. Compte tenu de la spécificité du climat méditerranéen et du réchauffement attendu, nous croyons que ce domaine mérite une attention particulière. Les observatoires hydroclimatiques de montagne l'objet du Réseau international pour l'hydrologie des bassins de recherche alpins (INARCH). INARCH (http://www.usask.ca/inarch/) est un effort collaboratif pour fournir une stratégie cohérente de mesure, partager les données et les outils pour améliorer la compréhension des processus hydrométéorologiques en montagne. Nous suggérons que notre observatoire de la neige libanais (bien que récent) se joigne à INARCH pour accroître sa visibilité et bénéficier des développements les plus récents dans le domaine de la désagrégation des modèle climatiques.

La neige étant une des variables les plus sensibles du cycle hydrologique à la température de l'air, le réchauffement climatique projeté pour les prochaines décennies

est susceptible d'avoir des implications profondes sur les ressources en eau régionales qui sont déjà surexploitées. Le modèle validé présenté dans cette thèse fournit un point de départ pour l'utilisation des données de réanalyse climatiques et des scénarios de changement climatique futur afin d'évaluer à plus long terme la vulnérabilité des systèmes hydrologiques libanais.

Pour cela, le défi principal reste de trouver une méthode adéquate pour simuler les transferts d'eau de fonte dans le karst. Une première approche pourrait être d'alimenter un modèle karstique simple tel que KARSTMOD avec notre fonte de neige simulée. Il reste un long chemin (peut-être une autre thèse?) pour aborder cette question, notamment pour quantifier les incertitudes étant donné la complexité du système karstique.

APPENDIX A1 - TOWARDS AN ENHANCED METHOD TO MAP SNOW COVER AREAS AND DERIVE SNOW-WATER EQUIVALENT IN LEBANON

APPENDIX A2 - METADATA FOR THE ARTICLES USED IN THE REVIEW

APPENDIX A3 - LIST OF DIFFERENT INDICATORS THAT CORRESPOND TO KEY RESEARCH AREAS

Journal of Hydrology 513 (2014) 274–282

Contents lists available at ScienceDirect

Journal of Hydrology

journal homepage: www.elsevier.com/locate/jhydrol

Towards an enhanced method to map snow cover areas and derive snow-water equivalent in Lebanon

Mario Mhawej *, Ghaleb Faour, Abbas Fayad, Amin Shaban

National Centre for Scientific Research, Beirut, Lebanon

ARTICLE INFO

Article history:
Received 17 August 2013
Received in revised form 9 February 2014
Accepted 25 March 2014
Available online 4 April 2014
This manuscript was handled by Andras Bardossy, Editor-in-Chief, with the assistance of Sheng Yue, Associate Editor

Keywords:
Snow water equivalent
MODIS
AMSR-E
New combing method
Water cycle
Lebanon

SUMMARY

Snow cover contributes to the definition of the hydrologic system of most River Basins in Lebanon. Despite its importance little is known about the proper quantification of snow cover extent and snow water equivalent (SWE), as well as the snow contribution to the hydrologic budget at the national scale. By taking advantage of the moderate-resolution optical sensors (MODIS) from both Terra and Aqua satellites it was possible to generate enhanced, eight-days, Terra-Aqua Combined (TAC) product set at a spatial resolution of 500 m. An innovative method that combines the AMSR-E SWE data (~25 km spatial resolution) and the enhanced TAC dataset was developed to derive a SWE product at a sub-pixel spatial resolution of 500 m. Both the enhanced TAC and the downscaled SWE were developed for the entire Lebanon. The enhanced TAC dataset was found to reduce cloud cover area by ~13% when compared to the original MOD10A2 dataset. Snow cover area was validated against ETM+ data and the SWE was assessed against in situ measurements; the overall accuracy of the snow cover maps was ~85%, whereas, the comparison between ground points measured and remotely sensed derived SWE indicates a poor correlation. This study concluded that while the use of TAC is well suited for the assessment of snow cover extent nationwide, the derived SWE from AMSR-E is not fully deployable in Lebanon. Meanwhile, a snow melt method that takes advantage from the remotely sensed SWE is needed to better achieve results suitable for hydrologic studies.

1. Introduction

The Lebanese mountains chains (i.e. Mount and the Anti-Lebanon) play a unique role in the distribution of rainfall and snow and eventually controlling the hydrologic behaviors of most river systems. The country's climate is characterized by the prevailing Mediterranean in the coastal and mountain areas and semi-arid to arid in the inland areas. The climate system and the topography of the country results in high differences and seasonal variability of precipitation and temperature. Precipitation ranges from 300 mm/year in the inland arid areas to more than 1200 mm/year over Mount Lebanon. Snow is more frequent at altitudes higher than 1200 m and has an estimated annual snowpack volume between 1200 and 2000 MCM/year (~30% to 40% of the annual precipitation) (Shaban et al., 2004; Aouad Rizk et al., 2005).

Snowmelt which usually occurs during spring, at the time where there is little contribution from rainfall, has great influence on the observed spring and river discharges. Despite their impact on the hydrologic regimes of most rivers, little is known about the snowpack dynamics in Lebanon. Same applies to snow accumulation and melting.

Remote sensing technology provides a mean to acquire information on the spatial distribution and thickness of snow cover at a relatively low cost. Satellite remote sensing primary data products used in this study are the snow cover area (SCA) and the snow water equivalent (SWE). Optical sensors are being used to derive accurate SCA and snow extent estimates at higher spatial resolution. The advantage of these sensors is attributed to the fact that snow contrasts greatly with its surroundings due to its high albedo (Gafurov and Bardossy, 2009). Despite their advantage, optical sensors such as MODIS and SPOT observations are limited to day time and are usually subject to cloud cover. Both snow cover area and snow extent lack the information about snow depth or water volume contained in the snowpack. In contrast to the optical sensors, passive microwave satellite remote sensors are known to provide snow thickness where there is no access to in situ snow depth measurements (Foster et al., 2005; Gao et al., 2010). These sensors are well known to provide SWE estimates, at regional scale, due to the coarser resolution offered (Clifford, 2010).

Previous researches suggest that remotely sensed SCA, snow extent, and SWE can enhance our understanding of snowpack

* Corresponding author. Tel.: +961 3 048958.
E-mail addresses: mario.mhawej@gmail.com (M. Mhawej), gfaour@cnrs.edu.lb (G. Faour), abbasfayad@yahoo.com (A. Fayad), geoamin@gmail.com (A. Shaban).

http://dx.doi.org/10.1016/j.jhydrol.2014.03.058
0022-1694/

distribution and improve the quantification of available water resources in remote areas (Yang et al., 2009). SCA has been successfully used in many studies to model snowmelt at the basin scale (Immerzeel et al., 2009; Powel et al., 2011; Gurung et al., 2011). The successful use of passive microwave SWE is usually subject to the study area topography and roughness and the snowpack depth (Andreadis and Lettenmaier, 2006).

Many literatures addressed the limitation found in the remotely derived SCA and SWE data products. Main focus areas, in the optical domain, concentrated on finding new algorithm to enhance the accuracy of snow products. For instance, Sirguey et al. (2009) developed a new methodology for the monitoring of the snow cover from MODIS NDSI data. Ault et al. (2006) and Gao et al. (2010) investigated new methods to enhance the accuracy of the MODIS data by minimizing cloud contamination. The combination between the two MODIS products Terra and Aqua was found to be useful in decreasing cloud effects (Xie et al., 2009). Studies in the microwave domain focused on finding new ways to improve SWE derived from the AMSR-E sensor using ground SWE measurements (Derksen, 2008; Langlois et al., 2008). Other studies focused on comparing and/or combining data from the AMSR-E with data from other sensors such as the SSM/I (Pulliainen, 2006; Vuyovich and Jacobs, 2011).

In order to better enhance the spatial resolution of SWE, different studies focused on integrating the optical and passive microwave sensors (Liang et al., 2008; Gao et al., 2010). Gao et al. (2010) used an enhanced method in order to derive cloud-free snow cover from the Terra-Aqua MODIS data and then developed a methodology in order to derive sub-pixel SWE data from the combined AMSR-E and MODIS systems.

This paper focuses on applying an algorithm for combining the Terra-Aqua MODIS data products into a single TAC (i.e. Terra-Aqua Combined) dataset. The development of TAC relies on methodologies such as the one used by Liang et al. (2008) and Gao et al. (2010). The new TAC product is validated against snow data product derived from Landsat ETM+. A new algorithm is developed in order to downscale the AMSR-E data using the MODIS newly derived TAC dataset. In contrast to the approach developed by Gao et al. (2010) where the AMSR-E data were equally distributed over the MODIS data, the proposed methodology accounts for statistical distribution of snow using a weighting factor based on the number of snow day(s) per year. This combination is sought to provide an enhanced dataset for Lebanon by combining snow cover area, snow extent, and SWE at a downscaled spatial resolution of 500 m. In situ measurements for snow depth and density are used in order to evaluate the accuracy of the sub-pixel derived SWE.

2. Study area

Lebanon, with an area of about 10,400 km^2, receives between 800 and 1500 mm of precipitation each year. The climate variability is highly influenced by the orographic effect of the country's topography and the prevailing Mediterranean climate which limits precipitation to the winter season. Lebanon is divided into four distinct physiographic regions – the coastal zone, the Mount Lebanon, the Bekaa Plain and the Anti-Lebanon. Fig. 1 illustrates the country's topography were the gradual increase in altitude is known to produce colder winters, increased precipitation and snow fall (UNEP, 2007). Snow cover remains for more than four months on mountain crests. Around 25% of the country's total area is covered by snow each year (Shaban et al., 2004). The snow cover area contributes to the feeding of 15 main river basin systems and more than 2000 springs. Snow also contributes to groundwater recharge via a number of aquiferous formations and karstic galleries (Shaban, 2010).

3. Datasets

Four data sets are used in this study. (i) The eight-day MODIS snow products of MOD10A2 (Terra) and MYD10A2 (Aqua) at a spatial resolution of 500 m are used to extract cloud free TAC product; (ii) the Enhanced Landsat Thematic Mapper-plus (ETM+) data with 30 m spatial resolution is used to validate the TAC algorithm; (iii) the AMSR-E/Aqua 5-day L3 SWE at 25 km spatial resolution is used to extract SWE and the combined MODIS and AMSR-E data are used to generate the SWE at sub-pixel scale; and (iv) in situ snow data are used to validate the SWE values.

3.1. MODIS snow cover products

The MODIS sensor is operational onboard two Earth Observation System (EOS) satellites, Terra and Aqua. The MODIS snow and ice products are being derived and provided through the Distributed Active Archive Center (DAAC) of the National Snow and Ice Data Center (NSIDC) since September 2000 for Terra and July 2002 for Aqua. The MOD10A2 and MYD10A2 8-Day L3 snow cover data consist of 1200 km by 1200 km tiles at a spatial resolution of 500 m gridded using a sinusoidal map projection. Data sets contain a data fields for maximum snow cover extent over an eight-day compositing period and a chronology of snow occurrence observations in compressed Hierarchical Data Format-Earth Observing System (HDF-EOS) format. The MODIS snow cover data for both sensors is based on a snow mapping algorithm that make use of the Normalized Difference Snow Index (NDSI) (Hall and Salomonso, 2004). MODIS snow cover images are coded raster. The maximum snow extent coded integer values include: 0 (missing data), 1 (no decision), 11 (night), 25 (land – no snow detected), 37 (lakes – inland water), 39 (ocean), 50 (cloud), 100 (lake ice), 200 (snow), 254 (saturated MODIS sensor detector), and 255 (fill – no data expected for pixel) (Hall and Salomonso, 2004).

3.2. AMSR-E SWE products

The AMSR-E instrument is a multi-frequency, dual-polarized passive microwave radiometer launched on onboard the NASA Earth Observing System (EOS) Aqua satellite in May 2002. AMSR-E provides global measurements of terrestrial, oceanic, and atmospheric variables for the investigation of water and energy cycles. The algorithms for the retrieval of SWE have been developed and improved by Tong and Velicogna (2010) and are based on the brightness temperature (Tb) difference between channels due to the attenuation of snow on the microwave radiation from the snow and underlying ground. The AMSR-E/Aqua 5-day L3 Global SWE EASE-Grid data were downloaded from the National Snow and Ice Data Center (NSIDC) in Boulder, Colorado (ftp://sidads.colorado.edu/pub/DATASETS/brightness-temperatures/polar-stereo/tools/). These Level-3 snow water equivalent (SWE) data sets contain SWE data and quality assurance flags mapped at 25 km Equal-Area Scalable Earth Grids (EASE-Grids) and covers the time period between June 2002 and October 2011. Data are stored in Hierarchical Data Format – Earth Observing System (HDF-EOS) format. The pixel values for SWE include: 0–240 (SWE values divided by 2 in (mm)), 247 (incorrect spacecraft altitude), 248 (off-earth), 252 (land or snow impossible), 253 (ice sheet), 254 (water), and 255 (missing data) (Tedesco et al., 2004).

3.3. Landsat ETM+ satellite data

Eighteen multispectral images were acquired from the Enhanced Landsat Thematic Mapper-plus (ETM+) instrument, avail-

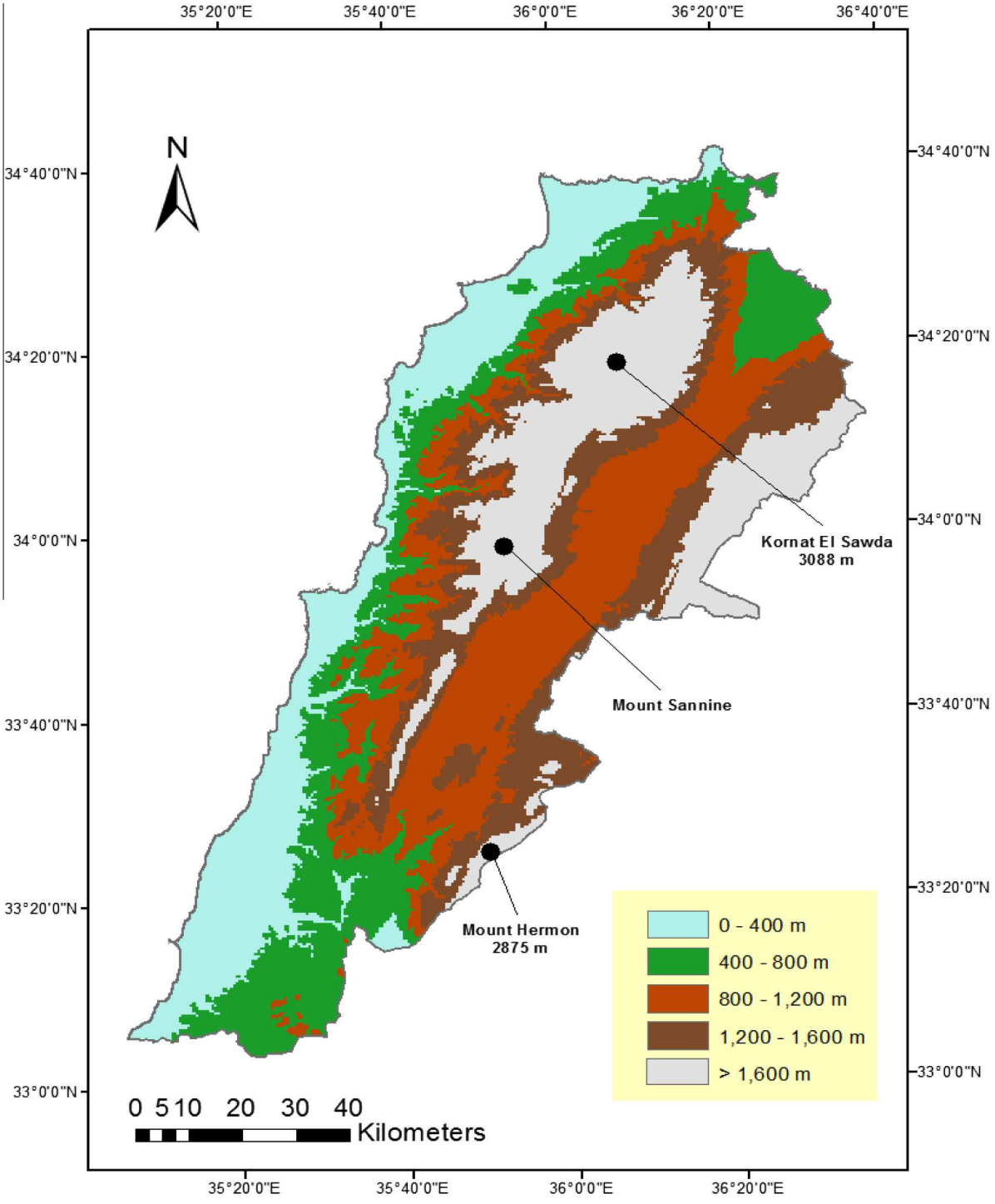

Fig. 1. Zonal classification of elevations in Lebanon.

able free of charge from the landsat.usgs.gov website. Each image contains eight bands representing one panchromatic band at 15 m spatial resolution, six bands covering the visible and short-wave infrared regions at 30 m spatial resolution, and one thermal infrared band at 60 m spatial resolution. Table 1 lists the ETM+ images that are used in this study along with their acquisition date. Snow cover is derived using Band 2 and Band 5 mainly because the snow reflects maximum in the visible part of the spectrum (i.e. Band 2 with wavelength centered at 0.56 μm) and has a reflectance near zero in the short-wave infrared part of the spectrum (i.e. band 5 with wavelength centered at 1.65 μm).

3.4. Field data

In situ snow depths and SWE calculations and were carried at seven different sites. To measure the depth of snow, a thin-walled tube with a sharp leading edge and a known diameter (10 cm) was

Table 1
Validation of MODIS against high spatial resolution Landsat ETM+ data.

Date	Snow area (landsat ETM+) in km^2	Snow area (MODIS) in km^2	Aerial difference (%)
December 26, 2004	1348	1358	0.8
January 11, 2005	1421	1439	1.2
January 27, 2005	1785	1666	−6.7
February 12, 2005	2038	1683	−17.4
March 16, 2005	735	455	−37.9
January 30, 2006	1388	1170	−15.7
January 1, 2007	1464	1559	6.5
January 17, 2007	1311	1162	−11.4
March 6, 2007	715	390	−45.5
March 22, 2007	582	305	−47.6
January 20, 2008	829	853	2.9
February 5, 2008	2964	2809	−5.2
February 21, 2008	3061	2696	−11.9
January 22, 2009	734	632	−13.9
February 7, 2009	492	333	−32.4
November 6, 2009	243	225	−7.4
January 12, 2011	606	535	−11.7
February 13, 2011	366	292	−20.1
		Overall aerial difference	−15.2

used. For each sample, the volume of snow is measured and the SWE is derived as function of the melted snow volume.

4. Methodology

The proposed methodology to combine MODIS and AMSR-E snow products includes four steps. The overall methodology and processing algorithms are provided in Fig. 2. The first step covered the preprocessing and the conversion of the original MODIS snow products into unified snow maps and then interpolating the AMSR-E data from the original 5-day to 8-day composite in order to time-overlay with the MODIS products. The second step consisted of combining the weekly Terra and Aqua MODIS snow cover product to generate the combined TAC snow cover products that maximizes snow extent and limits cloud coverage. The third step involved the calculation of the average snowing days per year from the snow cover dataset. The last step focused on implementing an algorithm to combine the MODIS and AMSR-E data set in order to downscale the raw AMSR-E SWE to a 500 m sub-pixel spatial resolution.

4.1. Data preprocessing

Eight day maximum snow extent and eight day snow cover variables were extracted from the MOD10A2 and MYD10A2 products. Daily snow cover was retrieved from the coded 8-day snow data. Actually, each daily snow cover image was coded in eight-bit ordered from right to left, meaning that the corresponding bit is set to on whenever snow was detected on that day (i.e. across a byte the bit 0 corresponds to day 1, bit 1 corresponds to day 2... and bit 7 to day 8 in the eight-day period). Information retrieval was achieved automatically using scripts developed under both MATLAB and ERDAS Imagine. To reduce the noise in the AMSR-E time series data median filter was applied. This data was then converted from five to eight-days using a spline interpolation (de Boor, 1978).

4.2. Generating the Terra Aqua Combined (TAC)

The development of the Terra Aqua Combined (TAC) was achieved by combining the two MODIS products MOD10A2 and MYD10A2 using the maximum snow coded integer values. Priority was assigned to the MOD10A2 obtained from the Terra Satellite namely because Terra snow product had a slightly better accuracy than the Aqua snow product (Xie et al., 2009). The new generated data set is a TAC snow cover time series extending from 2002 to 2012 at 500 m spatial resolution.

4.3. Mapping average snowy days per year

The TAC eight-day snow cover dataset was used to generate the yearly composite that represents the Snow Day per Year (SDY) product. These maps indicate the number of snow day(s) per year for each pixel.

4.4. Generating sub-pixel SWE data from the combined AMSR-E and TAC

In order to generate SWE at a 500 m spatial resolution MODIS and AMSR-E datasets were combined using spatial distribution in function of the probability and occurrence of days with snow cover over the entire year. The probability distribution is based on using the AMSR-E as a reference grid, and where Lebanon is represented by 56 pixels. The TAC was subdivided into 56 zones representing the same spatial extent of the AMSR-E grids. Since MODIS data is available at 500 m spatial resolution each AMSR-E pixel was overlaid by 2500 pixel representing the snow cover extent. The general equation is given as:

$$\mathrm{SWEsp} = \begin{cases} 0 & \text{if MODIS SCA} = 0 \\ \frac{2 * \mathrm{SWE}_{\mathrm{AMSR\text{-}E}} * \mathrm{SDY} * 2500}{\mathrm{SDT}} & \text{else} \end{cases}$$

where $\mathrm{SWE}_{\mathrm{AMSR\text{-}E}}$ is the AMSR-E SWE value, SDY is the average snow days per year for each MODIS pixel, and SDT is the sum of total snowing days per year combined for each AMSR-E pixel.

For each MODIS zone the sum of pixels with snow cover was calculated first, the outcome is a "Snow Day Total" map. The probability of the occurrence of snowy days for each pixel is then calculated by dividing the SDY by SDT. Noting that while the AMSR-E map gives the mean value of snow water equivalent in this pixel, there is 2500 values in MODIS for each AMSR-E pixel. Each AMSR-E SWE sub-pixel was derived by multiplying the pixel probability by the AMSR-E SWE at 25 km. Fig. 3 illustrates the comparison between probability distribution and mean value downscaling of AMSR-E data. The result is a 10 years (2002–2011), eight-days, SWE data set at a spatial resolution of 500 m.

5. Results

5.1. Accuracy assessment

5.1.1. Validation of TAC product

Fig. 4 shows the raw MOD10A2 product, which is usually associated with cloud contaminated areas and the derived TAC product for the year 2010. It can be easily distinguished how the accuracy increased between the MOD10A2 and the derived TAC product. Assessment revealed that the TAC dataset had ~13% reduced cloud coverage when compared to the MOD10A2 dataset (average over the time period between 2002 and 2011). In December 2010, the maximal cloud reduction was estimated at ~30%.

Snow surface derived for the high resolution ETM+ data at a spatial resolution of 30 m was compared to the derived TAC products. The result of the comparison is provided in Table 1. The comparison shows 98.5% correlation between the two products (i.e. ETM+ and TAC). The PBIAS revealed that the TAC product was underestimating the snow cover extent by 12.9% when compared to the ETM+ dataset. The aerial difference between the two datasets was estimated at ~15% with an STD of 20%. The results also

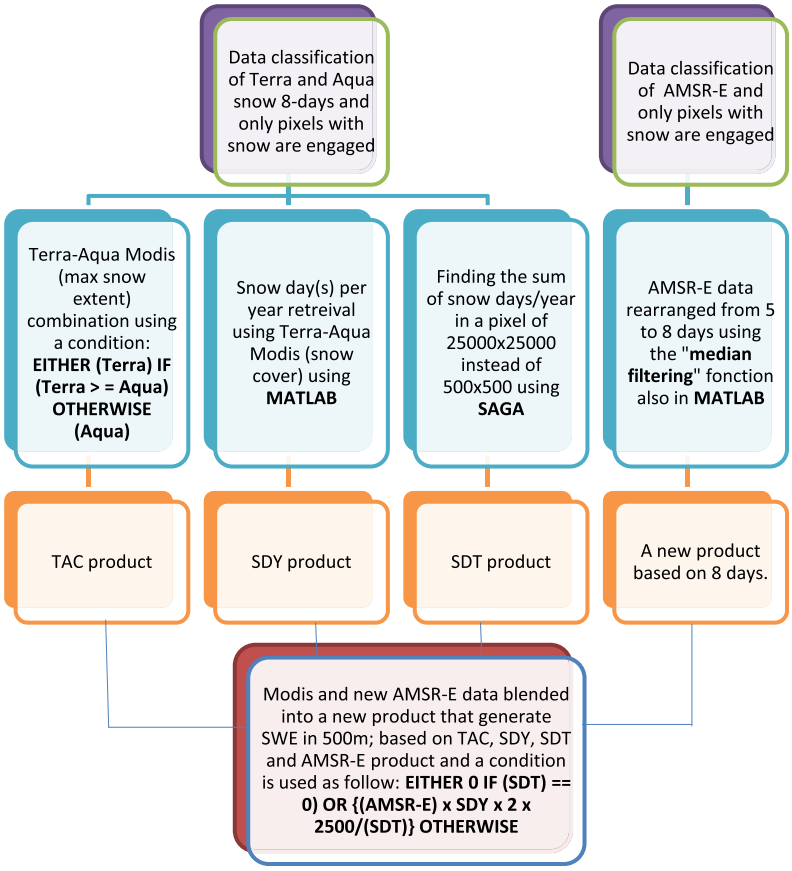

Fig. 2. Methodology for the derivation of TAC and sub-pixel SWE.

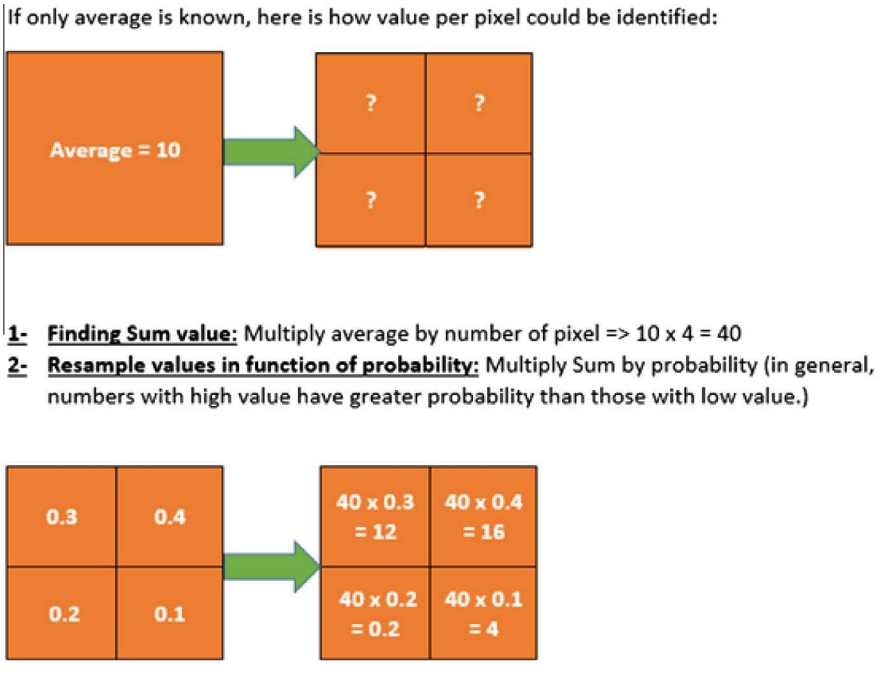

Fig. 3. Sub-pixel AMSR-E data extraction using probability distribution.

indicated that the TAC products had a better accuracy when the snow extent was large enough. In contrast when snow cover became scarce the accuracy of the TAC product reduced. This is justified by the fact that in sparse snow areas the probability of a pixel to be mapped as snow at a spatial resolution of 500 m (TAC) is less than that of a pixel mapped at a spatial resolution of 30 m (ETM+).

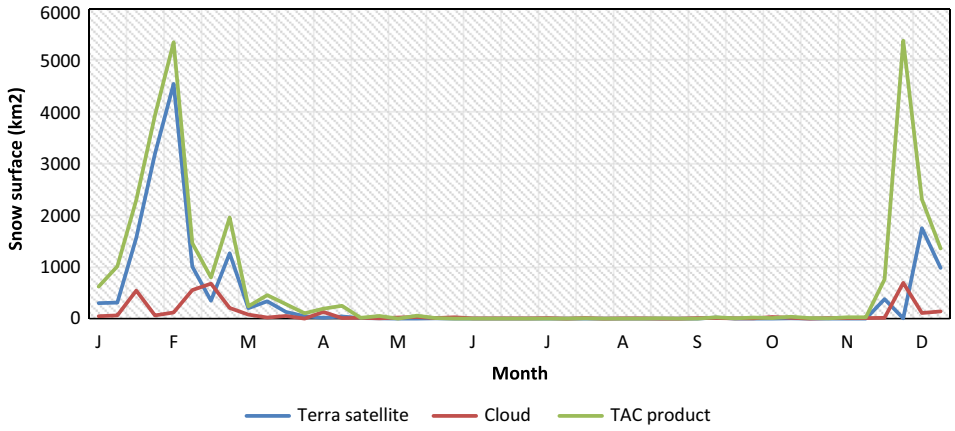

Fig. 4. Comparison between TAC snow, MOD10A2 raw data, and cloudextent in 2010.

5.1.2. Validation of the combined AMSR-E/TAC new product

While producing the eight-day AMSR-E dataset from the original five-day SWE using the "spline" function part of Matlab 2012, we noticed to have noisy values. As mentioned before, in order to minimize the noise, a "Median Filtering" was used. Fig. 5 shows the evaluation of four filters. It was obvious that level 5 is the best choice and was consequently used to filter the eight-day AMSR-E data.

Field measurements of SWE were carried over seven different locations in order to validate the eight-days AMSR-E SWE dataset. Results indicated poor correlation between AMSR-E SWE and ground measurements and a large PBIAS. The great variability between these observations is attributed to the fact that field measures were not fully representative of the topography and the extent of the study area; this conforms to other studies in the field (Gao et al., 2010). The retrieved SWE from regional scale passive microwave systems such as the AMSR-E is associated with the spatial heterogeneity, snow water content, and roughness which highly impacts the polarization effect and thus leads to increased bias. It is recommended that further studies investigate the impact of these factors in order to better understand their impact of the predicted SWE. Accordingly, it is difficult to directly make use of the SWE from AMSR-E. More ground sampling points and a coupled snow model are compulsory in order to capture snow accumulation.

5.2. Spatial and temporal variability of snow in Lebanon

Fig. 6 shows that the snow extent over the Lebanese mountains would remain for a maximum of ~89 days per year (average over 13 years between 2000 and 2012). Results revealed great variability in the spatial extent in function of the region. Table 2 summarizes snow cover extent by region calculated as the average over the time period between 2002 and 2012. It is obvious that at lower altitudes, between 0 and 500 m, the average snowing days is ~1 day per year. This value is more frequent in the coastal zones, the Northeast of Bekaa, and the South. Average snowing days at altitudes between 2500 and 3000 m was estimated at 65 days per year. Average snowing days reached their peaks over the mountain chains, namely at the Kornat El Sawda (3088 m). Snowing days were found to decrease gradually as the altitude declines on either sides of this peak – a clear example is found at the mountain of Jabal El Sheikh in the south of Lebanon. It was also evident that the mountain chains in Lebanon receive the largest amount of snow. Fig. 7 illustrates the snow cover extent with similar patterns over the Mount-Lebanon and the Anti-Lebanon ranges. The number of snowing days also dependent on the type of snow storm including its direction and source. Thus, tropical storms are often associated with large area coverage – for instance the snow storm during winter season 2001–2002. In contrast, regional snow storms are usually associated with short snowing days and less snow coverage.

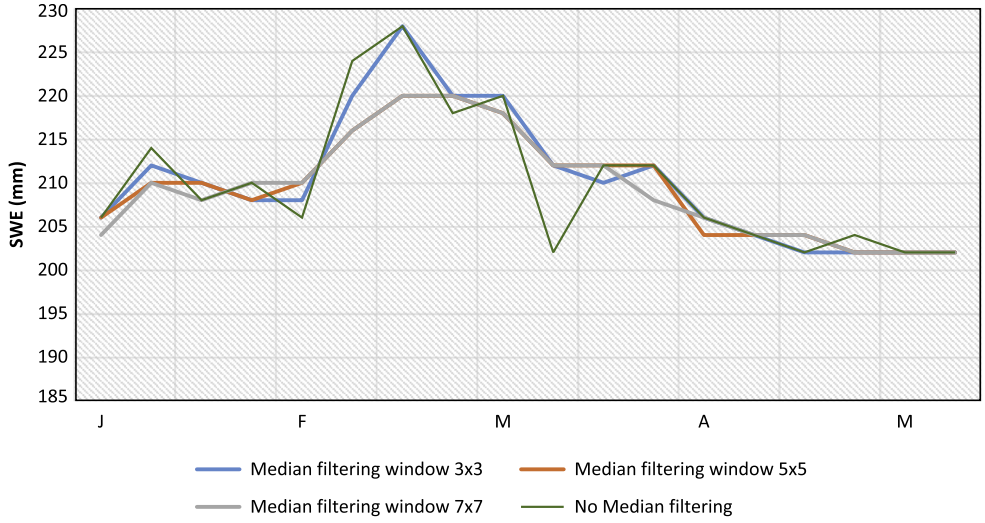

Fig. 5. Comparison between median filtered SWE and raw SWE in 2010.

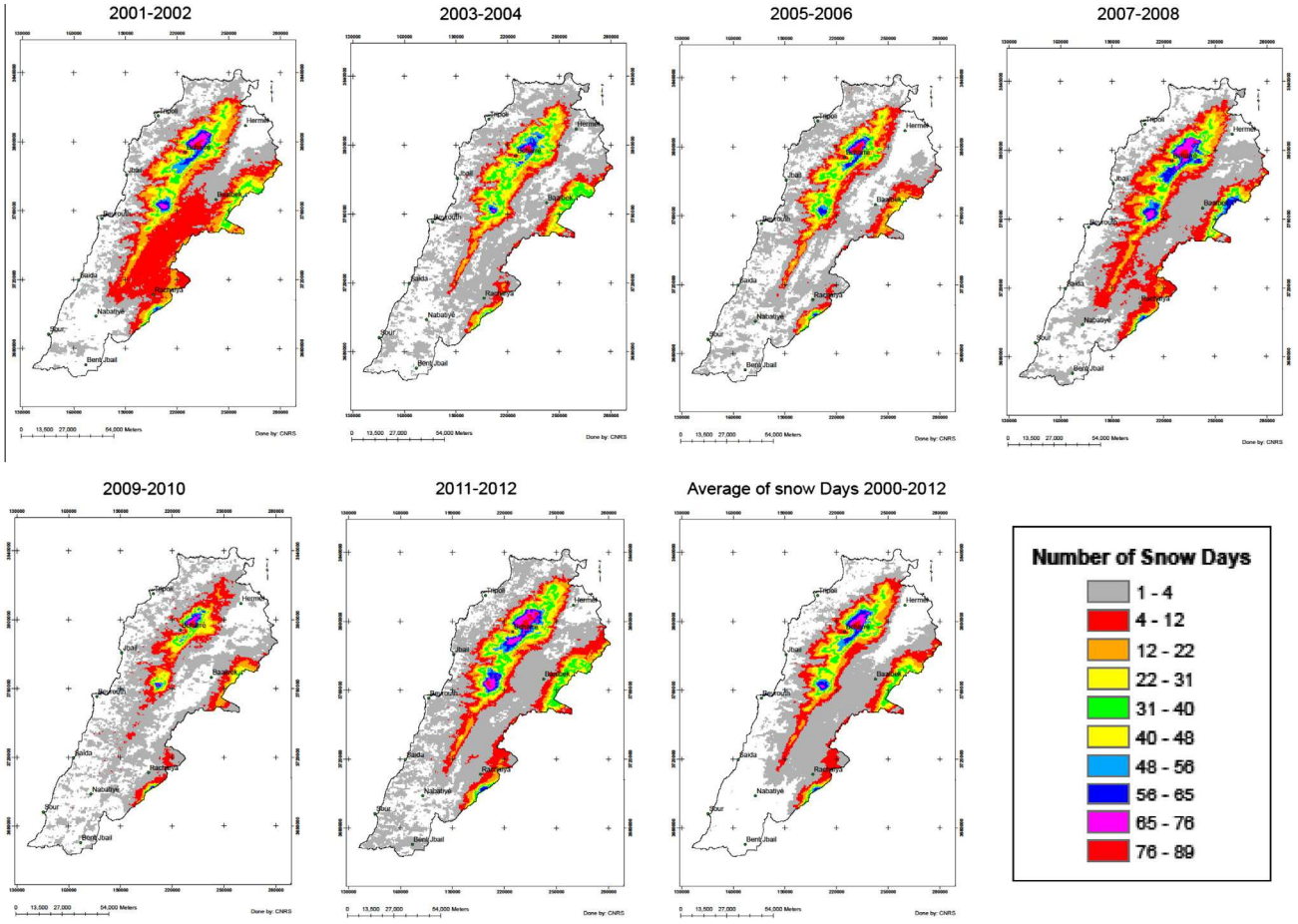

Fig. 6. Average number of snow day(s) per year between 2000 and 2012.

Table 2
Average of snow day per year considering altitude taken during twelve years, from year 2000 till 2012.

Altitude in meters	Number of day(s)
<500	<1
500–1000	1–2
1000–1500	3–4
1500–2000	15–16
2000–2500	37–38
>2500	65–66

Fig. 8 shows that the year 2004 had the largest snow surface area estimated at 1400 km^2. Meanwhile, the year 2000 had the smallest snow cover area estimated at ~550 km^2.

Fig. 9 illustrates snow fall occurrence on a monthly time scale. It was clear that snow usually occurs between October and June. The maximum snow coverage increases during the winter season. Snow cover peaks in early February (maximum extent ~3000 km^2) and usually remains to the middle of the spring season and in less scenarios until mid-June.

Fig. 10 shows the snow contribution to the overall hydrologic budget (i.e. inputs to surface runoff and groundwater recharge) and was compared to the total volume of precipitation between

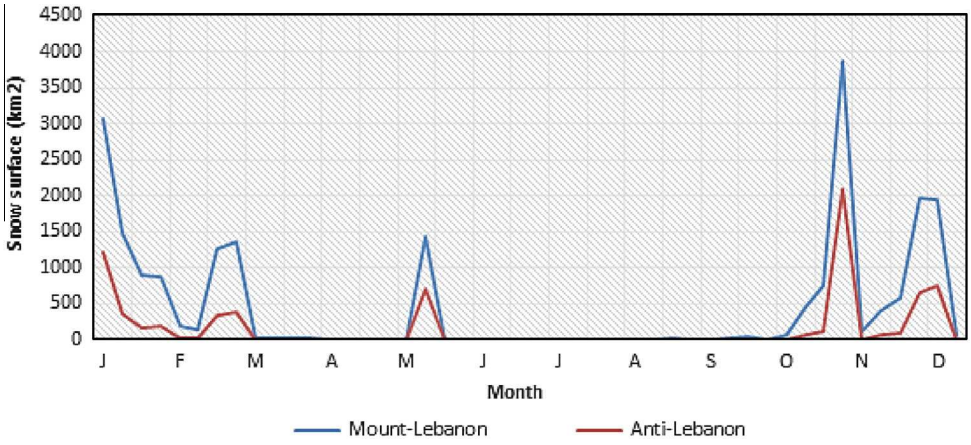

Fig. 7. Snow covers area (SCA) in Mount and Anti Lebanon in 2008.

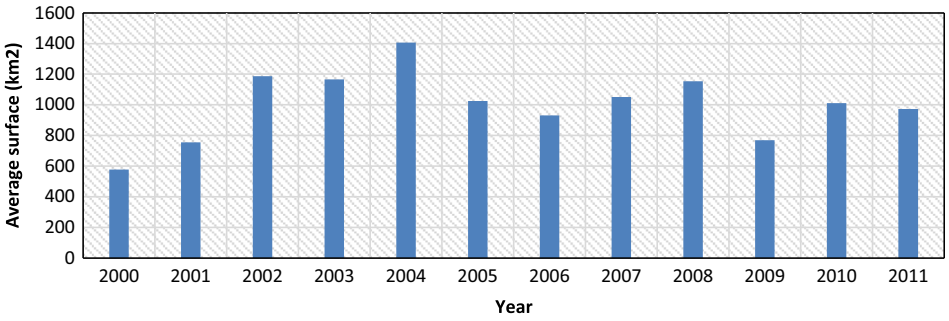

Fig. 8. Average yearly distribution of snow surface between 2000 and 2011.

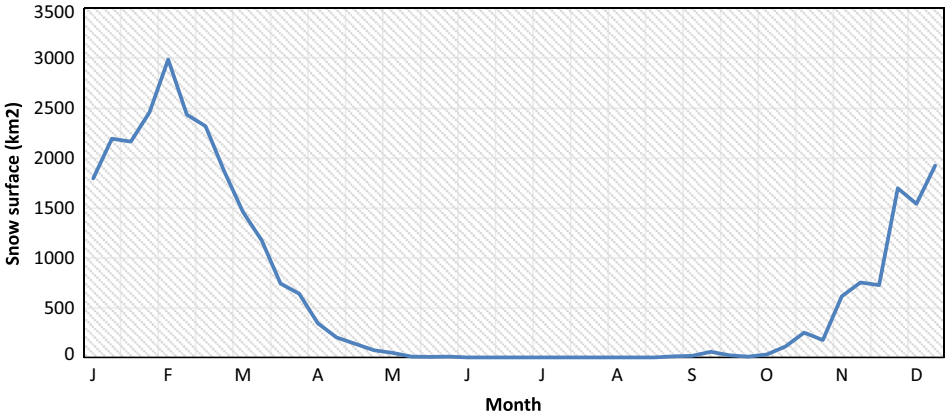

Fig. 9. Annual average snow surface distribution pattern (average 2000 and 2011).

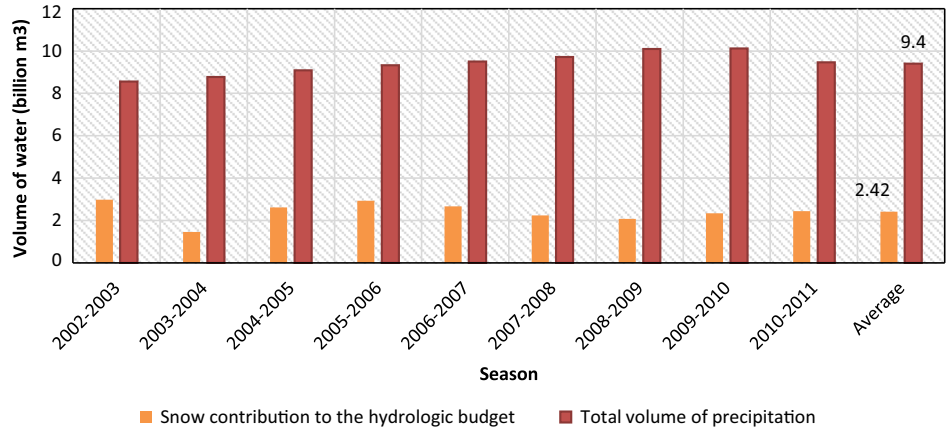

Fig. 10. Snow contribution to the hydrologic budget (i.e. surface runoff and groundwater recharge) compared to the total volume of precipitation.

2002 and 2011. It was clear that snow melt contributes to around 26% of the total hydrologic budget. The maximum snow contribution was found to be ~35% (2002–2003).

6. Discussion and conclusion

Both Terra and Aqua MODIS instruments can generate snow cover area with an acceptable spatial resolution of 500 m. AMSR-E instrument produces SWE data at a low spatial resolution of 25,000 m. Therefore, the aim of the research was to derive an enhanced snow extent area (TAC) data set and to measure snow water equivalent (SWE) over Lebanon. The TAC dataset minimized cloud contamination and the accuracy assessment of the TAC was validated against snow product derived using eighteen ETM+ snow products. Results revealed great correlation between the two datasets. The processing of the AMSR-E data using median filtering was used to generate eight-day noise-free curve from original five-day SWE data. The combination of both instruments was found to be practical in the derivation of sub-pixel SWE at 500 m spatial resolution.

Eight-day snow cover area and snow extent at 500 m spatial resolution over the time period between 2002 and 2012, as well as snow day(s) per year, were generated. The correlation between the volumes and spatial extent of snow in function of altitude was evaluated. It was evident that snow accounts, on the average, to around 26% of the total hydrologic budget in Lebanon. Such contribution represent feedbacks to the spring discharge mechanism during months were there is no precipitation. These outputs are

believed to help in the quantification of the hydrologic budget taking into consideration of the snow melt impacts on such system.

Acknowledgments

This work is done under the supervision of the Lebanese National Centre for Scientific Research (CNRS-L), Mansourieh, Lebanon. Special acknowledgment to Mr. Ali Termos for helping in some of the data generation process.

References

Andreadis, K.M., Lettenmaier, D.P., 2006. Assimilating remotely sensed snow observations into amacroscale hydrology model. Adv. Water. Resour. 29, 872–886. Remote Sens. Environ. 113, 40–49.

Aouad Rizk, A., Job, Jean-olivier, Khalil, S., Touma, T., Bitar, C., Bocquillon, C., Najem, W., 2005. Snow in Lebanon: a preliminary study of snow cover over Mount Lebanon and a simple snowmelt model. Hydrol. Sci. J. 50 (3), 555–569, ISSN 0262-6667.

Ault, Timothy W., Teresa Benkoa, Czajkwoski P., James, Cossa, Janet, Strublec, Alison, Spongbergb, Mark, Templinc, Christopher, GrossdKevin, 2006. Validation of the MODIS snow product and cloud mask using student and NWS cooperative station observations in the lower great lakes region. Remote Sens. Environ. 105 (4), 341–353.

Clifford, D., 2010. Global estimates of snow water equivalent from passive microwave instruments: history, challenges and future developments. Int. J. Remote Sens. 31 (14), 3707–3726.

de Boor, Carl, 1978. A practical guide to splines, Applied Mathematical Sciences, vol. 27. Springer-Verlag, NewYork.

Derksen, Chris, 2008. The contribution of AMSR-E 18.7 and 10.7 GHz measurements to improved boreal forest snow water equivalent retrievals. Remote Sens. Environ. 112 (5), 2701–2710.

Foster, J.L., Sun, C., Walker, J.P., Kelly, R., Chang, A., Dong, J., Powell, H., 2005. Quantifying the uncertainty in passive microwave snow water equivalent observations. Remote Sens. Environ. 94, 187–203.

Gafurov, A., Bardossy, A., 2009. Cloud removal methodology from MODIS snow cover product. Hydrol. Earth Syst. Sci. 13, 1361–1373.

Gao, Yang, Xie, Hongjie, Lub, Ning, Yaoc, Tandong, Liange, Tiangang, 2010. Toward advanced daily cloud-free snow cover and snow water equivalent products from TERRA-AQUA MODIS and AQUA AMSR-E measurements. J. Hydrol. 385, 23–35.

Gurung, Deo Raj, Kulkarni, Anil V., Giriraj, A., Aung, Khun San, Shrestha, Basanta, 2011. Monitoring of seasonal snow cover in Bhutan using remote sensing technique. Curr. Sci. India 101 (10), 1364–1370.

Hall Dorothy k., Salomonson Vicent V., 2004. MODIS/TERRA snow cover 8-day L3 global 500 m grid, version 5. Version Décembre 2006. <http://nsidc.org/data/docs/daac/modis_v5/mod10a2_modis_terra_snow_8-day_global_500m_grid.gd.html>.

Immerzeel, W.W., Droogers, P., de Jong, S.M., Bierkens, M.F.P., 2009. Large-scale monitoring of snow cover and runoff simulation in Himalayan river basins using remote sensing. Remote Sens. Environ. 113, 40–49.

Langlois, A., Scharien, R., Geldsetzerb, T., Iacozzaa, J., Barbera, D.G., Yackelb, J., 2008. Estimation of snow water equivalent over first year sea ice using AMSR-E and surface observations. Remote Sens. Environ. 112 (9), 3656–3667.

Liang, Tiangang, Zhang, Xuetong, Xie, Hongjie, Wu, Caixia, Feng, Qisheng, Huang, Xiaodong, Chen, Quangong, 2008. Toward improved daily snow cover mapping with advanced combination of MODIS and AMSR-E measurements. Remote Sens. Environ. 112 (10), 3750–3761.

Powel, Cynthia, Blesius, Leonhard, Davis, Jerry, Schuetzenmeister, Falk, 2011. Using MODIS snow cover and precipitation data to model water runoff for the Mokelumne River Basin in the Sierra Nevada, California (2000–2009). Global Planet Change 77 (1-2), 77–84.

Pulliainen, Jouni, 2006. Mapping of snow water equivalent and snow depth in boreal and sub-arctic zones by assimilating space-borne microwave radiometer data and ground-based observations. Remote Sens. Environ. 101 (2), 257–269.

Shaban Amin. 2010. Trans-boundary water resources of Lebanon: monitoring and assessment. <http://www.siagua.org/sites/default/files/documentos/documentos/libano.pdf>.

Shaban, Amin, Ghaleb, Faour, Khawlie, Mohamad, Abdallah, Chadi, 2004. Remote sensing application to estimate the volume of water in form of snow on Mount Lebanon. Hydrol. Sci. J. 49 (4), 653.

Sirguey, P., Mathieu, R., Arnaud, Y., 2009. Subpixel monitoring of the seasonal snow cover with MODIS at 250 m spatial resolution in the Southern Alps of New Zealand: methodology and accuracy assessment. Remote Sens. Environ. 113 (1), 160–181.

Tedesco Marco, Kelly Richard, Foster James, 2004. AMSR-E/Aqua L3 Global Snow Water Equivalent EASE-Grids. <http://nsidc.org/data/docs/daac/ae_swe_ease-grids.gd.html#> Contacts and Acknowledgments.

Tong, J., Velicogna, I.A., 2010. Comparison of AMSR-E/aqua snow products with in situ observations and MODIS snow cover products in the Mackenzie River Basin, Canada. Remote Sens. 2, 2313–2322.

UNEP (United Nations Environment Programme). January 2007. Lebanon post-conflict environment assessment. <http://www.unep.org/pdf/Lebanon_PCOB_Report.pdf>.

Vuyovich, Carrie, Jacobs, Jennifer M., 2011. Snowpack and runoff generation using AMSR-E passive microwave observations in the Upper Helmand Watershed, Afghanistan. Remote Sens. Environ. 115 (12), 3313–3321.

Xie, Hongjie, Wang, Xianwei, Liang, Tiangang, 2009. Development and assessment of combined terra and aqua MODIS snow cover products in Colorado plateau, USA and northern Xinjiang, China. J. Appl. Remote Sens. 3 (1).

Yang, D.Q., Zhao, Y.Y., Armstrong, R., Robinson, D., 2009. Yukon River streamflow response to seasonal snow cover changes. Hydrological Processes 23, 109–121.

Ref	JOR	Year	DOI
Abdelnour et al. 2011	WRR	2011	doi:10.1029/2010WR010165
Aguado 1985	WRR	1985	
Aguilar et al. 2010	HESS	2009	doi:10.5194/hess-14-2479-2010
Akyurek et al. 2010	IJRS	2010	http://dx.doi.org/10.1080/01431161.2010.483484
Akyurek et al. 2011	HP	2011	DOI: 10.1002/hyp.8090
Allocca et al. 2014	HESS	2014	doi:10.5194/hess-18-803-2014
Alvera & Garcia Ruiz 2000	AAAR	2000	DOI: 10.2307/1552397
Anderson 1968	WRR	1968	
Anderton et al. 2002	JH	2002	
Anderton et al. 2004	HP	2004	DOI: 10.1002/hyp.1319
Anghileri et al. 2016	WRR	2016	doi:10.1002/2015WR017864
Aouad et al. 2004	HSJ	2004	
Aouad-Rizk et al. 2005	HSJ	2005	http://dx.doi.org/10.1623/hysj.50.3.555.65023
Argus et al. 2014	GRL	2014	doi:10.1002/2014GL059570
Arnell 1999	GEC	1999	DOI: 10.1016/s0959-3780(99)00017-5
Ashfaq et al. 2013	JGR	2013	doi:10.1002/jgrd.50816, 2013
Avanzi et al. 2014	WRR	2014	http://dx.doi.org/10.1016/j.advwatres.2014.06.011
Ayala et al. 2014	WRR	2014	doi:10.1002/2013WR014960
Bacardit & Camarero 2010	AE	2010	doi:10.1016/j.atmosenv.2009.06.022
Bair et al. 2015	FES	2015	doi: 10.3389/feart.2015.00058
Bales et al. 2006	WRR	2006	doi:10.1029/2005WR004387
Bales et al. 2011	VZJ	2011	doi:10.2136/vzj2011.0001
Balsamo et al. 2015	HESS	2015	doi:10.5194/hess-19-389-2015
Barnett et al. 2005	N	2005	doi:10.1038/nature04141
Barnett et al. 2008	S	2008	DOI: 10.1126/science.1152538, PMID: 18239088
Bart et al. 2016	PLOS	2016	doi:10.1371/journal.pone.0161805
Beaty 1975	JG	1975	
Begueria et al. 2011	IJC	2011	DOI: 10.1002/joc.2218
Behrangi et al. 2015	JHM	2015	doi:10.1175/JHM-D-15-0061.1
Belmecheri et al. 2015	NCC	2015	DOI: 10.1038/NCLIMATE2809
Beniston & Stoffel 2014	STE	2014	http://dx.doi.org/10.1016/j.scitotenv.2013.11.122
Beniston 2003	CC	2003	DOI: 10.1023/a:1024458411589
Beniston 2006	HB	2006	DOI 10.1007/s10750-005-1802-0
Berg et l. 1991	HSJ	1991	http://dx.doi.org/10.1080/02626669109492547
Berghuijs et al. 2014	NCC	2014	
Berman et al. 2009	WRR	2009	doi:10.1029/2009WR008265
Bernier et al. 2003	HSJ	2003	10.1623/hysj.48.6.999.51428
Berris & Harr 1987	WRR	1987	
Beschta et al. 2000	JH	2000	
Biggs & Whitaker 2012	JH	2012	http://dx.doi.org/10.1016/j.jhydrol.2012.02.048
Bocchiola & Groppelli 2010	CRST	2010	doi:10.1016/j.coldregions.2010.06.001
Bocchiola & Rosso 2007	AWR	2007	doi:10.1016/j.advwatres.2006.03.002
Bocchiola 2014	AWR	2014	http://dx.doi.org/10.1016/j.advwatres.2014.04.017
Bonfils at al. 2008a	JC	2008	DOI: 10.1175/2008JCLI2397.1
Bonfils at al. 2008b	CC	2008	DOI 10.1007/s10584-007-9374-9
Boone et al. 2004	JC	2004	
Bormann et al. 2013	JH	2013	http://dx.doi.org/10.1016/j.jhydrol.2013.01.032
Boudhar et al. 2009	HSJ	2009	DOI: 10.1623/hysj.54.6.1094
Boudhar et al. 2010	IJAEOG	2010	doi:10.1016/j.jag.2009.09.008

Boudhar et al. 2016	HSJ	2016	http://dx.doi.org/10.1080/02626667.2014.965173
Bown et al. 2008	AG	2008	
Brands et. 2014	IJC	2014	DOI: 10.1002/joc.3788
Brekke et al. 2004	JAWRA	2004	
Brooks et al. 2016	JH	2016	http://dx.doi.org/10.1016/j.jhydrol.2015.12.004
Brown & Mote 2009	JC	2009	DOI: 10.1175/2008JCLI2665.1
Brown & Petkova 2007	IJC	2007	DOI: 10.1002/joc.1468
Brown et al. 2006	WRR	2006	doi:10.1029/2005WR004268
Brunetti et al. 2012	IJC	2012	DOI: 10.1002/joc.2233
Buckingham et al. 2015	JH	2015	http://dx.doi.org/10.1016/j.jhydrol.2015.02.042
Buisan et al. 2015	IJC	2015	DOI: 10.1002/joc.3978
Buisán et al. 2016	AMT (dis)	2016	doi:10.5194/amt-2016-197
Buttafuoco et al. 2011	TAC	2011	DOI 10.1007/s00704-011-0398-8
Caballero et al. 2007	WRR	2007	doi:10.1029/2005WR004192
Caldwell et al. 2009	CC	2009	DOI 10.1007/s10584-009-9583-5
Carenzo et al. 2016	AWR	2016	DOI: 10.1002/hyp.7085
Carreira et al. 2011	HGJ	2011	DOI 10.1007/s10040-010-0675-0
Castebrunet et al. 2012	CP	2012	doi:10.5194/cp-8-855-2012
Castebrunet et al. 2014	TCD	2014	doi:10.5194/tcd-8-581-2014
Castellarin 2014	JH	2014	http://dx.doi.org/10.1016/j.jhydrol.2014.03.050
Catalan 1989	WRR	1989	
Cayan et al. 1993	WRR	1993	
Cayan et al. 2001	BAMS	2001	
Cayan et al. 2008	CC	2008	DOI 10.1007/s10584-007-9377-6
Cayan et al. 2010	PNAS	2010	doi/10.1073/pnas.0912391107
Ceballos-Barbancho et al. 2008	JH	2008	doi:10.1016/j.jhydrol.2007.12.004
Chang & Yung 2010	JH	2010	doi:10.1016/j.jhydrol.2010.04.040
Chaouche et al. 2010	CRG	2010	doi:10.1016/j.crte.2010.02.001
Chaponnière et al. 2005	IJRS	2005	DOI: 10.1080/01431160500117758
Chaponniere et al. 2008	HP	2008	DOI: 10.1002/hyp.6775
Charbonneau et al. 1981	HSB	1981	http://dx.doi.org/10.1080/02626668109490899
Christensen et al. 2008	HP	2008	DOI: 10.1002/hyp.6961
Christy 2012	JHM	2012	DOI: 10.1175/JHM-D-11-040.1
Christy et al. 2006	JC	2006	
Church 1913	QJ	1913	
Clark et al. 2011	WRR	2011	doi:10.1029/2011WR010745
Clark et al. 2015a	WRR	2015	doi:10.1002/2015WR017198
Clark et al. 2015b	WRR	2015	doi:10.1002/2015WR017200
Cline et al. 1998	WRR	1998	
Coats & Goldman 2001	WRR	2001	
Coats 2006	CC	2006	DOI: 10.1007/s10584-005-9006-1
Coats 2010	CC	2010	DOI 10.1007/s10584-010-9828-3
Coats et al. 2013	CC	2013	DOI 10.1007/s10584-012-0425-5
Colbeck et al. 1979	EOS	1979	
Cooper et al. 2016	ERL	2016	doi:10.1088/1748-9326/11/8/084009
Coppola et al. 2014	STE	2014	http://dx.doi.org/10.1016/j.scitotenv.2014.03.003
Corbane et al. 2004	HSJ	2004	10.1623/hysj.50.2.355.61802
Cornwell et al. 2016	HESS	2016	doi:10.5194/hess-20-411-2016
Cortés et al. 2011	JH	2011	doi:10.1016/j.jhydrol.2011.05.013
Cortés et al. 2014	RSE	2014	http://dx.doi.org/10.1016/j.rse.2013.10.023

Cortes et al. 2016	WRR	2016	doi:10.1002/2015WR018376
Costa-Cabral et al. 2013a	CC	2013	DOI 10.1007/s10584-012-0630-2
Costa-Cabral et al. 2013b	CC	2013	DOI 10.1007/s10584-012-0529-y
Creamean et al. 2014	JGR	2014	doi:10.1002/2014JD021694
Creamean et al. 2015	ACP	2015	doi:10.5194/acp-15-6535-2015
Cristea et al. 2014	HP	2014	DOI: 10.1002/hyp.9909
Curtis et al. 2014	PLOS	2014	oi:10.1371/journal.pone.0106984
Dafis et al. 2016	IJC	2016	DOI: 10.1002/joc.4576
Daly et al. 2000	HP	2000	
Das et al. 2009	JHM	2009	DOI: 10.1175/2009JHM1095.1
Das et al. 2011	CC	2011	DOI 10.1007/s10584-011-0298-z
de Luis et al. 2010	GPC	2010	doi:10.1016/j.gloplacha.2010.06.006
Dedieu et al. 2014	STE	2014	http://dx.doi.org/10.1016/j.scitotenv.2014.04.078
Deems et al. 2013	JG	2013	doi:10.3189/2013JoG12J154
Delgado et al. 2010	JH	2010	doi:10.1016/j.jhydrol.2009.07.024
Demaria et al. 2013a	JHM	2013	DOI: 10.1175/JHM-D-12-047.0
Demaria et al. 2013b	JH	2013	http://dx.doi.org/10.1016/j.jhydrol.2013.08.027
Derin et al. 2016	JHM	2016	DOI: 10.1175/JHM-D-15-0197.1
Dettinger & Cayan 1995	JC	1995	
Dettinger & Cayan 2003	JH	2003	doi:10.1016/S0022-1694(03)00078-7
Dettinger 2011	JAWRA	2011	DOI: 10.1111/j.1752-1688.2011.00546.x
Dettinger 2013	CC	2013	DOI 10.1007/s10584-012-0501-x
Dettinger et al. 2004a	JHM	2004	
Dettinger et al. 2004b	CC	2004	
Dettinger et al. 2011	W	2011	doi:10.3390/w3020446
Dettinger et al. 2012	NH	2012	DOI 10.1007/s11069-011-9894-5
Dietz et al. 2012	IJRS	2012	http://dx.doi.org/10.1080/01431161.2011.640964
Dietz et al. 2012	RS	2012	doi:10.3390/rs4082432
Diffenbaugh et al. 2012	NCC	2012	DOI: 10.1038/NCLIMATE1732
Doll et al. 2014	WRR	2014	doi:10.1002/2014WR015595
Dong & Peters-Lidard 2010	JSTARS	2010	10.1109/JSTARS.2009.2039698
Dong et al. 2014	JHM	2014	DOI: 10.1175/JHM-D-13-060.1
Doummar et al. 2014	AGC	2014	http://dx.doi.org/10.1016/j.apgeochem.2014.06.004
Dozier 1987	RG	1987	
Dozier 1992	RG	1992	
Dozier and Painter 2004	AREP	2004	doi: 10.1146/annurev.earth.32.101802.120404
Dozier et al. 2008	AWR	2008	doi:10.1016/j.advwatres.2008.08.011
Dozier et al. 2009	RSE	2009	doi:10.1016/j.rse.2007.07.029
Dozier et al. 2016	WIRE	2016	doi: 10.1002/wat2.1140
Duan et al. 2016	STE	2016	http://dx.doi.org/10.1016/j.scitotenv.2016.08.213
Duran et al. 2013	IJC	2013	DOI: 10.1002/joc.3602
Durand et al. 2009	JAMC	2009	DOI: 10.1175/2009JAMC1810.1
Eckert et al. 2010a	JOC	2010	DOI: 10.1175/2010JCLI3312.1
Eckert et al. 2010b	CRST	2010	doi:10.1016/j.coldregions.2010.08.009
Eguen et al. 2012	NHESS	2012	doi:10.5194/nhess-12-1573-2012
El Kenawy et al. 2012	AR	2012	doi:10.1016/j.atmosres.2011.12.006
El Kenawy et al. 2013	IJC	2013	DOI: 10.1002/joc.3410
El Kenawy et al. 2015a	GPC	2015	http://dx.doi.org/10.1016/j.gloplacha.2015.08.013
El Kenawy et al. 2015b	AR	2015	http://dx.doi.org/10.1016/j.atmosres.2014.12.007
Elder et al. 1991	WRR	1991	

Elder et al. 1998	HP	1998	
Essery et al. 2013	AWR	2013	http://dx.doi.org/10.1016/j.advwatres.2012.07.013
Etchevers et al. 2001	JH	2001	
Etchevers et al. 2002	JGR	2002	DOI: 10.1029/2001JD000490
Falvey & Garreaud 2007	JHM	2007	DOI: 10.1175/JHM562.1
Famiglietti et al. 2011	GRL	2011	doi:10.1029/2010GL046442
Farley et al. 2011	GEC	2011	doi:10.1016/j.gloenvcha.2010.09.011
Fatichi et al. 2013	STE	2013	http://dx.doi.org/10.1016/j.scitotenv.2013.12.014
Favier et al. 2009	WRR	2009	0043-1397/09/2008WR006802
Feld et al. 2013	WRR	2013	doi:10.1002/wrcr.20318
Fernandez-Chacon et al. 2010	HP	2010	DOI: 10.1002/hyp.7597
Ferrari et al. 2013	TAC	2013	DOI 10.1007/s00704-013-0856-6
Ficklin et al. 2013	WRR	2013	doi:10.1002/wrcr.20248
Ficklin et al. 2013	CC	2013	DOI 10.1007/s10584-012-0566-6
Filippa et al. 2014	CRST	2014	http://dx.doi.org/10.1016/j.coldregions.2014.04.008
Franco et al. 2011	CC	2011	DOI 10.1007/s10584-011-0318-z
Franz & Karsten 2013	JH	2013	http://dx.doi.org/10.1016/j.jhydrol.2013.04.026
Franz et al. 2010	AWR	2010	doi:10.1016/j.advwatres.2010.05.004
Franz et al. 2014	JH	2014	http://dx.doi.org/10.1016/j.jhydrol.2014.07.008
Frei et al. 2012	ASR	2012	doi:10.1016/j.asr.2011.12.021
Friedman et al. 1992	JGR	1992	
Friedman et al. 2002	JGR	2002	doi:10.1029/2001JD000566
Fu et al. 2015	JGR	2015	doi:10.1002/2014JB011415
Fujihara et al. 2008	JH	2008	doi:10.1016/j.jhydrol.2008.01.024
Gallart et al. 2002	HESS	2002	
Gallart et al. 2011	PCE	2011	doi:10.1016/j.pce.2011.04.009
Gámiz-Fortis et al. 2011	JH	2011	doi:10.1016/j.jhydrol.2011.09.014
Gao & Giorgi 2008	GPC	2008	doi:10.1016/j.gloplacha.2008.02.002
Gao et al. 2010	RSE	2010	doi:10.1016/j.rse.2010.02.017
García et al. 2009	CRST	2009	doi:10.1016/j.coldregions.2009.07.009
Garcia et al. 2013	WRR	2013	doi:10.1002/wrcr.20140
García-Ruiz et al. 2010	G	2010	doi:10.1016/j.geomorph.2010.03.038
García-Ruiz et al. 2011	ESR	2011	doi:10.1016/j.earscirev.2011.01.006
García-Sellés et al. 2010	CRST	2010	doi:10.1016/j.coldregions.2010.08.003
Gascoin et al. 2011	TC	2011	doi:10.5194/tc-5-1099-2011
Gascoin et al. 2013	AWR	2013	http://dx.doi.org/10.1016/j.advwatres.2012.11.013
Gascoin et al. 2015	HESS	2015	doi:10.5194/hess-19-2337-2015
Giorgi & Piero Lionello 2008	GPC	2008	doi:10.1016/j.gloplacha.2007.09.005
Giorgi 2006	GRL	2006	doi:10.1029/2006GL025734
Girotto et al. 2014	HP	2014	DOI: 10.1002/hyp.9887
Giuntoli et al. 2013	JH	2013	http://dx.doi.org/10.1016/j.jhydrol.2012.12.038
Gleick 1987	WRR	1987	
Godsey et al. 2014	HP	2014	DOI: 10.1002/hyp.9943
Gomez-Landesa & Rango et al. 2002	HP	2002	DOI: 10.1002/hyp.1022
Gonzalez-Hidalgo et al. 2009	IJC	2009	DOI: 10.1002/joc.2115
Gottardi et al. 2012	JH	2012	doi:10.1016/j.jhydrol.2012.02.014
Goubanova & Li 2007	GPC	2007	doi:10.1016/j.gloplacha.2006.11.012
Goulden & Bales 2014	PNAS	2014	doi/10.1073/pnas.1319316111
Goulden et al. 2012	JGR	2012	doi:10.1029/2012JG002027
Grassa et al. 2006	AG	2006	doi:10.1016/j.apgeochem.2006.07.014

Grubisic et al. 2005	MWR	2005	
Guan et al. 2010	GRL	2010	DOI: 10.1175/MWR-D-11-00087.1
Guan et al. 2012	MWR	2012	DOI: 10.1175/MWR-D-11-00087.1
Guan et al. 2013a	WRR	2013	doi:10.1002/wrcr.20387
Guan et al. 2013b	WRR	2013	doi:10.1002/wrcr.20537
Guan et al. 2016	GRL	2016	doi: 10.1002/2016GL067978
Gunawardhana & Kazama 2012	HESS	2012	doi:10.5194/hess-16-1033-2012
Hall & Riggs 2007	HP	2007	DOI: 10.1002/hyp.6715
Hall et al. 2002	RSE	2002	http://dx.doi.org/10.1016/S0034-4257(02)00095-0
Hall et al. 2010	RSE	2010	doi:10.1016/j.rse.2009.10.007
Hamlet et al. 2005	JC	2005	
Hammersmark et al. 2008	RRA	2008	DOI: 10.1002/rra.1077
Hancock et al. 2013	RSE	2013	http://dx.doi.org/10.1016/j.rse.2012.10.004
Hanson et al. 2004	JH	2004	doi:10.1016/j.jhydrol.2003.10.006
Hanson et al. 2006	HGJ	2006	DOI 10.1007/s10040-006-0067-7
Harpold & Molotch 2015	GRL	2015	doi:10.1002/2015GL065855
Harpold 2016	AWR	2016	10.1016/j.advwatres.2016.03.017
Harpold et al. 2012	WRR	2012	doi:10.1029/2012WR011949
Harpold et al. 2014	WRR	2014	doi:10.1002/2013WR013935
Harpold et al. 2015	HP	2015	DOI: 10.1002/hyp.10400
Harpold et al. 2015a	HESS	2015	doi:10.5194/hess-19-2881-2015
Harr 1981	JH	1981	
Harr 1986	WRR	1986	
Harr et al. 1982	WRR	1982	
Harrington & Bales 1998	WRR	1998	
Hartmann et al. 2014	RG	2014	doi:10.1002/2013RG000443
Hay & Clark 2003	JH	2003	doi:10.1016/S0022-1694(03)00252-X
Hayhoe et al. 2004	PNAS	2004	
He et al. 2011a	AWR	2011	doi:10.1016/j.advwatres.2010.10.002
He et al. 2011a	WRR	2011	doi:10.1029/2010WR009753
He et al. 2012	HESS	2012	doi:10.5194/hess-16-815-2012
He et al. 2013	HR	2013	doi: 10.2166/nh.2012.441
Henn et al. 2015	WRR	2015	doi:10.1002/2014WR016736
Henn et al. 2016	JH	2016	http://dx.doi.org/10.1016/j.jhydrol.2016.08.009
Herrero & Polo 2012	HESS	2012	doi:10.5194/hess-16-3139-2012
Herrero et al. 2009	JH	2009	doi:10.1016/j.jhydrol.2009.03.021
Hidalgo et al. 2009	JC	2009	DOI: 10.1175/2009JCLI2470.1
Hidalgo-Munoz et al. 2015	WRR	2015	doi:10.1002/2014WR016826
Hinkelman et al. 2015	JHM	2015	DOI: 10.1175/JHM-D-14-0179.1
Hoerling et al. 2012	JC	2012	DOI: 10.1175/JCLI-D-11-00296.1
Howat & Tulaczyk 2005	JGR	2005	doi:10.1029/2005JF000356
Hreiche et al. 2007	HSJ	2007	http://dx.doi.org/10.1623/hysj.52.6.1119
Huang et al. 2012	JH	2012	doi:10.1016/j.jhydrol.2012.01.034
Hublart et al. 2015	HESS	2015	doi:10.5194/hess-19-2295-2015
Hunsaker et al. 2012	JAWRA	2012	DOI: 10.1111/j.1752-1688.2012.00641.x
Hüsler et al. 2014	TC	2014	doi:10.5194/tc-8-73-2014
Huth et al. 2004	HP	2004	DOI: 10.1002/hyp.1414
Ingraham & Taylor 1989	JH	1989	
Ingraham & Taylor 1991	WRR	1991	
Iroumé & Palacios 2013	JH	2013	http://dx.doi.org/10.1016/j.jhydrol.2013.09.031

Isotta et al. 2014	IJC	2014	DOI: 10.1002/joc.3794
Jefferson 2011	GRL	2011	doi:10.1029/2011GL048346
Jefferson et al. 2006	WRR	2006	doi:10.1029/2005WR004812
Jefferson et al. 2008	HP	2008	DOI: 10.1002/hyp.7041
Jepsen et al. 2012	WRR	2012	doi:10.1029/2011WR011006
Jepsen et al. 2016	JH	2016	http://dx.doi.org/10.1016/j.jhydrol.2015.12.010
Jepsen et al. 2016b	WRR	2016	doi:10.1002/2015WR017827
Jin et al. 2006	HP	2006	DOI: 10.1002/hyp.6126
Jones & Grant 1996	WRR	1996	
Jones 2000	WRR	2000	
Jung et al. 2012	JH	2012	http://dx.doi.org/10.1016/j.jhydrol.2012.08.002
Kapnick & Delworth 2013	JC	2013	DOI: 10.1175/JCLI-D-12-00528.1
Kapnick & Hall 2010	JC	2010	DOI: 10.1175/2010JCLI2903.1
Karpouzos et al. 2011	WEJ	2011	doi:10.1111/j.1747-6593.2010.00222.x
Kattelmann & Elder 1991	WRR	1991	
Kerkez et al. 2012	WRR	2012	doi:10.1029/2011WR011214
Kim & Kang 2007	JHM	2007	DOI: 10.1175/JHM599.1
Kim & Kang 2007	JHM	2007	DOI: 10.1175/JHM599.1
Kim 1997	WRR	1997	
Kim 2001	GRL	2001	
Kim 2004	CC	2004	
Kim et al. 1998	JC	1998	
Kinar & Pomeroy 2015	RG	2015	doi:10.1002/2015RG000481
Kirchner 2014	HESS	2014	doi:10.5194/hess-18-4261-2014
Kluver & Leathers 2015	IJC	2015	DOI: 10.1002/joc.4292
Knight et al. 2001	TPG	2001	DOI: 10.1111/0033-0124.00303
Knowles & Cayan 2002	GRL	2002	doi:10.1029/2001GL014339
Knowles 2002	WRR	2002	doi:10.1029/2001WR000360
Knowles 2015	JC	2015	DOI: 10.1175/JCLI-D-15-0051.1
Knowles and Cayan 2004	CC	2004	
Knowles et al. 2006	JC	2006	
Koeniger et al. 2016	HP	2016	DOI: 10.1002/hyp.10822
Kormos et al. 2016	WRR	2016	doi:10.1002/2015WR018125
Kostadinov & Lookingbill 2015	RSE	2015	http://dx.doi.org/10.1016/j.rse.2015.04.002
Kotlarski et al. 2015	IJC	2015	DOI: 10.1002/joc.4254
Kourgialas et al. 2010	JH	2010	doi:10.1016/j.jhydrol.2009.12.003
Kumar et al. 2016	WRR	2016	doi:10.1002/2016WR018607
Kyselý et al. 2012	GPC	2012	doi:10.1016/j.gloplacha.2012.06.010
Lafaysse et al. 2014	WRR	2014	doi:10.1002/2013WR014897
Lana-Renault et al 2007	JH	2007	http://dx.doi.org/10.2166/nh.2007.003
Lana-Renault et al 2014	HP	2014	DOI: 10.1002/hyp.9892
Lapo et al. 2015	WRR	2015	doi:10.1002/2014WR016259
Latron & Gallart 2008	JH	2008	doi:10.1016/j.jhydrol.2008.06.014
Lee & Liou 2012	AE	2012	doi:10.1016/j.atmosenv.2012.03.024
Leisenring & Moradkhani 2012	JH	2012	http://dx.doi.org/10.1016/j.jhydrol.2012.08.049
Leon and Pedrozo 2015	HP	2015	DOI: 10.1002/hyp.10226
Lespinas et al. 2010	CC	2010	http://dx.doi.org/10.1016/j.jhydrol.2014.01.033
Lespinas et al. 2014	JH	2014	DOI 10.1007/s10584-009-9668-1
Lettenmaier et al. 1990	WRR	1990	
Lettenmaier et al. 2015	WRR	2015	doi: 10.1002/2015WR017616

Leydecker and Melack 2000	JH	2000	
Li et al. 2011	C	2011	doi:10.1016/j.catena.2011.03.003
Li et al. 2012	RSE	2012	doi:10.1016/j.rse.2012.06.027
Lin et al. 2015	JGR	2015	doi:10.1002/2014JD022912
Liotta et al. 2013	AG	2013	http://dx.doi.org/10.1016/j.apgeochem.2013.03.012
Liou et al. 2013	ACP	2013	doi:10.5194/acp-13-11709-2013
Liu et al. 2013	HP	2013	DOI: 10.1002/hyp.9304
Livneh et al. 2010	JHM	2010	DOI: 10.1175/2009JHM1174.2
Livneh et al. 2015	NSD	2015	DOI: 10.1038/sdata.2015.42
Llasat et al. 2014	NHESS	2014	doi:10.5194/nhess-14-427-2014
Loarie et al. 2009	N	2009	doi:10.1038/nature08649
Long et al. 2015	WRR	2015	doi:10.1002/2014WR016853
Longépé et al. 2009	TGRS	2009	DOI:10.1109/TGRS.2008.2006048
López & Justribó 2010	HSJ	2010	http://dx.doi.org/10.1080/02626660903546126
Lopez-Bustins et al. 2008	GPC	2008	doi:10.1016/j.gloplacha.2011.03.003
López-Moreno & García-Ruiz 2004	HSJ	2004	http://dx.doi.org/10.1623/hysj.49.5.787.55135
López-Moreno & Latron 2008	HP	2008	DOI: 10.1002/hyp.6572
Lopez-Moreno & Nogues-Bravo, 2005	HP	2005	DOI: 10.1002/hyp.5840
Lopez-Moreno & Nogues-Bravo, 2006	HP	2006	DOI: 10.1002/hyp.6199
Lopez-Moreno & Vicente-Serrano 2008	JC	2008	DOI: 10.1175/2007JCLI1739.1
López-Moreno 2005	AAAR	2005	
López-Moreno et al. 2006a	HSJ	2006	http://dx.doi.org/10.1623/hysj.51.6.1039
Lopez-Moreno et al. 2006b	GRL	2006	doi:10.1029/2006GL028204
López-Moreno et al. 2006c	ESPL	2006	DOI: 10.1002/esp.1356
López-Moreno et al. 2007	CR	2007	
López-Moreno et al. 2008a	CR	2008	doi: 10.3354/cr00747
López-Moreno et al. 2008b	GPC	2008	doi:10.1016/j.gloplacha.2007.10.004
López-Moreno et al. 2008c	IJC	2008	DOI: 10.1002/joc.1645
López-Moreno et al. 2009	JH	2009	doi:10.1016/j.jhydrol.2009.06.049
López-Moreno et al. 2010a	HP	2010	DOI: 10.1002/hyp.7564
López-Moreno et al. 2010b	IJC	2010	DOI: 10.1002/joc.1945
López-Moreno et al. 2011a	GPC	2011	doi:10.1016/j.gloplacha.2011.03.003
López-Moreno et al. 2011b	TC	2011	doi:10.5194/tc-5-617-2011
López-Moreno et al. 2011c	HESS	2011	doi:10.5194/hess-15-311-2011
López-Moreno et al. 2012	HP	2012	DOI: 10.1002/hyp.9408
López-Moreno et al. 2013a	JH	2013	http://dx.doi.org/10.1016/j.jhydrol.2012.11.028
López-Moreno et al. 2013b	AWR	2013	http://dx.doi.org/10.1016/j.advwatres.2012.08.010
López-Moreno et al. 2013c	STE	2013	http://dx.doi.org/10.1016/j.scitotenv.2013.09.031
López-Moreno et al. 2014a	HP	2014	DOI: 10.1002/hyp.10245
López-Moreno et al. 2014b	IJC	2014	DOI: 10.1002/joc.3665
Lopez-Moreno et al. 2016	TC	2016	doi:10.5194/tc-10-681-2016
Lorenzo-Lacruz et al. 2012	JH	2012	doi:10.1016/j.jhydrol.2011.11.023
Loukas et al. 2007	WRM	2007	DOI 10.1007/s11269-006-9120-5
Lowry et al. 2010	HP	2010	DOI: 10.1002/hyp.7714
Lowry et al. 2011	WRR	2011	doi:10.1029/2010WR010086
Luce et al. 2013	S	2013	DOI: 10.1126/science.1242335
Luce et al. 2014a	WRR	2014	doi:10.1002/2013WR014844
Luce et al. 2014b	WRR	2014	doi:10.1002/2013WR014329
Lundberg et al. 2016	HP	2016	DOI: 10.1002/hyp.10703
Lundquist & Cayan 2002	JHM	2002	

Lundquist & Cayan 2007	JGR	2007	doi:10.1029/2006JD007561
Lundquist & Dettinger 2005	WRR	2005	doi:10.1029/2004WR003649
Lundquist & Flint 2006	JHM	2006	
Lundquist & Loheide 2011	WRR	2011	doi:10.1029/2010WR010050
Lundquist & Lott 2008	WRR	2008	doi:10.1029/2008WR007035
Lundquist et al. 2004	JHM	2004	
Lundquist et al. 2005	WRR	2005	doi:10.1029/2004WR003933
Lundquist et al. 2007	JHM	2007	DOI: 10.1175/2007JHM853.1
Lundquist et al. 2008	WRR	2008	doi:10.1029/2008JD009879
Lundquist et al. 2010	JHM	2010	DOI: 10.1175/2010JHM1264.1
Lundquist et al. 2013	WRR	2013	doi:10.1002/wrcr.20504
Lundquist et al. 2015a	WRR	2015	doi:10.1002/2014WR016585
Lundquist et al. 2015b	JHM	2015	DOI: 10.1175/JHM-D-15-0019.1
Lute & Abatzoglou 2014	WRR	2014	10.1002/2013WR014465
Lute et al. 2015	WRR	2015	10.1002/2014WR016267
Magand et al. 2014	JHM	2014	doi:10.1175/JHM-D-13-91.1
Majone et al. 2012	WRR	2012	doi:10.1029/2011WR010985
Manga 1996	WRR	1996	
Manga 1996	WRR	1996	
Manga 1997	WRR	1997	
Manga 1997	WRR	1997	
Manning et al. 2012	JH	2012	http://dx.doi.org/10.1016/j.jhydrol.2012.06.030
Marchane et al. 2015	RSE	2015	http://dx.doi.org/10.1016/j.rse.2015.01.002
Margulis et al. 2015	JHM	2015	DOI: 10.1175/JHM-D-14-0177.1
Margulis et al. 2016a	JHM	2016	DOI: 10.1175/JHM-D-15-0177.1
Margulis et al. 2016b	GRL	2016	doi:10.1002/2016GL068520
Markovich et al. 2016	HP	2016	doi: 10.1002/hyp.10851
Marks & Dozier 1992	WRR	1992	
Marks et al. 1992	WRR	1992	
Martelloni et al. 2013	HESS	2013	doi:10.5194/hess-17-1229-2013
Marti et al. 2015	TC	2015	doi:10.5194/tc-9-1773-2015
Marti et al. 2016	TCD	2016	doi:10.5194/tc-2016-11, 2016
Masiokas et al. 2006	JC	2006	
Masiokas et al. 2010	JHM	2010	DOI: 10.1175/2010JHM1191.1
Masiokas et al. 2016	TC	2016	doi:10.5194/tc-10-927-2016
Maurer & Duffy 2005	GRL	2005	doi:10.1029/2004GL021462
Maurer 2007	CC	2007	DOI 10.1007/s10584-006-9180-9
Maurer et al. 2007	JGR	2007	doi:10.1029/2006JD008088
Maurer et al. 2010a	HESS	2010	doi:10.5194/hess-14-1125-2010
Maurer et al. 2010b	JAWRA	2010	DOI: 10.1111/j.1752-1688.2010.00473.x
Mazurkiewicz et al. 2008	JH	2008	doi:10.1016/j.jhydrol.2007.12.027
McAdie 1913	MWR	1913	
McCabe & Dettinger 2002	JHM	2002	7541(2002)003<0013:PMAPOY>2.0.CO;2
McCabe & Legates 1995	IJC	1995	DOI: 10.1002/joc.3370150504
McCabe et al. 2007	BAMS	2007	DOI:10.1175/BAMS-88-3-319
McGuire & McDonnell 2010	WRR	2010	doi:10.1029/2010WR009341
McGuire et al. 2005	WRR	2005	doi:10.1029/2004WR003657
McGurk et al. 1993	JAWRA	1993	
Meixner et al. 1998	WRR	1998	
Meixner et al. 2016	JH	2016	http://dx.doi.org/10.1016/j.jhydrol.2015.12.027

Mernild et al. 2016a	IJC	2016	DOI: 10.1002/joc.4804
Mernild et al. 2016b	IJC	2016	DOI: 10.1002/joc.4828
Meromy et al. 2013	HP	2013	DOI: 10.1002/hyp.9355
Mhawej et al. 2014	JH	2014	http://dx.doi.org/10.1016/j.jhydrol.2014.03.058
Micheletty et al. 2014	HESS	2014	doi:10.5194/hess-18-4601-2014
Milano et al. 2012	CRG	2012	http://dx.doi.org/10.1016/j.crte.2012.07.006
Milano et al. 2013	JH	2013	http://dx.doi.org/10.1016/j.jhydrol.2013.07.010
Millares et al. 2009	HESS	2009	
Millares et al. 2014	G	2014	http://dx.doi.org/10.1016/j.geomorph.2013.09.038
Miller et al. 2003	JAWRA	2003	
Minnich 1986	JH	1986	
Mizukami & Perica 2008	JHM	2008	DOI: 10.1175/2008JHM981.1
Mizukami & Smith 2012	JH	2012	doi:10.1016/j.jhydrol.2012.01.030
Mizukami et al. 2011	JH	2011	doi:10.1016/j.jhydrol.2011.01.019
Molotch & Bales 2006	WRR	2006	doi:10.1029/2005WR004522
Molotch & Meromy 2014	HP	2014	DOI: 10.1002/hyp.10254
Molotch et al. 2005	HP	2005	DOI: 10.1002/hyp.5586
Montoya et al. 2014	GRL	2014	doi:10.1002/2014GL060588
Morán-Tejeda et al. 2010	GPC	2010	doi:10.1016/j.gloplacha.2010.03.003
Morán-Tejeda et al. 2011	HP	2011	DOI: 10.1002/hyp.7907
Morán-Tejeda et al. 2011a	JH	2011	doi:10.1016/j.jhydrol.2011.04.034
Moran-Tejeda et al. 2012a	REC	2012	DOI 10.1007/s10113-011-0236-7
Morán-Tejeda et al. 2012b	HSJ	2012	http://dx.doi.org/10.1080/02626667.2012.673722
Morán-Tejeda et al.2014	JH	2014	http://dx.doi.org/10.1016/j.jhydrol.2014.06.053
Mote 2003	GRL	2003	doi:10.1029/2003GL017258
Mote 2006	JC	2006	
Mote et al. 2005	BAMS	2005	DOI: 10.1175/BAMS-86-1-39
Muntan et al. 2009	NHESS	2009	
Musselman et al. 2012	AFM	2012	doi:10.1016/j.agrformet.2012.03.011
Nadal-Romero et al. 2016	HP	2016	DOI: 10.1002/hyp.10820
Neiman et al. 2014	JHM	2014	DOI: 10.1175/JHM-D-13-0183.1
Nogués-Bravo et al. 2007	GEC	2007	doi:10.1016/j.gloenvcha.2006.11.007
Nohara et al. 2006	JHM	2006	DOI: 10.1175/jhm531.1
Nolin & Daly 2006	JHM	2006	
Nolin et al. 2010	WRR	2010	doi:10.1029/2009WR008968
Notarnicola et al. 2013a	RS	2013	doi:10.3390/rs5010110
Notarnicola et al. 2013b	RS	2013	doi:10.3390/rs5041568
Novel et al. 2007	JH	2007	doi:10.1016/j.jhydrol.2006.10.029
Null et al. 2010	PLOS	2010	doi:10.1371/journal.pone.0009932
Null et al. 2013	CC	2013	DOI 10.1007/s10584-012-0459-8
Núñez et al. 2011	JH	2011	doi:10.1016/j.jhydrol.2011.05.035
Núñez et al. 2013	JH	2013	http://dx.doi.org/10.1016/j.jhydrol.2013.07.035
Oaida et al. 2015	JGR	2015	doi:10.1002/2014JD022444
Oroza et al. 2016	WRR	2016	doi: 10.1002/2016WR018896
Ouellette et al. 2013	WRR	2013	doi:10.1002/wrcr.20173, 2013
Oyarzún et al. 2014	JAE	2014	http://dx.doi.org/10.1016/j.jaridenv.2014.02.012
Pagán et al. 2016	ERL	2016	doi:10.1088/1748-9326/11/9/094026
Painter et al. 2003	RSE	2003	doi:10.1016/S0034-4257(02)00187-6
Painter et al. 2009	RSE	2009	doi:10.1016/j.rse.2009.01.001
Painter et al. 2016	RSE	2016	http://dx.doi.org/10.1016/j.rse.2016.06.018

Palmer et al. 2007	JH	2007	doi:10.1016/j.jhydrol.2006.12.008
Pandey et al. 1999	JGR	1999	
Pavelsky et al. 2011	JGR	2011	doi:10.1029/2010JD015479
Pavelsky et al. 2012	GRL	2012	doi:10.1029/2012GL052741
Pearson et al. 2016	B	2016	doi:10.5194/bg-12-3665-2015
Pellicciotti et al. 2008	HP	2008	DOI: 10.1002/hyp.7085
Pellicciotti et al. 2013	STE	2013	http://dx.doi.org/10.1016/j.scitotenv.2013.10.055
Penna et al. 2015	HP	2015	DOI: 10.1002/hyp.10347
Penna et al. 2016	JH	2016	http://dx.doi.org/10.1016/j.jhydrol.2016.03.040
Pepin et al. 2011	GRL	2011	doi:10.1029/2010JD014769
Pepin et al. 2015	NCC	2015	DOI: 10.1038/NCLIMATE2563
Perrot et al. 2014	WRR	2014	doi:10.1002/2013WR015243
Pierce & Cayan 2012	JC	2012	DOI: 10.1175/JCLI-D-12-00534.1
Pierce et al. 2008	JC	2008	DOI: 10.1175/2008JCLI2405.1
Pimentel et al. 2015	JHM	2015	DOI: 10.1175/JHM-D-14-0046.1
Pimentel et al. 2016	H	2016	doi:10.3390/hydrology3010010
Pitlick 1994	JH	1994	
Pokhrel et al. 2015	WRR	2015	doi:10.1002/2014WR015602
Pons et al. 2010	IJC	2010	DOI: 10.1002/joc.2016
Popovska & Bonacci 2007	HP	2007	DOI: 10.1002/hyp.6252
Pourrier et al. 2014	JH	2014	http://dx.doi.org/10.1016/j.jhydrol.2014.08.023
Powell et al. 2011	GPC	2011	doi:10.1016/j.gloplacha.2011.03.005
Pujol et al. 2007	HSJ	2007	http://dx.doi.org/10.1623/hysj.52.5.956
Queno et al. 2016	TC	2016	doi:10.5194/tc-10-1571-2016
Rademacher et al. 2005	WRR	2005	doi:10.1029/2003WR002805,
Ragettli et al. 2013	HP	2013	DOI: 10.1002/hyp.10055
Ragettli et al. 2016	PNAS	2016	10.1073/pnas.1606526113
Raleigh and Lundquist 2012	WRR	2012	doi:10.1029/2011WR010542
Raleigh et al. 2013a	RSE	2013	http://dx.doi.org/10.1016/j.rse.2012.09.016
Raleigh et al. 2013b	WRR	2013	doi:10.1002/2013WR013958
Raleigh et al. 2016	JHM	2016	DOI: 10.1175/JHM-D-14-0235.1
Ralph et al. 2016	BAMS	2016	DOI:10.1175/BAMS-D-14-00043.1
Ranzi et al. 1999	HP	1999	
Rauscher et al. 2008	GRL	2008	doi:10.1029/2008GL034424
Renard & Lall 2014	WRR	2014	doi:10.1002/2014WR016277
Revuelto et al. 2014	TC	2014	doi:10.5194/tc-8-1989-2014
Revuelto et al. 2015	WRR	2015	doi:10.1002/2014WR016496
Revuelto et al. 2016	JH	2016	http://dx.doi.org/10.1016/j.jhydrol.2015.12.015
Revuelto et al. 2016	HP	2016	DOI: 10.1002/hyp.10823
Rheinheimer et al. 2016	WRR	2016	doi:10.1002/2015WR018295.
Ribalaygua et al. 2013	STE	2013	http://dx.doi.org/10.1016/j.scitotenv.2013.06.089
Rice & Bales 2010	WRR	2010	doi:10.1029/2008WR007318
Rice et al. 2011	WRR	2011	doi:10.1029/2010WR009278
Risbey & Entekhabi 1996	JH	1996	
Rittger et al. 2013	AWR	2013	http://dx.doi.org/10.1016/j.advwatres.2012.03.002
Rittger et al. ?2016	AWR	2016	http://dx.doi.org/10.1016/j.advwatres.2016.05.015
Riverson et al. 2013	CC	2013	DOI 10.1007/s10584-012-0629-8
Rodriguez et al. 2016	HP	2016	DOI: 10.1002/hyp.10973
Rosenthal & Dozier 1996	WRR	1996	
Rousselot et al. 2012	TC	2012	doi:10.5194/tc-6-785-2012

Rutz et al. 2014	MWR	2014	DOI: 10.1175/MWR-D-13-00168.1
Saavedra et al. 2016	IJC	2016	DOI: 10.1002/joc.4795
Sade et al. 2014	JH	2014	http://dx.doi.org/10.1016/j.jhydrol.2014.07.048
Safeeq et al. 2016	IJC	2016	DOI: 10.1002/joc.4545
Sagredo & Lowell 2012	GPC	2012	doi:10.1016/j.gloplacha.2012.02.010
Sahoo et al. 2013	CC	2013	DOI 10.1007/s10584-012-0600-8
Sar?kaya et al. 2008	QSR	2008	doi:10.1016/j.quascirev.2008.01.002
Scanlon et al. 2012	WRR	2012	doi:10.1029/2011WR011312
Schlaepfer et al. 2012	GCB	2012	doi: 10.1111/j.1365-2486.2012.02642.x
Schmidli et al. 2002	IJC	2002	DOI: 10.1002/joc.769
Schneider & Matson 1977	RSE	1977	
Schulz & de Jong 2004	HESS	2004	doi:10.5194/hess-8-1076-2004
Seguí et al. 2010	JH	2010	doi:10.1016/j.jhydrol.2009.09.050
Senatore et al. 2011	JH	2011	doi:10.1016/j.jhydrol.2010.12.035
?ensoy & Uysal 2012	WRM	2012	DOI 10.1007/s11269-012-0079-0
Sensoy et al. 2006	HP	2006	DOI: 10.1002/hyp.6120
Serreze et al. 1999	WRR	1999	
Seth et al. 1999	GRL	1999	
Shaban et al. 2004	HSJ	2004	DOI: 10.1623/hysj.49.4.643.54432
Shamir & Georgakakos 2007	JH	2007	doi:10.1016/j.jhydrol.2006.10.007
Shamir & Georgakakos 2014	RSE	2014	http://dx.doi.org/10.1016/j.rse.2014.06.001
Shamir & Georgakakos et al. 2006	AWR	2006	doi:10.1016/j.advwatres.2005.06.010
Shaw et al. 2014	WRR	2014	doi:10.1002/2013WR014222
Simpson and Sienko 1998	JH	1998	
Simpson et al. 2004	WF	2004	
Singh et al. 2015	WRR	2015	doi:10.1002/2014WR015686
Slater et al. 2013	AWR	2013	http://dx.doi.org/10.1016/j.advwatres.2012.07.006
Smith et al. 1992	JGR	1992	
Smith et al. 2001	FB	2001	
Smith et al. 2013	JH	2013	http://dx.doi.org/10.1016/j.jhydrol.2013.08.040
Snyder et al. 2002	GRL	2002	DOI: 10.1029/2001GL014431
Snyder et al. 2004	JAWRA	2004	
Sobolowskia & Freib 2007	IJC	2007	DOI: 10.1002/joc.1395
Soncini & Bocchiola 2011	CRST	2011	doi:10.1016/j.coldregions.2011.06.011
Sonmez et al. 2014	IJC	2014	DOI: 10.1002/joc.3843
Soong & Kim, 1996	CC	1996	
Sorman & Beser 2013	HP	2013	DOI: 10.1002/hyp.9267
Sorman et al. 2009	HP	2009	DOI: 10.1002/hyp.7204
Souvignet et al. 2012	HSJ	2012	http://dx.doi.org/10.1080/02626667.2012.665607
Sproles et al. 2013	HESS	2013	doi:10.5194/hess-17-2581-2013
Sproles et al. 2016a	TCD	2016	doi:10.5194/tc-2016-66, 2016
Sproles et al. 2016b	WRM	2016	DOI: 10.1007/s11269-016-1271-4
Stehr et al. 2009	HSJ	2009	http://dx.doi.org/10.1623/hysj.54.6.1053
Stern et al. 2016	W	2016	doi:10.3390/w8100432
Stewart 2009	HP	2009	DOI: 10.1002/hyp.7128
Stewart 2013	CC	2013	DOI 10.1007/s10584-012-0567-5
Stewart et al. 2004	CC	2004	
Stewart et al. 2005	JC	2005	
Storck & Lettenmaier 2002	WRR	2002	doi:10.1029/2002WR001281
Struglia et al. 2004	JC	2004	

Sturm et al. 1995	JC	1995	
Sturm et al. 2010	JHM	2010	DOI: 10.1175/2010JHM1202.1
Sturm et al. 2015	WRR	2015	doi: 10.1002/2015WR017242
Sun et al. 2016	JC	2016	DOI: 10.1175/JCLI-D-15-0199.1
Surer & Akyurek 2012	HSJ	2012	http://dx.doi.org/10.1080/02626667.2012.729132
Surfleet & Tullos 2013	JH	2013	http://dx.doi.org/10.1016/j.jhydrol.2012.11.021
Svoma 2011	AAAR	2011	DOI: 10.1657/1938-4246-43.1.118
Szczypta et al. 2012	HESS	2012	doi:10.5194/hess-16-3351-2012
Szczypta et al. 2015	JH	2015	http://dx.doi.org/10.1016/j.jhydrol.2014.11.060
Tague & Grant 2004	WRR	2004	doi:10.1029/2003WR002629
Tague & Grant 2009	WRR	2009	doi:10.1029/2008WR007179
Tague & Peng 2013	JGR	2013	doi:10.1002/jgrg.20073
Tague 2009	HP	2009	DOI: 10.1002/hyp.7288
Tague et al. 2008	WRR	2008	doi:10.1029/2007WR006418
Tanaka et al. 2006	CC	2006	DOI: 10.1007/s10584-006-9079-5
Tang & Lettenmaier 2010	IJRS	2010	DOI: 10.1080/01431161.2010.483493
Taylor et al. 2001	WRR	2011	
Tekeli 2008	HP	2008	DOI: 10.1002/hyp.7093
Tekeli et al. 2005a	HSJ	2005	http://dx.doi.org/10.1623/hysj.2005.50.4.669
Tekeli et al. 2005b	RSE	2005	doi:10.1016/j.rse.2005.03.013
Tekeli et al. 2006	HP	2006	DOI: 10.1002/hyp.6114
Telesca et al. 2012	PA	2012	doi:10.1016/j.physa.2011.10.023
Telesca et al. 2014	JH	2014	http://dx.doi.org/10.1016/j.jhydrol.2014.10.037
Thirel et al. 2012	RSE	2012	http://dx.doi.org/10.1016/j.rse.2012.09.006
Tisseuil et al. 2010	JH	2010	doi:10.1016/j.jhydrol.2010.02.030
Tobin & Schwartz 2016	HP	2016	DOI: 10.1002/hyp.10859
Tramblay et al. 2013	HESS	2013	doi:10.5194/hess-17-3721-2013
Trujillo & Molotch 2014	WRR	2014	doi:10.1002/2013WR014753
Trujillo et al. 2012	NG	2012	DOI: 10.1038/NGEO1571
Valdés-Pineda et al. 2014	JH	2014	http://dx.doi.org/10.1016/j.jhydrol.2014.04.016
van Beek et al. 2011	WRR	2011	doi:10.1029/2010WR009791
van Huijgevoor et al. 2014	JH	2014	http://dx.doi.org/10.1016/j.jhydrol.2014.02.060
Vano et al. 2015	WRR	2015	doi:10.1002/2014WR015909
Vezza et al. 2010	WRM	2010	DOI 10.1007/s11269-010-9647-3
Vicuna & Dracup 2007	CC	2007	DOI 10.1007/s10584-006-9207-2
Vicuna et al. 2007	JAWRA	2007	DOI: 10.1111 ? j.1752-1688.2007.00038.x
Vicuna et al. 2011	CC	2011	DOI: 10.1007/s10584-010-9888-4
Vidal et al. 2010	IJC	2010	DOI: 10.1002/joc.2003
Viviroli & Weingartner 2004	HESS	2004	DOI: 10.5194/hess-8-1017-2004
Viviroli et al. 2007	WRR	2007	doi:10.1029/2006WR005653
Viviroli et al. 2011	HESS	2011	DOI: 10.5194/hess-15-471-2011
Vuyovich et al. 2014	WRR	2014	doi:10.1002/2013WR014734
Wada et al. 2011	WRR	2011	doi:10.1029/2010WR009792
Wayand et al. 2013	JHM	2013	DOI: 10.1175/JHM-D-12-0102.1
Wayand et al. 2015	WRR	2015	doi: 10.1002/2014WR016576
Waylen & Caviedes 1982	JH	1982	
Waylen & Caviedes 1990	JH	1990	
Welch et al. 2013	WRR	2013	doi:10.1002/wrcr.20100
White et al. 2010	JHM	2010	DOI: 10.1175/2009JHM1181.1
White et al. 2013	JAOT	2013	DOI: 10.1175/JTECH-D-12-00217.1

Williams & Melack 1991a	WRR	1991	
Williams & Melack 1991b	WRR	1997	
Williams & Rodoni 1997	WRR	1991	
Williams et al. 2001	WRR	2001	
Wolford et al. 1986	WRR	1986	
Wood et al. 2005	JGR	2005	doi:10.1029/2004JD004508
Wrzesien et al. 2014	IJC	2014	DOI: 10.1002/joc.4136
Wu et al. 2015	GRL	2015	doi:10.1002/2015GL064110
Xia et al. 2012	WRR	2012	doi:10.1029/2011WR011072
Xing et al. 2014	STE	2014	http://dx.doi.org/10.1016/j.scitotenv.2013.11.083
Yatheendradas et al. 2012	WRR	2012	doi:10.1029/2011WR011347
Yilmaz & Imteaz 2011	HSJ	2011	http://dx.doi.org/10.1080/02626667.2011.609173
Yilmaz et al. 2011	JH	2011	doi:10.1016/j.jhydrol.2011.09.031
Young et al. 2009	JAWRA	2009	DOI: 10.1111 ? j.1752-1688.2009.00375.x
Yucel et al. 2015	IJC	2015	DOI: 10.1002/joc.3974
Zaitchik & Rodell 2009	JHM	2009	DOI: 10.1175/2008JHM1042.1
Zampieri et al. 2015	STE	2015	http://dx.doi.org/10.1016/j.scitotenv.2014.06.036
Zegre et al. 2010	WRR	2010	doi:10.1029/2009WR008601
Zheng et al. 2016	TC	2016	doi:10.5194/tc-10-257-2016
Zhu et al. 2005	JAWRA	2005	
Zuazo et al. 2012	HSJ	2012	http://dx.doi.org/10.1080/02626667.2012.726994

Group	Category	Indicator	Abreviation
1. Science	1.1. Meteorology & climatology in mountains	Climate change & variability	Clim. Chan.
		Trends in climate & hydrology	Trend. Clim. Hyd.
		Trends in snowpack & hydrology	Trend. S.
		Clim. & meteo. in mountains	Clim. Met. Mnt.
		Climate and meteorological extremes	Clim. meteo. ext.
	1.2. Snow	Snow hydrometeorology	S. Hydm.
		Snowpack properties	S. Prop.
		Snow in forested regions	S. Forset
		Snowpack dynamics	S. Dyn.
		Glaciers	Gla.
	1.3. Hydrology	Hydrology in mountain regions	Hyd. Mnt.
		Hydrological processes in snow basins (inc. snow hydrology)	Hyd. Proc. S.
		Hydrological processes in mountains	Hyd. Proc. Mnt.
		Soil moisture and evapotranspiration	Soil Moist. ET.
		Snowmelt & runoff in mountains	S. Melt Runoff
		Hydrochemistry	Hydrochemistry
		Hydrogeology	Hyg.
		Hydrogeology in karst	Hyg. Karst
		Hydrology of extremes	Hyd. Ext.
2. Methods	2.1. Spatial distribution of snowpack	Remote sensing of snow	RSS
		Remote sensing application in meteo. & hydro.	Rem. Sen. Hyd,
	2.2. Snow indicators	Snow water equivalent	SWE
		Snow distribution	S. Dist.
		Snow obs. & measurements	S. Obs.
	2.3. Snow modeling & simulation	Energy & mass balance modeling	EBM
		Snow modeling	S. Mod.
	2.4. Hydrological modeling & simulation	Hydrological modeling and simulation	Hyd. Mod.
		Data assimilation & land surface modeling	Ass. Land Surf. Mod.
3. Data	3.1. Length of data used	Temporal extent and collection rate	-
	3.2. Source and type of data	Ground observations, projections, and reanalysis datasets	-
		Data assimilation (inc. data comparison from models)	-
		Global and national datasets	-
	3.3. Spatial scales	Extent of the study area	-
		Mountain elevation range	-
		Location of the study area	-